C-Job & Partners BV
Regulusplein 1
2132 JN Hoofddorp
The Netherlands
T +31 (0) 88 024 37 00
www.c-job.com

Powering a representative ROPAX ferry in 2050 with minimal greenhouse gas emissions

Project Nr:	Document Nr:	Status:	Revision:	Page:
17.509	000-100	FOR APPROVAL	0	1/158

© COPYRIGHT OF C-JOB, WHOSE PROPERTY, THIS DOCUMENT REMAINS. NO PART THEREOF MAY BE DISCLOSED, COPIED, DUPLICATED OR IN ANY OTHER WAY MADE USE OF EXCEPT WITH THE APPROVAL OF C-JOB.

(This page is intentionally left blank)

© COPYRIGHT OF C-JOB, WHOSE PROPERTY, THIS DOCUMENT REMAINS. NO PART THEREOF MAY BE DISCLOSED, COPIED, DUPLICATED OR IN ANY OTHER WAY MADE USE OF EXCEPT WITH THE APPROVAL OF C-JOB.

Thesis for the degree of MSc in Marine Technology in the specialization of *DPO*

Powering a representative ROPAX ferry in 2050 with minimal greenhouse gas emissions

By

J.J. Verbruggen

Performed at

C-Job Naval Architects

This thesis SDPO.18.021.m is classified as confidential in accordance with the general conditions for projects performed by the TUDelft.

June 20th, 2018

© COPYRIGHT OF C-JOB, WHOSE PROPERTY, THIS DOCUMENT REMAINS. NO PART THEREOF MAY BE DISCLOSED, COPIED, DUPLICATED OR IN ANY OTHER WAY MADE USE OF EXCEPT WITH THE APPROVAL OF C-JOB.

(This page is intentionally left blank)

© COPYRIGHT OF C-JOB, WHOSE PROPERTY, THIS DOCUMENT REMAINS. NO PART THEREOF MAY BE DISCLOSED, COPIED, DUPLICATED OR IN ANY OTHER WAY MADE USE OF EXCEPT WITH THE APPROVAL OF C-JOB.

Preface

The thesis in front of you is written as the completing work to obtain the title of Master of Science in Marine Technology at Delft University of Technology. After obtaining the degree of Bachelor of Science in Marine Technology at Delft University of Technology in 2016, I started with this master.

The research presented is carried out at C-Job Naval Architects, an independent naval architecture and engineering office, located in the Netherlands, with the objective to co-create ship designs with their clients. It was here, I first came into contact with an engineering firm that is eager to make the maritime world a better place by minimizing the emission of greenhouse gasses into the atmosphere. Contributing to this endeavor seemed like the right challenge for me to conclude my five years as student of Marine Technology at the Delft University of Technology.

Special thanks go to my supervisors who have contributed to the quality of this work. First, I would like to thank my supervisor at C-Job Naval Architects, Alexander van den Ing, for his valuable support, input and feedback throughout the research. Secondly, I thank my supervisor from the university, Robert Hekkenberg, for his continuous support and feedback during the whole process.

Furthermore, a word of thanks to my girlfriend, family, friends and colleagues who supported me both emotionally and intellectually during my studies and finally during this thesis.

Johannes Jacob Verbruggen
Hoofddorp, May 2018

© COPYRIGHT OF C-JOB, WHOSE PROPERTY, THIS DOCUMENT REMAINS. NO PART THEREOF MAY BE DISCLOSED, COPIED, DUPLICATED OR IN ANY OTHER WAY MADE USE OF EXCEPT WITH THE APPROVAL OF C-JOB.

(This page is intentionally left blank)

© COPYRIGHT OF C-JOB, WHOSE PROPERTY, THIS DOCUMENT REMAINS. NO PART THEREOF MAY BE DISCLOSED, COPIED, DUPLICATED OR IN ANY OTHER WAY MADE USE OF EXCEPT WITH THE APPROVAL OF C-JOB.

Summary

The International Maritime Organization (IMO) issued on the 13th of April 2018 a press release titled: *"UN body adopts climate change strategy for shipping"*. [1] This document illustrates the commitment of the IMO to significantly reduce the emission of greenhouse gasses (GHG) from international shipping in coming decades. However, the question arises whether the ambitious goals, set out in this press release, are feasible to be met.

This aim of this thesis is to investigate the economic and technological feasibility of powering a vessel while emitting minimal greenhouse gasses in 2050. The focus will be on power plant configuration consisting of an energy storage medium and energy converter. A case study, concerning a representative ROPAX ferry built in 2050, is performed to illustrate the feasibility of using such a power plant configuration.

Energy storage media considered are hydrogen, ammonia and batteries. The use of internal combustion engines, fuel cells and an ammonia reformer are also investigated. The performance of power plant configurations with respect to their estimated greenhouse gas emission, overall weight, required volume, initial investment cost and cost of the required energy per day of operation is evaluated and based on the results of this study several conclusions are drawn.

- First and foremost is the need to **reduce the price difference of hydrogen and ammonia compared to LNG**. Without this reduction, no single synthetic fuel can be considered economically feasible. Three options to reduce the price difference are identified:
  - a high LNG price including high emission tax;
  - a low commercial electric energy price; or
  - synthetic fuel production using excess renewable energy.

  Especially the last of these three is considered to be a feasible measure due to the expected presence of excess energy from solar and wind farms.
- The second conclusion is that using **fuel cells or batteries are the most environmentally friendly** option due to the emission of N_2O when using internal combustion engines.
- Thirdly, **all sustainable configurations require a considerable amount of space**.
- Furthermore, the combination of relative low electrical efficiencies and high hydrogen price result in high daily costs for hydrogen fueled internal combustion engines and PEMFCs.
- The initial investment cost and system weight of batteries-based configurations are high.

Following these conclusions, only three power plant configurations remain. Based on expected safety and logistical concerns and the expected potential for improvements, a single configuration was determined to be the most suitable to be used on a ROPAX ferry in 2050. This power plant configuration is composed of a **SOFC directly fueled by ammonia**.

After assessing the safety concerns associated with handling ammonia and the implications the established power plant configuration has on the general arrangement of the ship, it is concluded that the use of such a power plant configuration is highly likely to be feasible in 2050. However, it is recommended to perform a more in-depth analysis of required safety measures and operating characteristics of fuel cells in future research.

© COPYRIGHT OF C-JOB, WHOSE PROPERTY, THIS DOCUMENT REMAINS. NO PART THEREOF MAY BE DISCLOSED, COPIED, DUPLICATED OR IN ANY OTHER WAY MADE USE OF EXCEPT WITH THE APPROVAL OF C-JOB.

(This page is intentionally left blank)

© COPYRIGHT OF C-JOB, WHOSE PROPERTY, THIS DOCUMENT REMAINS. NO PART THEREOF MAY BE DISCLOSED, COPIED, DUPLICATED OR IN ANY OTHER WAY MADE USE OF EXCEPT WITH THE APPROVAL OF C-JOB.

Table of contents

Preface 5
Summary 7
List of Figures 12
List of Tables 15
Nomenclature 17
1 Introduction 19
1.1 Problem description and research objective 19
1.2 Report Structure 21
2 Representative characteristics & power plant configurations 22
2.1 Characteristics of a representative ROPAX ferry 22
2.2 Energy carriers 29
2.2.1 Not considered carbon free energy sources 31
2.2.2 Hydrogen (H_2) 33
2.2.3 Ammonia (NH_3) 34
2.2.4 Batteries 35
2.2.5 Overview 36
2.3 Energy converters 38
2.3.1 Internal Combustion Engine 38
2.3.2 Fuel Cell 39
2.3.3 Ammonia reformer 41
2.3.4 Electric motor and generator 42
2.3.5 Overview 42
2.4 Power plant configurations 43
2.4.1 Reference configuration 43
2.4.2 Stored hydrogen configurations 44
2.4.3 Stored ammonia configurations 44
2.4.4 Battery configurations 45
2.4.5 Overview 45
3 Power plant characteristics 46
3.1 Evaluation characteristics of power plant configurations 46
3.1.1 CO_2 equivalent pollutant emission 46
3.1.2 Energy cost per day operation 47
3.1.3 Initial investment cost 47
3.1.4 Total power plant volume 47
3.1.5 Total power plant mass 48
3.1.6 Overview of the evaluated characteristics and used formulas 48

© COPYRIGHT OF C-JOB, WHOSE PROPERTY, THIS DOCUMENT REMAINS. NO PART THEREOF MAY BE DISCLOSED, COPIED, DUPLICATED OR IN ANY OTHER WAY MADE USE OF EXCEPT WITH THE APPROVAL OF C-JOB.

3.2 Energy price ... 49
3.2.1 LNG price ... 49
3.2.2 Electricity prices ... 51
3.2.3 Hydrogen prices ... 52
3.2.4 Ammonia prices ... 55
3.2.5 Overview of energy prices ... 56
3.3 Energy storage characteristics ... 57
3.3.1 LNG storage ... 57
3.3.2 Hydrogen storage ... 57
3.3.3 Ammonia storage ... 58
3.3.4 Batteries ... 59
3.3.5 Overview of energy storage densities ... 61
3.4 Energy converter characteristics ... 62
3.4.1 Internal combustion engine ... 62
3.4.2 Fuel cell ... 65
3.4.3 Ammonia reformer ... 69
3.4.4 Overview ... 70
3.5 Summary ... 72
4 Power plant design ... 73
4.1 Default values ... 74
4.2 Sensitivity analysis ... 78
4.2.1 Conclusion 1: NH_3 becomes more appealing with increasing energy storage capacity 79
4.2.2 Conclusion 2: H_2 fueled ICEs and PEMFCs have relatively high daily energy costs ... 80
4.2.3 Conclusion 3: SOFCs and H_2 storage require much space ... 81
4.2.4 Conclusion 4: Batteries are expensive ... 82
4.2.5 Overview ... 83
4.3 Power plant used for a representative ROPAX ferry concept design ... 84
4.4 Summary ... 85
5 Proof of concept for a representative ROPAX ferry of 2050 ... 86
5.1 ROPAX ferry requirements ... 86
5.1.1 Passenger and car requirements ... 87
5.1.2 Power plant requirements ... 88
5.2 Safety concerns & regulation regarding the fuel ... 89
5.2.1 Properties of ammonia and LNG ... 89
5.2.2 IGC Code ... 91
5.2.3 IGF Code ... 92
5.3 General arrangement of a representative ROPAX ferry ... 93

© COPYRIGHT OF C-JOB, WHOSE PROPERTY, THIS DOCUMENT REMAINS. NO PART THEREOF MAY BE DISCLOSED, COPIED, DUPLICATED OR IN ANY OTHER WAY MADE USE OF EXCEPT WITH THE APPROVAL OF C-JOB.

5.4 Difference with current LNG powered vessels ... 97
5.5 Notable, out of scope, fuel saving measures ... 102
5.5.1 Waste heat recovery system ... 102
5.5.2 Solar panels ... 103
5.5.3 Wind assisted propulsion ... 104
5.5.4 Podded propulsor ... 104
5.6 Summary ... 106
6 Conclusion & recommendations ... 107
6.1 Conclusion ... 107
6.2 Recommendations ... 109
Bibliography ... 110
Appendices ... 123
A Market research plots ... 123
B Background information ... 130
B.1 Technology Readiness Levels (TRL) ... 130
B.2 Fuel cells ... 131
B.3 Ammonia reformer parasitic energy requirement ... 132
B.4 Conversion tables ... 133
B.5 Box & Whisker plot ... 134
C Literature data for energy carriers including storage system ... 135
C.1 Hydrogen at 350 bar ... 135
C.2 Hydrogen at 700 bar ... 135
C.3 Hydrogen at -253 °C ... 136
C.4 Ammonia at 10 bar ... 136
C.5 Li-ion batteries ... 136
C.6 Li-air batteries ... 137
C.7 Li-S batteries ... 138
C.8 Fuel cell electrical efficiencies ... 139
D Power plant analysis ... 140
D.1 All default values ... 140
D.2 As positive as possible ... 145
D.3 As negative as possible ... 146
D.4 Sensitivity analysis ... 147
D.5 Financial considerations ... 153
E Concept design ... 156
E.1 Passenger and car requirements ... 156
E.2 General Arrangement of MS Stavangerfjord ... 157

© COPYRIGHT OF C-JOB, WHOSE PROPERTY, THIS DOCUMENT REMAINS. NO PART THEREOF MAY BE DISCLOSED, COPIED, DUPLICATED OR IN ANY OTHER WAY MADE USE OF EXCEPT WITH THE APPROVAL OF C-JOB.

List of Figures

Figure 2-1: Status of vessels constructed from 1960-2010. [6] 23
Figure 2-2: Area of operation of vessels build between 2005 and 2015. [6] 23
Figure 2-3: Passenger and car capacity of ROPAX ferries build between 2005 and 2015. [6] 24
Figure 2-4: Number of vessels build per passenger capacity per decade. [6] 25
Figure 2-5: Number of vessels build per car capacity per decade. [6] 25
Figure 2-6: Passenger/car ratio per decade. [6] 25
Figure 2-7: Froude number of ROPAX ferries build between 2005 and 2015. [6] 26
Figure 2-8: Gross tonnage of ROPAX ferries as function of the number of cabins and cars. [6] 27
Figure 2-9: Total shipping CO_2 equivalent GHG emissions, 20-year and 100-year Global Warming potential. [12] 29
Figure 2-10: Global solar irradiance in kWh/m^2/day. [26] 32
Figure 2-11: Volumetric and gravimetric hydrogen density of different materials. The U.S. Department of Energy targets for the hydrogen storage system are also shown for comparison. [41] 34
Figure 2-12: Gravimetric and volumetric energy density of different energy carriers. [33] (NH_3 and Li-ion added) 36
Figure 2-13: Standardized layout of a power plant aboard a ferry. 43
Figure 2-14: Part of the power plant using ammonia as energy carrier and an ICE and generator as energy converter. 44
Figure 3-1: Henry Hub gas price in 2016 USD and mmBTU HHV according to the Energy Outlook 2017 by the U.S. Energy Information Administration. [74] 50
Figure 3-2: Hydrogen price per MWh HHV H2 as function of electricity price (l) and utilization factor (r). [81] 53
Figure 3-3: Hydrogen production cost estimation by C. Philibert. [85] 53
Figure 3-4: Range of gravimetric energy densities considered per type of battery based on literature. 59
Figure 3-5: Range of volumetric energy densities considered per type of battery based on literature. 59
Figure 3-6: Schematic diagram of a methane fueled solid oxide fuel cell system. [141] 65
Figure 3-7: Schematic representation of considered types of fuel cells. [63] 66
Figure 3-8: Electrical efficiency of fuel cells based on LHV based on literature. 69
Figure 4-1: GHG emissions from default values. 75
Figure 4-2: Energy cost per day using default values. 75
Figure 4-3: Weights for 1-day operation using default values. 76
Figure 4-4: Total volume required per power plant in case enough energy is stored for a 14-day operation. 79
Figure 4-5: Daily energy cost resulting from sensitivity analysis and using excess renewable energy to produce hydrogen and ammonia. 80
Figure 4-6: Total power plant volume determined by a variation study for a 1-day operational time. 81
Figure 4-7: Total power plant volume determined by a variation study for a 3.5-day operational time. 81
Figure 4-8: Investment cost of energy storage systems for a 1-day operational time. 82
Figure 4-9: Investment cost of total power plant for a 1-day operational time. 82
Figure 5-1: Schematic representation of used standard height and width of both a truck lane as well as a car lane. 87

© COPYRIGHT OF C-JOB, WHOSE PROPERTY, THIS DOCUMENT REMAINS. NO PART THEREOF MAY BE DISCLOSED, COPIED, DUPLICATED OR IN ANY OTHER WAY MADE USE OF EXCEPT WITH THE APPROVAL OF C-JOB.

Figure 5-2: Relevant figures for the position of a cylindric ammonia storage tank as provided in the IGC code. [192] 92
Figure 5-3: 3D views of the representative ROPAX ferry..... 93
Figure 5-4: The total general arrangement composed for a representative ROPAX ferry to be built in 2050 including an ammonia fueled SOFC. 95
Figure 5-5: Sideview of the representative ROPAX ferry..... 96
Figure 5-6: Required volumes of the power plants per component. 97
Figure 5-7: Required weights of the power plants per component. 98
Figure 5-8: Layout of the vessels below the waterline.[6,195] 100
Figure 5-9: First deck above the waterline for both vessels.[6,195] 101
Figure 5-10: Schematic representation of an integrated SOFC/GT system. [200] 102
Figure 5-11: Global solar irradiance in kWh/m^2/day. [26]..... 103
Figure 5-12: M/S Viking Grace equipped with a Flettner rotor. [205] 104
Figure 5-13: General layout of a podded propulsor. [206] 105
Figure 5-14: Different wake fields of a conventional twin screw ferry and podded propellers. [206] 105
Figure A-1: Car carrying capacity of ROPAX ferries between 1960 and 2010 per decade and a forecasted development for 2050. [6] 123
Figure A-2: Passenger/car ratio of ROPAX ferries between 1960 and 2010 per decade and a forecasted development for 2050. [6] 123
Figure A-3: Number of beds per maximum passenger capacity. [6] 123
Figure A-4: Froude number versus Passenger capacity. [6]..... 124
Figure A-5: Froude number versus Car capacity. [6] 124
Figure A-6: Gross tonnage of ROPAX ferries as function of the number of cabins and cars. [6] 124
Figure A-7: Displacement of a ROPAX ferry as function of gross tonnage and froude number. [6] .. 125
Figure A-8: Total MCR the engines of a ROPAX ferry as function of gross tonnage and Froude number. [6] 125
Figure A-9: Total MCR of the engines of a ROPAX ferry as function of displacement and Froude number. [6] 126
Figure A-10: Deadweight as function of displacement and number of cabins. [6] 126
Figure A-11: Deadweight as function of displacement and car carrying capacity. [6] 127
Figure A-12: Number of propellers and whether a ROPAX ferry has a bulbous bow or not displayed as function of the gross tonnage. [6]..... 127
Figure A-13: Displacement as function of the length between perpendiculars (Lbp). [6] 128
Figure A-14: Molded breadth (Bmold) as function of the length between perpendiculars (Lbp). [6]128
Figure A-15: Draught as function of the molded breadth (Bmold). [6] 129
Figure A-16: Length between perpendiculars as function of length over all. [6] 129
Figure B-1: Technology Readiness Levels according to NASA. [32]..... 130
Figure B-2: Schematic representation of a (a) Polymer Electrolyte Membrane fuel cell (PEMFC), (b) Alkaline fuel cell (AFC), (c) Phosphoric Acid fuel cell (PAFC), (d) Molten Carbonate fuel cell (MCFC) and (e) Solid Oxide fuel cell (SOFC). [63] 131
Figure B-3: Main elements of a SOFC system fed by natural gas. [211]..... 131
Figure B-4: Schematic layout of a power plant using an ammonia reformer. 132
Figure B-5: Example of a box & whisker plot including all previously discussed elements. [216] 134
Figure D-1: Energy cost per day 1st set. 141
Figure D-2: Investment costs for 1-day operation 1st set. 141
Figure D-3: Investment costs for 3.5-day operation 1st set. 142
Figure D-4: Investment costs for 14-day operation 1st set. 142
Figure D-5: Weights for 1-day operation 1st set. 142
Figure D-6: Weights for 3.5-day operation 1st set. 143
Figure D-7: Weights for 14-day operation 1st set. 143

© COPYRIGHT OF C-JOB, WHOSE PROPERTY, THIS DOCUMENT REMAINS. NO PART THEREOF MAY BE DISCLOSED, COPIED, DUPLICATED OR IN ANY OTHER WAY MADE USE OF EXCEPT WITH THE APPROVAL OF C-JOB.

Figure D-8: Volumes for 1-day operation 1st set. 143
Figure D-9: Volumes for 3.5-day operation 1st set. 144
Figure D-10: Volumes for 14-day operation 1st set. 144
Figure D-11: GHG emissions 1st set. 144
Figure D-12: Daily energy cost per configuration according to the sensitivity analysis. 147
Figure D-13: 1-day energy storage system investment cost per configuration according to the sensitivity analysis. 147
Figure D-14: 3.5-day energy storage system investment cost per configuration according to the sensitivity analysis. 148
Figure D-15: 14-day energy storage system investment cost per configuration according to the sensitivity analysis. 148
Figure D-16: Energy converter cost per power plant configuration according to the sensitivity analysis. 149
Figure D-17: Total weight of power plants per configuration for 1-day operation according to the sensitivity analysis. 149
Figure D-18: Total weight of power plants per configuration for 3.5-day operation according to the sensitivity analysis. 150
Figure D-19: Total weight of power plants per configuration for 14-day operation according to the sensitivity analysis. 150
Figure D-20: Total volume of power plants per configuration for 1-day operation according to the sensitivity analysis. 151
Figure D-21: Total volume of power plants per configuration for 3.5-day operation according to the sensitivity analysis. 151
Figure D-22: Total volume of power plants per configuration for 14-day operation according to the sensitivity analysis. 152
Figure D-23: Cumulative expenses over 10 years of operation of selected power plant configuration based on their default, best-case and worst-case scenarios. 154
Figure D-24: Cumulative expenses over 30 years of operation of selected power plant configuration based on their default, best-case and worst-case scenarios. 154
Figure D-25: Cumulative expenses over 45 years of operation of selected power plant configuration based on their default, best-case and worst-case scenarios. 155
Figure E-4: General arrangement of the MS Stavangerfjord part 1. [195] 157
Figure E-5: General arrangement of the MS Stavangerfjord part 2. [195] 158

© COPYRIGHT OF C-JOB, WHOSE PROPERTY, THIS DOCUMENT REMAINS. NO PART THEREOF MAY BE DISCLOSED, COPIED, DUPLICATED OR IN ANY OTHER WAY MADE USE OF EXCEPT WITH THE APPROVAL OF C-JOB.

List of Tables

Table 2-1: LNG key characteristics. [2,16] 30
Table 2-2: Hydrogen key characteristics. [29,33] 33
Table 2-3: Ammonia key characteristics. [2,35,40] 34
Table 2-4: Key parameters for the considered battery technologies. [42,45,47-50] 35
Table 2-5: Key characteristics of considered energy carriers. [2,4,16,29,33,35,38,40,42,47,48,56,57] 37
Table 2-6: Key characteristics of internal combustion engines. [6,38,58,62] 38
Table 2-7: Summary of fuel cell technologies according to DNV GL [60] and DOE [63]. 40
Table 2-8: Key characteristics of fuel cells. [38,59,66,67] 41
Table 2-9: Key characteristics of ammonia reformers. [38] 41
Table 2-10: Key characteristics of electric motors and generators. [6] 42
Table 2-11: Key characteristics of energy converters. [6,38,58,59,62,66,67] 42
Table 2-12: Summary of the considered power plant configurations. 45
Table 3-1: Evaluated power plant characteristics including units and formulas. 48
Table 3-2: Overview of the default, minimum and maximum price of LNG per component used. 50
Table 3-3: Overview of LCOE found in literature. 51
Table 3-4: Considered default, minimum and maximum electric energy price. 52
Table 3-5: Considered default, minimum and maximum hydrogen prices per storage condition. 54
Table 3-6: Considered default, minimum and maximum ammonia prices. 55
Table 3-7: Considered default, minimum and maximum energy prices. 56
Table 3-8: Considered default, minimum and maximum gravimetric densities per energy storage system. 61
Table 3-9: Considered default, minimum and maximum volumetric densities per energy storage system. 61
Table 3-10: Storage system investment prices. 61
Table 3-11: Main characteristics of an LNG-fueled internal combustion engine based on literature. 63
Table 3-12: Main characteristics of a hydrogen fueled internal combustion engine based on literature. 63
Table 3-13: Main characteristics of an ammonia fueled internal combustion engine based on literature. 64
Table 3-14: Characteristics of the ammonia reformer. 70
Table 3-15: Default, minimum and maximum efficiencies of energy converters used to assess power plant configurations. 70
Table 3-16: Specific masses of energy converters used to assess power plant configurations. 71
Table 3-17: Specific volumes of energy converters used to assess power plant configurations. 71
Table 3-18: Initial investment costs of energy converters used to assess power plant configurations. 71
Table 4-1: Default input values of the energy storage and energy converter units. 74
Table 4-2: Overview of configurations including discarded options after stage 1. 77
Table 4-3: Overview of configurations including discarded options. 83
Table 5-1: Definitions of chemical properties as stated by [191]. 89
Table 5-2: Safety related properties of ammonia and LNG. [191] 90
Table 5-3: Acute Exposure Guideline Levels (AEGL) of ammonia in ppm as defined by the U.S. Environmental Protection Agency. [191] 91
Table 5-4: Overview of relevant characteristics of the MS Stavangerfjord and the representative ferry of 2050. [195], [196] 97
Table 5-5: Overview of relevant characteristics of the MS Stavangerfjord and the representative ferry of 2050.[195,196] 99
Table B-1: Currency conversion table based on inflation. [212]. [213] 133

© COPYRIGHT OF C-JOB, WHOSE PROPERTY, THIS DOCUMENT REMAINS. NO PART THEREOF MAY BE DISCLOSED, COPIED, DUPLICATED OR IN ANY OTHER WAY MADE USE OF EXCEPT WITH THE APPROVAL OF C-JOB.

Table B-2: Conversion units used for the calculation of main characteristics of the power plant concepts. [214] 133
Table B-3: Explanation of the box & whisker plot elements. [215] 134
Table C-1: Gravimetric energy density of hydrogen stored at 350 bar according to literature. 135
Table C-2: Volumetric energy density of hydrogen stored at 350 bar according to literature. 135
Table C-3: Gravimetric energy density of hydrogen stored at 700 bar according to literature. 135
Table C-4: Volumetric energy density of hydrogen stored at 700 bar according to literature. 135
Table C-5: Gravimetric energy density of liquid hydrogen storage according to literature. 136
Table C-6: Volumetric energy density of liquid hydrogen storage according to literature. 136
Table C-7: Gravimetric energy density of compressed ammonia storage according to literature. ... 136
Table C-8: Volumetric energy density of compressed ammonia storage according to literature. 136
Table C-9: Gravimetric energy density of Li-ion batteries according to literature. 136
Table C-10: Volumetric energy density of Li-ion batteries according to literature. 137
Table C-11: Gravimetric energy density of Li-air batteries according to literature. 137
Table C-12: Volumetric energy density of Li-air batteries according to literature. 137
Table C-13: Gravimetric energy density of Li-S batteries according to literature. 138
Table C-14: Volumetric energy density of Li-S batteries according to literature. 138
Table C-15: Electric efficiencies based on LHV obtained from literature. 139
Table D-1: Default input values of the energy storage and energy converter units. 140
Table D-2: Output values of power plant configurations using default values. 140
Table D-3: Best-case input values of the energy storage and energy converter units. 145
Table D-4: Output values of power plant configurations using best-case values. 145
Table D-5: Worst-case input values of the energy storage and energy converter units. 146
Table D-6: Output values of power plant configurations using worst-case values. 146
Table E-1: Cabin and car requirements according to ferry operators. 156

© COPYRIGHT OF C-JOB, WHOSE PROPERTY, THIS DOCUMENT REMAINS. NO PART THEREOF MAY BE DISCLOSED, COPIED, DUPLICATED OR IN ANY OTHER WAY MADE USE OF EXCEPT WITH THE APPROVAL OF C-JOB.

Nomenclature

Roman variables

Variable	Description	Units
AM-REF	Ammonia reformer	
BC	Black carbon	
BoP	Balance of Plant	
CH_4	Methane	
CO_2	Carbon dioxide	
CoE	Cost of energy per day	USD/day
DNV GL	Det Norske Veritas Germanischer Lloyd	
DWT	Deadweight	ton
E	Energy (1 kWh = 3.6 MJ)	MJ
$E_{consumed}$	Consumed stored energy per day	GJ/day
EG	Electric generator	
EM	Electric motor	
$E_{net,el}$	Usable electrical energy per day	GJ/day
E_{stored}	Stored energy	GJ
FC	Fuel Cell	
Fn	Froude number ($v_s/\sqrt{g * L_{WL}}$)	-
GED	Gravimetric energy density (based on LHV)	GJ/ton
GHG	Greenhouse Gas	
GT	Gross tonnage	ton
H_2	Hydrogen	
ICE	Internal Cumbustion Engine	
IMO	International Maritime Organization	
LH2	Liquid Hydrogen	
LHV	Lower Heating Value of a fuel	MJ/kg
Li-air	Lithium air battery	
Li-ion	Lithium ion battery	
Li-S	Lithium sulfur battery	
LNG	Liquefied Natural Gas	
MCFC	Molten Carbonate Fuel Cell	
MCR	Maximum Continuous Rating	kW
NH_3	Ammonia	
NO_x	Nitrogen oxides ($NO+NO_2+N_2O$)	
NO	Nitric oxide	
N_2O	Nitrous oxide	
NO_2	Nitrogen dioxide	
P	Power	kW
pe_{CO_2eq}	CO_2 equivalent greenhouse gas emissions	g/kWh
PEMFC	Polymer Electrolyte Membrane Fuel Cell	
PM	Particulate matter	

© COPYRIGHT OF C-JOB, WHOSE PROPERTY, THIS DOCUMENT REMAINS. NO PART THEREOF MAY BE DISCLOSED, COPIED, DUPLICATED OR IN ANY OTHER WAY MADE USE OF EXCEPT WITH THE APPROVAL OF C-JOB.

$P_{net,el}$	Usable Electrical Power	kWe
PoE	Price of energy per GJ	USD/GJ
ppm	Parts Per Million	
PV	Photovoltaic	
ROPAX	Roll on/roll off passenger	
$S0_x$	Sulfur Oxides	
SOFC	Solid Oxide Fuel Cell	
spe	Specific pollutant emission	g/kWh
SPM	Specific mass	ton/MW
SPV	Specific volume	m^3/MW
Synthetic fuels	Hydrogen (H_2) and ammonia (NH_3)	
TRL	Technology Readiness Level	
VED	Volumetric energy density (based on LHV)	GJ/m^3
vol.%	Percentage of total volume	%
wt.%	Percentage of total weight	%

Greek variables

Variable	Description	Units
∇	Displacement	m^3
Δ	Difference	
ΔH	Lower heating value per mol	kJ/mol
η	Efficiency	
ρ	Density	kg/m^3

© COPYRIGHT OF C-JOB, WHOSE PROPERTY, THIS DOCUMENT REMAINS. NO PART THEREOF MAY BE DISCLOSED, COPIED, DUPLICATED OR IN ANY OTHER WAY MADE USE OF EXCEPT WITH THE APPROVAL OF C-JOB.

1 Introduction

The International Maritime Organization (IMO) issued on the 13th of April 2018 a press release titled: *"UN body adopts climate change strategy for shipping"*. [1] This document illustrates the commitment of the IMO to significantly reduce the emission of greenhouse gasses (GHG) from international shipping in coming decades. The vision of the IMO is to phase out the emission of GHGs as soon as possible within this century. The relevance of this is indicated by the fact that international shipping emits approximately 2.2 % of the total GHG worldwide in 2012, however it was not included in the Paris Agreement.

The goals set out in the previously mentioned press release imply the need to drastically reduce the emission of carbon dioxide, being the primary GHG emitted by ships, in the near future. These goals are defined as follows: [1]

1. ***carbon intensity of the ship to decline through implementation of further phases of the energy efficiency design index (EEDI) for new ships***
   to review with the aim to strengthen the energy efficiency design requirements for ships with the percentage improvement for each phase to be determined for each ship type, as appropriate;

2. ***carbon intensity of international shipping to decline***
   to reduce CO_2 emissions per transport work, as an average across international shipping, by at least 40% by 2030, pursuing efforts towards 70% by 2050, compared to 2008; and

3. ***GHG emissions from international shipping to peak and decline***
   to peak GHG emissions from international shipping as soon as possible and to reduce the total annual GHG emissions by at least 50% by 2050 compared to 2008 whilst pursuing efforts towards phasing them out as called for in the Vision as a point on a pathway of CO_2 emissions reduction consistent with the Paris Agreement temperature goals.

The use of liquified natural gas (LNG) as marine fuel is in recent studies, such as those performed by TNO, ECN and CE Delft [2] and IEA [3], considered to be a viable alternative to current marine fuels as MDO and HFO. This because there are large fields of natural gas available and the production cost of LNG is relatively low. This fuel is mainly composed of methane and is characterized by a high specific energy. The emission of carbon dioxide is reported to be reduced by up to 20 % when compared to conventional fuels. The use of LNG also considerably reduces the emission of particular matter (PM) and sulfur oxides (SO_X) making it highly attractive to be used in areas with strict emission regulation such as the Baltic Sea area. However, the use of LNG is not sufficient to reduce the GHG emissions to a level as specified in the objectives of the IMO as discussed above. Other measures are needed to meet these objectives.[4,5]

1.1 Problem description and research objective

The IMO has thus set the objective to drastically reduce the emission of greenhouse gasses in 2050 to only half the 2008 level. The GHG emission per ship is even required to decrease by 70 %. However what GHGs are important to be reduced and how is this possible? Is this feasible, both technologically as economically, to be achieved in 2050?

© COPYRIGHT OF C-JOB, WHOSE PROPERTY, THIS DOCUMENT REMAINS. NO PART THEREOF MAY BE DISCLOSED, COPIED, DUPLICATED OR IN ANY OTHER WAY MADE USE OF EXCEPT WITH THE APPROVAL OF C-JOB.

The International Council on Clean Transportation states that the main GHG emissions from ships are composed of four emissions, being: carbon dioxide (CO_2), methane (CH_4), black carbon (BC) and nitrous oxide (N_2O). These four emissions will therefore be considered during this thesis.

LNG is currently considered to be the least polluting fuel used in the maritime industry. However, using this fuel does not result in the desired GHG emission reduction in the year 2050 as is desired by the IMO. The use of other fuels and systems is required to achieve this reduction of GHGs in the future, resulting in a considerably different power plant design to be used on board future ships.

The objective of this thesis is therefore to come up with a power plant design emitting less greenhouse gasses than the quantities stated by the IMO. This solution should be economical and technological feasible in the year 2050. The feasibility of using such a power plant on board vessels will be illustrated by performing a case study for a representative ROPAX ferry to be built in 2050.

Considered power plant designs are reduced to basic sets of one type of energy carrier (e.g. a fuel) and one type of energy converter (e.g. an engine).

The above mentioned has resulted in the following main question:

What energy storage medium and energy converter will most likely be used on a representative ROPAX ferry with minimal greenhouse gas emission in 2050?

In order to come to a clear and substantiated answer of the main question, first the following sub-questions are to be answered:

1. *What requirements does the expected market of 2050 require the representative ROPAX ferry to have?*

Basic mission requirements of a representative ROPAX ferry to be built in 2050 are established by means of a market research.

2. *What power plant configuration, emitting minimal amounts of minimal greenhouse gasses, is expected to be the most economically and technologically feasible to be used on a ship in 2050?*

The economic and technologic feasibility of power plant configurations is assessed by evaluating their performance based on multiple evaluation characteristics considered to be important when designing ships.

3. *How does the selected power plant configuration affect the design of the representative ROPAX ferry compared to current LNG-fueled ferries?*

To illustrate the practical feasibility of using the established power plant configuration, a proof of concept is provided and directly compared to a present-day LNG-fueled ferry of similar size.

© COPYRIGHT OF C-JOB, WHOSE PROPERTY, THIS DOCUMENT REMAINS. NO PART THEREOF MAY BE DISCLOSED, COPIED, DUPLICATED OR IN ANY OTHER WAY MADE USE OF EXCEPT WITH THE APPROVAL OF C-JOB.

1.2 Report Structure

This report has started with an introduction to the problem, followed by the definition of the research objective and an overview of the reports structure.

Chapter 2 presents the outcome of a market research in the first section. This market research is performed to establish a basic set of characteristics, considered to be representative for a ROPAX ferry to be constructed in 2050. These vessel characteristics provide the bases for the operational requirements of the considered power plants in the remainder of this thesis and are simultaneously the answer to the first sub-question. Sections two, three and four of this chapter provide an overview of the considered energy storage media, energy converter units and the resulting simplified power plant configurations, respectively.

Chapter 3 begins with discussing the power plant characteristics which are assessed during the performance evaluation of each power plant. The calculation method of each characteristic is also provided in the first section. Since the price of the energy is found to be of great significance, the second section of this chapter discusses how the price of each source of energy is determined. Each energy source will be defined by a default, minimum and maximum price per unit energy. Default minimum and maximum values of the energy storage and energy converter characteristics are provided in, respectively, sections 3.3 and 3.4. This chapter ends with a summary.

The fourth chapter describes the selection process used to establish the most technologically, practically and economically feasible combination of energy storage medium and energy converter, referred to as a power plant configuration. The first section provides an initial assessment of the power plant configurations by solely using default values of characteristics as established in the third chapter. Several power plant configuration are discarded based on this assessment. Remaining power plant configurations are assessed based on the results of a sensitivity analysis performed in the second section. The last remaining power plant configurations are individually evaluated in the third section to establish a single most feasible configuration to be used onboard a 2050 representative ROPAX ferry. Conclusions following these sections are summarized in section 4.4, coming to a final answer to the second sub-question.

Chapter 5 provides a proof of concept for the use of the power plant established in chapter 4 on board a representative ROPAX ferry built in the year 2050 and therefore answers the last sub-question. Section 5.1 describes additional design requirements following from the passenger and power plant requirements. Additionally, safety concerns and differences with modern LNG-fueled ferries are discussed in sections 5.2 and 5.3, respectively. Section 5.5 describes notable fuel saving measures that are considered beyond the scope of this thesis but are considered to be highly feasible to be used on board this type of ferry. A summary of the findings is given in the summary at the end of this chapter.

This thesis is concluded in the last chapter in which also recommendations for future research are given.

© COPYRIGHT OF C-JOB, WHOSE PROPERTY, THIS DOCUMENT REMAINS. NO PART THEREOF MAY BE DISCLOSED, COPIED, DUPLICATED OR IN ANY OTHER WAY MADE USE OF EXCEPT WITH THE APPROVAL OF C-JOB.

2 Representative characteristics & power plant configurations

Before a feasible concept design for a ROPAX ferry to be constructed in 2050 can be delivered, clear boundaries and requirements are necessary. This ROPAX ferry of 2050 is required to have minimal greenhouse gas (GHG) emissions and should be able to carry hundreds of passengers and cars (100 – 2000 passengers and 100 – 1000 cars). To emit minimal amounts of greenhouse gasses alternative energy sources are considered. Using these initial requirements of the ferry, a set of representative characteristics is composed. These characteristics are determined in section 2.1 by means of a market research and will form a basis for the concept design of the ferry in chapter 5. Furthermore, section 2.2 describes which energy carriers will be considered. Section 2.3 will provide an overview of the different energy converters that are considered for the power plant configurations. Power plant configurations, evaluated in chapter 4, are composed by using the energy carriers and energy converters discussed in sections 2.2 and 2.3. These power plant configurations are described in section 2.4 of this chapter.

2.1 Characteristics of a representative ROPAX ferry

The initial description of this thesis mentions several basic requirements for the ROPAX ferry. The ferry must be able to transport at least several hundred passengers and cars. It is also required to operate outside territorial waters, meaning it should be able to sail in open seas and not only in coastal and inland waters. The expected characteristics of a representative ROPAX ferry build in 2050 are determined by means of a market research. This market research is performed by using an internal database of existing vessels available for employees of C-Job Naval Architects. This database is used to obtain trends concerning characteristics and age of ROPAX ferries build worldwide from 1960 till 2015. Because of the predefined requirements, several boundaries are implemented before determining trends. Only ferries that can carry at least a hundred passengers and a hundred cars are taken into account. Furthermore, only ferries capable of sailing in international waters are selected.

The remaining data is used to first establish an expected service life of a ROPAX ferry. Based on this expected lifetime, a selection of ferries is composed which will most probably be at the end of their service life in 2050. This selection is then used to determine a representative area of operation, passenger and car carrying capacity for a representative ferry of this selection. Trends concerning passenger and car carrying capacity of ferries build from 1960 till 2015 are determined using the database. These trends and the characteristics of the representative ferry are used to establish an expected set of requirements for a representative ferry build in 2050. These trends are considered to continue in the future and therefore do not account for any major changes in the requirements on a ferry for a given route.

The database is subsequently used to obtain correlations between the afore determined requirements of a representative ferry and its main dimensions, power requirements, energy requirements and service speed. These correlations are then used to estimate corresponding characteristics of the representative ferry build in 2050. These characteristics are used to determine power plant requirements in terms of output power and usable energy, used for the design of different power plant configurations in chapter 4.

© COPYRIGHT OF C-JOB, WHOSE PROPERTY, THIS DOCUMENT REMAINS. NO PART THEREOF MAY BE DISCLOSED, COPIED, DUPLICATED OR IN ANY OTHER WAY MADE USE OF EXCEPT WITH THE APPROVAL OF C-JOB.

First, the expected lifetime of a ROPAX ferry is established by evaluating the current status of the existing vessels and their year of construction. This results in Figure 2-1 show the percentage of vessels that have been scrapped or is in service per year of construction. From this graph it can be argued that most vessels are scrapped after 30 – 45 years of service. For this reason, the expected service life of a ROPAX ferry is established to be approximately 40 years. This means that a ROPAX ferry build in 2050 will probably replace ferries that were built around the year 2010. Ferries build between 2005 and 2015 are therefore selected to determine a representative area of operation, passenger and car carrying capacity for a representative ferry build in this period.

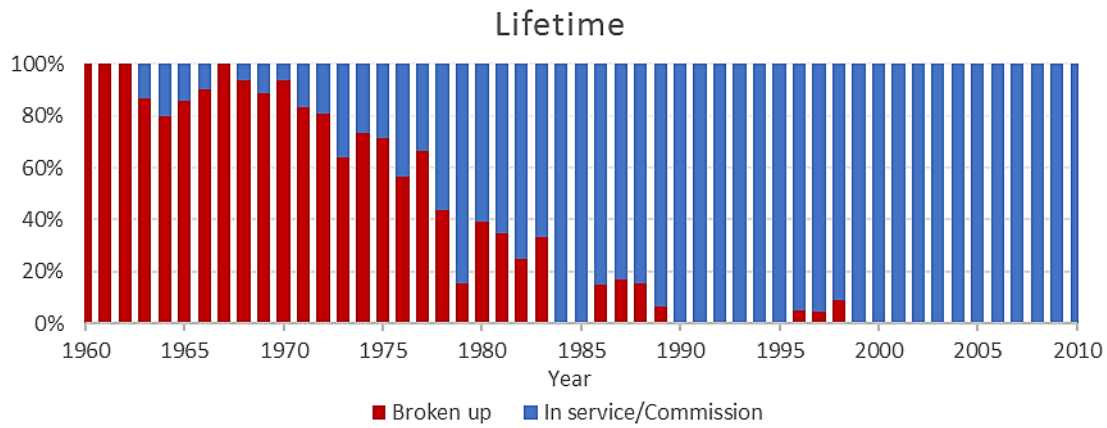

Figure 2-1: Status of vessels constructed from 1960-2010. [6]

According to this database, a total of 103 ferries have been built between 2005 and 2015. 27 of these ferries are currently operating in the Mediterranean Sea. Furthermore, 24 of these ferries operate in the Baltic Sea and 18 in the Yellow Sea. This is shown in Figure 2-2. After close examination of this selection of vessels, it appears that many vessels operating in the Mediterranean Sea have great similarities with vessels operating in the Baltic Sea. Several vessels sailing in the Mediterranean Sea even have sister ships operating in the Baltic Sea. For this reason, the Mediterranean and Baltic Sea are chosen as representative areas of operation.

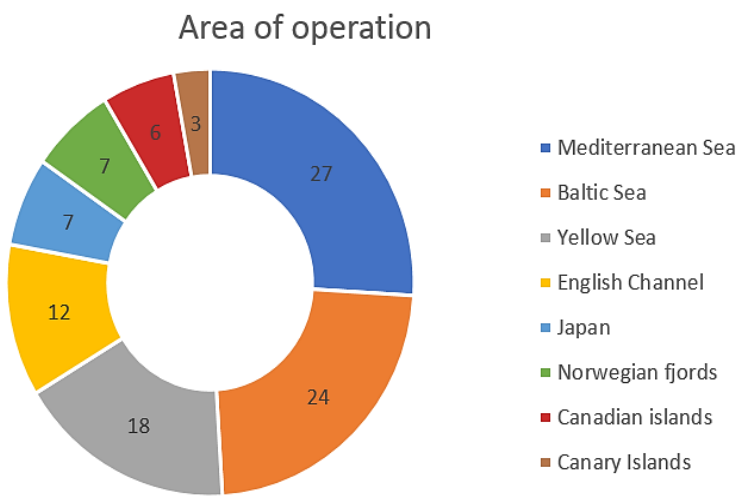

Figure 2-2: Area of operation of vessels build between 2005 and 2015. [6]

© COPYRIGHT OF C-JOB, WHOSE PROPERTY, THIS DOCUMENT REMAINS. NO PART THEREOF MAY BE DISCLOSED, COPIED, DUPLICATED OR IN ANY OTHER WAY MADE USE OF EXCEPT WITH THE APPROVAL OF C-JOB.

Using data of ferries build between 2005 and 2015, representative passenger and car carrying capacities are determined. These capacities are shown in Figure 2-3 per ferry. A cluster of very similar ferries, in terms of passenger and car capacity, is visible in this figure. These ferries are capable of transporting approximately 400 cars and 950 passengers. Because of the existence of this cluster and the fact that many of the ferries within this cluster are sailing in the Mediterranean of Baltic Sea, are afore mentioned car and passenger capacity considered to be representative for ferries build between 2005 and 2015. This is therefore also considered to be representative for ferries that will most probably be replaced in 2050.

From AIS data it appears that over half of the ferries within this cluster sail two trips per 24 hours with each trip having a distance of 150 to 200 miles. This is even more valid for vessels operating in the Mediterranean and Baltic Sea. Two-thirds of these vessels sail two trips a day. This dominating operational profile of ROPAX ferries is therefore regarded as representative operational profile for the representative ferry to be constructed in 2050.

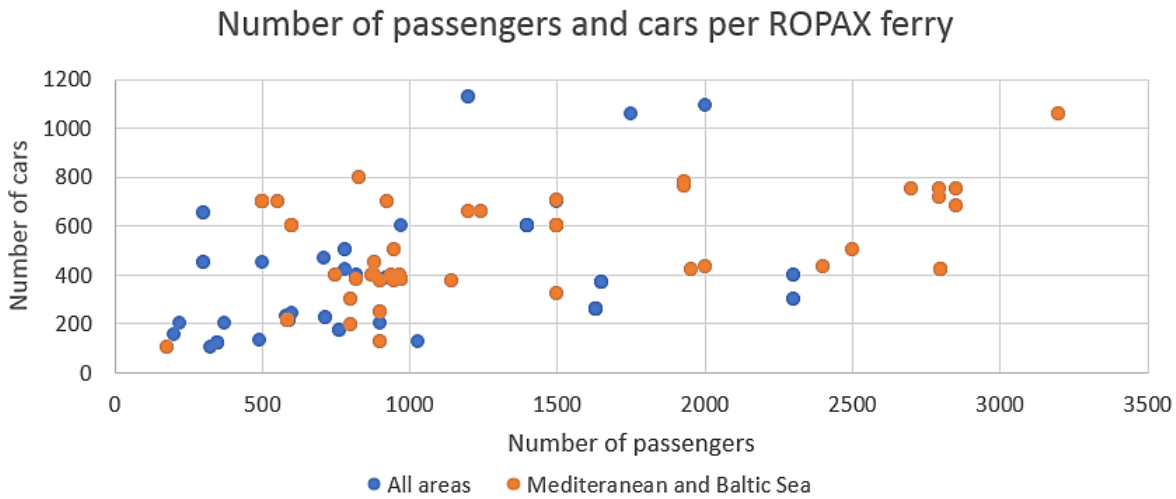

Figure 2-3: Passenger and car capacity of ROPAX ferries build between 2005 and 2015. [6]

Average car carrying capacity of ferries has increased almost linearly in the past 50 years (from ± 200 cars in the 1960s to over 400 cars in the beginning of the 21st century) according to Figure 2-5 and is expected to increase further in the future, as is shown in Figure A-1. From Figure 2-4 it appears that the number of passengers per vessel has been slowly increasing in the last decades, but with relatively large fluctuations. Figure 2-6 indicates a slowly converging passenger/car ratio over the last decades. This ratio seems to converge to approximately 2.5, shown in Figure A-2, which is coincidentally equal to the ratio of the series of ferries which are most likely to be replaced in 2050.

Taking the converging car/passenger ratio and the linear increase of car capacity over the period 1960 – 2010 into account, it is considered to be reasonable to assume that a representative ROPAX ferry of 2050 will be able to transport approximately 600 cars and 1500 passengers.

© COPYRIGHT OF C-JOB, WHOSE PROPERTY, THIS DOCUMENT REMAINS. NO PART THEREOF MAY BE DISCLOSED, COPIED, DUPLICATED OR IN ANY OTHER WAY MADE USE OF EXCEPT WITH THE APPROVAL OF C-JOB.

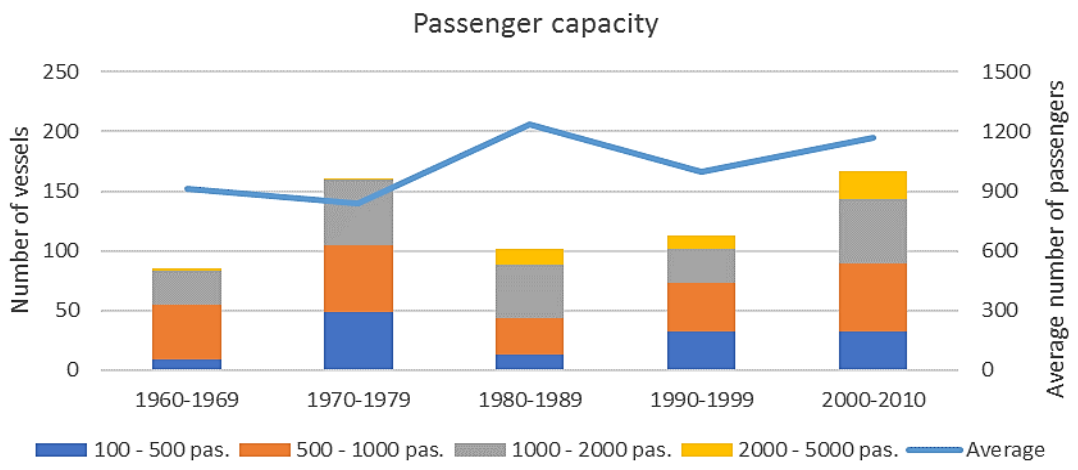

Figure 2-4: Number of vessels build per passenger capacity per decade. [6]

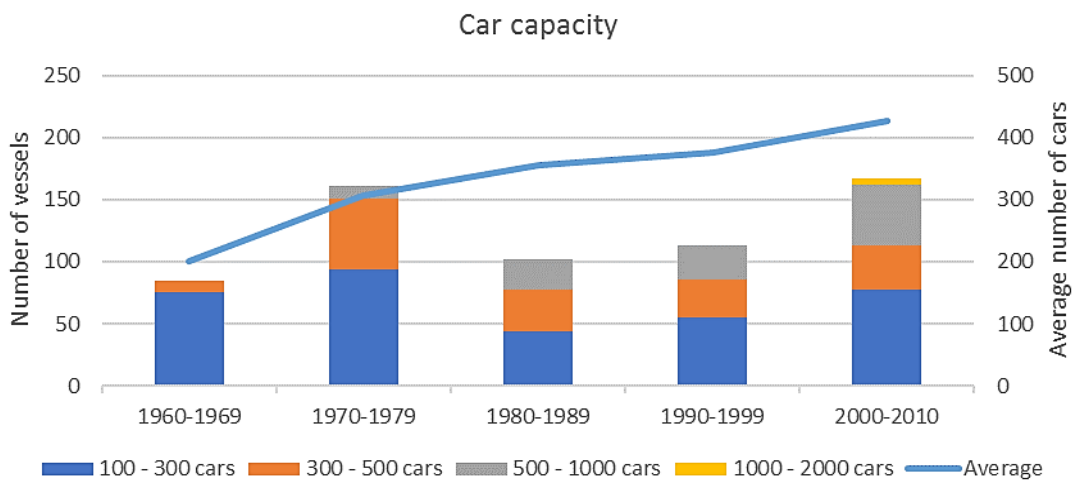

Figure 2-5: Number of vessels build per car capacity per decade. [6]

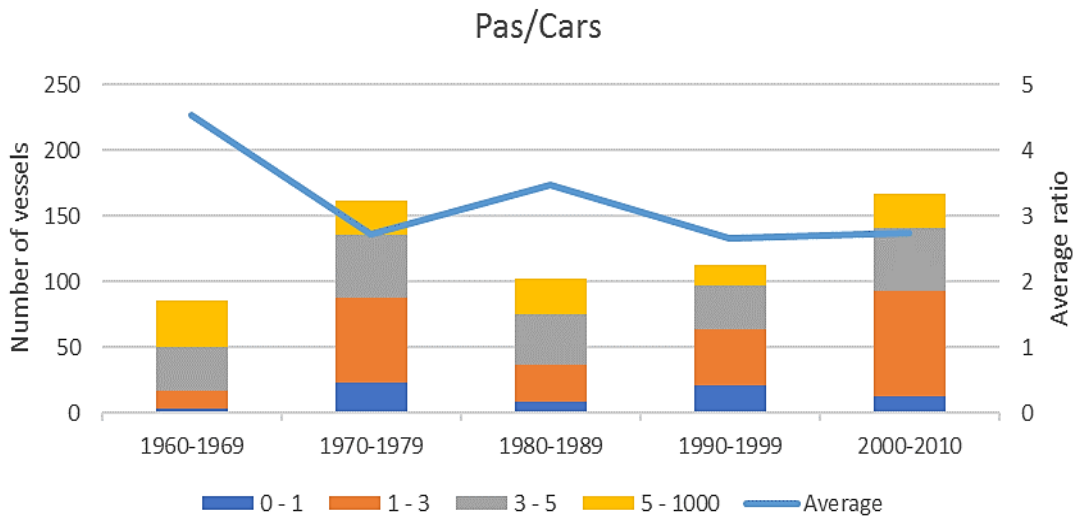

Figure 2-6: Passenger/car ratio per decade. [6]

© COPYRIGHT OF C-JOB, WHOSE PROPERTY, THIS DOCUMENT REMAINS. NO PART THEREOF MAY BE DISCLOSED, COPIED, DUPLICATED OR IN ANY OTHER WAY MADE USE OF EXCEPT WITH THE APPROVAL OF C-JOB.

Using the afore mentioned internal database, the required number of beds is estimated based on the maximum passenger capacity. This is plotted in Figure A-3 and reveals a representative value of 0.8 beds per passenger, resulting in 1200 beds on board the representative ROPAX ferry of 2050.
The fact that there are less beds than the maximum passenger capacity can be explained by the fact that a ferry rarely transports its maximum number of passengers. Reducing the number of beds results in less cabins (on average there are 3 beds per cabin [6]) and therefore in a somewhat smaller vessel. This saves money during construction and operation of the vessel. Approximately 400 cabins will be present on a representative ferry with given passenger and car capacity.

A frequently used way of increasing the passenger capacity for peak periods is the use of airplane-type seats as sleeping facility. These require far less space compared to full cabins while providing a place to sleep. [7]

Given the afore determined estimated capacity of a representative ferry of 2050, main dimensions and speed of such a ferry can be estimated. From the data, it appears that the vast majority of the ROPAX ferries have a design service speed between Froude number 0.2 and 0.4, as shown in Figure A-4 and Figure A-5. Considering vessels build between 2005 and 2015, the governing velocity is at Froude numbers of around 0.3 (see Figure 2-7). It is therefore determined that a representative design speed is equal to approximately Fn = 0.3.

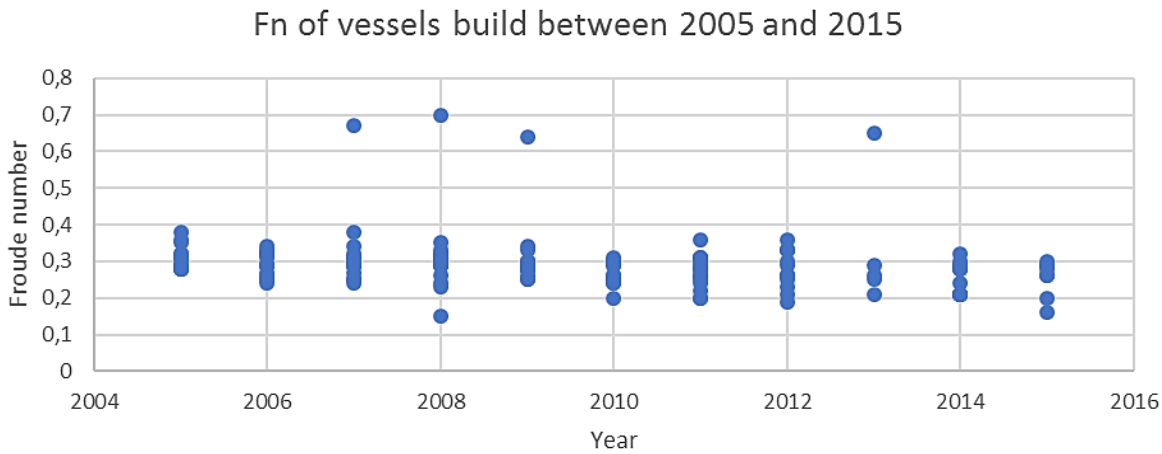

Figure 2-7: Froude number of ROPAX ferries build between 2005 and 2015. [6]

Because this Froude number is lower than 0.4, the main source of resistance is frictional resistance. Given this fact, it can be justifiably assumed that the use of a multihull will not provide any beneficial affect with respect to the resistance. Multihulls are characterized by a higher frictional resistance given the same displacement and dimensionless velocity (Fn) which increases the fuel consumption [8], [9]. Vessels shown in Figure 2-7 operating at Fn > 0.5 are exclusively multihull vessels. For this reason, a monohull is considered to be a representative hull configuration for a ROPAX ferry of 2050.

Port limits of ports in the Baltic and Mediterranean Sea impose limitations on maximum measurements of vessels and therefore also on ROPAX ferries. Current limitations are taken into account when designing the representative ROPAX ferry of 2050. After consulting internal sources, it becomes clear that ports, currently used by ROPAX ferries of afore mentioned capacities, require vessels to have a draft of less than 9 meters. Length and breadth limitations of these ports do not impose problems, because current vessels do not come close to these limitations. [6]

© COPYRIGHT OF C-JOB, WHOSE PROPERTY, THIS DOCUMENT REMAINS. NO PART THEREOF MAY BE DISCLOSED, COPIED, DUPLICATED OR IN ANY OTHER WAY MADE USE OF EXCEPT WITH THE APPROVAL OF C-JOB.

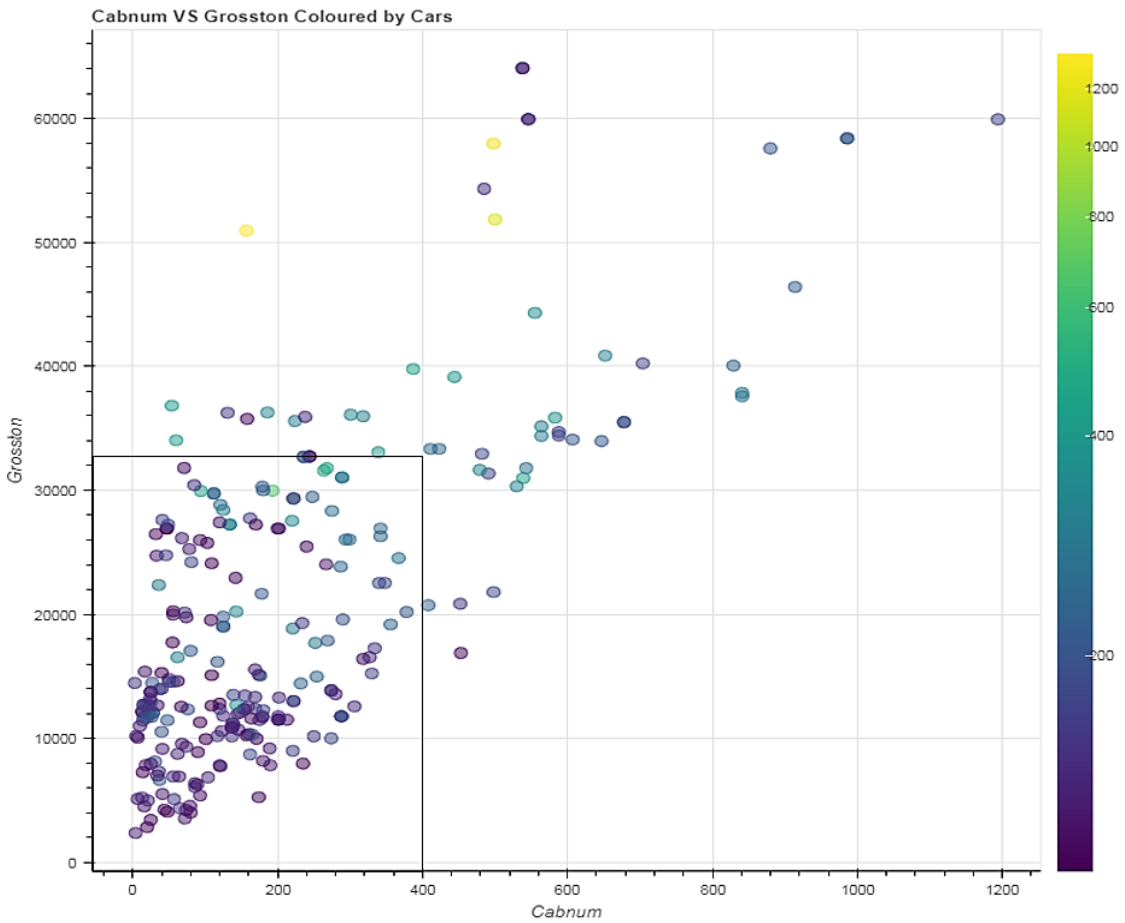

Figure 2-8: Gross tonnage of ROPAX ferries as function of the number of cabins and cars. [6]

Given a capacity of 1 500 passengers and 600 cars, in combination with 400 cabins and a service speed of Fn = 0.3, the gross tonnage (GT) of the ROPAX ferry can be estimated. Figure 2-8, obtained from the internal database, shows the GT of vessels as function of the number of cabins and the car carrying capacity. The number of cabins and the number of cars influence the GT of a vessel because they both require a certain amount of space and the GT is by definition a function of the enclosed space of a vessel. [10] From Figure 2-8 follows that a vessel with approximately 400 cabins and 600 cars has a GT of approximately 33 000 ton. A gross tonnage of 33 000 ton is by definition equal to 110 000 m^3 enclosed volume.[1]

Required engine power and expected displacement are determined by using similar graphs which are found in appendix A (Figure A-6 – Figure A-16). Resulting from these graphs are an expected displacement of 18 000 m^3 (Figure A-7) and an MCR of 28 000 kW (Figure A-8). Based on the displacement, number of cabins and car carrying capacity (Figure A-10 and Figure A-11), a deadweight (DWT) of 6 000 ton is estimated. Figure A-12 indicates that ROPAX ferries with a GT above 20 000 ton are equipped with two propellers and a bulbous bow. Figure A-13 – Figure A-16 are provide an indication of the length between perpendiculars, molded breadth, draft and length overall, which are 170 m, 26 m, 6.2 m and 185 m, respectively.

[1] The International Convention on Tonnage Measurement of Ships defines gross tonnage by the formula GT = K_1V, where V is the total volume of all enclosed spaces in the ship in cubic meters and K_1 is a constant calculated by $K_1 = 0.2 + 0.02 \log_{10} V$. [10]

© COPYRIGHT OF C-JOB, WHOSE PROPERTY, THIS DOCUMENT REMAINS. NO PART THEREOF MAY BE DISCLOSED, COPIED, DUPLICATED OR IN ANY OTHER WAY MADE USE OF EXCEPT WITH THE APPROVAL OF C-JOB.

From internal sources it appears that a representative refueling interval of similar sized ferries is equal to once a week. However, the maximum stored fuel on board such a vessel is on average sufficient to operate for 14 days. A representative fuel capacity for this size of ferry is therefore approximately 900 m^3 HFO. [6] Using this fuel capacity, theoretical maximum refueling interval and fuel characteristics (ρ_{HFO} = 1010 kg/m^3, specific energy = 40.5 MJ/kg) an average energy consumption is estimated to be equal to 2.6 TJ/day.

In conclusion, a representative ferry to be built in 2050 has the following parameters:

- monohull
- 1500 passengers
- 600 cars
- 1200 beds in 400 cabins
- service speed Fn = 0.3
- 18 000 m^3 displacement
- 28 000 kW MCR
- 33 000 ton GT (equal to 110 000 m^3 enclosed volume)
- 6 000 ton DWT
- 170 m length between perpendiculars
- 185 m length over all
- 26 m molded breadth
- 6.2 m draft
- 2 propellers
- bulbous bow
- two trips per 24 hours
- 150 – 200 miles per trip
- 2.6 TJ/day fuel consumption

© COPYRIGHT OF C-JOB, WHOSE PROPERTY, THIS DOCUMENT REMAINS. NO PART THEREOF MAY BE DISCLOSED, COPIED, DUPLICATED OR IN ANY OTHER WAY MADE USE OF EXCEPT WITH THE APPROVAL OF C-JOB.

2.2 Energy carriers

Minimization of greenhouse gas emissions is one of the most important requirements for the representative ferry of 2050. Greenhouse gasses considered are carbon dioxide (CO_2), methane (CH_4) and nitrous oxide (N_2O). These are the three main greenhouse gasses contributing to the enhanced greenhouse effect according to the in 2013 published Fifth Assessment Report of the Intergovernmental Panel on Climate Change (IPCC) [11]. GHGs emitted by the shipping industry are also dominated by CO_2, CH_4 and N_2O emissions, but also by black carbon or soot (BC) as can be seen in Figure 2-9 . BC emissions will therefore also be taken into. These emissions are typically measured as part of the particular matter (PM) emissions of an engine. [12]

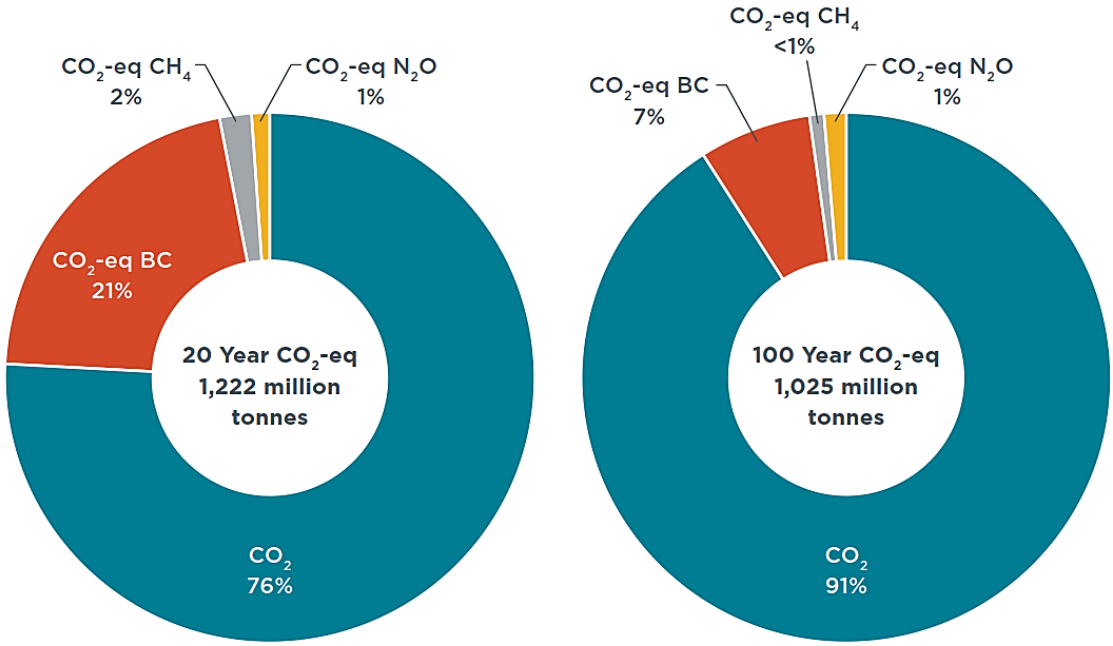

Figure 2-9: Total shipping CO_2 equivalent GHG emissions, 20-year and 100-year Global Warming potential. [12]

Special emphasis will be put on the minimization of carbon related emissions, because these amount to over 80 % of the total global radiative forcing [11]. IPCCs Fifth Assessment Report (2013) describes radiative forcing as:

Radiative forcing (RF) is a concept used for quantitative comparisons of the strength of different human and natural agents in causing climate change. Positive RFs lead to a global mean surface warming and negative RFs to a global mean surface cooling. [13]

Carbon related emissions originate from burning carbon containing fuels (such as fossil fuels, biomass and biofuels) and these are therefore not considered as energy carrier for a ferry of 2050.

SO_X emissions are not considered to be a greenhouse gas and are therefore not included in the consideration. These emissions do not contribute to the enhanced greenhouse effect but do cause acid rain damaging nature. This is the reason, legislation limiting the amount of SO_X emitted by ships exists in various areas named Sulphur Emission Control Areas or SECAs. Examples of such areas are the Baltic Sea and North Sea. [14]

NO_X emissions are composed of nitric oxide (NO), nitrogen dioxide (NO_2) and nitrous oxide (N_2O). Although IMO legislation limits the maximum amount of total NO_X, only N_2O emissions, when emitted from ships, contribute to global warming. This is the reason why only N_2O emissions are displayed in

© COPYRIGHT OF C-JOB, WHOSE PROPERTY, THIS DOCUMENT REMAINS. NO PART THEREOF MAY BE DISCLOSED, COPIED, DUPLICATED OR IN ANY OTHER WAY MADE USE OF EXCEPT WITH THE APPROVAL OF C-JOB.

Figure 2-9. The amount of N_2O emitted is in general only a few percent of the total NO_X emissions which will be taken into account in the remainder of the thesis. However, emissions from engines are generally documented as NO_X and this definition will therefore also be used during this thesis. [11-14]

A special case is LNG. This fuel is not considered a solution to reduce GHG emissions but is used as reference energy carrier. This fossil fuel is in recent studies, such as those performed by TNO, ECN and CE Delft [2] and IEA [3], considered to be a viable alternative to current marine fuels as MDO and HFO. This because there are large fields of natural gas available and the relatively low production cost of LNG. LNG is already used in marine applications, an example of this is the Viking Grace which is an LNG powered ROPAX ferry operating in the Baltic Sea. PM and SO_x emissions are greatly reduced, and NO_x emissions are also slightly reduced when MDO is replaced by LNG. Reduction of SO_x emissions is currently the main reason operators use LNG. This fuel does not require scrubbers to comply with modern regulation in Sulphur Emission Control Areas (SECAs) due to its neglectable (0.004 wt.%) sulfur content. PM emissions are negligible when using LNG. CO_2 emissions are reduced because of the higher specific energy of LNG compared to e.g. MDO (49 MJ/kg and 42 MJ/kg respectively) resulting in a lower fuel consumption. However, methane emissions are currently increased when using LNG because of methane slip. Methane has a higher global warming potential than CO_2 [15] which currently nullifies much of the positive effect of reduced CO_2 production. LNG has the potential to reduce GHG emissions by up to 20 %, if methane emissions can be reduced. This fuel is stored in cryogen tanks at -162 °C, therefore resulting in a relatively big and heavy storage tank. [4,5,14]

Table 2-1: LNG key characteristics. [2,16]

	DENSITY [KG/M³]	STORAGE PRESSURE [BAR]	STORAGE TEMPERATURE [°C]	SPECIFIC ENERGY [MJ/KG]	ENERGY DENSITY [MJ/L]
LNG	456	Ambient	-162	49	22.3

Subsection 2.2.1 will address carbon free energy sources that are not considered and the reason why these are not considered. Energy carriers that will be considered are hydrogen, ammonia and batteries. Every considered energy carrier, the reason for the energy carrier and its general characteristics are described in subsections 2.2.2, 2.2.3 and 2.2.4. Both mass and volume are important parameters when designing a vessel, because it greatly affects its carrying capacity and performance. Key characteristics of energy carriers are therefore indicated.

Specific energy represents the amount of energy stored per unit mass of an energy storage medium and can therefore be taken as a rough indicator for the mass of the total energy storage.

Energy density is representative for the amount of energy stored in per unit volume given a certain energy carrier and is therefore characteristic for the volume of the energy storage system.

Storage conditions are included because these could impose the need for additional systems, such as a cooling unit, to keep the energy carrier in its intended state.

This section will be concluded with an overview of the considered energy carriers.

© COPYRIGHT OF C-JOB, WHOSE PROPERTY, THIS DOCUMENT REMAINS. NO PART THEREOF MAY BE DISCLOSED, COPIED, DUPLICATED OR IN ANY OTHER WAY MADE USE OF EXCEPT WITH THE APPROVAL OF C-JOB.

2.2.1 Not considered carbon free energy sources

Apart from the carbon containing energy carriers, several carbon-free sources are also considered not applicable for a representative ferry in 2050. The most important sources of energy, according to the International Energy Agency (IEA), [17] are discussed in this subsection. These sources of energy are nuclear power, wind energy and solar energy. The reason why these are not taken into account will be discussed per source.

Nuclear power

The reason why nuclear power is not considered an option is because of the strong public opposition towards this source of energy. Nuclear energy results in hazardous radioactive nuclear waste which will be around for many centuries which is not considered to be desirable. Massive areas will become inhabitable in the event of an accident, which also could result in the deaths of thousands of people per accident. [18]

Wind energy

Wind energy is regarded as one of the most feasible sources of 'green' energy in the near future because of the global abundance of wind, especially at sea. Although wind energy is a growing source of renewable energy, it is considered not feasible to use wind energy as primary source of energy on a ROPAX ferry in 2050. This because of the following reasons:

- Wind energy requires large (dynamic) components with a high center of gravity and considerable weight. This is not beneficial for the stability of the ferry and could impose problems during the concept design stage.
    - Sails have a large area and could therefore impose a large side force, which could result in a considerable heeling moment due to the large heeling arm.
    - Flettner rotors are smooth vertical cylinders which are rotating and by doing so generate a lift force. This effect is also known as the Magnus-effect. This device is capable of significantly reducing the fuel consumption on board a vessel but is not suited as primary source of energy or energy converter. [19]
    - A kite is considered an instable and unpredictable method of utilizing wind energy and is therefore not widely accepted in the shipping industry. Ships sailing at speeds over 17 knots (as will be the case for the representative ferry of 2050) are not suitable for this technology because the efficiency of the system decreases as the ship speed increases. [20]
    - A wind turbine on the deck could serve as a source of electric energy, which can be used for propulsion or hotel services. However, both vertical [21] and horizontal [22] axis wind turbines are relatively heavy and tall, which again decreases the stability of the vessel. Wind turbines also impose considerable drag and heeling forces, negatively influencing the performance of the vessel.
- Heeling of a ROPAX ferry during transit is considered a big issue because of passenger comfort.
- Wind conditions are inconsistent, resulting in considerable uncertainties regarding the amount of propulsive power a wind-based system is able to generate at a given time and location. A ferry is bound to a timetable, requiring a predictable traveling time which cannot be guaranteed when using wind energy as primary source of energy.

© COPYRIGHT OF C-JOB, WHOSE PROPERTY, THIS DOCUMENT REMAINS. NO PART THEREOF MAY BE DISCLOSED, COPIED, DUPLICATED OR IN ANY OTHER WAY MADE USE OF EXCEPT WITH THE APPROVAL OF C-JOB.

Solar energy

The use of solar energy has increased considerably in recent years and it is expected to become the number one source of renewable energy in the near future [23]. However, this source of energy requires a very large area to produce enough energy to supply the ROPAX ferry with enough energy to operate. The following case is used to provide a very rough estimate of the required size of such a system on a ferry.

A fuel consumption of 50 tons of LNG per day is obtained from Viking Line [24]. This is equal to an energy consumption of approximately 2.4 TJ/day. Given the fact that 1 kWh is equal to 3.6 MJ, a total of $6.6*10^5$ kWh is required per day. From Figure 2-10, a solar irradiance[2] of 6 kWh/m^2/day is assumed for the Mediterranean Sea. This means that a total of $1.1*10^5$ m^2 of solar panels is required to propel the vessel, if all solar energy is converted to electric energy. The Viking Grace has a length overall of 218 m and a breadth of 31.8 m which results in a total top area of 218 * 31.8 ≈ $6.9*10^3$ m^2. This is just over 6 % of the total required area. When taking into account that this calculated top area is the surrounding square area of the vessel and therefore overestimates the deck area and the system efficiency is far less than 100 % (current system efficiencies are typically 15 % [25-27]), it can be assumed that this source of energy will never be enough to supply the whole vessel with energy. For this reason, this source of energy is not regarded as primary source of energy.

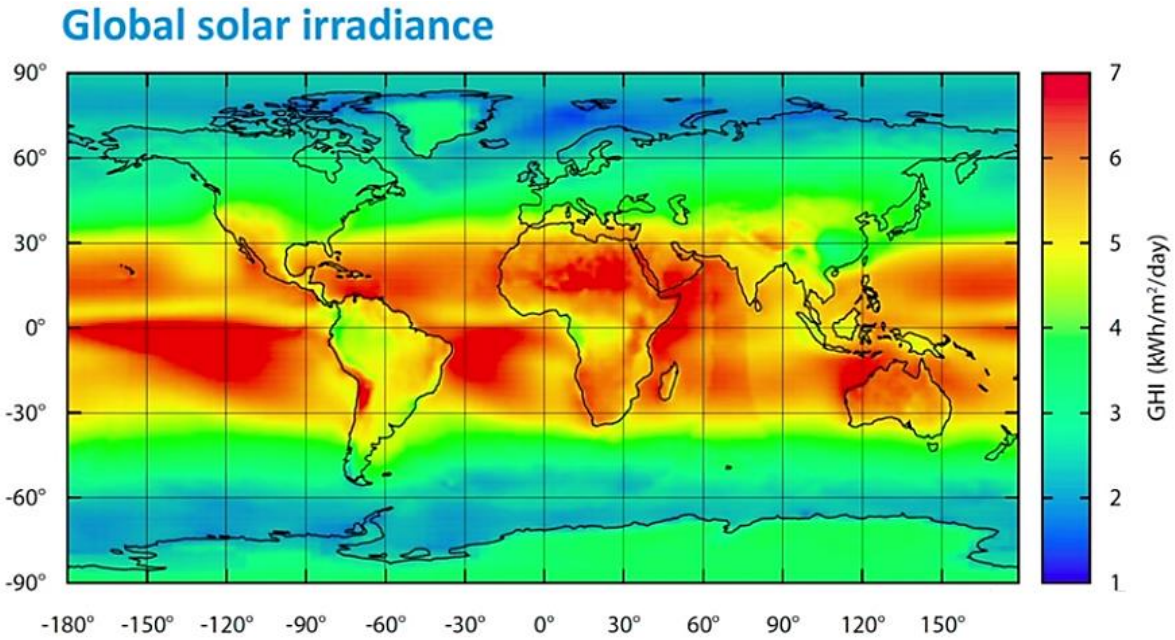

Figure 2-10: Global solar irradiance in kWh/m^2/day. [26]

[2] Solar irradiance is the solar radiation energy per unit area per unit time.

© COPYRIGHT OF C-JOB, WHOSE PROPERTY, THIS DOCUMENT REMAINS. NO PART THEREOF MAY BE DISCLOSED, COPIED, DUPLICATED OR IN ANY OTHER WAY MADE USE OF EXCEPT WITH THE APPROVAL OF C-JOB.

2.2.2 Hydrogen (H_2)

Many governments, including those of the USA, Japan, Germany and Denmark, actively investigate and subsidize research for the use of hydrogen as clean fuel of the future and are aiming at a so-called 'hydrogen economy'. The fact that hydrogen has a high specific energy density (LHV) of 120 MJ/kg is considered to be a great advantage. Hydrogen is therefore considered to be a significant source of energy in future mobile applications. It can already be produced without any GHG emissions by means of electrolysis using renewable energy resources, although this form of production is currently not economically feasible [28]. Hydrogen can be stored in many ways, but the most technological feasible and currently used are pressurized and liquified hydrogen (LH_2). Typical storage pressures of hydrogen are 350 bar and 700 bar. This type of hydrogen storage is considered the most mature storage method for the moment, but it requires a large volume (energy density of pressurized hydrogen is 2.64 MJ/L and 4.08 MJ/L for respectively 350 and 700 bar) and part of the energy is lost during pressurization of the hydrogen gas. Further research is required before this method can be used in commercial applications. Cryogenic liquid hydrogen storage is also possible using current technology. This form of storage has a high volumetric energy density (8.50 MJ/L) compared to compressed hydrogen as can be seen in Table 2-2. Despite these positive characteristics several serious drawbacks limit the use of this form of storage. Up to 40 % of the energy is lost during the liquefying process and boil-off also imposes efficiency losses. [29,30]

Other methods used for on-board hydrogen storage are known, but many of these require much more research before it can be applied on commercial scale. Chemical and physical storage methods make use of different materials to store the hydrogen. Examples of these kind of storage materials are: carbon nanotubes, metal glasses, lithium nitrides, complex hydrides and liquid organic hydrogen carriers (LOHC). Many of these materials require a large amount of research and development (most of them are currently not passed TRL 3[3]) and are therefore not considered to be applicable for large scale commercial use in 2050 and are therefore not considered in this thesis. This decision was made based on mutual consent after discussing this with the company supervisor. [29-32]

Pure hydrogen will be considered as possible fuel for ROPAX ferries in 2050. Two storage methods of pure hydrogen are considered, namely pressurized hydrogen (at 350 bar and at 700 bar) and liquified hydrogen (at -253 °C).

Only NO_X emissions are possible when using hydrogen as fuel, meaning that the emission of CO_2, CH_4 and PM can be neglected. This is due to the fact that hydrogen does not contain carbon. [14]

Table 2-2: Hydrogen key characteristics. [29,33]

	DENSITY [KG/M³]	STORAGE PRESSURE [BAR]	STORAGE TEMPERATURE [°C]	SPECIFIC ENERGY [MJ/KG]	ENERGY DENSITY [MJ/L]
LH_2	70.8	Ambient	-253	120	8.50
H_2 (350 BAR)	22	350	Ambient	120	2.64
H_2 (700 BAR)	37	700	Ambient	120	4.50

[3] Technology Readiness Levels (TRL) is a measure used to assess the maturity level of a certain technology. TRL 3 indicates a successful analytical and experimental proof-of-concept. See appendix B for more information and an overview of all Technology Readiness Levels according to NASA. [32]

© COPYRIGHT OF C-JOB, WHOSE PROPERTY, THIS DOCUMENT REMAINS. NO PART THEREOF MAY BE DISCLOSED, COPIED, DUPLICATED OR IN ANY OTHER WAY MADE USE OF EXCEPT WITH THE APPROVAL OF C-JOB.

2.2.3 Ammonia (NH_3)

Another chemical compound frequently considered a viable fuel for the future is liquid anhydrous ammonia. This can be produced from hydrogen and nitrogen and has a higher volumetric H_2 density than compressed or liquified hydrogen, as can be seen in Figure 2-11.

Ammonia can directly be used as fuel without any carbon related GHG hydrogen carrier (17.6 wt.% H_2, 105 kg H_2 per m^3). Decomposing ammonia into hydrogen and nitrogen can be done by using a catalyst or at high temperatures (over 300 °C). Other advantages of ammonia are the possibility to store it as a liquid at relatively mild conditions (-33 °C or 10 bar) and the already existing large annual global production ($140*10^6$ tons in 2016 [34]). However, there are also downsides to this chemical compound. This compound is hazardous to life above certain concentrations because it attacks the skin and lungs/respiratory system. This could impact the public acceptance of ammonia as fuel. However, most humans detect ammonia's odor at concentrations of approximately 20 ppm and ammonia levels above 35 ppm are considered immediately dangerous to life and health. [35-38]

Ammonia stored at 10 bar will be used as possible energy storage medium both as hydrogen carrier as well as fuel itself. This storage condition is the less expensive than ammonia stored at -33 °C for systems storing <3000 tons NH_3 according to Vincent Hans from Proton Ventures. [39] This recommendation is in line with information obtained from the Power to Ammonia report. [40] The representative ROPAX ferry, composed in section 2.1, stores approximately 900 m^3 HFO. Energy content of 900 m^3 HFO is equal to approximately 2000 tons NH_3, resulting in the recommendation to store ammonia at 10 bar.

Again, due to the absence of carbon in the fuel, only NO_X emissions are possible when using ammonia as fuel. [14]

Table 2-3: Ammonia key characteristics. [2,35,40]

	DENSITY [KG/M³]	STORAGE PRESSURE [BAR]	STORAGE TEMPERATURE [°C]	SPECIFIC ENERGY [MJ/KG]	ENERGY DENSITY [MJ/L]
NH_3	603	10	Ambient	18.6	11.3

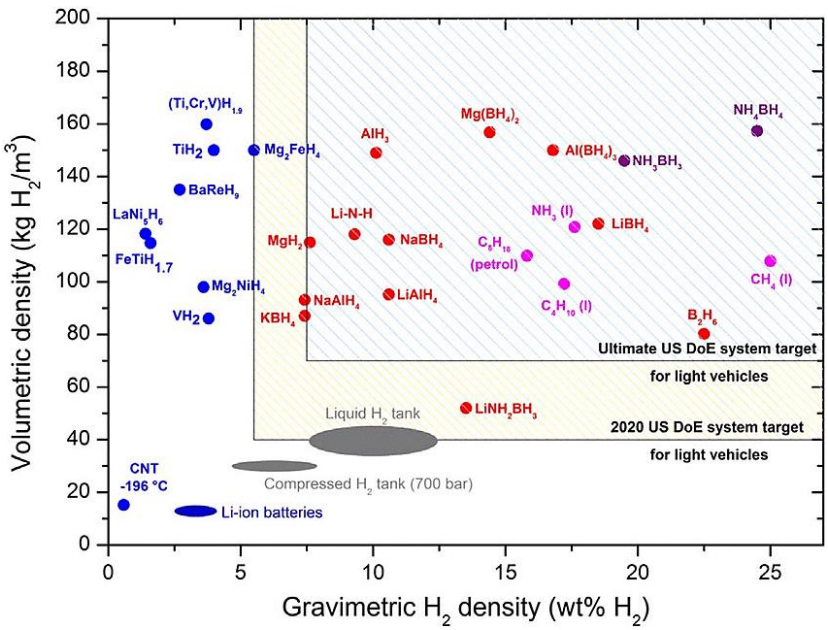

Figure 2-11: Volumetric and gravimetric hydrogen density of different materials. The U.S. Department of Energy targets for the hydrogen storage system are also shown for comparison. [41]

© COPYRIGHT OF C-JOB, WHOSE PROPERTY, THIS DOCUMENT REMAINS. NO PART THEREOF MAY BE DISCLOSED, COPIED, DUPLICATED OR IN ANY OTHER WAY MADE USE OF EXCEPT WITH THE APPROVAL OF C-JOB.

2.2.4 Batteries

Apart from chemical storage methods, as discussed in previous sections, are also forms of electrical storage considered. Electrical storage in the form of batteries to be precise. Most commonly used rechargeable batteries are lead acid and lithium-ion (Li-ion). Serious challenges are anticipated when using batteries as primary energy storage medium. The amount of energy stored per unit mass (specific energy) and unit volume (energy density), respectively 0.49 MJ/kg and 1.08 MJ/L for Li-ion batteries, [42] are both a reason for concern. Recent developments promise batteries (such as sodium-ion [43] and lithium-air [44] batteries) with a higher specific energy and energy density, but these technologies are currently not technological and/or commercially feasible and even those are very heavy. Despite these difficulties, several types of batteries will be considered. The selection of these types of batteries is based on an in 2015 published paper by O. Sapunkov, et al. named "Quantifying the promise of 'beyond' Li–ion batteries". [45] This paper basically relates the status of different technologies to the number of papers that are published per technology. Technologies discussed in this paper are: Li-ion, lithium–air (Li-air), lithium–sulfur (Li–S), sodium-ion (Na–ion), sodium–air (Na-air), redox-flow and magnesium-ion (Mg-ion). [46]

Each of the afore mentioned battery technologies will be compared to each other of the basis of energy density, specific energy, TRL and year of introduction. These are considered to be key values which indicate the battery's size (energy density), weight (specific energy) and technological maturity (TRL). All these values are documented in Table 2-4 (source of the information is given between square brackets).

Table 2-4: Key parameters for the considered battery technologies. [42,45,47-50]

	DENSITY [KG/M^3]	ENERGY DENSITY [MJ/L]	SPECIFIC ENERGY [MJ/KG]	TRL	YEAR OF INTRODUCTION
LI-ION	2200	1.08	0.49	9	1976
LI-AIR	±2000	25 (theoretical)	12.5 (theoretical)	4	1970
LI-S	±700	1.26	1.8	5	2001
NA-ION		Unknown	0.32	3	2012
NA-AIR		Unknown	4 (theoretical)	2	2011
MG-AIR		Unknown	8 (theoretical)	2	1999
REDOX-FLOW		0.036	0.029 – 0.29	7	1884

Li-ion batteries are currently the standard type of batteries used aboard newbuild ships and are therefore considered. [51]

Li-air is also considered because this technology promises a high energy density and specific energy, resulting in a relatively small and light weighted battery pack. However, this technology is currently not past its laboratory stage (TRL4) despite the fact that the technology was already known in 1970. This is a result of limited rechargeability of the batteries. The best Li-air batteries today are only rechargeable for a very limited number of cycles (100 cycles at most). This is due to several phenomena such as degradation and passivation of the electrodes and electrolyte decomposition. [42] For more information concerning the limited rechargeability of state of the art Li-air batteries, see [42], [45], [52] and [53].

© COPYRIGHT OF C-JOB, WHOSE PROPERTY, THIS DOCUMENT REMAINS. NO PART THEREOF MAY BE DISCLOSED, COPIED, DUPLICATED OR IN ANY OTHER WAY MADE USE OF EXCEPT WITH THE APPROVAL OF C-JOB.

A newer type of battery has also great potential and is therefore taken into account. This is the lithium-sulfur type of battery. As can be seen in Table 2-4, energy density and specific energy of this type of batteries are both higher, and therefore better, compared to current Li-ion batteries. This combined with the fact that the technology has already been proven outside a laboratory is deemed to be sufficient cause to include this type of batteries in the consideration. Li-S batteries are currently plagued by a decaying capacity due to the corrosion of the lithium anode. See [45], [54], [52] and [55] for more information about these problems.

Na-ion, Na-air and Mg-air batteries are not considered because of its low TRL and the absence of any information concerning energy density. These technologies are not laboratory tested resulting in a large uncertainty about the performance of the technologies.

Redox-flow batteries have been researched since 1884 and the technology has advanced to TRL 7, but the energy density is approximately 30 times lower than that of Li-ion batteries. [47] This is considered to be infeasible aboard a ROPAX ferry causing this technology to be removed from the consideration.

Batteries do not emit greenhouse gasses at all. [14]

2.2.5 Overview

In summary, three primary energy carriers are considered which are:

- hydrogen – stored at 350 bar
  – stored at 700 bar
  – stored at -253 °C
- ammonia – stored at 10 bar
- batteries – Li-ion
  – Li-air
  – Li-S

Basic characteristics of already commercially available energy carriers are shown in Figure 2-12.

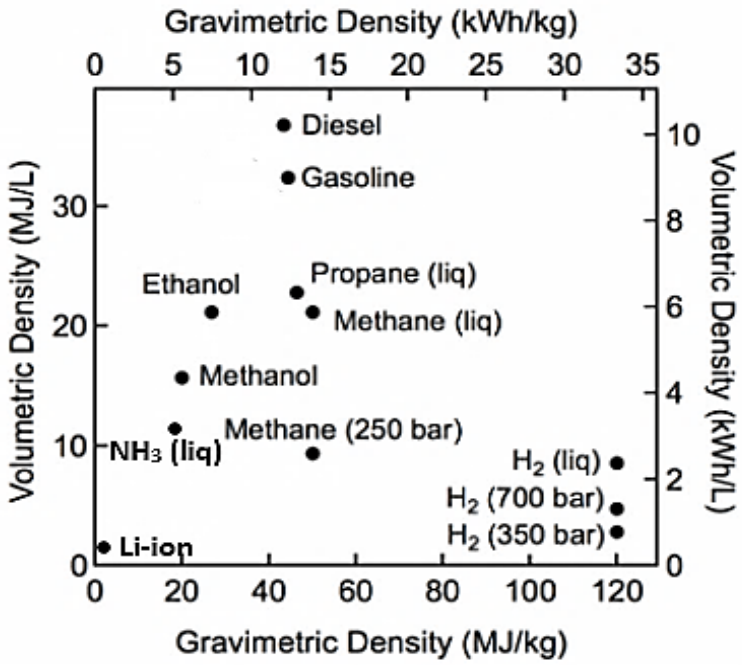

Figure 2-12: Gravimetric and volumetric energy density of different energy carriers. [33] (NH_3 and Li-ion added)

© COPYRIGHT OF C-JOB, WHOSE PROPERTY, THIS DOCUMENT REMAINS. NO PART THEREOF MAY BE DISCLOSED, COPIED, DUPLICATED OR IN ANY OTHER WAY MADE USE OF EXCEPT WITH THE APPROVAL OF C-JOB.

Table 2-5 provides key characteristics of all these energy carriers and the reference energy carrier, LNG. These characteristics are key in assessing the performance of each carrier and therefore the suitability of each carrier aboard a ROPAX ferry in 2050.

Table 2-5: Key characteristics of considered energy carriers. [2,4,16,29,33,35,38,40,42,47,48,56,57]

	LNG	LH_2	H_2 (350 BAR)	H_2 (700 BAR)	NH_3	LI-ION	LI-AIR	LI-S
DENSITY [KG/M³]	456	70.8	22	34	603	2200	±2000	±700
STORAGE PRESSURE [BAR]	Ambient	Ambient	350	700	10	Ambient	Ambient	Ambient
STORAGE TEMPERATURE [°C]	-162	-253	Ambient	Ambient	Ambient	Ambient	Ambient	Ambient
SPECIFIC ENERGY [MJ/KG]	49	120	120	120	18.6	0.49	12.5	1.8
ENERGY DENSITY [MJ/L]	22.3	8.50	2.64	4.08	11.3	1.08	25	1.26
AUTO-IGNITION TEMPERATURE [°C]	537	571	534	534	651	-	-	-
FLAMMABILITY [% VOLUME IN AIR]	5-15	4-75	4-75	4-75	16-25	-	-	-
GHG EMITTIED	CO_2, CH_4, N_2O	N_2O	N_2O	N_2O	N_2O	-	-	-
TRL	9	8	9	8	9	9	4	5

NO_X emissions, and thus also N_2O emissions, are still possible when using hydrogen and ammonia and are therefore indicated in the table. However, latest research show that the amount of NO_X emitted when using hydrogen or ammonia is virtually zero when using fuel cells and very low when using an internal combustion engine.[38,58,59]

Particular matter emissions are considered to be negligible for all fuels. These emissions only occur when heavier carbon-based fuels are used. [14]

© COPYRIGHT OF C-JOB, WHOSE PROPERTY, THIS DOCUMENT REMAINS. NO PART THEREOF MAY BE DISCLOSED, COPIED, DUPLICATED OR IN ANY OTHER WAY MADE USE OF EXCEPT WITH THE APPROVAL OF C-JOB.

2.3 Energy converters

Each energy carrier requires an energy converter to convert its stored energy (chemical or electric) to usable energy. Several different energy converters are considered for this transition and are described below. Basic working principals of every energy converter are given as well as their approximated characteristic weight (mass per unit power), volume (volume per unit power) and efficiency. Both mass and weight are very important parameters when designing a vessel and are therefore given for every converter. The characteristic volume of a converter is determined as the product of its overall length, breadth and height. Efficiency of the converter affects the required amount of energy stored on board and is therefore key in estimating the required energy storage capacity. First is an internal combustion engine discussed. The second subsection concerns several types of fuel cells after which the third subsection describes an ammonia reformer. Subsection four provides general characteristics of electric motors and generators. Characteristics of these converters are summarized at the end of this section.

Internal combustion engines and fuel cells are considered to be key energy converters in the future. [60] These converters are expected to be able to convert the energy carriers, discussed in section 2.2, into usable energy. Electric motors and generators are required for different power plant configurations (see section 2.4), but future developments are not investigated. This is in accordance with the wishes of C-Job, based on the limited expected technological improvements for these energy converters. Characteristic mass, volume and efficiency of electric motors and generators in 2050 will therefore be considered the same as those of current electric motors and generators.

2.3.1 Internal Combustion Engine

Internal combustion engines (ICE) are currently the most commonly used energy converters on-board ships. These units are reliable and applicable for LNG, hydrogen and a mixture of hydrogen and ammonia. Although ICEs are not the most fuel-efficient energy converters, investment costs are relatively low, and the technology is already widely used and known. This type of converters is therefore taken into account. The working principle of ICEs using hydrogen and a mixture of hydrogen and ammonia is very similar to modern diesel and gas fueled spark ignited ICEs. Ammonia requires a small amount of hydrogen (5 wt.% or more) to efficiently start the fuel ignition.

ICEs typically require 15 m^3 and 12 ton per unit power output (MCR in MW). Typical efficiencies are between 35 and 47 %. These values correspond with medium speed engines commonly used on ROPAX ferries. [6,38,61]

Table 2-6: Key characteristics of internal combustion engines. [6,38,58,62]

	SPECIFIC VOLUME [M^3/MW]	SPECIFIC MASS [TON/MW]	OPERATING TEMPERATURE [°C]	FUEL	EFFICIENCY [%]
ICE	15	12	>800	LNG H_2 H_2+NH_3	35 – 47

© COPYRIGHT OF C-JOB, WHOSE PROPERTY, THIS DOCUMENT REMAINS. NO PART THEREOF MAY BE DISCLOSED, COPIED, DUPLICATED OR IN ANY OTHER WAY MADE USE OF EXCEPT WITH THE APPROVAL OF C-JOB.

2.3.2 Fuel Cell

Many institutions and manufacturers are developing fuel cells expected to be applicable to various types of application including transportation. Hydrogen fueled PEMFCs are currently the most widely developed type of fuel cells and are already used in several transportation related projects. However, other types are also emerging, and promising results are provided for these systems as well.
Five main types of fuel cells, according to U.S. Department of Energy (DOE), [63] currently known are:

- Polymer Electrolyte Membrane Fuel Cell (PEMFC)
- Alkaline Fuel Cell (AFC)
- Phosphoric Acid Fuel Cell (PAFC)
- Molten Carbonate Fuel Cell (MCFC)
- Solid Oxide Fuel Cell (SOFC)

A fuel cell directly converts chemical energy into electric energy. The basic layout of a fuel cell consists of an electrolyte between two electrodes (an anode and cathode). Fuel is supplied to the anode of the fuel cell and oxygen (in the form of outside air) is supplied to the cathode. Chemical reactions at the electrodes causes the fuel and oxygen to react into charged ions and negatively charged electrons. Charged ions pass through the electrolyte in the middle to the other side of the fuel cell. The electrons flow by means of an electrical circuit outside the fuel cell from the anode to the cathode. This flow of electrons outside the cell is also known as electric energy and can thus be used to power external systems. Both the charged ions and the electrons react after this transport at the electrodes to uncharged chemical compounds which are then transported away from the fuel cell. The formation of chemical compounds is an exothermic reaction which produces heat. This heat can be used to power e.g. a turbine when the temperature is high enough (several hundred degrees Celsius). [63], [64]

A fuel cell system is composed of stacked fuel cells and Balance of Plant (BoP) components. This BoP maintains the fuel and fuel cell stack at the required operating conditions. This includes but is not limited to heaters, coolers, pumps, compressors, humidifiers and fuel processing units. The BoP is a major part of the total weight and volume of a fuel cell system and this will therefore be taken into account during the evaluation of the system weight and volume. In literature it is very common to address complete fuel cell systems as fuel cell and this will therefore also be used in the remainder of this report. [57], [65]

Each type of fuel cell uses different electrodes which results in different charged ions passing through the electrolyte. Figure B-2 shows schematic representations of the different fuel cell types. Table 2-7 provides an overview of each fuel cell type, which charged ion passes through the electrolyte, characteristic operating temperatures, electrical efficiencies and which type of fuel can be used. There are also benefits, and challenges given per type as well as a qualitative size indication. Information in this table is retrieved from two sources: an in 2017 by DNV GL published report named "*Study on the use of fuel cells in shipping"* [60] and a living document composed by the Fuel Cell Technologies Office (part of the U.S. Department of Energy) called "*Fuel Cell Technologies Office Multi-Year Research, Development, and Demonstration Plan"* [63].

© COPYRIGHT OF C-JOB, WHOSE PROPERTY, THIS DOCUMENT REMAINS. NO PART THEREOF MAY BE DISCLOSED, COPIED, DUPLICATED OR IN ANY OTHER WAY MADE USE OF EXCEPT WITH THE APPROVAL OF C-JOB.

Table 2-7: Summary of fuel cell technologies according to DNV GL [60] and DOE [63].

	MOBILE ION	OPERATING TEMPERATURE	ELECTRICAL EFFIENCY	POSSIBLE FUELS	SIZE	BENEFITS	CHALLENGES
PEMFC	H^+	<120 °C	50 – 60 %	- Hydrogen	Small	- High power-to-weight ratio - Commercially available - Short start-up time	- Expensive catalyst - Sensitive to fuel impurities (e.g. CO and sulfur)
AFC	OH^-	<100 °C	50 – 60 %	- Hydrogen	Small	- Low cost - Quick start-up	- CO_2 poisoning - Pure O_2 needed
PAFC	H^+	150 – 200 °C	40 %	- LNG - Methanol - Diesel - Hydrogen	Large	- Heat recovery possible - Increased tolerance to fuel impurities	- Expensive catalyst - Low power density - Low efficiency - Sulfur sensitivity - Long start-up time
MCFC	CO_3^{2-}	600 – 700 °C	50 %	- LNG - Methanol - Diesel - Hydrogen	Large	- Heat recovery possible - Not easily contaminated - Fuel flexibility	- Long start-up time - Less flexible towards changing power demands - Low power density - High temperature corrosion and breakdown of cell components
SOFC	O^{2-}	500 – 1000 °C	60 %	- LNG - Methanol - Diesel - Hydrogen - (Ammonia in the near future)	Medium	- Heat recovery possible - Not easily contaminated - Fuel flexibility	- Less flexible towards changing power demands - Long start-up time - High temperature corrosion and breakdown of cell components

© COPYRIGHT OF C-JOB, WHOSE PROPERTY, THIS DOCUMENT REMAINS. NO PART THEREOF MAY BE DISCLOSED, COPIED, DUPLICATED OR IN ANY OTHER WAY MADE USE OF EXCEPT WITH THE APPROVAL OF C-JOB.

Based on Table 2-7 and recommendations provided by the afore mentioned reports (constructed by DNV GL [60] and U.S. Department of energy [63]) are PEMFC, SOFC and MCFC considered in this thesis.

AFC is not considered because it requires very clean hydrogen and pure oxygen to function well. This would require an additional system in which oxygen is stored which is deemed infeasible.

A PAFC is deemed infeasible because it is relative size, low efficiency and high investment costs.

PEMFC and MCFC will only use hydrogen as fuel, while SOFC will use either hydrogen or ammonia as its fuel. [38,59,66]

Each type of fuel cell requires another volume and mass to be able to produce a unit power. A PEMFC is considered to be relatively light weighted and small, resulting in a volume requirement of 0.65 m^3/MW and a weight of 1 ton/MW. A MCFC on the other hand requires a volume of 50 m^3/MW and a weight of 40 ton/MW. A SOFC is heavier than a PEMFC, but lighter than a MCFC. It weights approximately 31 m^3/MW and requires 12.5 ton per MW power.

Table 2-8: Key characteristics of fuel cells. [38,59,66,67]

	SPECIFIC VOLUME [M^3/MW]	SPECIFIC MASS [TON/MW]	OPERATING TEMPERATURE [°C]	FUEL	ELECTRICAL EFFICIENCY [%]
PEMFC	0.65	1.0	<120	H_2	50 – 60
SOFC	31	12.5	500 – 1000	H_2 NH_3	Up to 60
MCFC	50	40	600 – 700	H_2	Up to 60

2.3.3 Ammonia reformer

Ammonia can be used as hydrogen carrier, but this requires an ammonia reforming unit. Reforming of ammonia can be done by using a catalyst or at high temperatures (>600 °C). Only catalytic reforming options are evaluated because these require less energy to reform the same amount of ammonia. [38] These options are also more reliable in terms of percentage of ammonia reformed. This is key to prevent ammonia poisoning of fuel cells. Ammonia permanently damages the anode catalyst and the membrane of the fuel cell resulting in a relatively short lifetime, lower efficiency and high maintenance cost. [66], [68]

Table 2-9: Key characteristics of ammonia reformers. [38]

	VOLUME/POWER [M^3/MW]	MASS/POWER [TON/MW]	OPERATING TEMPERATURE [°C]	FUEL	EFFICIENCY [%]
AM-REF	-	-	200 – 800	NH_3	80 – 90

© COPYRIGHT OF C-JOB, WHOSE PROPERTY, THIS DOCUMENT REMAINS. NO PART THEREOF MAY BE DISCLOSED, COPIED, DUPLICATED OR IN ANY OTHER WAY MADE USE OF EXCEPT WITH THE APPROVAL OF C-JOB.

2.3.4 Electric motor and generator

As previously mentioned, electric motors (EM) and generators (EG) are needed for different power plant configurations, but any future developments are not investigated. This is in accordance with the wishes of the corporate supervisor. Characteristic mass, volume and efficiency of electric motors and generators in 2050 will therefore be considered the same as those of current electric motors and generators. These characteristics are determined from an internal database of machinery, based on vendor data, within C-Job Naval Architects.

Electric motors require approximately 4.6 m^3 per MW output power. The mass per MW output power is determined to be equal to 4.0 ton. A typical efficiency of electromotors is 96 %.

Generators are assumed to operate with 97 % efficiency. Typical volume and mass per MW electric output power are 3.8 m^3 and 3.9 ton. [6]

Table 2-10: Key characteristics of electric motors and generators. [6]

	SPECIFIC VOLUME [M^3/MW]	SPECIFIC MASS [TON/MW]	OPERATING TEMPERATURE [°C]	FUEL	EFFICIENCY [%]
EM	4.6	4.0	Ambient	-	96
EG	3.8	3.9	Ambient	-	97

2.3.5 Overview

In conclusion, several energy converters are considered during the composition of the power plant concepts. First an ICE for burning of LNG, hydrogen and an ammonia and hydrogen mixture resulting in usable mechanical energy. Furthermore, PEMFC, SOFC and MCFC are considered for converting hydrogen into electric energy. An ammonia fueled SOFC will also be evaluated as well as an ammonia reformer. Electric motors and generators are also considered, but not further investigated. Characteristic values presented in Table 2-11 remain unchanged in various future scenarios. Table 2-11 provides an overview of typical characteristics for the afore mentioned energy converters.

Table 2-11: Key characteristics of energy converters. [6,38,58,59,62,66,67]

	ICE	PEMFC	SOFC	MCFC	AM-REF	EG	EM
SPECIFIC VOLUME [M^3/MW]	15	0.65	31	50		3.8	4.6
SPECIFIC MASS [TON/MW]	12	1.0	12.5	40		3.9	4.0
OPERATING TEMPERATURE [°C]	>800	<120	500 –1000	600 –700	200 –800	Ambient	Ambient
FUEL	LNG H_2 H_2+NH_3	H_2	H_2 NH_3	H_2	NH_3	-	-
EFFICIENCY [%]	35 – 47	50 – 60	Up to 60	Up to 60	80 – 90	97	96

© COPYRIGHT OF C-JOB, WHOSE PROPERTY, THIS DOCUMENT REMAINS. NO PART THEREOF MAY BE DISCLOSED, COPIED, DUPLICATED OR IN ANY OTHER WAY MADE USE OF EXCEPT WITH THE APPROVAL OF C-JOB.

2.4 Power plant configurations

Previously discussed energy carriers and energy converters are the basis for the power plant configurations that will be evaluated in chapter 4. This section will establish which configurations will be considered and what their general layout will be. The configurations are grouped based on their energy source and summarized in Table 2-12 at the end of this section. First, the LNG-based reference configuration will be established. Configurations with hydrogen, ammonia and batteries are then subsequently composed resulting in a wide range of different power plant configurations. These power plant configurations will be composed of only one kind of energy carrier and one kind of energy converter. The choice for using only one kind of energy carrier and one kind of energy converter per power plant configuration is made to be able to compare the effect of using certain energy carriers or converters to each other.

These power plants are simplified representations of the eventual configuration meaning that the number of engines and tanks are not necessarily equal to one. In the event of NO_X emissions exceeding current emission legislation, a NO_X reducing plant is added to the system. This results in a change in total weight, volume, efficiency and investment costs of the system. Whether this NO_X reducing plant is required or not, is determined in chapter 3.

2.4.1 Reference configuration

As previously mentioned, LNG is used as a reference energy carrier for the representative ROPAX ferry of 2050. This fuel will be converted into mechanical energy by means of an ICE and subsequently converted to electrical energy by a shaft generator. Electrical energy is distributed to onboard energy consumers and the electrical motor driving the propeller.

Such a configuration is currently used on several ROPAX ferries amongst which the Viking Grace. This is currently one of the few LNG fueled ROPAX ferries in operation. It is equipped with:

- two 200 m^3 LNG storage tanks
- four 7 600 kW ICEs
- four 7 300 kW generators
- two fixed pitch propellers
- two 10.5 MW electric motors, one for each propeller

It is striking to see that the amount of stored energy is far less than for a conventional diesel fueled ferry of similar size and capacity (according to the internal C-Job database approximately 900 m^3 HFO). This is causes the Viking Grace to have a theoretical operational time of 3.5 days based on fuel capacity and average fuel consumption. [6], [24]

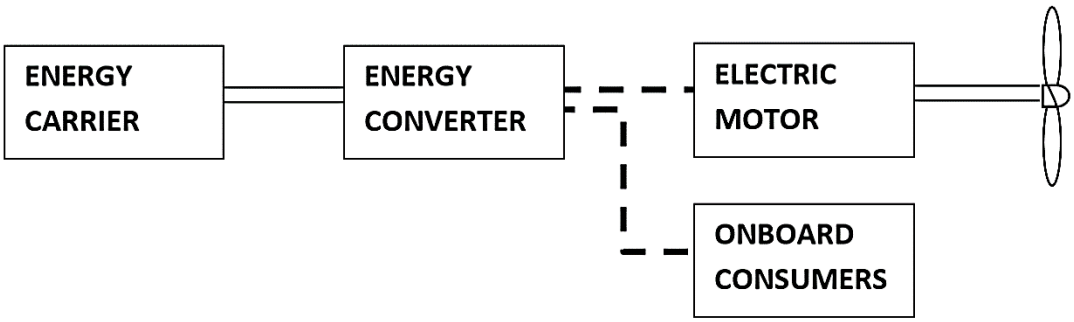

Figure 2-13: Standardized layout of a power plant aboard a ferry.

© COPYRIGHT OF C-JOB, WHOSE PROPERTY, THIS DOCUMENT REMAINS. NO PART THEREOF MAY BE DISCLOSED, COPIED, DUPLICATED OR IN ANY OTHER WAY MADE USE OF EXCEPT WITH THE APPROVAL OF C-JOB.

Figure 2-13 shows a schematic representation of the afore mentioned power plant layout. This will be the standard layout of every power plant concept evaluated in chapter 4. Mechanical connections are represented by solid lines and electrical transport is represented by dashed lines between the components.

Only the kind of energy converter and energy carrier changes. The required electrical output power and energy of the energy converter will remain the same throughout the power plant evaluation. Power requirement of a NO_X reducing installation, if needed, will be subtracted from the output power of the energy converter. This configuration is summarized in Table 2-12.

2.4.2 Stored hydrogen configurations

Hydrogen can be used in both ICE and FC which results in a large number of configurations for this source of energy. On top of that, hydrogen can be stored in several ways, contributing to the number of different configurations.

Hydrogen driven configuration 1 (HC1) is very similar to the reference configuration. The only difference is the fuel. ICEs in combination with generators are used to produce electric energy for the propulsion and onboard consumers. Because three different hydrogen storage methods are considered, three versions of this configuration are evaluated. Version 1 (HC1.1) makes use of hydrogen stored at 350 bar, version 2 (HC1.2) uses of hydrogen stored at 700 bar and version 3 (HC1.3) contains liquified hydrogen storage.

The second stored hydrogen configuration (HC2) makes use of PEMFCs for all energy conversion. This means that no ICEs and generators are needed. Due to the low temperatures in these cells are virtually no NO_X emissions expected. [60]

HC3 replaces PEMFCs by SOFCs but is identical to HC2 in every other aspect. This also applies to HC4 which uses MCFCs instead of PEMFCs. This results in 12 different power plant versions with pure hydrogen stored on board.

All of these configurations are summarized in Table 2-12.

2.4.3 Stored ammonia configurations

After the use of hydrogen as energy carrier is the use of ammonia also possible. For this medium are five different configurations established.

The first configuration (AC1), which gets its energy from ammonia, contains ICEs as energy converters. This configuration requires an ammonia reformer to obtain a blended fuel which contains at least 5 wt.% of hydrogen. The remainder of the system is equal to the reference configuration. Figure 2-14 shows this part of the power plant.

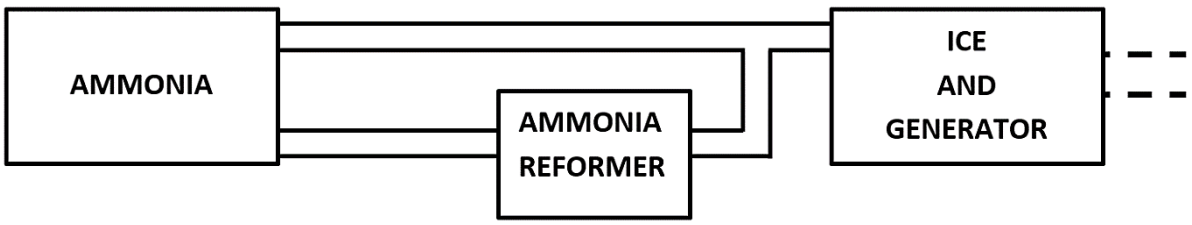

Figure 2-14: Part of the power plant using ammonia as energy carrier and an ICE and generator as energy converter.

Ammonia configuration 2 (AC2) makes use of a reformer to reform all ammonia to hydrogen and nitrogen. This pure hydrogen is used to fuel PEMFCs as is done in HC2. Similar configurations exist with SOFCs (AC3) and MCFCs (AC4).

© COPYRIGHT OF C-JOB, WHOSE PROPERTY, THIS DOCUMENT REMAINS. NO PART THEREOF MAY BE DISCLOSED, COPIED, DUPLICATED OR IN ANY OTHER WAY MADE USE OF EXCEPT WITH THE APPROVAL OF C-JOB.

Lastly, an ammonia configuration with an ammonia fueled SOFCs is evaluated. This is the last configuration that will be considered and brings the total ammonia fueled power plant configurations to 5.

All of these configurations are summarized in Table 2-12.

2.4.4 Battery configurations

Lastly, configurations with batteries as only energy carrier are considered. These configurations do not require additional energy converters, because the energy is already electrically discharged. Battery configuration 1 (BC1) uses Li-ion batteries, BC2 uses Li-air batteries and BC3 Li-S batteries.

These configurations are summarized in Table 2-12.

2.4.5 Overview

This brings the total amount of power configuration to 21. These configurations are summarized in Table 2-12. The name of every configuration is given in the first column. The second and third column indicate which energy carrier and converter are used per configuration. The last column mentions additional components that could be necessary for the individual power plant to comply with regulation.

Table 2-12: Summary of the considered power plant configurations.

CONFIGURATION	ENERGY CARRIER	ENERGY CONVERTER	ADDITIONAL COMPONENTS
REFERENCE	LNG	ICE+EG	NO_X reducing plant (if necessary)
HC1.1	H_2 at 350 bar	ICE+EG	NO_X reducing plant (if necessary)
HC1.2	H_2 at 700 bar	ICE+EG	NO_X reducing plant (if necessary)
HC1.3	LH_2	ICE+EG	NO_X reducing plant (if necessary)
HC2.1	H_2 at 350 bar	PEMFC	
HC2.2	H_2 at 700 bar	PEMFC	
HC2.3	LH_2	PEMFC	
HC3.1	H_2 at 350 bar	SOFC	
HC3.2	H_2 at 700 bar	SOFC	
HC3.3	LH_2	SOFC	
HC4.1	H_2 at 350 bar	MCFC	
HC4.2	H_2 at 700 bar	MCFC	
HC4.3	LH_2	MCFC	
AC1	NH_3	ICE+EG Ammonia reformer	NO_X reducing plant (if necessary)
AC2	NH_3	PEMFC Ammonia reformer	
AC3	NH_3	SOFC Ammonia reformer	
AC4	NH_3	MCFC Ammonia reformer	
AC5	NH_3	SOFC	
BC1	Li-ion		
BC2	Li-air		
BC3	Li-S		

© COPYRIGHT OF C-JOB, WHOSE PROPERTY, THIS DOCUMENT REMAINS. NO PART THEREOF MAY BE DISCLOSED, COPIED, DUPLICATED OR IN ANY OTHER WAY MADE USE OF EXCEPT WITH THE APPROVAL OF C-JOB.

3 Power plant characteristics

Chapter 2 resulted in 21 different power plant configurations which will be evaluated based on key power plant characteristics. Section 3.1 will discuss which key characteristics are used during this evaluation and how these characteristics are determined. Reasons for considering each characteristic will be provided as well as which factors influence the characteristics. Section 3.2 discusses how future energy prices are estimated, because current production methods of e.g. hydrogen are not considered to be sustainable, resulting in an overall increase of GHG emissions compared to current propulsion methods. See section 3.2 for more information. Main characteristics of energy storage systems and energy converters are subsequently determined in sections 3.3 and 3.4. These main characteristics will be used in chapter 4 to estimate the performance of each configuration, based on the evaluation characteristics as established in section 3.1. Presented information is summarized in section 3.5.

3.1 Evaluation characteristics of power plant configurations

As previously mentioned, different power plant configurations are compared to each other by assessing their individual performance based on several key characteristics. These characteristics are determined by using power plant requirements as determined in section 2.1. These requirements are the output electrical power and usable electrical energy per day which are assumed to be constant for every power plant configuration regardless of the weight or volume of the power plant configuration.

The following section will describe each evaluated characteristic including the method used for calculating/determining every characteristic. Every power plant is required to be able to provide the same amount of electrical power and usable electrical energy per day and these values are therefore used as input for the calculations. Paragraph 3.1.1 concerns the CO_2 equivalent pollutant emission of a power plant. Sections 3.1.2 – 3.1.5 respectively discuss the daily energy cost, initial investment cost, total power plant volume and mass. 3.1.6 provides a short recapitulation of afore mentioned considered key power plant characteristics.

3.1.1 CO_2 equivalent pollutant emission

A primary objective of the project is to reduce greenhouse gas emissions of the vessel. GHG emissions are, therefore, considered a very important characteristic, which should be minimized. It is common practice to measure emission in specific pollutant emission (spe), defined as the emitted mass of a pollutant per produced unit of energy (g/kWh). [64] Produced energy is measured at the output of the energy converter (e.g. at the flange of the ICE in the case of a diesel engine). This is scaled by multiplying this specific pollutant emission with the output power of energy converter divided by the useable electrical power. In case of an ICE, this is equal to the following formula:

$$spe = spe_{ICE} * \frac{P_{ICE}}{P_{net,el}}$$

As stated in section 2.2, CO_2, CH_4 and N_2O emissions are taken into consideration as GHGs. However, these gasses have a different impact on the environment and enhanced global warming effect. The impact of GHGs is expressed by a 100-year Global Warming Potential (GWP), relative to that of CO_2, by the Intergovernmental Panel on Climate Change (IPCC). GWP is a way to assess the potential climate impact associated with specific emissions over a specified period. This takes the radiative forcing and atmospheric lifetime of the GHGs relative to CO_2 into account. IPCC states that the 100-year GWP of CH_4 is 21 times as high as that of CO_2 The GWP of N_2O is 310 times that of CO_2. [13]

© COPYRIGHT OF C-JOB, WHOSE PROPERTY, THIS DOCUMENT REMAINS. NO PART THEREOF MAY BE DISCLOSED, COPIED, DUPLICATED OR IN ANY OTHER WAY MADE USE OF EXCEPT WITH THE APPROVAL OF C-JOB.

CO_2 equivalent pollutant emission (pe_{CO_2eq}) of the different power plants will be determined by taking the afore mentioned GWP into account. This results in the following formula for the CO_2 equivalent pollutant emission:

$$pe_{CO_2eq} = spe_{CO_2} + 21 * spe_{CH_4} + 310 * spe_{N_2O}$$

3.1.2 Energy cost per day operation

A significant part of the operational costs of a vessel are energy costs. Minimizing energy costs is, therefore, very important to operators. These costs are estimated by multiplying the total energy consumption per day ($E_{consumed}$, measured in GJ/day) by the energy price (PoE) in USD/GJ, resulting in the following expression for the cost of energy (CoE) expressed in US dollars per day:

$$CoE = E_{consumed} * PoE$$

Due to the fact that every power plant is required to supply the vessel with the same amount of electrical energy per day, measured at the output of the energy converter, this method is considered to be a fair comparison of the energy costs.

The amount of energy consumed per day is determined by using the required usable energy per day ($E_{net,el}$), as defined in section 2.1, divided by the product of the efficiencies of used power converters. This results in the following formula:

$$E_{consumed} = \frac{E_{net,el}}{\prod \eta}$$

Configurations AC1 – AC4 require an ammonia reformer to obtain pure hydrogen from ammonia. This process requires energy, supplied in the form of thermal or electric energy. Thermal energy can be obtained from waste heat present in the exhaust gas flow. In the event of insufficient thermal energy supply by the exhaust gas flow, electrical energy is extracted from the energy converter to ensure a sufficient supply of hydrogen to the energy converter. Extracting electrical energy from the energy converter results in a decrease in overall efficiency and increase in required electrical output power of the energy converter. This effect will be considered when determining the main characteristics of the power plant. Appendix B.3 illustrates this effect in the form of a calculation example.

3.1.3 Initial investment cost

Besides the fuel costs, initial investments are also of considerable importance to operators. These costs are, therefore, estimated by taking the sum of the cost (in USD) of every main component of the configuration. The main components of the power plants considered are the energy storage system (including the fuel conditioning system, fuel storage tank(s) and battery packs) and energy converter(s). Prices of these components are estimated by means of literature research.

3.1.4 Total power plant volume

Required volumes of systems are very important to ferry operators, because this has a considerable impact on the carrying capacity of the ferry. A ROPAX ferry requires a relatively large enclosed volume (GT) to carry its payload, as already discussed in section 2.1 and shown in Figure 2-8 and Figure A-6 – Figure A-11. This results in a wish to minimize system volumes, resulting in more available space for the transport of passengers and cars.

Required volumes of the energy converters and energy storage systems are considered in cubic meters (m^3) and summated to estimate the total power plant volume.

© COPYRIGHT OF C-JOB, WHOSE PROPERTY, THIS DOCUMENT REMAINS. NO PART THEREOF MAY BE DISCLOSED, COPIED, DUPLICATED OR IN ANY OTHER WAY MADE USE OF EXCEPT WITH THE APPROVAL OF C-JOB.

Required storage volume of energy carriers is determined as function of the energy density (ED) in GJ/m^3. The amount of energy stored on board ($E_{stored} = E_{consumed} * refueling\ interval$) divided by this energy density results in the volume of the energy carrier including the storage tank.

The required volume of the fuel tank is multiplied by $4/\pi$, in case of a cylindrical fuel tank, resulting in a boxed volume surrounding the cylindrical tank. This to account for the fact that space at the sides of such a tank rarely can be utilized. [6]

For every energy converter is a specific volume (SPV) determined in m^3/MW. The required volume of an energy converter is therefore a function of the output power of the energy converter. The total volume of the power plant is therefore equal to:

$$V = \sum \left(\frac{4}{\pi}\right) * \frac{E_{stored}}{ED} + \sum SPV * P_{out}$$

3.1.5 Total power plant mass

Besides the cost and volume of a system, mass is also an important characteristic. The total mass of the power plant is calculated by a summation of the mass of every main component of the system. These components are the same as those considered for the volume calculation. Mass of the fuel is also determined resulting in a fixed and variable weight per power plant concept. All masses are determined with the unit metric ton (1 ton = 1000 kg).

The following parameters are used to determine the weight of every component.

- SPE: Specific energy of an energy carrier including storage tank based on the lower heating value in GJ/ton
- SPM: Specific mass of an energy converter per unit output power (ton/MW)
- LHV: Lower heating value of the fuel in GJ/ton

This results in the following expression:

$$m = \sum \frac{E_{stored}}{SPE} + \sum SPM * P_{out}\,, \qquad m_f = \frac{E_{stored}}{LHV}$$

3.1.6 Overview of the evaluated characteristics and used formulas

This last part of section 3.1 summarizes all afore mentioned characteristics that will be valuated, and the formulas used to evaluate them. This summary is provided in Table 3-1.

Table 3-1: Evaluated power plant characteristics including units and formulas.

CHARACTERISTIC	UNIT	FORMULA
CO_2 equivalent pollutant emission	g/kWh	$pe_{CO_2eq} = spe_{CO_2} + 21 * spe_{CH_4} + 310 * spe_{N_2O}$
Cost of Energy	USD/day	$CoE = E_{consumed} * PoE$
Initial investment	USD	$Initial\ investment = \sum component\ price$
Total volume	m^3	$V = \sum \left(\frac{4}{\pi}\right) * \frac{E_{stored}}{ED} + \sum SPV * P_{out}$
Total mass including fuel	ton	$m = \sum \frac{E_{stored}}{SPE} + \sum SPM * P_{out}$
Total mass excluding fuel	ton	$m = \sum \frac{E_{stored}}{SPE} - \frac{E_{stored}}{LHV} + \sum SPM * P_{out}$

© COPYRIGHT OF C-JOB, WHOSE PROPERTY, THIS DOCUMENT REMAINS. NO PART THEREOF MAY BE DISCLOSED, COPIED, DUPLICATED OR IN ANY OTHER WAY MADE USE OF EXCEPT WITH THE APPROVAL OF C-JOB.

3.2 Energy price

Section 3.1.2 states that the cost of energy per day is determined by multiplying the energy consumption of a configuration by the price of the energy carrier. The method of determining the energy consumption per day has been given in this section, but the price of energy (PoE) is still not known. This price will therefore be determined in the following paragraphs. The price of LNG is determined in paragraph 3.2.1. Next, the prices of electricity, hydrogen and ammonia are determined in paragraph 3.2.2, 3.2.3 and 3.2.4, respectively. Hydrogen prices are determined per storage condition.

Every price of energy used from this point forward are given as 2017 equivalent U.S. dollars (USD). Table B-1 found in appendix B provides an overview of conversion units used to scale currency to 2017 equivalent USD. Conversion factors for energy units, such as BTU (British thermal units), are given in Table B-2. A minimum, default and maximum expected price will be given for every energy storage medium. All prices of energy will be defined as 2017 equivalent U.S. dollars per gigajoule stored energy based on the lower heating value of the storage medium (USD/GJ). Only resource and production costs are taken into account. Additional costs, for example transportation costs, are therefore not considered.

3.2.1 LNG price

Since LNG is used as reference source of energy, a method to determine the cost of LNG per unit energy is required. DNV GL defines the price of LNG fuel to be equal to the sum of Henry Hub Gas price and liquefaction cost. [69] This formula will be used for the estimation of the LNG price in 2050 with one modification, a CO_2 tax is added to the equation.

$$PoE_{LNG} = Henry\ Hub\ gas + liquefaction\ cost + CO_2\ equivalent\ emisstion\ tax$$

Several governments are planning to implement a form of emission taxation in the future. Amongst these governments are European governments, New Zealand, Korea, China, Japan and Mexico. Emission prices vary between 1 and 412 USD per ton CO_2 equivalent GHG emission. For example, European GHG emission tax is currently 6 USD/ton CO_2 equivalent while Switzerland has implemented a carbon tax of 87 USD/ton CO_2 equivalent according to the World Bank. [70] A report by composed by the World Energy Council in 2013, suggests an emission price of 26 – 90 USD/ton CO_2 to be implemented in the future. [71] Cefic, an International Non-Profit Association representing chemical companies across Europe, considers CO_2 price up to 412 USD/ton CO_2. 79 USD/ton CO_2 is used in the Current Policy Initiatives (CPI) scenario of the EU Energy Roadmap aiming to reduce GHG emissions by 40 % in 2050 compared to 1990. [72] Since burning of one ton of natural gas results in approximately 2.8 ton CO_2, [73] a price of 1 USD/ton CO_2 equivalent is approximately equal to 0.0639 USD/GJ burned gas. When estimating the price of LNG in 2050, a CO_2 equivalent emission tax between 0 and 412 USD/ton CO_2 equivalent is taken into account. 0 USD/ton CO_2 will be the default value since there are currently no CO_2 taxes implemented in the considered areas of operation.

According to DNV GL, liquefaction costs are estimated to be between 3 and 5 USD/mmBTU (2.84 – 4.74 USD/GJ). [69] These values are therefore used as minimum and maximum liquefaction costs. A default value of 4 USD/mmBTU will be used.

© COPYRIGHT OF C-JOB, WHOSE PROPERTY, THIS DOCUMENT REMAINS. NO PART THEREOF MAY BE DISCLOSED, COPIED, DUPLICATED OR IN ANY OTHER WAY MADE USE OF EXCEPT WITH THE APPROVAL OF C-JOB.

The U.S. Energy Information Administration expects the Henry Hub gas price to be 3.57 – 11.04 USD/GJ with 6.25 USD/GJ as reference case. This can be seen in Figure 3-1 shown below. [74] These values for the Henry Hub gas price are used as minimum, maximum and default gas prices.

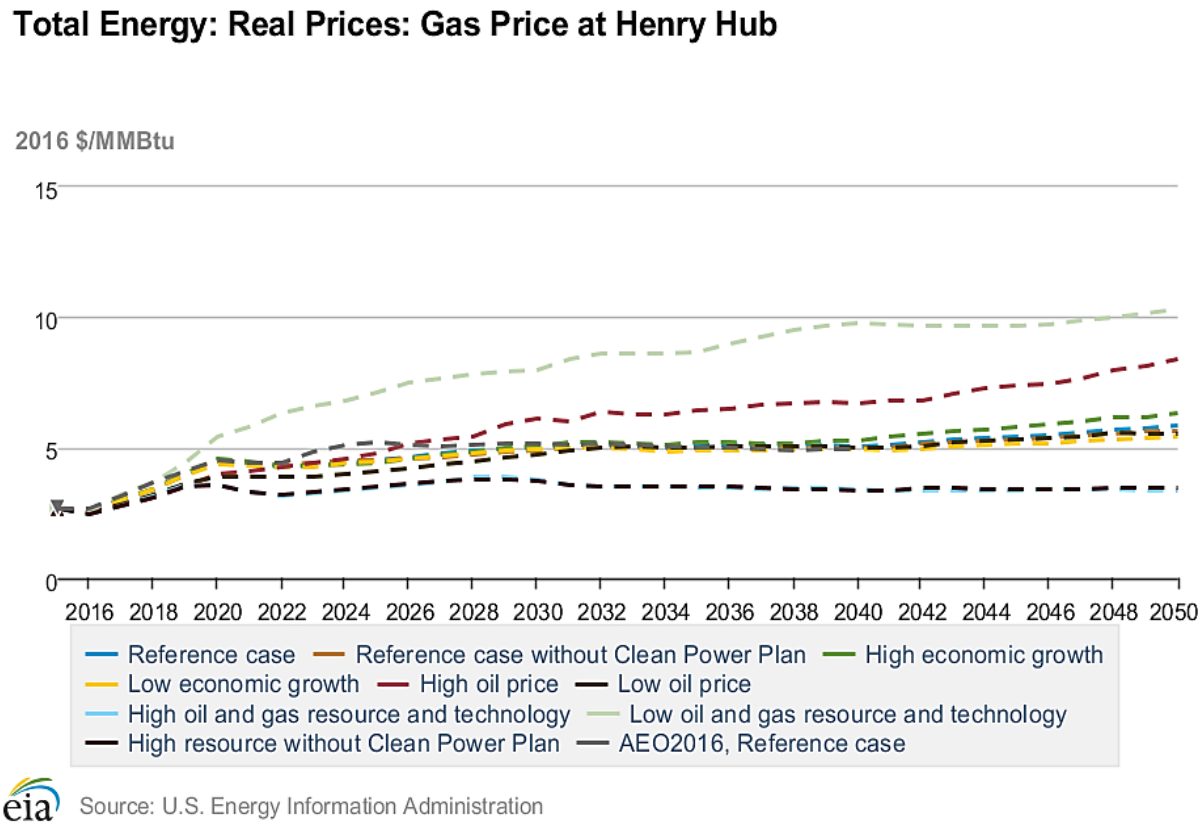

Figure 3-1: Henry Hub gas price in 2016 USD and mmBTU HHV according to the Energy Outlook 2017 by the U.S. Energy Information Administration. [74]

Given the previous defined minimum, default and maximum prices a default LNG price of 10.04 USD/GJ is estimated. Table 3-2 provides an overview of previously defined minimum, default and maximum prices.

Table 3-2: Overview of the default, minimum and maximum price of LNG per component used.

USD/GJ	DEFAULT	MINIMUM	MAXIMUM
HENRY HUB GAS PRICE	6.25	3.57	11.04
LIQUEFACTION COSTS	3.79	2.84	4.74
CO_2 EQUIVALENT EMISSION TAX	0.00	0.00	26.33 (412 USD/ton CO_2)
TOTAL	**10.04**	**6.41**	**42.11**

© COPYRIGHT OF C-JOB, WHOSE PROPERTY, THIS DOCUMENT REMAINS. NO PART THEREOF MAY BE DISCLOSED, COPIED, DUPLICATED OR IN ANY OTHER WAY MADE USE OF EXCEPT WITH THE APPROVAL OF C-JOB.

3.2.2 Electricity prices

Because this project is revolving around GHG emission minimization during the operation of a vessel, only electricity produced using renewable sources of energy is used for this project. Prices of energy originating from solar and wind are taken into account during the price estimation of electricity, because these two sources of energy are considered to be the most feasible sources of large scale renewable energy. [71], [75]

The levelized cost of energy (LCOE) is used to estimate the price of electric energy in 2050. The levelized cost of energy is defined as the total lifetime cost of a system divided by its total energy production during its life. [76] This is represented by the following formula obtained from U.S. Department of Energy [76]:

$$LCOE = \frac{\sum_{t=1}^{n} \frac{I_t + M_t + F_t}{(1+r)^t}}{\sum_{t=1}^{n} \frac{E_t}{(1+r)^t}}$$

I_t Investment expenditures in year t (including financing)
M_t Operations and maintenance expenditures in year t
F_t Fuel expenditures in year t
E_t Electricity generation in year t
r Discount rate
n Life of the system

Several LCOE are found in literature and are presented in Table 3-3.

Table 3-3: Overview of LCOE found in literature.

AVERAGE [USD/GJ]	MINIMUM [USD/GJ]	MAXIMUM [USD/GJ]	TYPE OF SOURCE	SOURCE
	19	28	2013 World Energy Council on solar plant	[71]
	16	23	2013 World Energy Council on onshore wind	[71]
23			2016 performance offshore wind farm (Borssele I/II)	[77]
17			2016 performance offshore wind farm (Borssele III/IV)	[77]
6			2016 performance solar farm (Abu Dhabi)	[77]
14	12	17	2016 Industry expert opinion onshore solar farm	[78]
29	23	41	2016 Industry expert opinion offshore wind farm	[78]
39	16	43	2016 European Commission research	[75]
16	16	18	2017 Lappeenranta University of Technology research	[79]
15	8	19	2017 Agora Energiewende research	[80]

© COPYRIGHT OF C-JOB, WHOSE PROPERTY, THIS DOCUMENT REMAINS. NO PART THEREOF MAY BE DISCLOSED, COPIED, DUPLICATED OR IN ANY OTHER WAY MADE USE OF EXCEPT WITH THE APPROVAL OF C-JOB.

Using the data presented above, a minimum and maximum electricity price of 6 and 43 USD/GJ, respectively, are assumed. Averaging all presented prices, a value of 20 USD/GJ is obtained. This will be the default electricity price. These values are shown in Table 3-4.

Table 3-4: Considered default, minimum and maximum electric energy price.

USD/GJ	DEFAULT	MINIMUM	MAXIMUM
ELECTRICITY PRICE	20.00	6.00	43.00

3.2.3 Hydrogen prices

Steam methane reforming (SMR) is currently the most used method of hydrogen production. Methane reacts at high temperature (700 °C – 1000 °C) and pressure (3 – 25 bar) with steam and decomposes into hydrogen and carbon monoxide (CO). Produced CO and steam are subsequently reacted to produce CO_2 and hydrogen using the so-called water-gas shift reaction. These reactions are represented by the following equations. [33]

Steam methane reforming (SMR):

$$CH_4 + H_2O \rightarrow CO + 3\,H_2$$

Water gas shift reaction:

$$CO + H_2O \rightarrow CO_2 + H_2$$

During the production of 1 kg H_2, a total of 8.9 kg CO_2 is emitted. [40] This is more GHG emission per unit energy than would be emitted when methane is used in an ICE. Using hydrogen produced via SMR is therefore considered more harmful to the environment compared to directly burning natural gas in an ICE and thus more harmful than the reference case used in this thesis. Hydrogen will therefore be considered to be produced using another method.

The International Energy Agency (IEA) considers the use of electricity as most feasible CO_2 free hydrogen production method. When using electricity to decompose water into hydrogen and oxygen a minimum of 39.4 kWh per kg hydrogen produced is required. However, state of the art technologies require approximately 53 kWh electrical energy to produce 1 kg hydrogen. This is equal to 1.59 GJ of electrical energy per GJ H_2. This factor will be used when calculating the hydrogen production costs. The price of electrical energy is considered to be equal to the electric energy price determined in paragraph 3.2.2. This to ensure a GHG free production of hydrogen. When electricity produced using conventional methods would be used for the production of hydrogen, CO_2 equivalent GHG emissions are approximately 3 times as high as when using SMR. [40,81]

Capital costs for the production plant of hydrogen are estimated to be 20 USD/MWh, based on HHV of H_2 (6.57 USD/GJ LHV of H_2), according to the IEA. [81] Figure 3-2 shows this as well as a hydrogen price estimation based on electricity price. Note that this relation is based on the higher heating value (HHV) of hydrogen and the assumption that 1.2 GJ electric energy is required to produce 1 GJ HHV H_2 (1.42 GJ electricity per GJ LHV H_2 or 47 kWh/kg H_2). This energy requirement is theoretically possible with state of the art technologies, however practical values are higher, 53 kWh/kg H_2, as previously mentioned. [40,82,83]

© COPYRIGHT OF C-JOB, WHOSE PROPERTY, THIS DOCUMENT REMAINS. NO PART THEREOF MAY BE DISCLOSED, COPIED, DUPLICATED OR IN ANY OTHER WAY MADE USE OF EXCEPT WITH THE APPROVAL OF C-JOB.

Taking into account capital costs for the production plant (6.57 USD/GJ LHV of H_2) and Best Available Technique (BAT) specific power consumption equal to 53 kWh_{el}/kg H_2 (1.59 $GJ_{el}/GJ_{LHV,H2}$), the following equation for the cost of hydrogen emerges:

$$H_2 = 6.57 + 1.59 * Electricity\ price\ [USD/GJ]$$

This expression for the production cost of hydrogen is verified by the book *Compendium of Hydrogen Energy Volume 1* [84] and the IEA report *Technology Roadmap: Hydrogen and Fuel Cells* [81]. Hydrogen production cost estimation given by C. Philibert in his in 2017 published report *Renewable Energy for Industry: From green energy to green materials and fuels* is somewhat lower compared to the above-mentioned formula. Figure 3-3 provides his findings concerning the price of hydrogen taking into account the full load hours (FLH) of a combined solar and wind farm. [85]

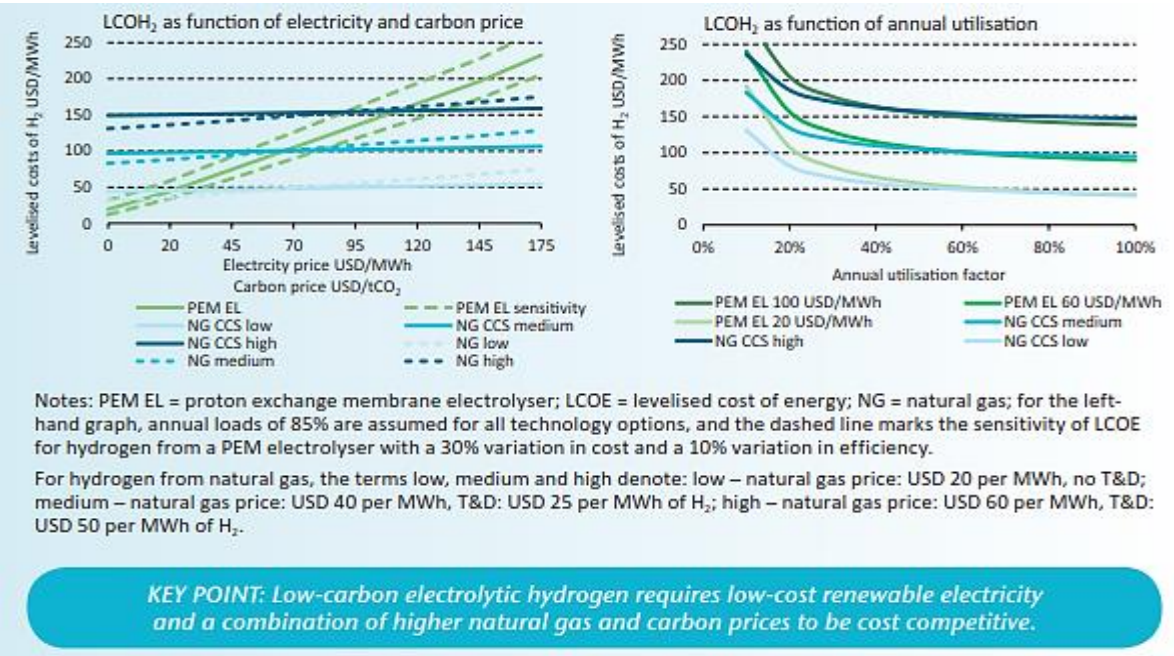

Figure 3-2: Hydrogen price per MWh HHV H2 as function of electricity price (l) and utilization factor (r). [81]

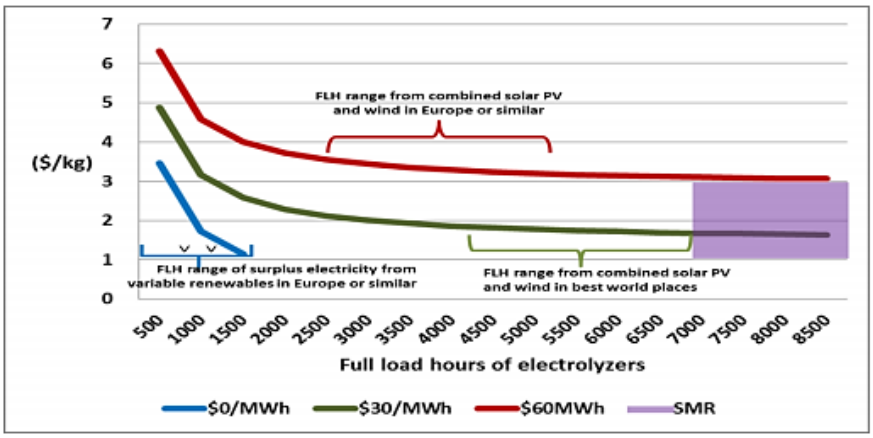

Assumptions: Capex of electrolysers $ 450/kW (NEL 2017), WACC 7%, lifetime 30 years, efficiency 70% (IEA 2015); cost of hydrogen from SMR $ 1 to 3/kg H_2.depending on natural gas prices.

Figure 3-3: Hydrogen production cost estimation by C. Philibert. [85]

© COPYRIGHT OF C-JOB, WHOSE PROPERTY, THIS DOCUMENT REMAINS. NO PART THEREOF MAY BE DISCLOSED, COPIED, DUPLICATED OR IN ANY OTHER WAY MADE USE OF EXCEPT WITH THE APPROVAL OF C-JOB.

Due to the fact that hydrogen is stored at extreme conditions, required energy to bring hydrogen to its intended storage condition makes up a considerable part of the total required energy. The cost of this required energy is taken into account by incorporating it into the expression for the price of hydrogen.

Liquefaction of hydrogen typically requires 40 MJ/kg H_2 produced when using a liquefaction plant capacity (>1000 kg H_2/h). [86] This additional energy requirement results in an increase in required energy of 0.33 GJ per GJ H_2 equivalent. The total formula for the cost of liquid hydrogen will therefore be:

$$H_2\ (-253\ ℃) = 6.57 + 1.92 * Electricity\ price$$

The cost of compressed hydrogen is estimated in a similar way. Compression of hydrogen requires 16.5 MJ/kg H_2 (0.14 GJ/GJ H_2 equivalent) when compressing it to 350 bar. 22 MJ/kg hydrogen (0.18 GJ/GJ H_2 equivalent) is required to compress it to a final pressure of 700 bar. [86] This results in the following formulas for the compressed hydrogen price:

$$H_2\ (350\ bar) = 6.57 + 1.73 * Electricity\ price$$
$$H_2\ (700\ bar) = 6.57 + 1.77 * Electricity\ price$$

These prices are valid for cases when hydrogen is manufactured by using commercial energy, however another option is to utilize otherwise wasted excess energy from renewable resources to produce hydrogen. This is also described by C. Philibert and shown in Figure 3-3. [85] Based on this research is the hydrogen price produced from excess energy determined to be 12.50 USD/GJ.

These three formulas, used when commercial electrical energy is used to produce hydrogen, result in the default, minimum and maximum hydrogen prices shown in Table 3-5. The price of hydrogen when produced using excess energy is provided between brackets.

Table 3-5: Considered default, minimum and maximum hydrogen prices per storage condition.

USD/GJ	DEFAULT	MINIMUM	MAXIMUM
ELECTRICITY PRICE	20.00	6.00	43.00
H_2 AT 350 BAR	41.17 (12.50)	16.95	80.96
H_2 AT 700 BAR	41.97 (12.50)	17.19	82.68
H_2 AT -253 °C	44.97 (12.50)	18.09	89.13

© COPYRIGHT OF C-JOB, WHOSE PROPERTY, THIS DOCUMENT REMAINS. NO PART THEREOF MAY BE DISCLOSED, COPIED, DUPLICATED OR IN ANY OTHER WAY MADE USE OF EXCEPT WITH THE APPROVAL OF C-JOB.

3.2.4 Ammonia prices

The price of ammonia is strongly linked to the price of hydrogen. This is due to the fact that ammonia is produced from hydrogen using the Haber-Bosch Process. This process combines nitrogen and hydrogen at 350-550 °C and 100-300 bar over iron-based catalyst resulting in an exothermic reaction.

Haber-Bosch process:

$$3\,H_2 + N_2 \rightarrow 2\,NH_3$$

Current production methods use natural gas to produce hydrogen resulting in the emission of 1.8 ton CO_2/ton ammonia. Producing ammonia using electric energy requires 10.4 kWh/kg NH_3 according to a report by Energy Valley, Hanze University of Applied Sciences and Proton Ventures BV. [82] Specific power consumption for the production of ammonia is estimated to be 7.1 – 11 kWh/kg NH_3, depending on the production process, according to the Institute for Sustainable Process Technology (ISPT) report. [40] 7 – 8 kWh/kg NH_3 is the target use, defined by the U.S. Department of Energy, for a Solid State Ammonia Synthesis (SSAS) system. However, this technology is not yet proven. [72]

Conventional ammonia production methods as well as the use of grey energy are not considered for the production of ammonia. These production methods would result in more GHG emissions than when conventional hydrocarbon fuels would be burned, resulting in a net increase of GHG emissions. For this reason, only the use of energy obtained from renewable energy sources is considered.

Ammonia production is assumed to consume 10.4 kWh (37.44 MJ) electrical energy per kg NH_3 as defined by [82]. Since ammonia is pressurized, an additional 1.27 MJ electric energy is required per kg NH_3. This results in a total required energy input of 38.71 MJ/kg NH_3 = 2.08 GJ electrical energy required to produce 1.00 GJ of ammonia equivalent. [40,82]

Capital costs to produce ammonia are estimated to be 2.69 USD/GJ. This follows from a study performed by C. Philibert of the Renewable Energy Division at the International Energy Agency. [85] These capital costs are required when the plant is producing ammonia for 55 % of the time. This utilization factor is consistent with the amount of full load hours of electrolysers using energy from a combined solar and wind plant, as shown in Figure 3-3.
When only using excess renewable energy, an estimated ammonia price of 10.00 USD/GJ is used. This is based on estimations used by C. Philibert and statements from the International Transport Forum, Proton Ventures, Hanzehogeschool and Stichting Energy Valley.[82,85,87]

This results in the following expression for the price of ammonia:

$$NH_3 = 2.69 + 2.08 * Electricity\ price$$

Table 3-6: Considered default, minimum and maximum ammonia prices.

USD/GJ	DEFAULT	MINIMUM	MAXIMUM
ELECTRICITY PRICE	20.00	6.00	43.00
NH_3	44.29 (10.00)	15.17	92.13

© COPYRIGHT OF C-JOB, WHOSE PROPERTY, THIS DOCUMENT REMAINS. NO PART THEREOF MAY BE DISCLOSED, COPIED, DUPLICATED OR IN ANY OTHER WAY MADE USE OF EXCEPT WITH THE APPROVAL OF C-JOB.

3.2.5 Overview of energy prices

Table 3-7 provides an overview of all considered energy prices. Energy prices of hydrogen and ammonia are considerably higher than those of LNG and electricity for renewable energy sources. The price of LNG would need to increase dramatically to exceed the price of synthetic fuels (hydrogen and ammonia) produced using commercial electric energy. Synthetic fuel prices can compete with LNG prices when excess renewable energy is used for the production of synthetic fuels.

Table 3-7: Considered default, minimum and maximum energy prices.

USD/GJ	DEFAULT	MINIMUM	MAXIMUM
LNG	10.04	6.41	42.11
ELECTRICITY	20.00	6.00	43.00
H_2 AT 350 BAR	41.17 (12.50)	16.95	80.96
H_2 AT 700 BAR	41.97 (12.50)	17.19	82.68
H_2 AT -253 °C	44.97 (12.50)	18.09	89.13
NH_3	44.29 (10.00)	15.17	92.13

© COPYRIGHT OF C-JOB, WHOSE PROPERTY, THIS DOCUMENT REMAINS. NO PART THEREOF MAY BE DISCLOSED, COPIED, DUPLICATED OR IN ANY OTHER WAY MADE USE OF EXCEPT WITH THE APPROVAL OF C-JOB.

3.3 Energy storage characteristics

Energy carrier characteristics mentioned in section 2.2 form the basis for the energy storage volume and weight. However, these characteristics are only valid for the energy carrier itself and do therefore not take the characteristics of the storage tank into account. The effect of the energy storage method on the total weight and volume of the energy storage will be determined in the following sections. Most safety measures, such as minimal distance between tanks, are not considered, except for the maximum tank filling level. Required volume for cylindrically shaped storage tanks will be obtained by multiplying the storage tank volume by $4/\pi$ to fit the tank in a square box surrounding the tank, as described in paragraph 3.1.4. This is justified by the fact that this added space cannot be used due to the shape of the tank. [6] Volumetric (GJ/m^3) and gravimetric energy densities (GJ/ton) will be defined for every energy storage method. An estimated initial investment cost is also determined per storage method.

First, LNG storage characteristics are determined in paragraph 3.3.1. Hydrogen storage systems are considered next (3.3.2), followed by ammonia storage (3.3.3) and batteries (3.3.4). All characteristics are summarized in tables found in paragraph 3.3.5.

3.3.1 LNG storage

LNG fuel tanks used on board ships are mostly cylindrically shaped. From supplier data, it appears that such a tank is capable of storing 25.4 GJ/ton and 15.3 GJ/m^3 bare tank volume. Taking wasted space into account, the energy storage per volume is 12.0 GJ/m^3. [88] Volumetric and gravimetric energy densities (VED & GED) obtained from publications by Hirose [89] and Van Biert et al. [38] confirm the supplier data.

Supplier data indicates a storage tank price of approximately 400 USD/GJ stored LNG. [88]

Due to safety regulations are LNG fuel tanks required to have a filling level of 95 % or less. This will be taken into account during the volume and weight estimation of the tank.

3.3.2 Hydrogen storage

Hydrogen is known to require a relatively large amount of space and extreme storage conditions compared to hydrocarbon-based fuels. Multiple studies have been performed to optimize hydrogen storage systems. Many of these researches concern a hydrogen storage tank on board a fuel cell electric vehicle (FCEV) due to governmental incentives to develop systems to use hydrogen as future fuel for road vehicles and thereby creating a 'hydrogen economy'. [30,59,74,86]

Gravimetric and volumetric energy densities obtained from supplier data and research papers are documented in appendix C, Table C-1 – Table C-6. From these data, following energy density ranges are obtained:

H_2 at 350 bar

- Gravimetric density: 3.0 – 15.0 GJ/ton Default value: 7.0 GJ/ton
- Volumetric density: 1.8 – 2.4 GJ/m^3 Default value: 2.0 GJ/m^3

H_2 at 700 bar

- Gravimetric density: 2.4 – 13.2 GJ/ton Default value: 6.5 GJ/ton
- Volumetric density: 2.0 – 4.0 GJ/m^3 Default value: 3.2 GJ/m^3

H_2 at -253 °C

- Gravimetric density: 6.6 – 15.0 GJ/ton Default value: 9.0 GJ/ton
- Volumetric density: 4.0 – 5.4 GJ/m^3 Default value: 4.3 GJ/m^3

© COPYRIGHT OF C-JOB, WHOSE PROPERTY, THIS DOCUMENT REMAINS. NO PART THEREOF MAY BE DISCLOSED, COPIED, DUPLICATED OR IN ANY OTHER WAY MADE USE OF EXCEPT WITH THE APPROVAL OF C-JOB.

Especially gravimetric energy densities are reported over a wide range due to the use of different storage tank materials. Maximum GED values are reached by hypothetical composite materials. [30]
Volumetric energy densities are limited by the energy density of pure hydrogen given in Table 2-2. This results in a considerably smaller range of storage densities. Default values as defined above originate from existing systems. [89]
Maximum filling levels of hydrogen storage tanks are not known and therefore considered equal to 100 %.

Concerning the cost of a hydrogen storage system, the U.S. Department of Energy has set a target value of 2 USD/kWh in 2015. This was not met according to several researches. Current system costs are estimated to be 13 USD/kWh H_2 for a 350 bar storage system, 15 USD/kWh H_2 for a 700 bar storage system and 5 USD/kWh H_2 for a liquid H_2 storage system. [82,90-95]
A default price indication of 2 USD/kWh (560 USD/GJ) hydrogen is assumed when calculating the hydrogen storage system cost since much active research is performed on this subject. Current storage prices are taken into account as maximum price estimations.

3.3.3 Ammonia storage

Ammonia storage is widely used in e.g. rail and stationary applications. Regulations regarding maximum filling levels exist but vary slightly per country and industry. European regulations allow a maximum filling level of 88 % (0.53 kg NH_3/L net tank volume), [96] however, U.S. Regulation only allows 85 % filling level. [97], [98] Due to the fact that the operational area of the representative ROPAX ferry is intercontinental, a maximum filling level of 85 % is used.

Table C-7 provides an overview of gravimetric energy densities found in research papers and supplier data. Volumetric energy densities are documented in Table C-8. These tables are found in appendix C.4.

NH_3 at 10 bar

- Gravimetric density: 13.0 – 14.6 GJ/ton Default value: 13.6 GJ/ton
- Volumetric density: 10.4 – 10.7 GJ/m^3 Default value: 10.5 GJ/m^3

Volumetric energy densities approach pure ammonia energy densities (11.3 GJ/m^3) resulting in a relatively narrow rang of possible VED. Gravimetric densities are influenced by the construction material of the storage tank, resulting in a considerably larger range of possible densities compared to the volumetric density.

Supplier data estimates the price of an ammonia storage tank to be approximately 40 USD/GJ ammonia stored. This price is not expected to drop significantly in the future due to the already relatively low price and limited expected technological improvement in the furure. 40 USD/GJ will therefore be used as investement price of an ammonia storage system.[39,99]

© COPYRIGHT OF C-JOB, WHOSE PROPERTY, THIS DOCUMENT REMAINS. NO PART THEREOF MAY BE DISCLOSED, COPIED, DUPLICATED OR IN ANY OTHER WAY MADE USE OF EXCEPT WITH THE APPROVAL OF C-JOB.

3.3.4 Batteries

Configuration BC1, BC2 and BC3 make use of different battery technologies as already explained in section 2.2.4. Industry experts expect considerable technological improvements of especially Li-air and Li-S batteries in coming decades.[42,52,53]

Due to the expected technological developments, large uncertainties concerning volumetric and gravimetric energy densities of different battery technologies arise. A range of VEDs and GEDs is defined for each type of battery, based on literature research. Appendices C.5, C.6 and C.7 provide an overview of expected practical volumetric and gravimetric energy densities according to this literature research. This data is used to compose Figure 3-4 and Figure 3-5, providing a graphical representation of the statistical variance of the obtained data. Appendix B.5 provides more information about this type of plot. Figure 3-4 shows the variation of GEDs obtained from literature per battery technology. VED variations per technology are illustrated in Figure 3-5.

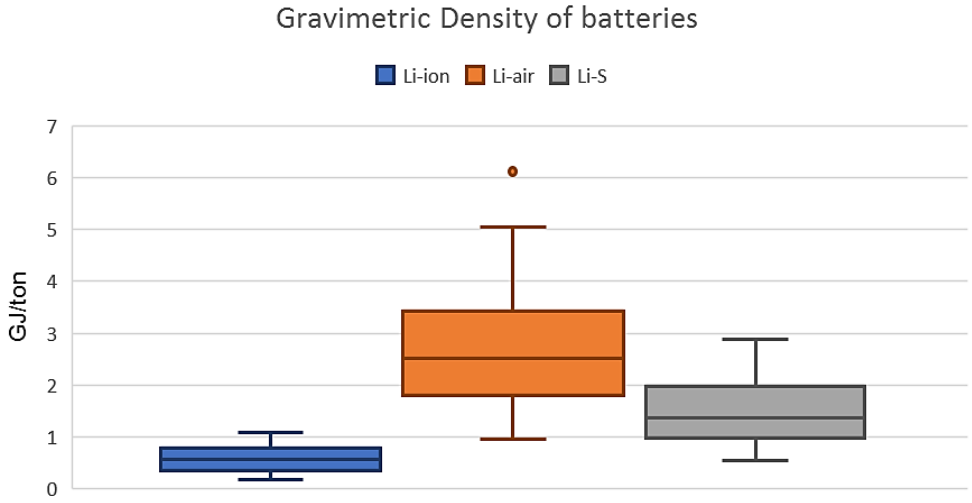

Figure 3-4: Range of gravimetric energy densities considered per type of battery based on literature.

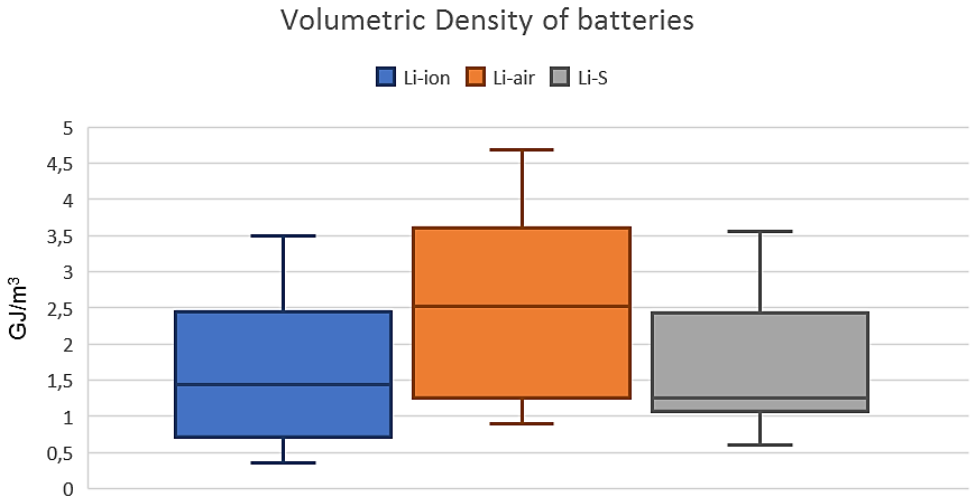

Figure 3-5: Range of volumetric energy densities considered per type of battery based on literature.

© COPYRIGHT OF C-JOB, WHOSE PROPERTY, THIS DOCUMENT REMAINS. NO PART THEREOF MAY BE DISCLOSED, COPIED, DUPLICATED OR IN ANY OTHER WAY MADE USE OF EXCEPT WITH THE APPROVAL OF C-JOB.

Based on this data are the following battery energy density variations obtained:

Li-ion

- Gravimetric density: 0.18 – 1.08 GJ/ton Default value: 0.58 GJ/ton
- Volumetric density: 0.36 – 3.49 GJ/m^3 Default value: 1.44 GJ/m^3

Li-air

- Gravimetric density: 0.97 – 6.12 GJ/ton. Default value: 2.52 GJ/ton
- Volumetric density: 0.90 – 4.68 GJ/m^3 Default value: 2.52 GJ/m^3

Li-S

- Gravimetric density: 0.54 – 2.88 GJ/ton. Default value 1.36: GJ/ton
- Volumetric density: 0.61 – 3.56 GJ/m^3 Default value 1.26: GJ/m^3

Battery characteristics are defined by minimal and maximal values of the obtained range and its median. This median is used as default value. Default values determined for Li-ion batteries are approximately equal to reported GEDs and VEDs of existing Li-ion batteries. [89]

Volumetric and gravimetric energy densities of batteries are defined by the amount of energy stored. This, however, is not equal to the amount of usable energy from batteries. The amount of usable energy from batteries is defined by the roundtrip efficiency. This efficiency is 80 – 95 % for Li-ion batteries. A general accepted standard effeciency is 90 % for this type of batteries. [53,100]

Li-air batteries are predicted to have a roundtrip efficiency between 80 and 90 %. An efficiency of 85 % is generally assumed in literature.[52,101]

Predicted roundtrip efficiencies for Li-S batteries vary from 78 – 91 %. 85 % is regarded as standard efficiency. [102]

Li-ion prices are projected to drop from approximately 250 USD/kWh now to as low as 73 USD/kWh in the future. The U.S. Advanced Battery Consortium has defined a price of less than 150 USD/kWh to be an achievable goal in the near future. Li-ion prices are therefore defined to be 73 USD/kWh (20 000 USD/GJ) as default value and 150 USD/kWh (42 000 USD/GJ) as maximum. [87,103-105]
Li-air and Li-S battery prices are not known due to the fact that such systems are not yet available. When fundamental and technological issues are resolved, a price of approximately 200 USD/kWh is speculated to be achievable. This price has a large margin of error and can only be achieved when numerous practical issues are overcome. 200 USD/kWh (56 000 USD/GJ) will be used as default price, keeping in mind that this could be very different and that these technologies could fail to work at all. [42,105,106]

© COPYRIGHT OF C-JOB, WHOSE PROPERTY, THIS DOCUMENT REMAINS. NO PART THEREOF MAY BE DISCLOSED, COPIED, DUPLICATED OR IN ANY OTHER WAY MADE USE OF EXCEPT WITH THE APPROVAL OF C-JOB.

3.3.5 Overview of energy storage densities

Main characteristics of energy storage systems have been described in the past section. These characteristics are used in chapter 4 to determine the total weight, mass, investment cost and daily energy consumption per power plant configuration. Volumetric and gravimetric energy densities are defined for every energy storage system as well as initial investment costs. Each characteristic is defined by a minimum, default and maximum value, based on literature and supplier data. Table 3-8 provides an overview of defined gravimetric energy densities, Table 3-9 summarizes volumetric energy densities and initial investment costs are displayed in Table 3-10.

Maximum filling levels are defined for LNG and ammonia storage systems according to current regulation. Batteries are characterized by a roundtrip efficiency defined per battery type.

Table 3-8: Considered default, minimum and maximum gravimetric densities per energy storage system.

GJ/TON	DEFAULT	MINIMUM	MAXIMUM
LNG	25.4		
H_2 AT 350 BAR	7.0	3.0	15.0
H_2 AT 700 BAR	6.5	2.4	13.2
H_2 AT -253 °C	9.0	6.6	15.0
NH_3	13.6	13.0	14.6
LI-ION	0.58	0.18	1.08
LI-AIR	2.52	0.97	6.12
LI-S	1.36	0.54	2.88

Table 3-9: Considered default, minimum and maximum volumetric densities per energy storage system.

GJ/M^3	DEFAULT	MINIMUM	MAXIMUM
LNG	15.3		
H_2 AT 350 BAR	2.0	1.8	2.4
H_2 AT 700 BAR	3.2	2.0	4.0
H_2 AT -253 °C	4.3	4.0	5.4
NH_3	10.5	10.4	10.7
LI-ION	1.44	0.36	3.49
LI-AIR	2.52	0.90	4.68
LI-S	1.26	0.61	3.56

Table 3-10: Storage system investment prices.

USD/GJ	DEFAULT	MINIMUM	MAXIMUM
LNG	400		
H_2 AT 350 BAR	560 (2 USD/kWh)	560 (2 USD/kWh)	3 600 (13 USD/kWh)
H_2 AT 700 BAR	560 (2 USD/kWh)	560 (2 USD/kWh)	4 200 (15 USD/kWh)
H_2 AT -253 °C	560 (2 USD/kWh)	560 (2 USD/kWh)	1 400 (5 USD/kWh)
NH_3	40		
LI-ION	20 000 (73 USD/kWh)	20 000 (73 USD/kWh)	42 000 (150 USD/kWh)
LI-AIR	56 000 (200 USD/kWh)	56 000 (200 USD/kWh)	∞ (not possible)
LI-S	56 000 (200 USD/kWh)	56 000 (200 USD/kWh)	∞ (not possible)

From these tables it is clear that ammonia storage is considerably cheaper than other systems and the weight and volume of such a system is relatively certain due to a narrow range of gravimetric and volumetric energy densities. This is the result of the fact that such systems already exist, and relatively mild storage conditions of ammonia compared to other fuels.

© COPYRIGHT OF C-JOB, WHOSE PROPERTY, THIS DOCUMENT REMAINS. NO PART THEREOF MAY BE DISCLOSED, COPIED, DUPLICATED OR IN ANY OTHER WAY MADE USE OF EXCEPT WITH THE APPROVAL OF C-JOB.

3.4 Energy converter characteristics

Each type of energy converter has different favorable and unfavorable characteristics. A selection of these characteristics is evaluated during the power plant comparison. Engine efficiency, GHG emissions, specific mass and specific volume of each energy converter is therefore reported in the sections below. These characteristics are determined at 85 % MCR, also known as continuous service rating (CSR). Each characteristic will be defined by a minimum, maximum and default value based on literature and supplier data. Results of this paragraph and of paragraph 3.3 are used to determine evaluation parameters, established in section 3.1, for each power plant discussed in chapter 4.

Characteristics of internal combustion engines are described per operating fuel in paragraph 3.4.1. An LNG-fueled ICE is discussed first. This engine will be used in the default configuration of chapter 4 and will therefore be defined solely by a default specific mass (ton/MW), specific volume (m^3/MW) and efficiency. Investment costs are considered to be variable. Characteristics of hydrogen fueled ICEs and ICEs fueled by an ammonia hydrogen mixture are subsequently discussed. Characteristics of these engines will be defined by a minimum, default and maximum value.

3.4.2 concerns fuel cell characteristics based on existing systems, expert opinion and literature. PEMFCs are discussed first, MCFCs second, third are hydrogen fueled SOFCs and ammonia fueled SOFCs are last.

Ammonia reformer characteristics are discussed in subsection 3.4.3.

Lastly, a summary of established energy converter characteristics is given in 3.4.4.

3.4.1 Internal combustion engine

ICEs fueled by three different fuels, but using the same technique, are taken into consideration as stated in paragraph 2.3.1.

LNG fueled ICE

LNG fueled engines are currently used in maritime operations and characteristics of these engines are therefore used when assessing required weight, volume and emissions of the reference configuration. Size, weight and efficiency of state of the art LNG fueled engines are taken into account when assessing LNG fueled engines of 2050. From manufacturer data it appears that a typical gas engine weights approximately 12 ton/MW MCR and requires a volume of 15 m^3/MW MCR resulting in an overall density of 0.8 ton/m^3. These engines have a typical specific energy consumption of approximately 7500 kJ/kWh, equal to an efficiency of 48 %.[6,107] This is in accordance with the range of 40 – 50 % found in literature. [108]

A price level of 125 – 350 USD/kW is generally assumed for diesel engines. [64,109,110] This will therefore be used during the power plant evaluation. A default price of 350 USD/kW will be used due to limited expected technological improvements for this type of energy converter. These prices will also be used for a hydrogen and ammonia fueled engine, because these engines operate in a similar manner and no commercial prices of H_2 and NH_3 fueled ICEs are provided in literature. [99]

Diesel generator sets are assumed to cost as low as 1000 USD/kW output energy according to a report composed for the New Zealand Electricity Commission. [111] CSIRO, IEA and the U.S. Department of Energy report prices between 800 and 3000 USD/kW for a natural gas fueled power plant.[112-114] Diesel generator prices for maritime applications are generally estimated to be 750 USD/kW. [6] Taking engine prices into account, generator prices are estimated to be 400 USD/kW.

© COPYRIGHT OF C-JOB, WHOSE PROPERTY, THIS DOCUMENT REMAINS. NO PART THEREOF MAY BE DISCLOSED, COPIED, DUPLICATED OR IN ANY OTHER WAY MADE USE OF EXCEPT WITH THE APPROVAL OF C-JOB.

Greenhouse gas emissions are dominated by CO_2 emissions. These are estimated to be 450 g/kWh based on supplier data and literature. [73,107,115,116]

CH_4 emissions (sometimes called methane slip) are typically equal to 4 – 8 g/kWh. Literature advises to use 5 g/kWh.[115-117]

Due to the IMO Tier III regulations are NO_X emissions of gas fueled engines kept below 2 g/kWh. This implies that a NO_X reducing unit will not be necessary on board and is therefore not considered for the reference case. NO_X emissions are considered to be equal to 1.5 g/kWh. [6,107,115-117]

Table 3-11: Main characteristics of an LNG-fueled internal combustion engine based on literature.

ICE + LNG		DEFAULT	MINIMUM	MAXIMUM
Efficiency	[%]	48	40	50
CO_2	[g/kWh]	450		
CH_4	[g/kWh]	5		
NO_X	[g/kWh]	1.5		
Specific volume	[m^3/MW]	15		
Specific mass	[ton/MW]	12		
Investment price	[USD/kW]	350	125	350

Hydrogen fueled ICE

Research institutes as well as manufacturers are investigating hydrogen fueled internal combustion engines (HICE). Most of these researches concern combustion processes of hydrogen within the engine and hereby induced emissions. Hydrogen is characterized by a higher flame speed and combustion temperature compared to LNG. These characteristics are favorable for the formation of NO_X. However, controlling the air/fuel ratio, compression ratio and ignition timing makes it possible to control combustion temperature and mean effective pressure (BMEP) resulting in lower NO_x emissions. This also negatively affects the engine efficiency. Based on data obtained from research papers, it is determined that HICEs are capable of meeting IMO Tier III regulations and therefore do not require a NO_X reducing unit. NO_X emissions are considered to be the maximum allowable amount (2 g/kWh), because lowering NO_X emissions has a negative effect on the efficiency of the engine.

Reported efficiencies vary between 40 and 55 %. When taking the determined maximum NO_X emission, an efficiency of 43% seems to be representative.

Hydrogen fueled engines are larger and heavier than engines fueled by fossil fuels. This results in a specific volume of 15 – 20 m^3/MW and 12 – 16 ton/MW. [14,58,118-123]

Table 3-12: Main characteristics of a hydrogen fueled internal combustion engine based on literature.

ICE + H_2		DEFAULT	MINIMUM	MAXIMUM
Efficiency	[%]	43	40	55
CO_2	[g/kWh]	0	0	0
CH_4	[g/kWh]	0	0	0
NO_X	[g/kWh]	2	1	2
Specific volume	[m^3/MW]	18.5	15	20
Specific mass	[ton/MW]	15	12	16
Investment price	[USD/kW]	350	125	350

© COPYRIGHT OF C-JOB, WHOSE PROPERTY, THIS DOCUMENT REMAINS. NO PART THEREOF MAY BE DISCLOSED, COPIED, DUPLICATED OR IN ANY OTHER WAY MADE USE OF EXCEPT WITH THE APPROVAL OF C-JOB.

Ammonia fueled ICE

Ammonia is characterized by a low burning velocity and narrow flammability limit (15 – 25 % in air). This imposes difficulties at the start of the combustion process. However, these problems are solved by adding a small amount of hydrogen. As mentioned before, hydrogen in characterized by a high flame speed and flame temperature which improves the combustion process. [124]

Multiple researches concern efficiencies and emissions of ICEs fueled by different ammonia/hydrogen mixtures. Volumetric percentages of 5 – 30 % hydrogen are investigated, but 10 vol.% hydrogen seems to be the most common composition.[85,124-126]

NO_X emissions are a serious problem when using ammonia in an ICE. The use of ammonia lowers the maximum combustion temperature resulting in less thermal NO_X formation. However, due to the presence of nitrogen in the fuel itself, more NO_X originating from the fuel are formed. Literature states that NO_X emissions could be reduced to below 1 g/kWh, but can also exceed IMO Tier III limits, depending on engine characteristics and ignition conditions (e.g. ignition timing and air-fuel ratio). To prevent the use of a NO_X reducing unit, a maximum NO_X emission of 2 g/kWh will be used. This will be at the expense of efficiency similar to a hydrogen engine. Uncombusted ammonia could be present in the engine exhaust, however, little research has been done regarding these emissions. Reported concentrations of ammonia in the exhaust gas are below 100 ppm. More research is required to fully understand and model the amount of unburned ammonia.[14,85,126-131]

Efficiencies between 40 and 55 % have been reported, but most paper report efficiencies of approximately 45 %. These numbers are therefore used in the evaluation. Weights and main dimensions of ammonia fueled engines are not given in literature. However, since one paper describes a test with ammonia/hydrogen mixtures in an engine designed for pure hydrogen fuel, similar volume and mass requirements are assumed.[124,129-132]

Table 3-13: Main characteristics of an ammonia fueled internal combustion engine based on literature.

ICE + NH_3		DEFAULT	MINIMUM	MAXIMUM
Efficiency	[%]	45	40	55
CO_2	[g/kWh]	0	0	0
CH_4	[g/kWh]	0	0	0
NO_X	[g/kWh]	2	1	2
Specific volume	[m^3/MW]	18.5	15	20
Specific mass	[ton/MW]	15	12	16
Investment price	[USD/kW]	350	125	350

© COPYRIGHT OF C-JOB, WHOSE PROPERTY, THIS DOCUMENT REMAINS. NO PART THEREOF MAY BE DISCLOSED, COPIED, DUPLICATED OR IN ANY OTHER WAY MADE USE OF EXCEPT WITH THE APPROVAL OF C-JOB.

3.4.2 Fuel cell

Efficiencies, specific masses and specific volumes are estimated for each type of fuel cell. Fuel cell systems are composed of fuel cell stacks and Balance of Plant (BoP) components as already explained in section 2.3.2. The total weight and volume of a fuel cell is greatly influenced by the BoP components. Specific volumes and masses of fuel cells will be determined, based on manufacturer data and literature. These volumes and masses are corrected to obtain feasible specific masses and volumes for 2050. Expert opinion [133] states that fuel cell systems will considerably reduce in weight and volume in coming decades. This is due to a better integration of BoP components, advances in technology and application changes for the systems. GHG emissions of fuel cells are considered negligible due to the fuel and combination of operating conditions. No carbon containing fuels are used, resulting in zero fuel related CO_2 and CH_4 emissions. NO_X formation is negligible due to the combination of low pressure and operating temperatures within the fuel cell.[14,38,60,134-139]

Notable differences of considered fuel cell systems compared to present day systems

Figure 3-6 provides an example of a SOFC fueled by natural gas which is currently the most common fuel for operational SOFCs and MCFCs. A 3D representation of such a fuel cell can be found in appendix B, Figure B-3. This configuration requires the decomposition of methane (CH_4) into H_2 and CO_2 before the fuel can be used in the SOFC. This decomposition occurs at the reformer unit as shown in Figure 3-6. Both fuel cell types convert up to 90 % of the supplied H_2 into water and electric energy. Remaining H_2 leaving the anode of the fuel cell is burned in the tail gas combustor to prevent the emission of unburned fuel and to supply heat to the preheater/reformer. The reformer requires this heat to decompose methane into H_2 and CO_2. [140]

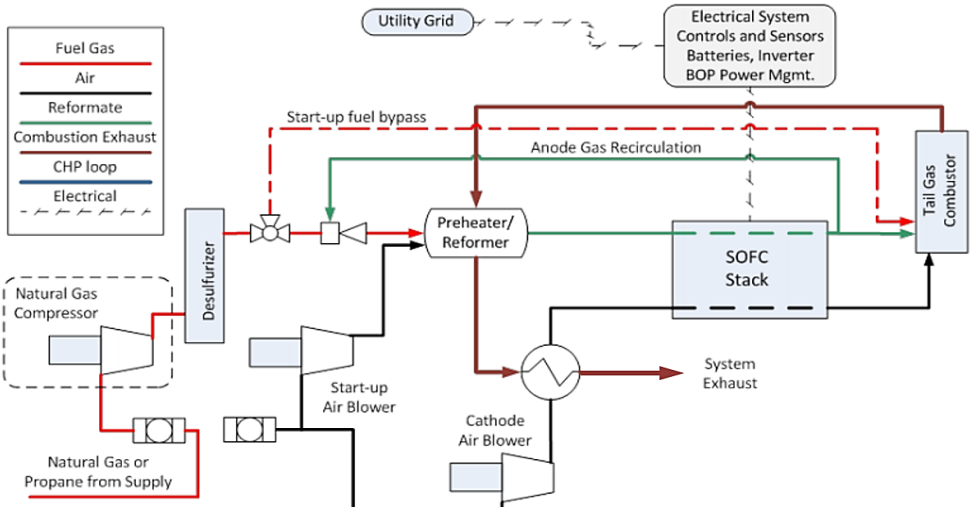

Figure 3-6: Schematic diagram of a methane fueled solid oxide fuel cell system. [141]

Fuel reformers are not required for the operation of a fuel cell when it is fueled by pure hydrogen. This results in more available waste heat from the tail gas combustor (this remains required to prevent unburned fuel to be emitted) resulting in the possibility to generate additional power by means of a waste heat recovery system. However, such a system is not included in the BoP of the considered configurations because the amount of waste heat that can be utilized to generate additional electrical output power is not known due to a lack of research on this subject.

When an ammonia reformer is required for a configuration, it is considered as a separate system and not part of the BoP mass and volume.

© COPYRIGHT OF C-JOB, WHOSE PROPERTY, THIS DOCUMENT REMAINS. NO PART THEREOF MAY BE DISCLOSED, COPIED, DUPLICATED OR IN ANY OTHER WAY MADE USE OF EXCEPT WITH THE APPROVAL OF C-JOB.

A MCFC uses CO_2 for the transportation of oxygen ions through the membrane of the fuel cell as can be seen in Figure 3-7. Present day MCFC systems are fueled by natural gas and use CO_2 originating from this fuel for the transportation of oxygen ions. Considered MCFC systems are fueled by pure hydrogen and therefore require internally recirculating CO_2 to operate. CO_2 slip is assumed to be negligible due to the lack of information concerning CO_2 slip of such a system. [60,135]

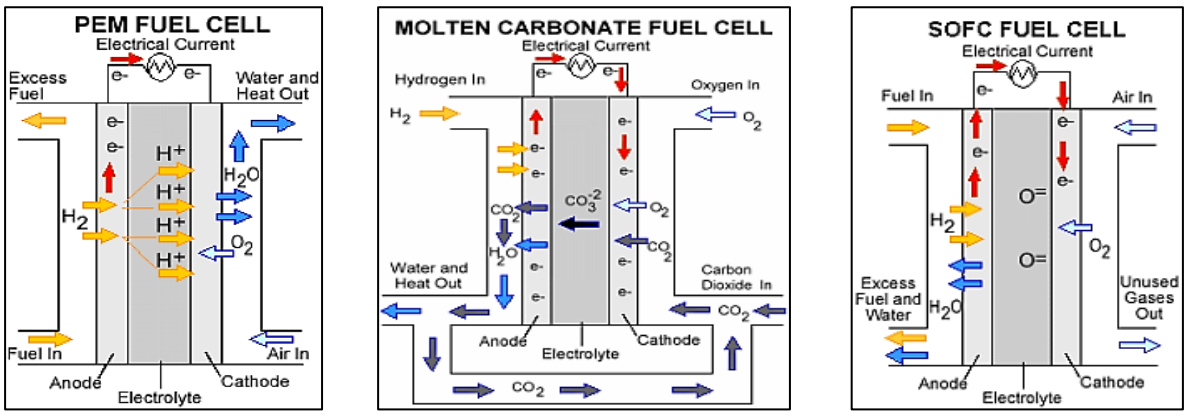

Figure 3-7: Schematic representation of considered types of fuel cells. [63]

Proton Exchange Membrane Fuel Cell (PEMFC) systems

PEMFCs are currently predominantly researched for mobile applications due to its relatively low specific volume and weight. Most researches are therefore focused on road transport and thus relatively small power requirement. [63,142,143] Reported specific weights (SPM) of PEMFCs are ranging from 2 – 13 ton/MW. Most of these systems require approximately 5 ton/MW. [38,144-146] Experts expect a specific mass of approximately 1 ton/MW in the future.[38,63,133] Based on this information is a maximum SPM of 5 ton/MW assumed, a default SPM of 1 ton/MW and a minimum of 0.5 ton/MW. This is based on fuel cell performance equal to current, expected future and two times as good as expected performance, respectively. Minimal values for specific weight and specific volume are for PEMFCs and MCFC based on systems performing two times as good as expert opinion states. This to account for the fact that the impact of future developments on such systems is highly uncertain resulting in the possibility that future systems perform considerably better than expected.

Specific volumes (SPV) of PEMFCs are currently 7 m^3/MW on average. However expert opinion predicts that only a tenth of this volume will be required in the future, resulting in an expected specific volume of 0.7 m^3/MW.[38,63,135,145-147] A maximum SPV of 7 m^3/MW will be used and a minimum of 0.4 m^3/MW. 0.7 m^3/MW will be used as default specific volume for PEMFCs.

- Specific volume: Range: 0.4 – 7 m^3/MW Default: 0.7 m^3/MW
- Specific mass: Range: 0.5 – 5 ton/MW Default: 1 ton/MW

The U.S. Department of Energy has reported a PEMFC system cost of approximately 50 USD/kW for mass produced automotive sized fuel cells. Future targets are 40 and 30 USD/kW for this kind of PEMFCs. Larger scale systems are expected to be more expensive due to a lower production quantity. The price of such systems is estimated to be 600 USD/kW, but considerable cost improvements are expected by experts. A minimum price for large scale PEMFC systems is therefore estimated to be 300 USD/kW. [63,81,133,148,149]

© COPYRIGHT OF C-JOB, WHOSE PROPERTY, THIS DOCUMENT REMAINS. NO PART THEREOF MAY BE DISCLOSED, COPIED, DUPLICATED OR IN ANY OTHER WAY MADE USE OF EXCEPT WITH THE APPROVAL OF C-JOB.

Molten Carbonate Fuel Cell (MCFC) systems

Although MCFCs have been actively researched in the past and they are considered to be the most developed type of fuel cell, the capital investment cost is still very high. This in combination with the limited electrical efficiency and low power density has resulted in a declining interest in this type of fuel cells. Current available MCFC systems are reported to require 125 ton/MW and 500 m^3/MW. These systems are used for land-based electricity generation in which weight and volume does not play a significant role during the design process. Expert opinion states that future MCFCs will require approximately 40 ton/MW and 50 m^3/MW. [38,133,134,150-152] Based on this data and expert opinion are the following MCFC characteristics determined to be used:

-
- Specific volume: Range: 25 – 500 m^3/MW Default: 50 m^3/MW
- Specific mass: Range: 20 – 125 ton/MW Default: 40 ton/MW

Maximum values are determined to be equal to current system requirements, default values are equal to achievable values according to expert opinion. Minimum values are half the achievable values according to experts.[38,133,151]

MCFC are currently very expensive with prices over 5000 USD/kW. Given the expected limited future development of these fuel cells, experts estimate that such systems will cost approximately 1000 USD/kW in the future. These will be minimal and maximal considerate prices for these systems. A default price of 2000 USD/kW is used.[38,103,133]

Hydrogen fueled Solid Oxide Fuel Cell (H_2 SOFC) systems

Current SOFC systems are designed for land based electric power generation and not required to be space or weight efficient, similar to MCFCs. Commercially available systems are currently fueled by natural gas and require ±125 m^3/MW and ±50 ton/MW.[38,150,153-155] Existing SOFC system concept designs are claiming a specific volume requirement of 33.3 m^3/MW and 8.7 ton/MW specific mass. [156] According to expert opinion, a SOFC volume and mass of 30 m^3/MW and 12 ton/MW is to be expected in the future.[38,133] One paper estimates future SOFC SPV and SPM to be 7 m^3/MW and 3 ton/MW. [151] Expert opinion will be used as default values for the SOFC. Minimal SPM and SPV are obtained from [151] and maximal values are equal to existing SOFC characteristics. This results in the following values for SOFC characteristics:

- Specific volume: Range: 7 – 125 m^3/MW Default: 30 m^3/MW
- Specific mass: Range: 3 – 50 ton/MW Default: 12 ton/MW

These values are based on natural gas fueled SOFC system including a fuel reformer and desulfurization unit. These units are not required when fueled by pure hydrogen, but the effect of these units is considered to be within the uncertainty of future systems. [133]

Large scale production price estimations of SOFCs are reported to be as low as 750 USD/kW. However, these reported systems are fueled by natural gas and therefore include unnecessary systems such as waste heat recovery systems and fuel reformers. This, in combination with expert expectation that SOFCs will improve considerably, it is estimated that a SOFC system could cost as low as 400 USD/kW.

© COPYRIGHT OF C-JOB, WHOSE PROPERTY, THIS DOCUMENT REMAINS. NO PART THEREOF MAY BE DISCLOSED, COPIED, DUPLICATED OR IN ANY OTHER WAY MADE USE OF EXCEPT WITH THE APPROVAL OF C-JOB.

Ammonia fueled Solid Oxide Fuel Cell (NH_3 SOFC) systems

Direct ammonia fueling of SOFCs has been proven to be possible with current technology and SOFCs. Especially Ni-YSZ[4] anodes are recommended because nickel acts as a catalyst for the decomposition of ammonia at the anode and therefore speeding up the decomposition, reaching a very high conversion. An ammonia fueled SOFC system possesses several favorable qualities with respect to natural gas fueled SOFCs. This includes the absence of a fuel reformer and the cooling effect of ammonia on the fuel cell, resulting in less cooling air required at the cathode of the fuel cell. Therefore, a direct ammonia fueled SOFC will require smaller heat exchangers for the air flow and less parasitic power losses. Concluding from this it can be stated that a NH_3 fueled SOFC system requires less volume and weight for auxiliary components compared to a H_2 fueled SOFC system. However, from the same researches it appears that the power density of the fuel cell stack slightly decreases due to the ammonia reforming. Information from literature has proven insufficient to establish a specific volume and mass for future NH_3 SOFC systems. Based on this information and expert opinion, specific volume and mass are assumed to be equal for a H_2 and NH_3 fueled SOFC system.[133,136,157-167]

No investment cost estimations are available for ammonia fueled SOFC. Due to the great similarity between hydrogen and ammonia fueled SOFCs, are similar prices as for hydrogen fueled SOFCs assumed.

Efficiency

Electrical efficiencies of the different fuel cell systems are determined using reported electrical efficiencies retrieved from manufacturer data and research papers. Table C-15 in appendix C provides an overview of found electrical efficiencies. This data is visualized in Figure 3-8 and based on this are the following efficiencies determined:

- PEMFC: Range: 35 – 65 % Default: 47 %
- MCFC: Range: 40 – 55 % Default: 50 %
- SOFC: Range: 43 – 68 % Default: 55 %
- NH_3 SOFC: Range: 47 – 70 % Default: 60 %

From this figure it appears that a PEMFC has the lowest average electrical efficiency, but also the potential to achieve high electrical efficiencies. This is due to the fact that PEMFC systems are considered to be the future energy converter for road transport as previously mentioned. This has resulted in a wide range of different reported PEMFC compositions and therefore different electrical efficiencies.[168,169]

[4] Yttria stabilized zirconia ($(ZrO_2)_{0.85}(Y_2O_3)_{0.15}$ or YSZ) is currently the most commonly used anode material in SOFCs and is also the most actively researched anode material. Ni-YSZ is a mixture of YSZ and nickel oxide (NiO) powder and is also used in known SOFCs. [137], [156]

© COPYRIGHT OF C-JOB, WHOSE PROPERTY, THIS DOCUMENT REMAINS. NO PART THEREOF MAY BE DISCLOSED, COPIED, DUPLICATED OR IN ANY OTHER WAY MADE USE OF EXCEPT WITH THE APPROVAL OF C-JOB.

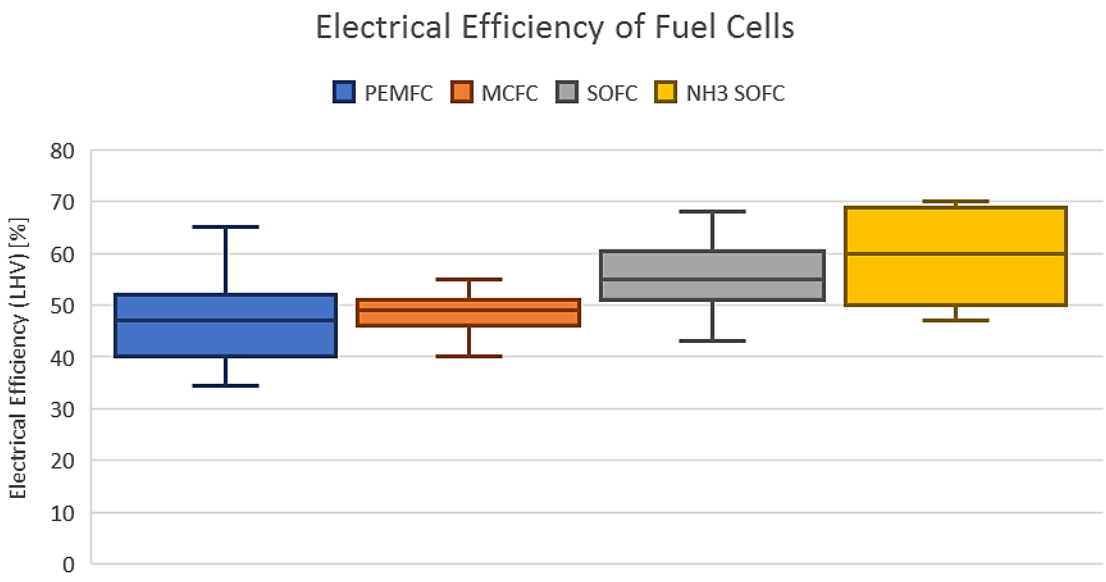

Figure 3-8: Electrical efficiency of fuel cells based on LHV based on literature.

MCFC have been actively researched in the past, however due to the mediocre electrical efficiency and low energy density, interest in these fuel cells has decreased considerably in past decades. This has resulted in a relative narrow range of reported electrical efficiencies. [170]

Experts consider the SOFC to be the large-scale energy converter of the future. This is due to its relatively high electrical efficiency and the possibility to recover energy from waste heat. This has resulted in an increased interest in these fuel cells, resulting in a wide range of reported electrical efficiencies. An ammonia fueled SOFC is characterized by higher efficiencies compared to a hydrogen fueled SOFC because of the cooling effect of ammonia on the fuel cell and the fact that these cells are reported to operate at a higher temperature.[38,155,158,171,172]

3.4.3 Ammonia reformer

Configurations AC1 – AC4 require an ammonia reformer to obtain hydrogen from ammonia. Three basic types of reformers currently exist: thermal, electric and catalytic. Thermal and electric reformers are currently used in industry and are available for commercial use. These types of reformers are relatively large compared to catalytic reformers. Typical thermal and electric reformers require approximately 25 m^3/MW hydrogen gas, while catalytic reformers only require 0.01 – 0.6 m^3/MW reactor volume. Although reactor volume is not equal to the total volume of a reformer, it can be regarded as an indication. Future ammonia reformers are estimated to require 8 m^3/MW and 4 ton/MW. These estimations are based on the opinion of several experts found in different research papers. Large deviations from these characteristics will be used when assessing the configurations as is documented in Table 3-14.[173-180]

© COPYRIGHT OF C-JOB, WHOSE PROPERTY, THIS DOCUMENT REMAINS. NO PART THEREOF MAY BE DISCLOSED, COPIED, DUPLICATED OR IN ANY OTHER WAY MADE USE OF EXCEPT WITH THE APPROVAL OF C-JOB.

The energy efficiency of the ammonia reformer is defined as:

$$\eta_{reformer} = \frac{3 * \Delta H_{H_2}}{2 * \Delta H_{NH_3} + E_{el} + Q}$$

Where ΔH_{H_2} is equal to the LHV of hydrogen (242.7 kJ/mol) and ΔH_{NH_3} is equal to the LHV of ammonia (320.1 kJ/mol). Since two moles ammonia decomposes in three moles hydrogen, the LHV of hydrogen and ammonia are multiplied by three and two, respectively. Electrical energy (E_{el}) and heat (Q) are externally added. [181]

Reported energy efficiencies of ammonia reformers are ranging from 88 – 97 %. 90 % energy efficiency seems to be the standard practical value used. Less efficient reformers are often not considered to be sufficiently effective.[38,178-187]

Ammonia reformers are already produced at approximately 250 USD/kW hydrogen output. [173] This will therefore be used as price for an ammonia reformer.

Table 3-14: Characteristics of the ammonia reformer.

NH_3 REFORMER		DEFAULT	MINIMUM	MAXIMUM
Efficiency	[%]	90	88	97
CO_2	[g/kWh]	0	0	0
CH_4	[g/kWh]	0	0	0
NO_X	[g/kWh]	0	0	0
Specific volume	[m^3/MW]	8	4	20
Specific mass	[ton/MW]	4	2	10
Investment price	[USD/MW]	250		

3.4.4 Overview

From previous paragraphs it appears that greenhouse gasses are emitted when an internal combustion engine is used. Carbon related emissions only occur when a carbon containing fuel is used, but NO_X emissions are likely to occur using any fuel. Furthermore, ICEs are not expected to drastically evolve in coming decades, but fuel cells are expected to improve considerably. However, characteristics of these fuel cells are highly uncertain due to expected significant improvements of fuel cells. This has resulted in a wide range of documented and expected specific masses, specific volumes, investment costs and efficiencies. Considered values are documented in Table 3-15 – Table 3-18.

Table 3-15: Default, minimum and maximum efficiencies of energy converters used to assess power plant configurations.

%	DEFAULT	MINIMUM	MAXIMUM
ICE on LNG	48		
ICE on Hydrogen	43	40	55
ICE on Ammonia	45	40	55
PEMFC	47	35	65
MCFC	50	40	55
SOFC on Hydrogen	55	43	68
SOFC on Ammonia	60	47	70
Ammonia Reformer	90	88	97
EG	97		

© COPYRIGHT OF C-JOB, WHOSE PROPERTY, THIS DOCUMENT REMAINS. NO PART THEREOF MAY BE DISCLOSED, COPIED, DUPLICATED OR IN ANY OTHER WAY MADE USE OF EXCEPT WITH THE APPROVAL OF C-JOB.

Table 3-16: Specific masses of energy converters used to assess power plant configurations.

TON/MW	DEFAULT	MINIMUM	MAXIMUM
ICE on LNG	12		
ICE on Hydrogen	15	12	16
ICE on Ammonia	15	12	16
PEMFC	1	0,5	5
MCFC	40	20	125
SOFC on Hydrogen	12	3	50
SOFC on Ammonia	12	3	50
Ammonia Reformer	4	2	10
EG	3.9		

Table 3-17: Specific volumes of energy converters used to assess power plant configurations.

M^3/MW	DEFAULT	MINIMUM	MAXIMUM
ICE on LNG	15		
ICE on Hydrogen	18,5	15	20
ICE on Ammonia	18,5	15	20
PEMFC	0,7	0,4	7
MCFC	50	25	500
SOFC on Hydrogen	30	7	125
SOFC on Ammonia	30	7	125
Ammonia Reformer	8	4	20
EG	3.8		

Table 3-18: Initial investment costs of energy converters used to assess power plant configurations.

USD/KW	DEFAULT	MINIMUM	MAXIMUM
ICE on LNG	350	125	350
ICE on Hydrogen	350	125	350
ICE on Ammonia	350	125	350
PEMFC	300	300	600
MCFC	2 000	1 000	5 000
SOFC on Hydrogen	750	400	1 200
SOFC on Ammonia	750	400	1 200
Ammonia Reformer	250		
EG	400		

© COPYRIGHT OF C-JOB, WHOSE PROPERTY, THIS DOCUMENT REMAINS. NO PART THEREOF MAY BE DISCLOSED, COPIED, DUPLICATED OR IN ANY OTHER WAY MADE USE OF EXCEPT WITH THE APPROVAL OF C-JOB.

3.5 Summary

The first section of chapter 2 describes general operational requirements of a representative ROPAX ferry build in 2050 based on a market research. Following sections assess different energy carriers and energy converters which could be used to supply a future ferry with the energy it requires to operate. This ended in the composition of different power plant configurations that will be assessed in chapter 4. These configurations are simplified representations containing only main components of a power plant, being an energy storage system and one or more energy converters. An overview of considered power plant configurations can be found in section 2.4, Table 2-12.

After defining power plant configurations that will be evaluated, assessment characteristics are determined in the first section of chapter 3. These characteristics are used to qualitatively compare different power plant configurations in chapter 4. Power plant characteristics that will be evaluated are:

- CO_2 equivalent pollutant emission
- Daily energy cost
- Initial investment cost
- Total power plant volume
- Total power plant mass

The price of energy is determined in section 3.2. The price of LNG is defined as the summation of the gas price, liquefaction cost and a carbon emission price. Future electricity price estimations are based on studies concerning future prices of renewable energy. Hydrogen and ammonia produced using electric energy are considered for the price estimation of these synthetic fuels linking it directly to commercial electricity prices. Price estimations for hydrogen and ammonia fabricated by utilizing excess energy from renewable energy resources are also given. An overview of these prices is given in Table 3-7.

Main characteristics of energy storage systems and energy converters are described in sections 3.3 and 3.4, respectively. These main characteristics are used to determine the weight, volume, daily energy cost, investment cost and CO_2 equivalent pollutant emission of each power plant configuration as is described in section 3.1. Characteristics are defined by a minimum, default and maximum value based on literature, expert opinion and supplier data. The results of this study are summarized in paragraphs 3.3.5 and 3.4.4.

© COPYRIGHT OF C-JOB, WHOSE PROPERTY, THIS DOCUMENT REMAINS. NO PART THEREOF MAY BE DISCLOSED, COPIED, DUPLICATED OR IN ANY OTHER WAY MADE USE OF EXCEPT WITH THE APPROVAL OF C-JOB.

4 Power plant design

Given all previously determined energy carrier, energy storage and energy converter characteristics, a variation study is performed to determine the most feasible power plant configuration for a representable ROPAX ferry constructed in 2050. This study is performed in three stages, each stage eliminating power plant configurations until a single configuration is left to be used during the concept design of the ferry.

Stage 1 is named the default stage. Established default values of energy storage system and energy converter characteristics, determined in sections 3.3 and 3.4 of the previous chapter, are used to determine main characteristics of each power plant configuration and compare the results. This is described in section 4.1.

The second stage is a sensitivity analysis in which power plant characteristics, such as weight and volume, are determined by a variance study. Random values for energy storage system and energy converter characteristics, between predefined minimum and maximum values, are used to obtain a range of power plant characteristics for each power plant configuration. By defining numerous sets of random variables, used to calculate power plant characteristics, a wide variety of possible future scenarios is obtained. The result of this study is a dataset of over 170 different unbiased scenarios. Resulting power plant characteristics are documented in box and whisker plots to provide a graphical representation of the data. These plots are shown in appendix D.4. Section 4.2 elaborates on conclusions drawn from this data and section 4.2.5 provides an overview of eliminated configurations as a result of these conclusions.

From the remaining power plant configurations, a single power plant configuration is deemed to be the most feasible option for a representative ROPAX ferry of 2050. This is the last stage of this study and described in section 4.3. This one remaining power plant configuration will be used for the concept design of a representative ferry as will be discussed in chapter 5.

Since an LNG-based configuration is used as reference configuration, a 3.5-day theoretical operation time is regarded as standard operational time (see section 2.4.1). 1 and 14-day operations are also used because a theoretical operation time of 14 days is currently considered to be representative for ROPAX ferries fueled by conventional fuels (see section 2.1) and 1-day operation is a considered to be feasible for battery powered vessels. A one-day operational time is also considered a minimal operational time given the operational profile of the representative vessel as determined in section 2.1. This operational profile includes two trips a day, but because of uncertainty concerning the exact energy consumption during a trip (caused by variation in for example weather conditions) it has been determined that a vessel is required to be capable of storing sufficient energy to theoretically operate a full day without refueling/recharging.

All results are documented in appendix D. First, input values of the energy storage systems and energy converters are provided in overview tables, such as Table 4-1 shown on the next page. Numerical output results of the calculations are given in the subsequent table. Plots showing a graphical representation of the numerical output are also provided in this appendix. Relevant plots are shown in following sections, providing graphical representations of discussed power plant characteristics.

Names of power plant configurations, as displayed in figures providing key characteristics of power plant configurations such as Figure 4-1, correspond to the names as defined in Table 2-12. Table 4-2, located on page 77, also provides an overview of every evaluated configuration.

© COPYRIGHT OF C-JOB, WHOSE PROPERTY, THIS DOCUMENT REMAINS. NO PART THEREOF MAY BE DISCLOSED, COPIED, DUPLICATED OR IN ANY OTHER WAY MADE USE OF EXCEPT WITH THE APPROVAL OF C-JOB.

4.1 Default values

Established default values of every energy storage system and energy converter unit, defined in sections 3.3 and 3.4, are used to determine the weight, volume, daily energy price, investment cost and CO_2 equivalent GHG emission of every power plant configuration. These power plant characteristics are calculated according to the calculation method as described in section 3.1. Table 4-1 provides an overview of all default input values of energy storage systems and energy converters as defined in chapter 3. Table D-2, found in appendix D.1, provides numerical results of the power plant characteristics obtained by using these input values and formulas as defined in section 3.1. Figure D-1 – Figure D-11 present graphical representations of these results.

Table 4-1: Default input values of the energy storage and energy converter units.

ENERGY STORAGE SYSTEM INPUT									
		LNG	LH_2	350 BAR H_2	700 BAR H_2	NH_3	LI-ION	LI-AIR	LI-S
ENERGY PRICE	USD/GJ	10,04	44,97	41,17	41,97	44,29	20	20	20
GRAVIMETRIC DENSITY	GJ/ton	25,4	9	7	6,5	13,6	0,58	2,52	1,36
VOLUMETRIC DENSITY	GJ/m³	15,3	4,3	2	3,2	10,5	1,44	2,52	1,26
STORAGE EFFICIENCY	%	100	100	100	100	100	90	85	85
MAX. FILLING LEVEL	%	95	100	100	100	85	100	100	100
ENERGY STORAGE PRICE	USD/GJ	400	560	560	560	40	20 000	56 000	56 000

ENERGY CONVERTER INPUT									
		LNG ICE	H_2 ICE	NH_3 ICE	PEMFC	MCFC	SOFC	NH_3 SOFC	AM-REF
SPECIFIC MASS	ton/MW	12	15	15	1	40	12	12	4
SPECIFIC VOLUME	m³/MW	15	18,5	18,5	0,7	50	30	30	8
ELECTRICAL EFFICIENCY	%	47	42	44	47	50	53	55	90
INVESTMENT PRICE	USD/kW	350	350	350	300	2 000	750	750	250
CO_2 EMISSION	g/kWh	450	0	0	0	0	0	0	0
CH_4 EMISSION	g/kWh	5	0	0	0	0	0	0	0
NO_X EMISSION	g/kWh	1.5	2	2	0	0	0	0	0

Values presented in Table 4-1 already show that only internal combustion engines are considered to emit GHGs. This is also shown in Figure 4-1. Since the performance of ICEs is limited by the amount of NO_X emitted, as discussed in section 3.4.1, are these energy converters not considered a perfect solution, but also not discarded solely based on this emission.

© COPYRIGHT OF C-JOB, WHOSE PROPERTY, THIS DOCUMENT REMAINS. NO PART THEREOF MAY BE DISCLOSED, COPIED, DUPLICATED OR IN ANY OTHER WAY MADE USE OF EXCEPT WITH THE APPROVAL OF C-JOB.

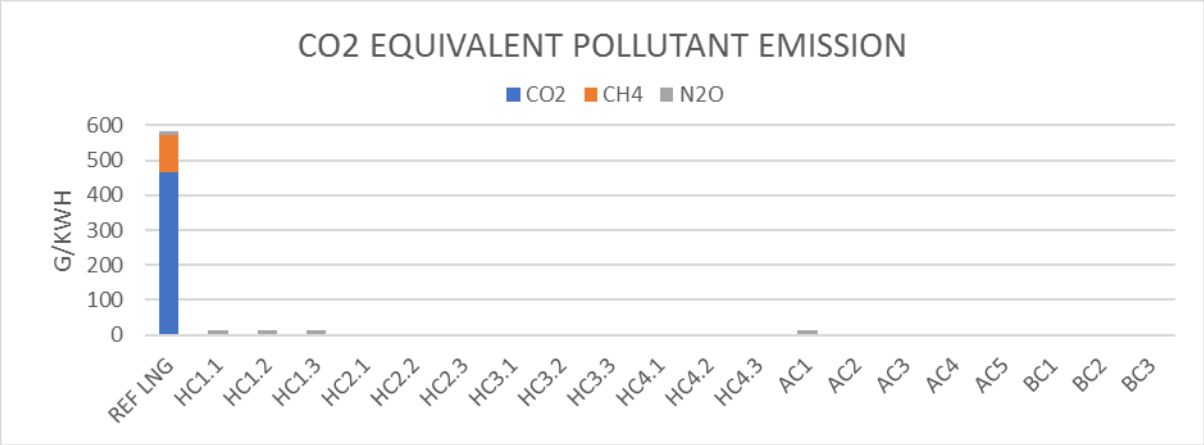

Figure 4-1: GHG emissions from default values.

Figure 4-2 shows the estimated cost of energy per day operation for all configurations. This figure shows a high cost per day when using hydrogen or ammonia with respect to LNG cost. This leads to the conclusion that synthetic fuels can only be economically feasible in the case of:

- a high LNG price including high emission tax;
- a low commercial electric energy price; or
- synthetic fuel production using excess renewable energy.

Energy costs per day of operation for configurations using ICEs (HC1.1, HC1.2, HC1.3 and AC1) are higher compared to fuel cell configurations due to a lower electrical efficiency of the energy converter resulting in a lower overall efficiency. Since the energy cost per day of operation is defined to be a function of the required output electrical energy of the power plant, the overall power plant efficiency and the price of input energy per GJ, as explained in section 3.1.2, does a decrease in overall efficiency result in an increase in required energy input, resulting in a higher daily energy cost. A PEMFC in combination with stored ammonia and an ammonia converter (AC2) is even more expensive due to the parasitic power requirement of the ammonia reformer. This high energy cost in combination with the sensitivity of a PEMFC for fuel impurities (see Table 2-7) is considered to be sufficient cause to reject configuration AC2 as possible solution.

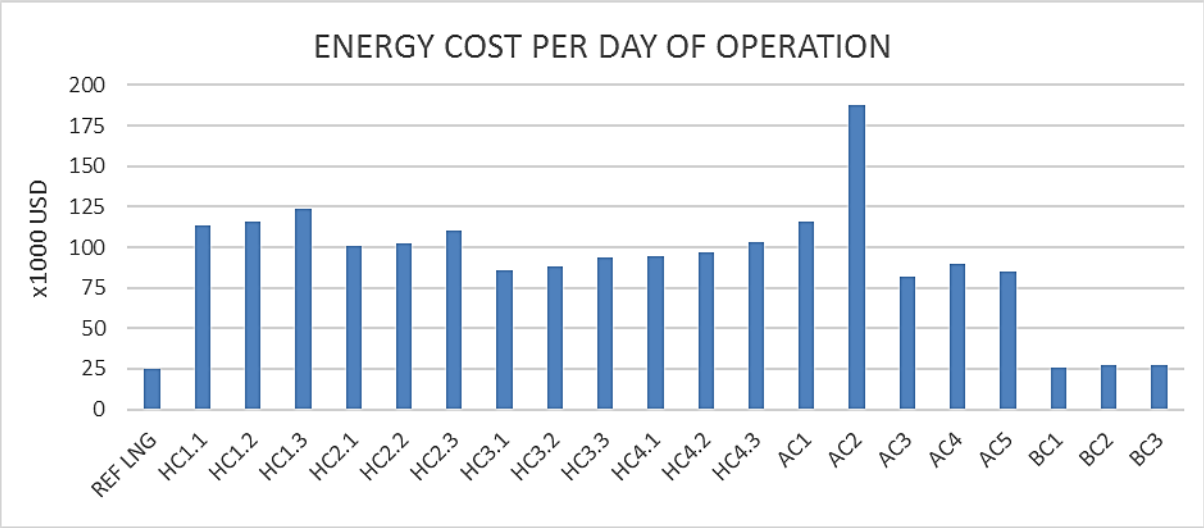

Figure 4-2: Energy cost per day using default values.

© COPYRIGHT OF C-JOB, WHOSE PROPERTY, THIS DOCUMENT REMAINS. NO PART THEREOF MAY BE DISCLOSED, COPIED, DUPLICATED OR IN ANY OTHER WAY MADE USE OF EXCEPT WITH THE APPROVAL OF C-JOB.

Battery configurations are not recommended for multiple day operations due to a high investment cost and weight of batteries shown in Figure D-2 till Figure D-7. Investment prices for battery configurations are expected to exceed those of all other configurations when a theoretical operational time of 3.5 days or 14 days is used. This is also valid for considered minimal battery prices and maximal ICE and FC prices as can be concluded from the results presented in appendices D.2 and D.3. These two appendices respectively present the best possible and worst-case scenarios of every power plant configuration showing that the most positive expected investment costs of battery configurations exceed the worst-case scenario investment cost of the reference case (38 million USD for the worst-case scenario LNG-based configuration and 86 – 994 million USD for the best-case battery configurations with a multiple day theoretical operational time).

Molten carbonate fuel cells are not considered to be a viable alternative for future power plants due to a limited electrical efficiency, high specific mass, high investment cost and limited expected future improvements resulting from decreasing interest, as already mentioned in paragraph 3.4.2. Figure 4-3 illustrates that the expected weight of MCFCs (grey parts of configurations HC4.1, HC4.2, HC4.3 and AC4) exceeds total power plant weights of all other fuel-based systems.
This figure also shows a high expected weight of Li-ion batteries (BC1). This weight is not considered high enough to immediately discard this configuration, but it is considered to be a negative attribute and will therefore be documented in Table 4-2.

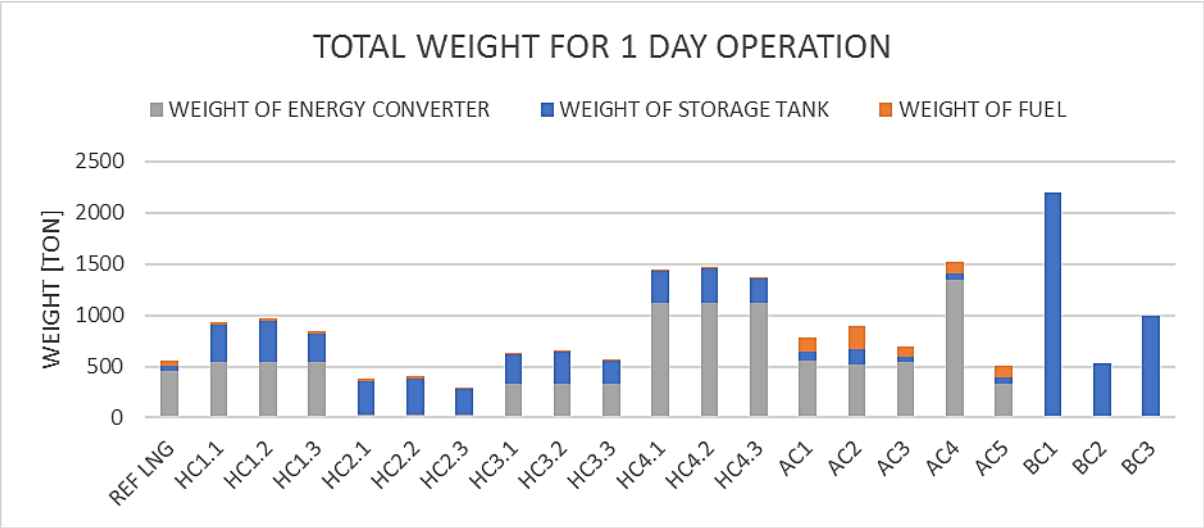

Figure 4-3: Weights for 1-day operation using default values.

© COPYRIGHT OF C-JOB, WHOSE PROPERTY, THIS DOCUMENT REMAINS. NO PART THEREOF MAY BE DISCLOSED, COPIED, DUPLICATED OR IN ANY OTHER WAY MADE USE OF EXCEPT WITH THE APPROVAL OF C-JOB.

Concluding from afore mentioned information are battery configurations discarded for multiple day operations.

MCFC based configurations are discarded due to a combination of negative attributes such as limited expected improvements and high specific weight of the system.

A PEMFC in combination with ammonia is discarded due to a high expected daily energy cost, caused by the parasitic energy requirement of the ammonia reformer.

Internal combustion engines are characterized by being the only type of energy converter emitting CO_2 equivalent GHG emissions but not yet discarded from the consideration. These engines are also characterized by a relatively lower electrical efficiency compared to fuel cells resulting in somewhat higher expected daily energy cost.

Li-ion batteries are relatively heavy, but also not yet discarded.

Table 4-2 provides an overview of all considered configurations and whether they are discarded or not. Discarded configurations are indicated by a red box with the word NO. Several configurations possess negative attributes, such as a low overall electrical efficiency, but these characteristics are not deemed severe enough to immediately discard these configurations. Such configurations are indicated by a yellow box with NEG. in it. This table will be repeated at the end of section 4.2 in which the findings of this section are included, resulting in fewer feasible power plants.

Table 4-2: Overview of configurations including discarded options after stage 1.

CONFIGURATION	ENERGY CARRIER	ENERGY CONVERTER			1-DAY	3,5-DAY	14-DAY
REFERENCE	LNG	ICE	EG		NO	**REF**	NO
HC1.1	H_2 at 350 bar	ICE	EG		NEG.	NEG.	NEG.
HC1.2	H_2 at 700 bar	ICE	EG		NEG.	NEG.	NEG.
HC1.3	LH_2	ICE	EG		NEG.	NEG.	NEG.
HC2.1	H_2 at 350 bar	PEMFC					
HC2.2	H_2 at 700 bar	PEMFC					
HC2.3	LH_2	PEMFC					
HC3.1	H_2 at 350 bar	SOFC					
HC3.2	H_2 at 700 bar	SOFC					
HC3.3	LH_2	SOFC					
HC4.1	H_2 at 350 bar	MCFC			NO	NO	NO
HC4.2	H_2 at 700 bar	MCFC			NO	NO	NO
HC4.3	LH_2	MCFC			NO	NO	NO
AC1	NH_3	ICE	EG	AM-REF	NEG.	NEG.	NEG.
AC2	NH_3	PEMFC		AM-REF	NO	NO	NO
AC3	NH_3	SOFC		AM-REF			
AC4	NH_3	MCFC		AM-REF	NO	NO	NO
AC5	NH_3	SOFC					
BC1	Li-ion				NEG.	NO	NO
BC2	Li-air					NO	NO
BC3	Li-S					NO	NO

© COPYRIGHT OF C-JOB, WHOSE PROPERTY, THIS DOCUMENT REMAINS. NO PART THEREOF MAY BE DISCLOSED, COPIED, DUPLICATED OR IN ANY OTHER WAY MADE USE OF EXCEPT WITH THE APPROVAL OF C-JOB.

4.2 Sensitivity analysis

A sensitivity study is performed in which power plant characteristics, such as weight and volume, are determined by a variance study. This method uses random values within predefined ranges, as discussed in sections 3.2.5, 3.3.5 and 3.4.4, for each characteristic of each energy storage system and energy converter. Using these sets of values as input, key power plant characteristics are determined and documented. Numerous sets of randomly assigned characteristic values result in unbiased ranges of values per key power plant characteristic. A statistical analysis of these results is performed to evaluate the performance of each configuration.

Section 4.1 has identified economic challenges of using synthetic fuels produced from commercial energy. Synthetic fuels are therefore assumed to be fabricated using excess energy from renewable resources. This is considered the most feasible solution because the carbon emission tax required to make the synthetic fuels feasible is extremely high. For example, an emission tax of ~400 $/ton CO_2 equivalent would result in an LNG price roughly equal to the default price of synthetic fuels, current estimations for future carbon taxes rarely exceed 100 $/ton CO_2 equivalent. [71]

A low commercial electric energy price could be possible, but this would require highly efficient systems and low investment prices. Although this is expected for future solar and wind farms, it is by most researches not expected to be feasible to generate electric energy at an average levelized cost of only 6 $/GJ (which would be the required price of electric energy to obtain synthetic fuel prices comparable to default LNG prices). Only the best performing wind and solar farms are expected to produce energy at such a low cost.

The existence of excess energy, when generating electric energy using solar and wind farms, has already been established in section 3.2.3. Utilizing this energy to fabricate ammonia and hydrogen would reduce the price of these synthetic fuels considerably, as discussed in the same section.

Electric energy prices used for battery configurations are commercial energy prices. This because electric energy is required to charge the batteries of the ferry whenever it arrives and not only when excess energy is available.

Numerous sets of randomly assigned characteristic values result in ranges of values per key power plant characteristic. Appendix D.4 provides a graphical overview of the results of this study. These results lead to multiple conclusions with respect to weight, volume and cost of a configuration, energy converter or energy storage system. These conclusions are discussed in sections 4.2.1 – 4.2.4 which also provide relevant figures for these conclusions. Each conclusion will eliminate one or more power plant configurations from the consideration. 4.2.5 summarizes the result of section 4.2 in a table similar to
Table 4-2 found on the previous page. Remaining configurations will be assessed in section 4.3 to come to one configuration that will be used in the concept design.

Figures provided in sections 4.2.1 – 4.2.4 only show still considered configurations (e.g. when a configuration is discarded in section 4.2.2, it will not be shown in a figure used in section 4.2.3). Figures provided in appendix D.4 include all configurations.

© COPYRIGHT OF C-JOB, WHOSE PROPERTY, THIS DOCUMENT REMAINS. NO PART THEREOF MAY BE DISCLOSED, COPIED, DUPLICATED OR IN ANY OTHER WAY MADE USE OF EXCEPT WITH THE APPROVAL OF C-JOB.

4.2.1 Conclusion 1: NH_3 becomes more appealing with increasing energy storage capacity

Energy storage in the form of ammonia becomes more appealing with increasing required energy storage capacity. This is the result of a relative narrow range of gravimetric and volumetric energy densities of the storage system due to relatively mild storage conditions and favorable characteristics of ammonia, as is documented in Table 2-3 and paragraph 3.3.3, resulting in a relatively high volumetric and gravimetric energy density. The volumetric energy density of ammonia storage systems in particular is considerably higher than those of hydrogen storage systems or batteries, resulting in less required volume for ammonia configurations. Figure D-10 shows the amount of volume required for the energy storage and energy converter as calculated using default values. This figure shows that the total required volume of a power plant, given a theoretical operational time of 14 days, is highly dominated by the required volume of the energy storage system. This effect can also be seen by comparing Figure D-20, Figure D-21 and Figure D-22 to each other. The difference between these figures originates from the difference in the amount of energy stored because the volume required for the energy converter is not affected by the theoretical operational time.

However, Figure D-22 also shows that a system containing sufficient energy for a 14-day autonomous operation requires a large amount of volume. Although best case scenario ammonia configurations approach volumetric requirements of the reference configuration, all configurations are deemed too large to be feasible on board a ROPAX ferry. This is due to the fact that current operational power plants on board ROPAX ferries in general do not exceed 2000 m^3 (displayed as a blue line in Figure 4-4). Since 14-day operational time configurations require over double this volume, an operational time of 14 days is not considered to be representative for a future ROPAX ferry.

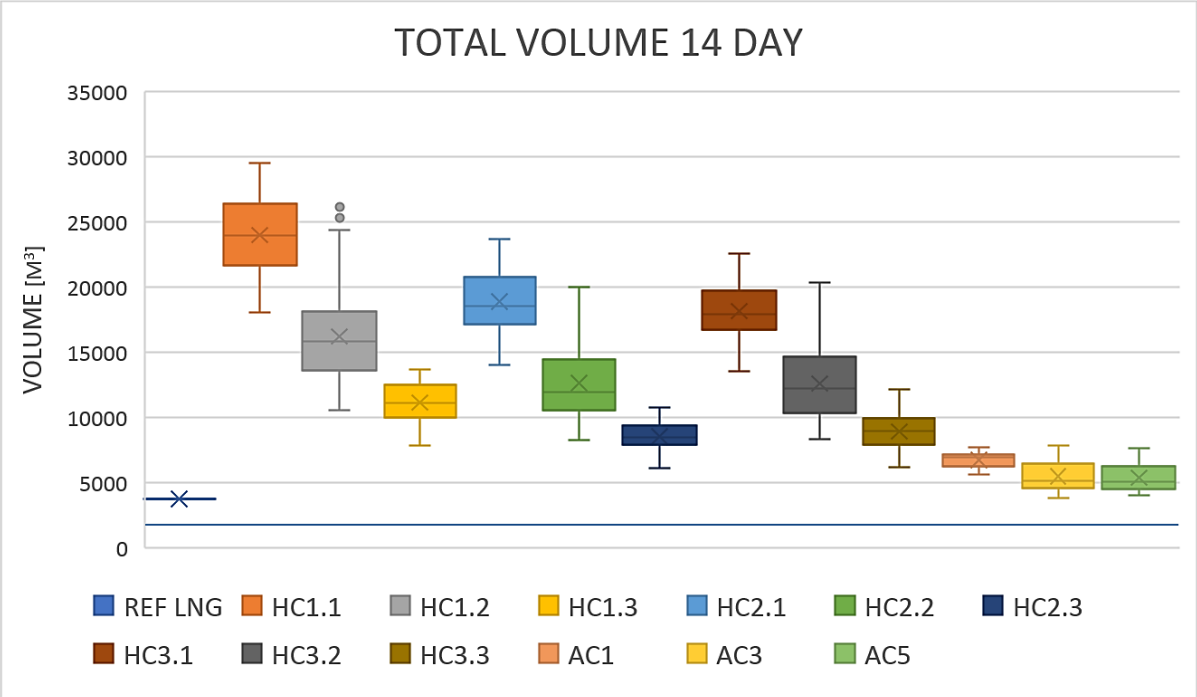

Figure 4-4: Total volume required per power plant in case enough energy is stored for a 14-day operation.

Discarded:

- All 14-day configurations, due to high required volumes

© COPYRIGHT OF C-JOB, WHOSE PROPERTY, THIS DOCUMENT REMAINS. NO PART THEREOF MAY BE DISCLOSED, COPIED, DUPLICATED OR IN ANY OTHER WAY MADE USE OF EXCEPT WITH THE APPROVAL OF C-JOB.

4.2.2 Conclusion 2: H_2 fueled ICEs and PEMFCs have relatively high daily energy costs

Section 3.4.1 already mentions high NO_X emissions and low efficiencies of hydrogen fueled internal combustion engines. NO_X emissions of ICEs were already shown in Figure 4-1, but not deemed sufficient cause to discard these configurations. However, the low efficiency of an ICE results in a relatively high energy cost per day, as is shown in Figure 4-5. These costs, in combination with high NO_X emission, is reason for a strong reluctance to choose these configurations, but it not considered to be decisive enough to discard these configurations as power plant option.

Configuration AC1 also suffers from high NO_X emissions and relatively low efficiency, but daily energy costs are considerably lower compared to hydrogen fueled ICEs configurations due to a lower ammonia price compared to hydrogen, when produced using excess renewable energy.

Daily costs of configurations HC2.1, HC2.2 and HC2.3 are also relatively high due to the limited efficiency of PEMFCs, but these are considered not to emit any GHGs.

Battery configurations BC1, BC2 and BC3 display a wide range of energy costs per day due to a variety of commercial electricity prices.

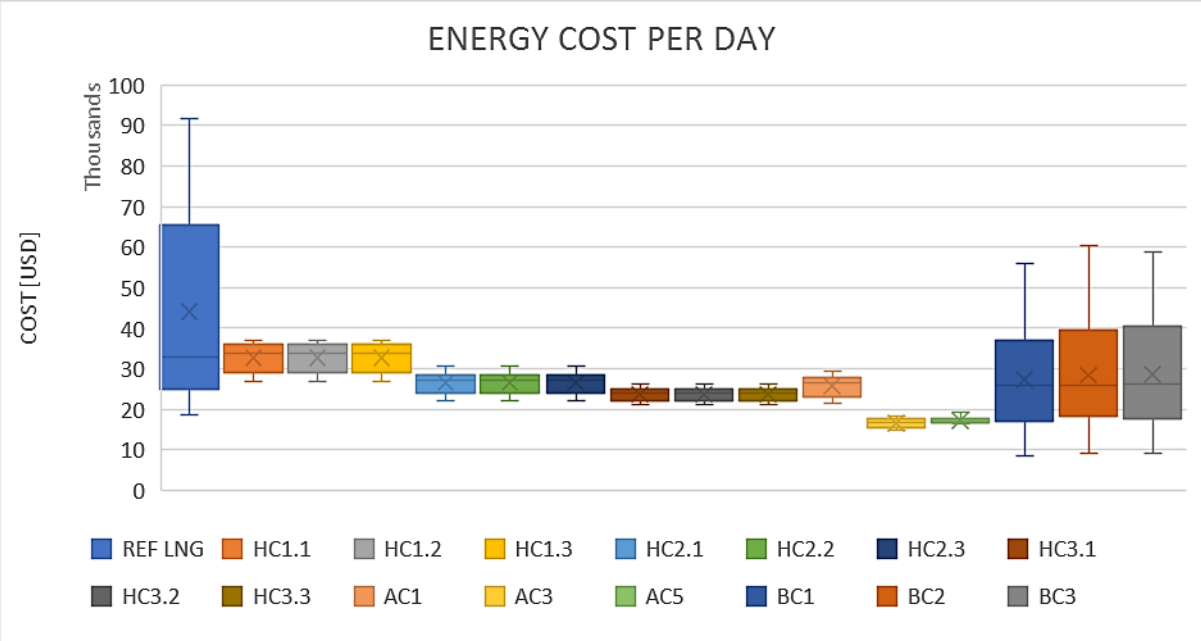

Figure 4-5: Daily energy cost resulting from sensitivity analysis and using excess renewable energy to produce hydrogen and ammonia.

Negative attribute defined:

- Hydrogen fueled ICEs (HC1.1, HC1.2 and HC1.3), due to a combination of high NO_X emissions and relatively high expected energy costs per day of operation.
- Hydrogen fueled PEMFCs (HC2.1, HC2.2 and HC2.3) have a relatively high expected energy costs per day.
- Battery configurations (BC1, BC2 and BC3) have a relatively large variation concerning expected energy costs per day.

© COPYRIGHT OF C-JOB, WHOSE PROPERTY, THIS DOCUMENT REMAINS. NO PART THEREOF MAY BE DISCLOSED, COPIED, DUPLICATED OR IN ANY OTHER WAY MADE USE OF EXCEPT WITH THE APPROVAL OF C-JOB.

4.2.3 Conclusion 3: SOFCs and H_2 storage require much space

The volume of configurations using SOFCs in combination with a theoretical energy storage capacity of one day is highly dominated by the volume requirement of the SOFC. The large range of possible SOFC specific volumes result in a relatively large variation in required volumes for these configurations. These large volumetric deviations are also observed for SOFC-based configuration designed for a 3.5-day operational time, but the volumetric energy densities of hydrogen storage systems also impose considerable variations in required power plant volumes. This is shown in Figure 4-6 and Figure 4-7.

These ranges of uncertainty concerning the volume of power plants results in excluding configurations using SOFCs from a theoretical 1-day operational time.

Compressed hydrogen storage systems are dismissed for an theoretical operational time of 3.5 days because of the large required volumes and deviations.

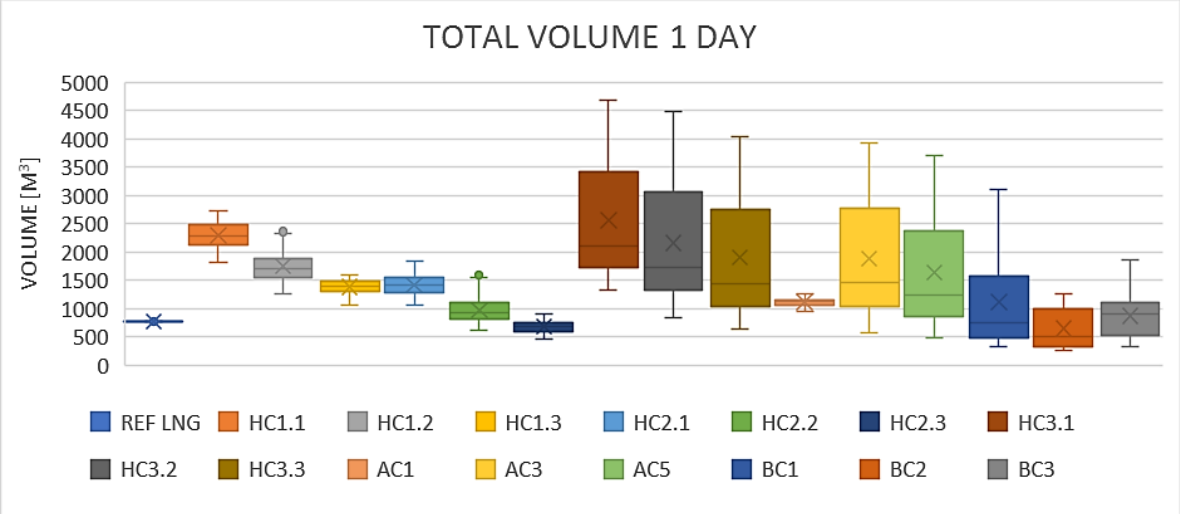

Figure 4-6: Total power plant volume determined by a variation study for a 1-day operational time.

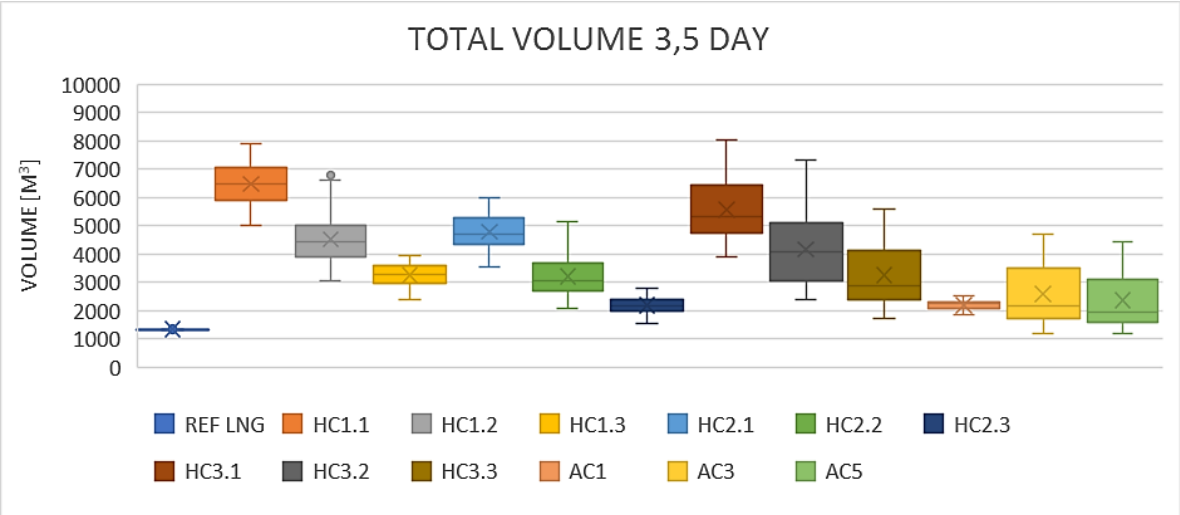

Figure 4-7: Total power plant volume determined by a variation study for a 3.5-day operational time.

Discarded:

- 1-day configurations using SOFCs (HC3.1, HC3.2, HC3.3, AC3 and AC5), due to relatively high required volumes
- 3.5-day configurations using compressed hydrogen (HC1.1, HC1.2, HC2.1, HC2.2, HC3.1 and HC3.2), due to substantial required volumes

© COPYRIGHT OF C-JOB, WHOSE PROPERTY, THIS DOCUMENT REMAINS. NO PART THEREOF MAY BE DISCLOSED, COPIED, DUPLICATED OR IN ANY OTHER WAY MADE USE OF EXCEPT WITH THE APPROVAL OF C-JOB.

4.2.4 Conclusion 4: Batteries are expensive

Energy costs per day are in paragraph 4.2.2 already indicated not to be in favor of battery configurations, compared to synthetic fuels produced using excess energy, due to a large commercial electric energy price variation. Figure 4-8 indicates the investment cost of 1-day energy storage systems. This figure shows that batteries are expected to be much more expensive than other energy storage systems, even under the most favorable conditions for batteries. Total power plant costs do not exceed the most favorable advanced battery price as is shown in Figure 4-9.

This, in combination with the fact that Li-air and Li-S batteries are not yet proven to be applicable in mobile applications and the technological challenges of these batteries that need to be solved, results in the decision to discard configurations BC2 and BC3.

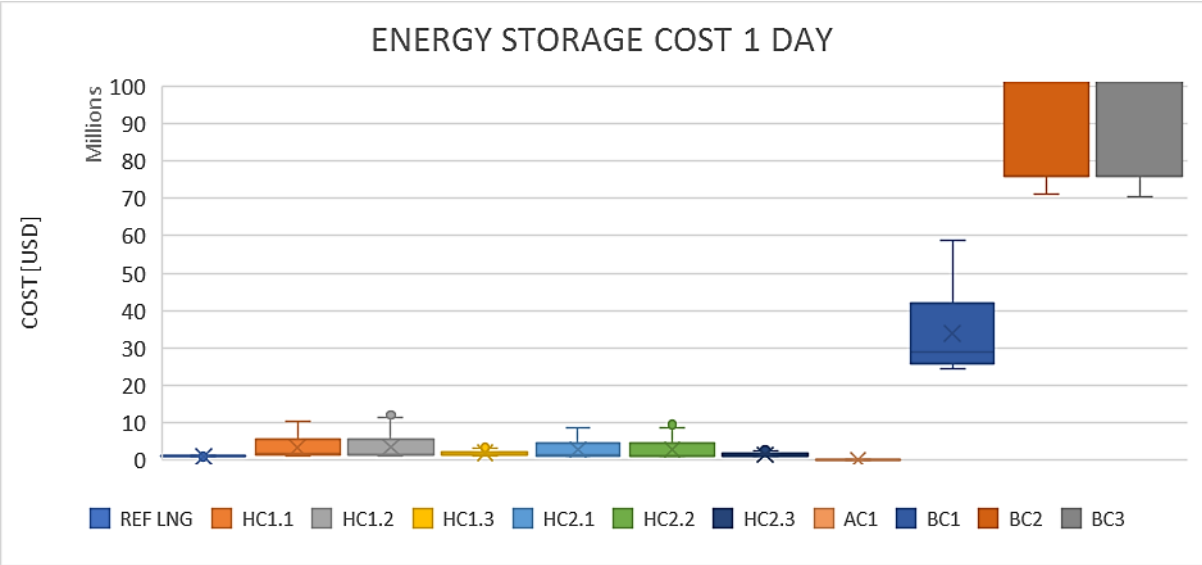

Figure 4-8: Investment cost of energy storage systems for a 1-day operational time.

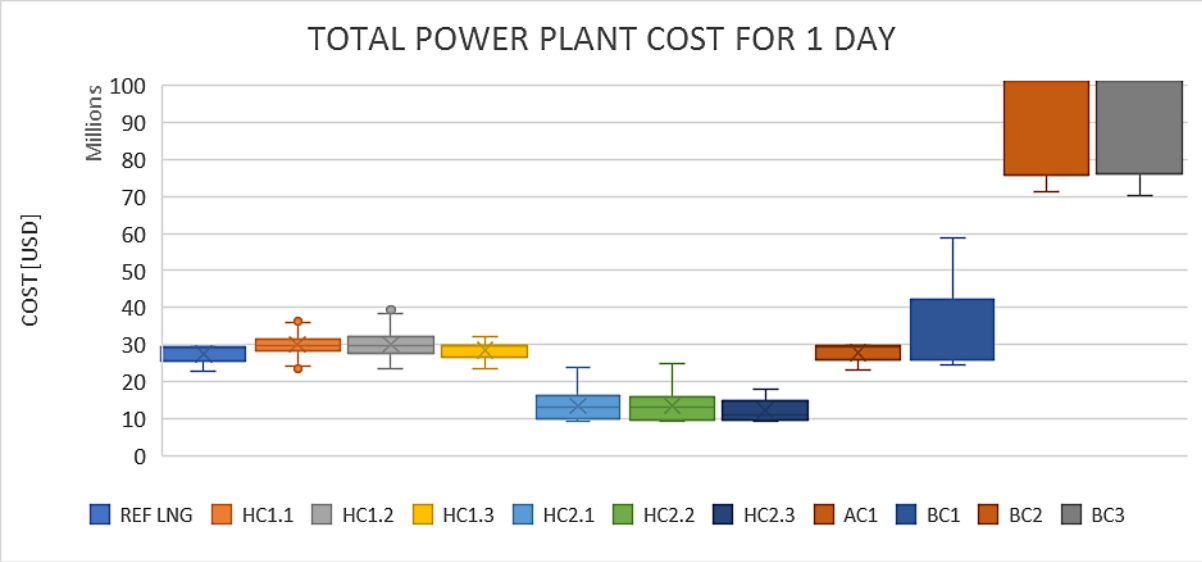

Figure 4-9: Investment cost of total power plant for a 1-day operational time.

Discarded:

- BC2 and BC3, due to a combination of high investment costs, high uncertainty concerning technological developments and large variation in energy cost per day.

© COPYRIGHT OF C-JOB, WHOSE PROPERTY, THIS DOCUMENT REMAINS. NO PART THEREOF MAY BE DISCLOSED, COPIED, DUPLICATED OR IN ANY OTHER WAY MADE USE OF EXCEPT WITH THE APPROVAL OF C-JOB.

4.2.5 Overview

Previous paragraphs all have eliminated several configurations for various reasons. Table 4-3 provides an overview of all considered configurations and whether they are discarded or not. Discarded configurations are indicated by a red box with the word NO and the number of the paragraph in which the configuration is discarded.

Several configurations possess negative attributes, such as a high required volume, but these characteristics are not deemed severe enough to immediately discard these configurations. Such configurations are indicated by a yellow box with NEG.(paragraph number) in it.

Table 4-3: Overview of configurations including discarded options.

CONFIGURATION	ENERGY CARRIER	ENERGY CONVERTER			1-DAY	3.5-DAY	14-DAY
REFERENCE	LNG	ICE	EG		NO (4.1)	**REF**	NO (4.1)
HC1.1	H_2 at 350 bar	ICE	EG		NEG.(4.2.2)	NO (4.2.3)	NO (4.2.1)
HC1.2	H_2 at 700 bar	ICE	EG		NEG.(4.2.2)	NO (4.2.3)	NO (4.2.1)
HC1.3	LH_2	ICE	EG		NEG.(4.2.2)	NEG.(4.2.2)	NO (4.2.1)
HC2.1	H_2 at 350 bar	PEMFC			NEG.(4.2.2)	NO (4.2.3)	NO (4.2.1)
HC2.2	H_2 at 700 bar	PEMFC			NEG.(4.2.2)	NO (4.2.3)	NO (4.2.1)
HC2.3	LH_2	PEMFC			NEG.(4.2.2)	NEG.(4.2.2)	NO (4.2.1)
HC3.1	H_2 at 350 bar	SOFC			NO (4.2.3)	NO (4.2.3)	NO (4.2.1)
HC3.2	H_2 at 700 bar	SOFC			NO (4.2.3)	NO (4.2.3)	NO (4.2.1)
HC3.3	LH_2	SOFC			NO (4.2.3)		NO (4.2.1)
HC4.1	H_2 at 350 bar	MCFC			NO (4.1)	NO (4.1)	NO (4.1)
HC4.2	H_2 at 700 bar	MCFC			NO (4.1)	NO (4.1)	NO (4.1)
HC4.3	LH_2	MCFC			NO (4.1)	NO (4.1)	NO (4.1)
AC1	NH_3	ICE	EG	AM-REF	NEG. (4.1)	NEG. (4.1)	NO (4.2.1)
AC2	NH_3	PEMFC		AM-REF	NO (4.1)	NO (4.1)	NO (4.1)
AC3	NH_3	SOFC		AM-REF	NO (4.2.3)		NO (4.2.1)
AC4	NH_3	MCFC		AM-REF	NO (4.1)	NO (4.1)	NO (4.1)
AC5	NH_3	SOFC			NO (4.2.3)		NO (4.2.1)
BC1	Li-ion				NEG.(4.2.2)	NO (4.1)	NO (4.1)
BC2	Li-air				NO (4.2.4)	NO (4.1)	NO (4.1)
BC3	Li-S				NO (4.2.4)	NO (4.1)	NO (4.1)

Table 4-3 indicates one reference configuration (LNG fueled ICE theoretically capable of operating for 3.5 days) as defined in section 2.4.1. 49 configurations have been eliminated from the consideration for various reasons as discussed in sections 4.1 and 4.2. Eleven configurations possess identified negative attributes, which were not deemed immediate showstoppers. However, these configurations are not considered for the representative ROPAX ferry concept design, discussed in chapter 5, due to these negative attributes. This leaves three configurations open for consideration. Section 4.3 will address these three configurations and determine which will be used for the concept design.

© COPYRIGHT OF C-JOB, WHOSE PROPERTY, THIS DOCUMENT REMAINS. NO PART THEREOF MAY BE DISCLOSED, COPIED, DUPLICATED OR IN ANY OTHER WAY MADE USE OF EXCEPT WITH THE APPROVAL OF C-JOB.

4.3 Power plant used for a representative ROPAX ferry concept design

As previously stated, three configurations are considered to have no severe negative characteristics. These systems all use SOFCs and are theoretically capable of operating for 3.5 days without refueling. From these three systems, one is chosen to be implemented for the concept design a ROPAX ferry in 2050. This choice is made in cooperation with C-Job Naval Architects by evaluating positive and negative aspects of each power plant concept. The remainder of this paragraph will discuss which configuration will be used during the concept design and reasons why the other two remaining configurations are not used.

Configuration AC3 requires an ammonia reformer, resulting in higher investment costs, volume and mass of the power plant. This ammonia reformer also requires a portion of the waste heat from the fuel cell to convert ammonia into hydrogen and nitrogen. This reduces the amount of available waste heat that could be utilized by a waste heat recovery system. Although a waste heat recovery system is not actively investigated, it is considered to be a feasible system to be used on board future vessels using SOFCs. Configurations not requiring an ammonia reformer have the potential to utilize more waste heat for the generation of additional electric energy compared to configurations which do require a reformer. This would reduce the fuel consumption of vessels without a reformer, resulting in less operational costs. For this reason, configuration AC3 is not incorporated in the concept design of a representative ROPAX ferry.

Configuration HC3.3 requires liquid hydrogen and configuration AC5 uses ammonia as energy storage medium. Ammonia from excess energy is already mentioned to be less expensive than hydrogen produced from excess energy. This results in lower daily energy costs, as shown in Figure 4-5. Ammonia possesses other favorable characteristics compared to liquid hydrogen, apart from the price difference.

Liquid hydrogen is stored at -253 °C, an extreme storage condition compared to ammonia, which is stored at 10 bar. The low temperature of hydrogen is likely to cause several logistical problems concerning large scale storage and on land transportation. Ammonia is already transported and stored on a large scale around the world and is proven not to suffer from severe logistical problems. [40], [188]

Hydrogen is extremely flammable and explosive when leaked to the environment due to a low required ignition energy, high flame speed and large flammability range, as can be seen in Table 2-5. On the other hand, ammonia is toxic to animals and the environment resulting in safety concerns when using it as fuel on board a passenger ship. [41], [56], [98]

Taking logistical challenges and safety concerns into account, it is decided that ammonia would be a more preferable energy carrier than liquid hydrogen. This means that configuration AC5 will be used for the concept design of the representative ferry of 2050.

© COPYRIGHT OF C-JOB, WHOSE PROPERTY, THIS DOCUMENT REMAINS. NO PART THEREOF MAY BE DISCLOSED, COPIED, DUPLICATED OR IN ANY OTHER WAY MADE USE OF EXCEPT WITH THE APPROVAL OF C-JOB.

4.4 Summary

After evaluating all 21 different power plant configurations and three different theoretical operational times, several conclusions are drawn concerning positive and negative attributes of energy storage and energy conversion methods per theoretical operational time. These conclusions are used to choose the power plant configuration most likely to be used onboard a ROPAX ferry in 2050. Each of these conclusions are summarized below.

First is the need to reduce the price of hydrogen and ammonia with respect to LNG. Three options are identified to accomplish this:

- a high LNG price including high emission tax;
- a low commercial electric energy price; or
- synthetic fuel production using excess renewable energy.

Especially the last of these three is considered to be a feasible measure due to the expected presence of excess energy from solar and wind farms.

The second conclusion is that using fuel cells or batteries are the most environmentally friendly option due to the emission of NO_X, and thus N_2O, when using internal combustion engines.

Thirdly, all sustainable configurations require a considerable amount of space and, consequently, a 14-day theoretical operational time is not considered feasible for any configuration. However, it has been concluded that ammonia fueled configurations are best suited for longer operational times due to the relative high energy storage density with respect to hydrogen or batteries. Following from this, it is also concluded that compressed hydrogen requires considerable amounts of space, making it only feasible for very short operational times. This also applies to batteries. SOFCs are also expected to require considerable amounts of space, but the effect of this decreases when the energy storage capacity increases. This makes SOFCs better suited for multiple day theoretical operational time.

The combination of relative low electrical efficiencies and high hydrogen price has resulted in discarding the hydrogen fueled internal combustion engines and PEMFCs.
The initial investment price of advanced batteries (Li-air and Li-S), in combination with their high weight, has led to the conclusion that advanced batteries are not suited to be used on such a large ship.
Molten carbonate fuel cells are not considered to be a suitable energy converter to be used on board future vessels due to a combination of negative attributes such as limited expected improvements and high specific weight of the system.

After these conclusions were drawn, three power plant configurations remained (see paragraph 4.3). These were closely examined and based on expected safety and logistical concerns and the expected potential for improvements, a single configuration was determined to be the most feasible to be used on a ROPAX ferry in 2050. This power plant configuration is composed of a SOFC directly fueled by ammonia.

© COPYRIGHT OF C-JOB, WHOSE PROPERTY, THIS DOCUMENT REMAINS. NO PART THEREOF MAY BE DISCLOSED, COPIED, DUPLICATED OR IN ANY OTHER WAY MADE USE OF EXCEPT WITH THE APPROVAL OF C-JOB.

5 Proof of concept for a representative ROPAX ferry of 2050

Section 2.1 has resulted in an estimation concerning the requirements of a ROPAX ferry build in 2050 which could be considered to be representative for ferries build at that time. After extensive literature research, future performance expectations of considered energy storage systems and energy converters were established in chapter 3. Chapter 4 describes the variation study performed to determine the most feasible power plant configuration to be used to power the predefined ROPAX ferry.

The following chapter will incorporate the most feasible power plant configuration, as defined in chapter 4, into a concept design of a ROPAX ferry, complying with the requirements of the representative ROPAX ferry as defined in section 2.1. These requirements will be discussed and elaborated on in section 5.1. Since ammonia is a toxic gas, serious safety concerns arise which will be discussed in 5.2. This section will also discuss current regulation. Section 5.3 will discuss the concept design of the ferry. Power plant related differences between an existing LNG-fueled ferry and the ammonia-fueled ferry of 2050 are discussed in section 5.4. The last section will discuss four fuel saving measures that are considered to be feasible to be used given the design of the vessel and the power plant. All information will be shortly summarized at the end of this chapter.

5.1 ROPAX ferry requirements

As previously stated, ferry requirements determined in section 2.1 are used to compose a concept design of a ROPAX ferry using the power plant configuration chosen in section 4.3. These requirements are:

- monohull
- 1500 passengers
- 600 cars
- 1200 beds in 400 cabins
- service speed Fn = 0.3
- 18 000 m^3 displacement
- 28 000 kW MCR
- 33 000 ton GT (equal to 110 000 m^3 enclosed volume)
- 6000 ton DWT
- 170 m length between perpendiculars
- 185 m length over all
- 26 m molded breadth
- 6.2 m draft
- 2 propellers
- bulbous bow
- two trips per 24 hours
- 150 – 200 miles per trip
- 1.15 TJ/day electrical energy per day
- Solid oxide fuel cell (SOFC) directly fueled by pressurized ammonia

Sections 5.1.1 and 5.1.2 will discuss further requirements resulting from these initial requirements. Requirements imposed by the passenger and car capacity of the ferry are discussed in section 5.1.1. 5.1.2 will elaborate on the requirements of the power plant.

© COPYRIGHT OF C-JOB, WHOSE PROPERTY, THIS DOCUMENT REMAINS. NO PART THEREOF MAY BE DISCLOSED, COPIED, DUPLICATED OR IN ANY OTHER WAY MADE USE OF EXCEPT WITH THE APPROVAL OF C-JOB.

5.1.1 Passenger and car requirements

The representative ROPAX ferry of 2050 is required to be able to carry approximately 600 cars and 1500 passengers. A total of 1200 beds in 400 cabins has also been specified to be representative for this ferry. This has been established in section 2.1 and will form the basis of the following section.

Garage requirements

Based on literature and information provided by ferry operators (see [189] and appendix E.1), a standard sized passenger car is estimated to measure 5 m in length. This is a length most commonly used by ferry operators and is therefore used to estimate the required total length of the car lanes on board the ferry. This amounts to 3000 lane meters. A standardized car height is equal to 2.1 m and a lane width of 2.3 is commonly used for passenger cars. However, operators also offer the possibility of transporting trucks, trailers and lorries which require more lane width and height compared to passenger cars. Lanes suitable for these large vehicles are in general 3.1 m wide and have a clearance height of 4.8 m.[6,189]

Little information is available concerning the amount of lane meters suited for trucks with respect to the amount of lane meters designated for passenger cars. Moreover, available information is inconsistent and therefore deemed insufficient to be used during this thesis. Nevertheless, the need to be able to carry trucks is established. This causes the garage to have two standard lane widths and heights. A lane designated for passenger cars requires a clearance height of at least 2.1 m and a width of 2.3 m. A lane suited for a truck will be 3.1 m wide and 4.8 high. Because of the structural requirements of the decks, a total standard garage deck height including stiffeners is determined to be 5.8 m. These dimensions are obtained from existing vessels. A standard car lane, including construction, will be 2.9 m high, resulting in a clearance height of 2.4 m. Figure 5-1 provides a graphic representation of the used lane height, lane width and deck height. A total of approximately 3000 lane meters will be present in the general arrangement, as can be seen in section 5.3, Figure 5-4.

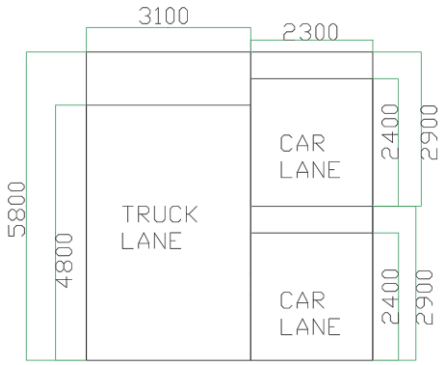

Figure 5-1: Schematic representation of used standard height and width of both a truck lane as well as a car lane.

Cabin requirements

A floor area of 8 – 10 m^2 per standard passenger cabin is common on board ROPAX ferries according to ferry operators. These cabins are generally equipped with two or four berths resulting in a required area per berth of 2 – 4 m^2 (see appendix E.1). Due to the presence of luxurious cabins, an average required cabin floor area per berth equal to 4 m^2 is assumed during the design of the ROPAX ferry. This complies with currently existing ROPAX ferries [6] and spatial requirements used in an article assessing the applicability of the EEDI (Energy Efficiency Design Index) for ROPAX vessels [190].

© COPYRIGHT OF C-JOB, WHOSE PROPERTY, THIS DOCUMENT REMAINS. NO PART THEREOF MAY BE DISCLOSED, COPIED, DUPLICATED OR IN ANY OTHER WAY MADE USE OF EXCEPT WITH THE APPROVAL OF C-JOB.

Public spaces

It is common for this type of ferry to have a deck accommodating public spaces. These public spaces include a tax-free shop, restaurants, seating areas, a sun deck and a galley. This deck is located between the car decks and the accommodation decks. This can also be seen in the general arrangement provided in section 5.3.

5.1.2 Power plant requirements

Chapter 4 has resulted in the selection of an ammonia fueled SOFC, theoretically capable of operating for 3.5 days, as most feasible power plant in 2050. The fuel cell currently requires a considerable amount of space but is expected to improve significantly in coming decades as established in section 3.4.2. Expected default requirements of a fuel cell, stated in section 3.4.2, will therefore be used when incorporating the fuel cell into the design of the ferry. These default values are: an electrical efficiency of 60 %, a required mass of 12 ton/MW and required volume of 30 m^3/MW. This amounts to an estimated required space of 840 m^3 and weight of 336 ton, as calculated in section 4.1.

The previously assumed electrical efficiency of the fuel cell results in a required ammonia storage capacity of 360 ton ammonia. Considering the maximum filling level of a pressurized ammonia tank (85%) and characteristics of the storage tank, a total storage volume of 700 m^3 is required. Currently existing compressed ammonia storage tanks are known to have a storage capacity of 450 m^3. Therefore, two of these tanks will be used on board the ROPAX ferry.

Besides the already defined power plant components, batteries are required on board this ferry. This is due to two reasons:

1. A SOFC takes a considerable amount of time to heat up before it can be used to generate power.
2. A SOFC is not capable of rapidly increasing the output electrical power.

Heating up current fuel cell systems takes between 30 minutes and several hours, depending on for example the design and operating temperature.

Increasing the amount of electrical output power of the fuel cell also takes some time. This results in the need for onboard batteries to provide additional power when a rapid output power increase is required. Batteries could provide additional power while the fuel cell power output is slowly increased. The amount of time to increase the power is again dependent on the design of the fuel cell itself[5]. Scaling down the output power can be done instantly. [133]

Calculating the amount of required electric energy storage capacity is found to be impossible due to a lack of information concerning the exact operational profile of the vessel, the operating characteristics of future fuel cells and practical experience of using fuel cells on board vessels. Based on expert opinion a required electric energy storage capacity of 50 GJ is assumed. This is approximately equal to delivering 28 MW (MCR of the power plant) for half an hour. This amounts to an estimated Li-ion battery weight of 96 ton and required volume of 39 m^3. These characteristics will therefore be incorporated into the design. [133]

[5] E.g. a fuel cell by Sunfire currently delivers its maximum power at 33 A, but is only capable of increasing its current by 2 A/min.

© COPYRIGHT OF C-JOB, WHOSE PROPERTY, THIS DOCUMENT REMAINS. NO PART THEREOF MAY BE DISCLOSED, COPIED, DUPLICATED OR IN ANY OTHER WAY MADE USE OF EXCEPT WITH THE APPROVAL OF C-JOB.

5.2 Safety concerns & regulation regarding the fuel

Using ammonia to propel a vessel is technologically feasible, but safety concerns arise due to the toxicity of ammonia, as already mentioned in section 2.2.3. At the moment of writing this thesis, no existing regulation directly applies for the use of ammonia as fuel on board a ship. Existing regulation concerning the transportation of ammonia (IGC Code) and the use of a gaseous fuel (IGF Code) are reviewed to provide an indication of required safety measures. Despite the fact that these codes are not intended for vessels using pressurized ammonia as fuel, it is considered a good basis of a preliminary safety assessment. This is confirmed by Bureau Veritas which states that these two codes will form the basis of future regulation for ammonia fueled ships if and when these ships are developed. Until regulation, intended for ships using ammonia as fuel, is in place, an extensive hazard and safety analysis of the vessel is required to prove that the vessel is safe to operate. This analysis should be performed during the basic design of a vessel. [6]

First, safety related properties of ammonia are compared to those of LNG. The IGC Code will be discussed in the second section and afterwards the IGF Code in the third section. The goal of these codes will be discussed as well as required safety measures to ensure a safe operation. Location restrictions of the ammonia storage tanks are determined using these codes and used in the concept design of the vessel.

5.2.1 Properties of ammonia and LNG

Since LNG is used as reference fuel, a direct comparison with ammonia is made. Since the exact composition of LNG is dependent on its origin, a common simplification is to use the characteristics of methane. This is justified by the fact that LNG is mostly methane. An overview of properties related to safety are documented in Table 5-2. From this data, several differences are obtained:

- LNG is more flammable than ammonia
- Ammonia is very toxic and LNG not toxic at all
- Ammonia is more easily stored than LNG
- Ammonia is easily detected by its smell, LNG is odorless
- Both gasses are lighter than air

Table 5-1: Definitions of chemical properties as stated by [191].

Flashpoint	The flashpoint (of a volatile material) is the lowest temperature at which it can vaporize to form an ignitable mixture in air.
Auto-Ignition Temperature	The lowest temperature at which the substance will spontaneously ignite in a normal atmosphere without an external source of ignition.
Vapor Pressure	Vapor pressure is the pressure of a vapor in thermodynamic equilibrium with its condensed phases in a closed system.
Critical Temperature	The critical temperature of a substance is the temperature at and above which vapor of the substance cannot be liquefied, no matter how much pressure is applied.
Critical Pressure	The critical pressure of a substance is the pressure required to liquefy a gas at its critical temperature.
GHS Hazard Statements	GHS (Globally Harmonized System of Classification and Labelling of Chemicals) is a United Nations system to identify hazardous chemicals and to inform users about these hazards. GHS has been adopted by many countries around the world and is now also used as the basis for international and national transport regulations for dangerous goods.

© COPYRIGHT OF C-JOB, WHOSE PROPERTY, THIS DOCUMENT REMAINS. NO PART THEREOF MAY BE DISCLOSED, COPIED, DUPLICATED OR IN ANY OTHER WAY MADE USE OF EXCEPT WITH THE APPROVAL OF C-JOB.

Table 5-2: Safety related properties of ammonia and LNG. [191]

	Ammonia	LNG (Methane)
Molecular Formula	NH_3	CH_4
Molecular Weight	17.031 g/mol	16.043 g/mol
Density	0.6818 g/L	0.7168 g/L
Boiling Point	-33 °C	-161 °C
Melting Point	-78 °C	-183 °C
Flashpoint	132 °C	-188 °C
Auto-Ignition Temperature	651 °C	537 °C
Flammability	15 – 26 vol.% in air	5 – 15 vol.% in air
Vapor pressure	1013 kPa at 26 °C	62.13 MPa at 25 °C
Critical Temperature	132 °C	-83 °C
Critical Pressure	111.5 atm	45.8 atm
Physical State; Appearance	Colorless gas Pungent, suffocating odor	Colorless gas Odorless
GHS Hazard Statements	H221: Flammable gas H314: Causes severe skin burns and eye damage H331: Toxic if inhaled H400: Very toxic to aquatic life H411: Toxic to aquatic life with long lasting effects	H220: Extremely flammable gas H315: Causes skin irritation H319: Causes serious eye irritation H335: May cause respiratory irritation H351: Suspected of causing cancer
Pictograms		

These differences imply considerable differences with respect to safe handling and use on board ships. Due to the low flammability of ammonia, as indicated by a high flashpoint, no serious difficulties to comply with fire safety regulation are to be expected. Due to the low flammability with respect to LNG, similar or even less extensive fire safety regulation are to be expected for the use of ammonia.

The toxicity of ammonia is the main safety concern of involved parties. Even small concentrations of ammonia in the air can cause serious health risks as shown in Table 5-3. The facts that ammonia is lighter than air and is easily detected by its smell before dangerous concentrations are reached, can be considered favorable attributes when reviewing the safety of ammonia. The fact that ammonia is lighter than air can be used to prevent human casualties in case of a leak by venting ammonia above the vessel. This would release the toxic vapor into the atmosphere, potentially resulting in considerable environmental damage, but it could safe human lives. Safety measures need to be taken to prevent leakage of ammonia to the environment. Toxic gas detectors should be present to warn the people in case of a leak. The fact that ammonia can be smelled before dangerous concentrations are reached, could function as an alarming system for the people onboard.

© COPYRIGHT OF C-JOB, WHOSE PROPERTY, THIS DOCUMENT REMAINS. NO PART THEREOF MAY BE DISCLOSED, COPIED, DUPLICATED OR IN ANY OTHER WAY MADE USE OF EXCEPT WITH THE APPROVAL OF C-JOB.

Table 5-3: Acute Exposure Guideline Levels (AEGL) of ammonia in ppm as defined by the U.S. Environmental Protection Agency. [191]

Exposure Time	AEGL 1 (Discomfort)	AEGL 2 (Impaired Escape)	AEGL 3 (Life Threatening/Death)
10 minutes	30	220	2700
30 minutes	30	220	1600
1 hour	30	160	1100
4 hours	30	110	550
8 hours	30	110	390

Storage conditions of ammonia are relatively mild compared to that of LNG. LNG is stored at an extreme low temperature of -162 °C while ammonia is stored at 10 bar. These conditions both result in the need for tested and certified equipment for the safe handling of the fuel.

5.2.2 IGC Code

The International Code for the Construction and Equipment of Ships Carrying Liquefied Gases in Bulk or IGC Code is currently used for bulk carriers transporting ammonia. It provides an international standard for the safe carriage of liquefied gasses, such as ammonia, by prescribing the design and construction standards of ships transporting these gasses. Required equipment to minimize the risk to the ship, its crew and the environment are also prescribed.

The IGC Code specifically dictates the need for suitable respiratory and eye protection equipment for emergency escape purposes for every person on board, as well as decontamination showers and eyewash stations. Toxic vapor detectors are required in rooms where an ammonia leak could occur e.g. the ammonia storage room and all spaces containing gas piping, gas equipment or gas consumers. This to monitor the integrity of the ammonia containment, handling and auxiliary systems.

The location of ammonia storage tanks is to be at least a distance of B/15 from the moulded line of the bottom at centerline. This distance is equal to the vertical extent of bottom damage as specified in 2.3.1.2.3 of the IGC Code.

Ammonia storage tanks shall be located at a minimum distance of d = 0.8 m from the outer shell as indicated in 2.4.2 of the IGC Code.

According to regulation 3.5.3.5.1 of this code, a minimal distance of 380 mm is required between the surface of the curved ammonia storage tank and structural elements such as stiffeners. A minimal distance of 450 mm is required as clearance between the tank and the ships structure to which structural elements are attached.

A distance of 380 mm is required between a storage tank and a flat surface of ship structure or another storage tank. This is prescribed by regulation 3.5.3.5.3. [192]

© COPYRIGHT OF C-JOB, WHOSE PROPERTY, THIS DOCUMENT REMAINS. NO PART THEREOF MAY BE DISCLOSED, COPIED, DUPLICATED OR IN ANY OTHER WAY MADE USE OF EXCEPT WITH THE APPROVAL OF C-JOB.

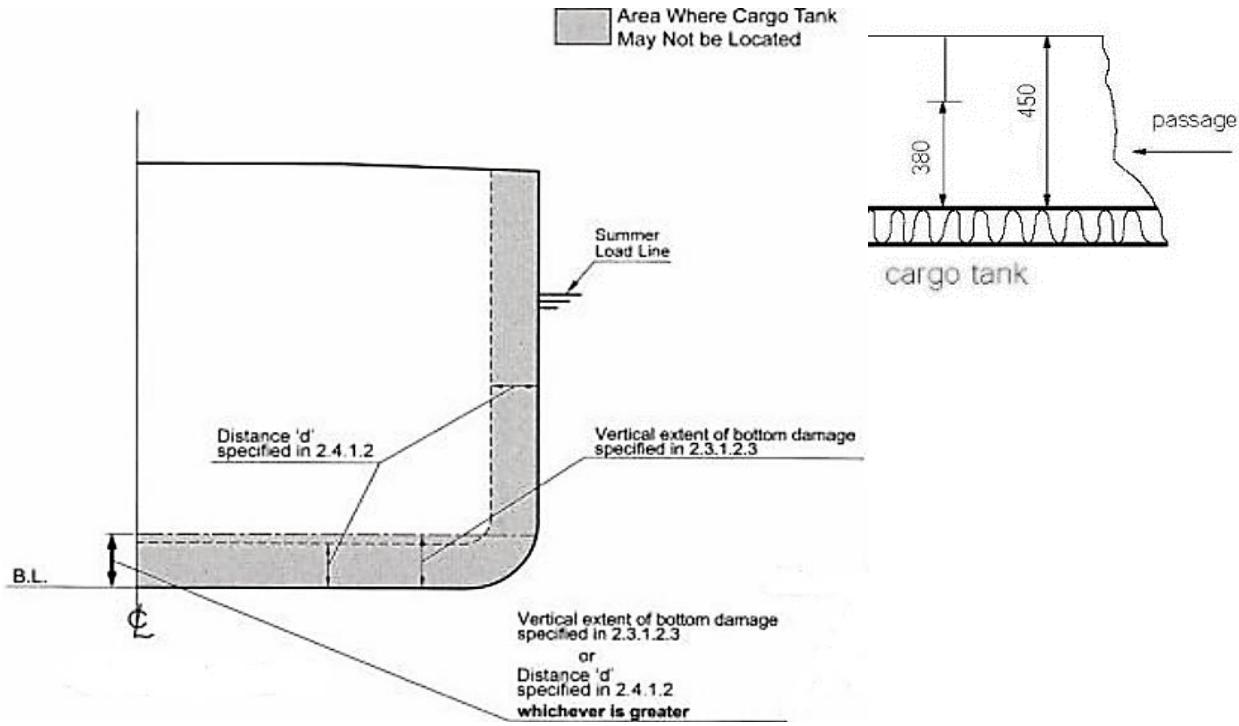

Figure 5-2: Relevant figures for the position of a cylindric ammonia storage tank as provided in the IGC code. [192]

5.2.3 IGF Code

The International Code of Safety for Ships using Gases or other Low-Flashpoint Fuels (IGF Code) is based on natural gas fueled ships. This code also applies to other gaseous or low-flashpoint[6] fuels that are not specified in this code, such as ammonia. These fuels will have to comply with the functional requirements of the IGF Code.

Regulation 5.3.3.1 states that fuel tanks shall be located at a minimum distance of B/5 inboard from the ship side at the summer load line. This to protect the tanks from external damage caused by collision or grounding.

5.3.3.4.1 dictates that for passenger ships, the boundary of the fuel tank should be located a minimal distance of B/10 from the aft terminal of the ship. Where the shell plating is located inboard of B/5, a minimal distance of B/15 applies.

Fuel tanks are to be placed 0.08L aft of the forward perpendicular as required by regulation 5.3.3.7 of the IGF Code and SOLAS regulation II-1/8.1 for passenger ships.

Functional requirements regarding the design of the fuel containment system, such as the storage tanks and pressure relief system, are provided in chapter 6 of the IGF Code. This to reduce the risk to personnel, ship and environment to a level equivalent to conventional oil fueled ships. Various functional requirements for bunkering, pipes, fuel supply to consumers, fire safety, explosion prevention, ventilation and electric installations are provided in subsequent chapters. These functional requirements apply for all gas fueled vessels, but given regulation is solely applicable for natural gas fueled vessels, resulting in the need for actual regulation for ammonia fueled ships. [193]

[6] Gaseous fuels or liquid fuels having a flashpoint lower than otherwise permitted under paragraph 2.1.1 of SOLAS regulation II-2/4 (60 °C)

© COPYRIGHT OF C-JOB, WHOSE PROPERTY, THIS DOCUMENT REMAINS. NO PART THEREOF MAY BE DISCLOSED, COPIED, DUPLICATED OR IN ANY OTHER WAY MADE USE OF EXCEPT WITH THE APPROVAL OF C-JOB.

5.3 General arrangement of a representative ROPAX ferry

This part of chapter 5 is used to describe the general arrangement of the ROPAX ferry of 2050 as composed for this thesis. This arrangement is composed to provide an indication of the layout of such a ferry, implying the feasibility of this design. Ferry designs internally available at C-Job Naval Architects were used during the composition as source of inspiration.

The layout of the ferry will be described and is shown in Figure 5-4 and Figure 5-5. Figure 5-3 provides 3D representations of the ferry as composed. This ferry complies with dimension and volume restrictions as composed in section 2.1. A conventional underwater hull form is used including a bulbous bow and skeg. Using a bulbous bow is advised by both the statistical data and the book *"Practical Ship Design"*. This reduces the resistance of the ship and therefore the fuel consumption. A skeg is used to improve the course stability of the vessel. Podded propulsors are used because electric energy has to be used for the propulsion of the vessel and these units are characterized by a favorable effect on the overall efficiency of the propulsion, as described in section 5.5.4. Lastly, fin stabilizers (not shown in the 3D views) are used to improve the passenger comfort by reducing the rolling motions.[6,194]

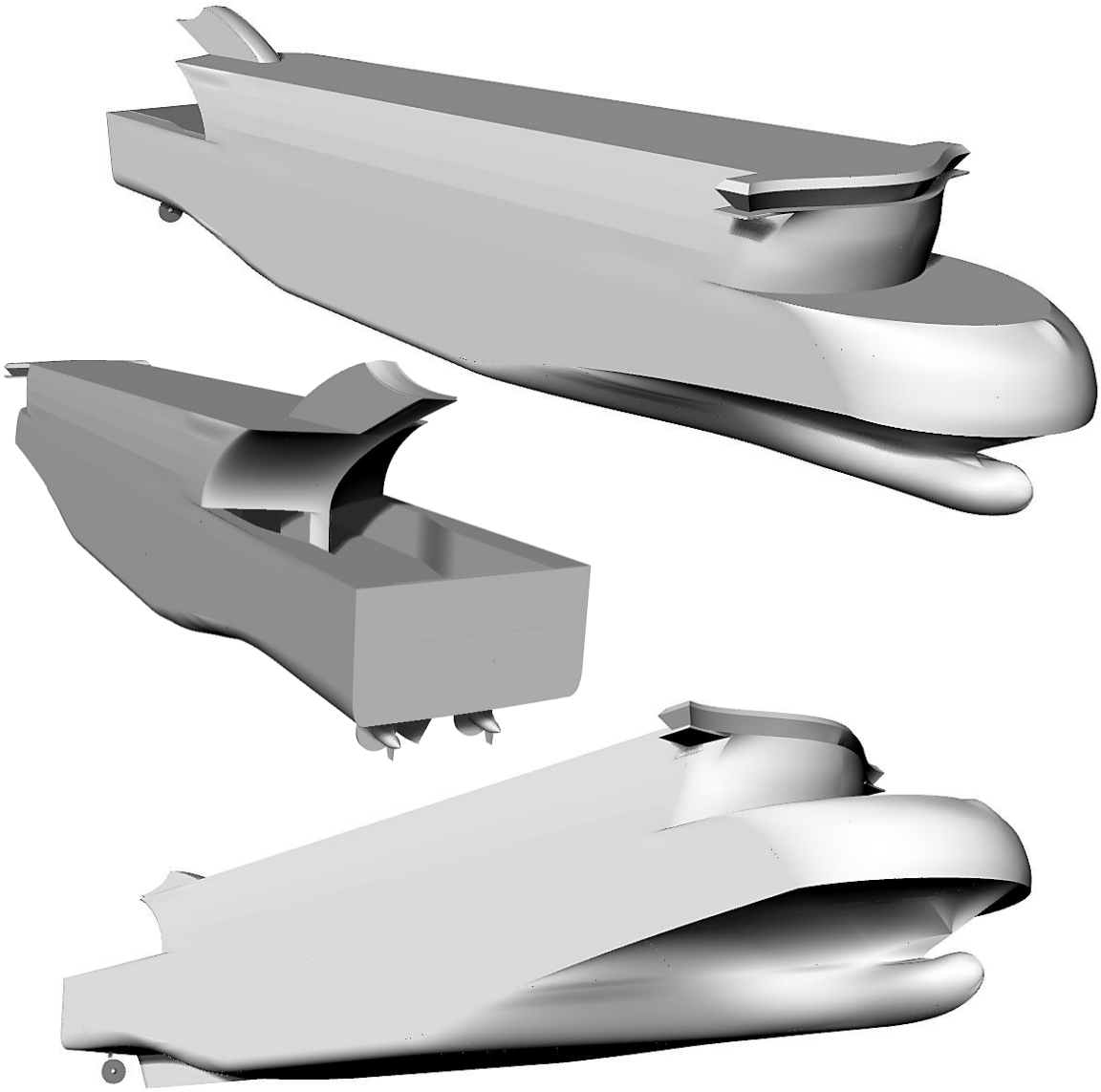

Figure 5-3: 3D views of the representative ROPAX ferry.

© COPYRIGHT OF C-JOB, WHOSE PROPERTY, THIS DOCUMENT REMAINS. NO PART THEREOF MAY BE DISCLOSED, COPIED, DUPLICATED OR IN ANY OTHER WAY MADE USE OF EXCEPT WITH THE APPROVAL OF C-JOB.

Following the 3D views of the previous page, a description of the layout of the ferry is given. This description will exclude the bottom three decks because these are discussed in section 5.4. Figure 5-4 provides the layout of every deck and Figure 5-5 provides a sideview of the vessel including colored areas representing various purposes of indicated decks. Spaces indicated as Technical Space include, but are not limited to, ballast water tanks, pump rooms and ventilation shafts. The layout of each deck will be described in the following paragraphs.

Deck 4

This deck starts at a height of 9 100 mm above the keel and is 5 800 mm in height. This deck is mostly used to house trucks onboard which enter the deck by the stern door. A total of 950 lane meters suited for trucks are present at this deck. A tiltable ramp enables cars to reach deck 3 with 530 lane meters suited for passenger cars.

Due to the highly flared bow of the vessel, considerable amounts of technical space are available at the bow. This is indicated by the inclusion of a contour at 12 000 mm. Staircases and elevators are also indicated enabling the passengers to reach decks 5, 6 and 7.

Deck 5

Deck 5 can be accessed by trucks and cars by the opened stern door and a shore-based ramp. This deck accommodates 620 lane meters for trucks and 430 lane meters for passenger cars. A tiltable ramp enables passenger cars to reach deck 6. 210 meters of the truck lanes are not enclosed and are therefore suited for trucks and lorries equipped with a cooling unit. These units are required to be parked outside due to the emission of exhaust gasses. Lifeboats are situated on decks 5 and 6 on both sides of the ferry.

Deck 6

This deck houses most of the mooring equipment of the ferry and is situated at a height of 17 800 mm above the keel line. Cars from deck 5 access this deck by the tiltable ramp. A total of 460 lane meters is available for passenger cars at this deck.

This concludes the garage decks. A total of 1420 lane meters is available to park passenger cars. 1570 truck lane meters are present resulting in a total amount of 2990 lane meters.

Deck 7

Deck 7 is a public deck at 20 700 mm above the keel. This deck accommodates shops, lounges, restaurants and an outside sundeck. Staircases and elevators from the garage decks end here and staircases and elevators to the accommodation decks start here.

© COPYRIGHT OF C-JOB, WHOSE PROPERTY, THIS DOCUMENT REMAINS. NO PART THEREOF MAY BE DISCLOSED, COPIED, DUPLICATED OR IN ANY OTHER WAY MADE USE OF EXCEPT WITH THE APPROVAL OF C-JOB.

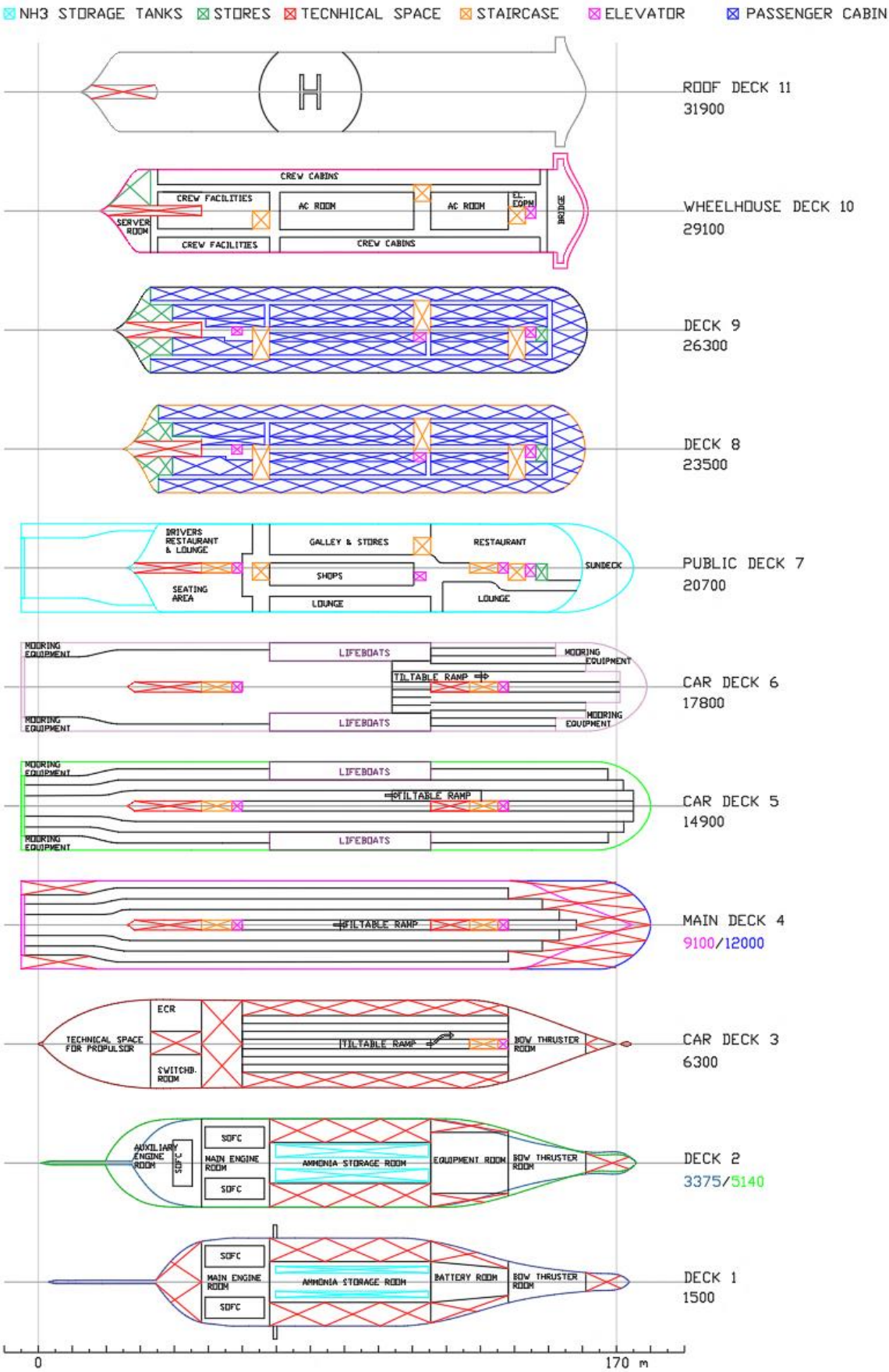

Figure 5-4: The total general arrangement composed for a representative ROPAX ferry to be built in 2050 including an ammonia fueled SOFC.

© COPYRIGHT OF C-JOB, WHOSE PROPERTY, THIS DOCUMENT REMAINS. NO PART THEREOF MAY BE DISCLOSED, COPIED, DUPLICATED OR IN ANY OTHER WAY MADE USE OF EXCEPT WITH THE APPROVAL OF C-JOB.

Decks 8 & 9

Located at 23 500 and 26 300 mm height, decks 8 and 9 are mainly occupied with passenger cabins. A total area of 4 700 m^2 is reserved for passenger cabins on these two decks. Passengers can enter these decks by elevator or stairs located at three different locations. Stores are also indicated on these decks.

Deck 10

Crew cabins and AC rooms are situated at the tenth deck. The bridge, crew facilities and server room are also located at this deck.

Roof

The top of the ferry accommodates a helicopter deck and has space reserved for the funnel. The roof is located 31 900 mm from the keel line.

Figure 5-5 provides a side view of the ferry, clearly showing the decks with passenger cabins and the parts of the garage reserved for cars of trucks as described above. The engine room, battery room and ammonia storage room are also indicated in this figure. The location of the podded propulsor is also shown in this figure, as well as the stern door, tiltable ramps, bulbous bow and skeg. Note that the colors of the decks are the same as those used in Figure 5-4.

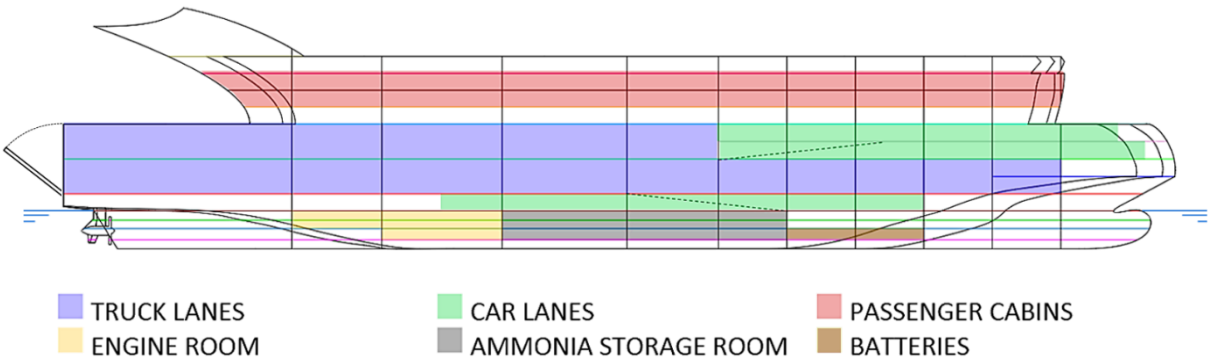

Figure 5-5: Sideview of the representative ROPAX ferry.

© COPYRIGHT OF C-JOB, WHOSE PROPERTY, THIS DOCUMENT REMAINS. NO PART THEREOF MAY BE DISCLOSED, COPIED, DUPLICATED OR IN ANY OTHER WAY MADE USE OF EXCEPT WITH THE APPROVAL OF C-JOB.

5.4 Difference with current LNG powered vessels

Differences with respect to the fuel, fuel storage system and energy converter properties have been established in previous chapters. However, the effect of these properties on the design of the ferry has not been investigated yet. This will be done in the following section, discussing the layout of the general arrangement as composed for the representative ROPAX ferry of 2050. This will be directly compared to an LNG-fueled ferry, MS Stavangerfjord, currently operating in the Baltic Sea.

The full general arrangement of the MS Stavangerfjord can be found in appendix E. This chapter will only discuss the decks used for the power plants of each design. General arrangements of these vessels as presented in this chapter are of equal scale.

First, volumes and weights of the MS Stavangerfjord are compared to power plant characteristics of the reference power plant (LNG fueled ICE+generator) and the power plant established in section 4.3 (ammonia fueled SOFC). This comparison is made using Figure 5-6 and Figure 5-7, each displaying the most favorable, default and least favorable volume or weight estimations of the reference power plant and AC5. Afterwards, general arrangements of the MS Stavangerfjord and the representative ROPAX ferry of 2050 are directly compared.

The two vessels display great similarities with respect to the total volume (gross tonnage), draft and passenger and car capacity. However, there are also considerable differences. MS Stavangerfjord is 15 m shorter, somewhat wider and has approximately a hundred cabins less. Table 5-4 provides an overview of the vessels characteristics.

Table 5-4: Overview of relevant characteristics of the MS Stavangerfjord and the representative ferry of 2050. [195], [196]

		MS Stavangerfjord	2050 ROPAX ferry
Ship characteristics	Length overall	170 m	185 m
	Breadth	27.5 m	26 m
	Draft	6.35 m	6.2 m
	Gross Tonnage	32 500 ton	33 000 ton
	Passengers	1500	1500
	Cabins	306	400
	Cars	600	600

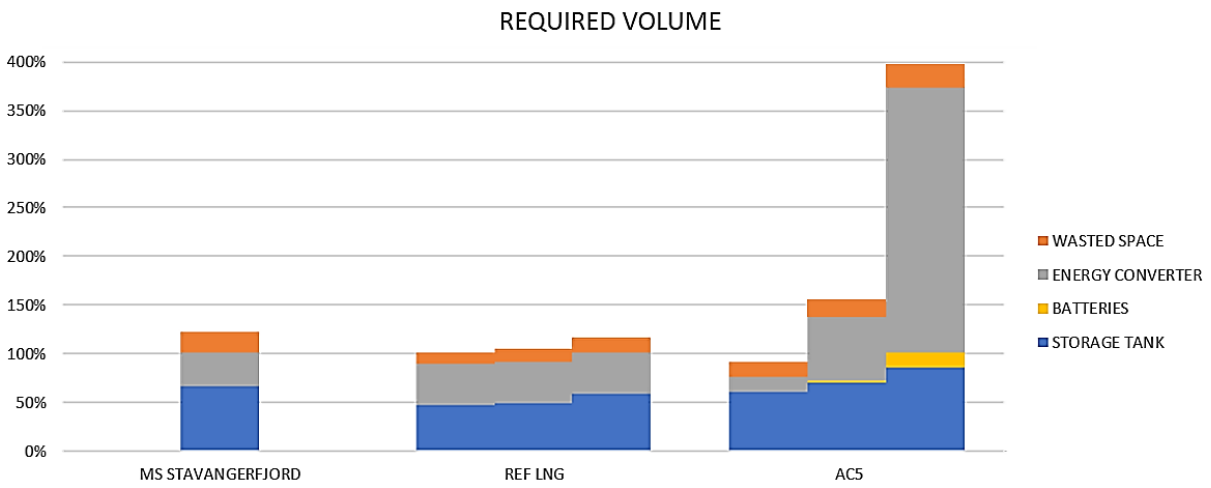

Figure 5-6: Required volumes of the power plants per component.

© COPYRIGHT OF C-JOB, WHOSE PROPERTY, THIS DOCUMENT REMAINS. NO PART THEREOF MAY BE DISCLOSED, COPIED, DUPLICATED OR IN ANY OTHER WAY MADE USE OF EXCEPT WITH THE APPROVAL OF C-JOB.

Figure 5-6 provides the power plant volumes of the MS Stavangerfjord, reference power plant configuration and that of the power plant configuration established in section 4.3 (AC5). This figure displays the volumes as percentage of the bare volume of the powerplant onboard the MS Stanvangerfjord, meaning all engines, generators and cylindric tank volumes together are equal to 100 % in case to the MS Stavangerfjord. The amount of wasted space (defined as the volumtric difference of the cylindric tank and the enclosing box similar to section 3.1.4) is also indicated. It is striking to see that the energy converter volumetric requirements of the reference configuration do not differ much from the MS Stavangerford. However, the MS Stavangerfjord is capable of storing more fuel than the calculations for the reference configuration indicate to be necessary. MS Stavangerfjord only has a total installed power of 26 MW MCR and the propeller is directly driven, thus eliminating the need for large electric generators. This has reduced the volume of the energy converters. The required volume variations of configuration AC5, caused by uncertainties concerning the performance future ammonia fueled SOFC, are significant. This greatly affects the required volume of the energy converter (SOFC) and the amount of required fuel. Fuel volumetric requirements are primarily influenced by the electric efficiency of the energy converter and not the energy density of the energy storage itself. This because both the energy density of LNG and ammonia are fairly certain as has been established in section 3.3. The volumetric requirements of batteries have a limited effect on the total required volume.

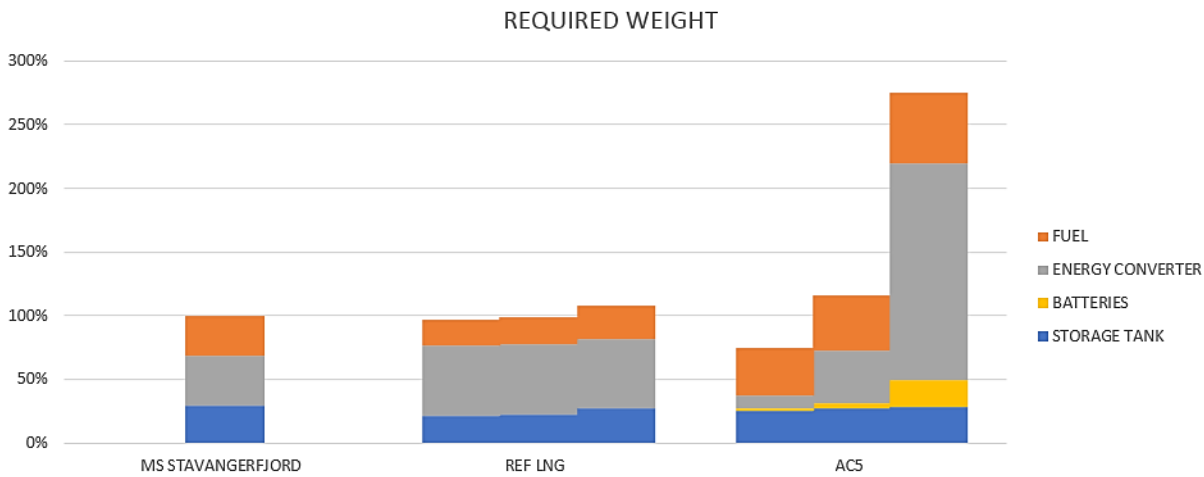

Figure 5-7: Required weights of the power plants per component.

The relative large amount of fuel and the absence of electric generators on board MS Stavangerfjord is even more clear to see in Figure 5-7. In this figure, the weight of the energy converter of the reference case is estimated to be significantly larger than that of the MS Stravangerfjord and the weight of the fuel is less. Again, the performance of future ammonia fueled SOFC is crucial when it comes to the overall weight of the power plant. The effect of batteries has increased with respect to the volume requirement due to the relative high density of batteries.

© COPYRIGHT OF C-JOB, WHOSE PROPERTY, THIS DOCUMENT REMAINS. NO PART THEREOF MAY BE DISCLOSED, COPIED, DUPLICATED OR IN ANY OTHER WAY MADE USE OF EXCEPT WITH THE APPROVAL OF C-JOB.

During the design of the representative ROPAX ferry, the default future scenario is used to estimate the required volume and weight of the individual power plant components. Table 5-5 provides an overview of the relevant characteristics of the MS Stavangerfjord and the representative ferry.
The representative ferry is equipped with two ammonia tanks with a total ammonia storage capacity of more than required by the default future scenario. This because the tanks that are used are currently available.

Table 5-5: Overview of relevant characteristics of the MS Stavangerfjord and the representative ferry of 2050.[195,196]

			MS Stavangerfjord	2050 ROPAX ferry
Ship characteristics	Length overall		170 m	185 m
	Breadth		27.5 m	26 m
	Draft		6.35 m	6.2 m
	Gross Tonnage		32 500 ton	33 000 ton
	Passengers		1500	1500
	Cabins		306	400
	Cars		600	600
Energy storage			LNG	Ammonia + Li-ion
Fuel tank	Dimensions	Length	19.1 m	45 m
		Diameter	5.3 m	3.7 m
	Single tank weight		~ 120 ton	~ 102 ton
	Storage capacity		2 x 296 m^3	2 x 450 m^3
	Total fuel weight		~ 260 ton	~ 460 ton
Battery	Volume		-	39 m^3
	Weight		-	97 ton
Energy converter	Types		4 x Rolls-Royce B3540V12PG 2 x MAN 6L21/31 1 x MAN 7L21/31 2 x Marelli MJBM 630 SC6	SOFC
	Total converter volume		436 m^3	840 m^3
	Total converter weight		325 ton	336 ton
	Total converter power		26.1 MW	28 MW
Total power plant	Weight		825 ton	1100 ton
	Block volume		1550 m^3	2000 m^3

When considering the power plant itself, significant differences are observed.

First, the size of the fuel tanks. Because of the lower volumetric energy density of ammonia, with respect to LNG, a larger storage volume is required to store sufficient ammonia. The fact that a tank storing pressurized ammonia is only allowed to have a maximum filling level of 85 % (a filling level of up to 95 % is allowed for LNG vessels) also increases the required volumetric storage quantity. However, despite the large volume of the vessel, a lower tank weight is required, caused by the already established favorable storage conditions of ammonia with respect to LNG.

© COPYRIGHT OF C-JOB, WHOSE PROPERTY, THIS DOCUMENT REMAINS. NO PART THEREOF MAY BE DISCLOSED, COPIED, DUPLICATED OR IN ANY OTHER WAY MADE USE OF EXCEPT WITH THE APPROVAL OF C-JOB.

The total occupied volume of the storage tanks does not differ significantly, again due to the favorable storage conditions of ammonia w.r.t. LNG. An LNG tank requires a considerable amount of insulation material, resulting in a considerably thicker wall. The difference of storage conditions has also resulted in a considerably different length to diameter ratio of the storage tanks. An ammonia storage tank is considerably longer, but its diameter is considerably less when compared with the LNG tanks. The fact that the considered ammonia tank has a lower diameter, resulted in the possibility to locate a partial car deck at water level, as shown in Figure 5-9.

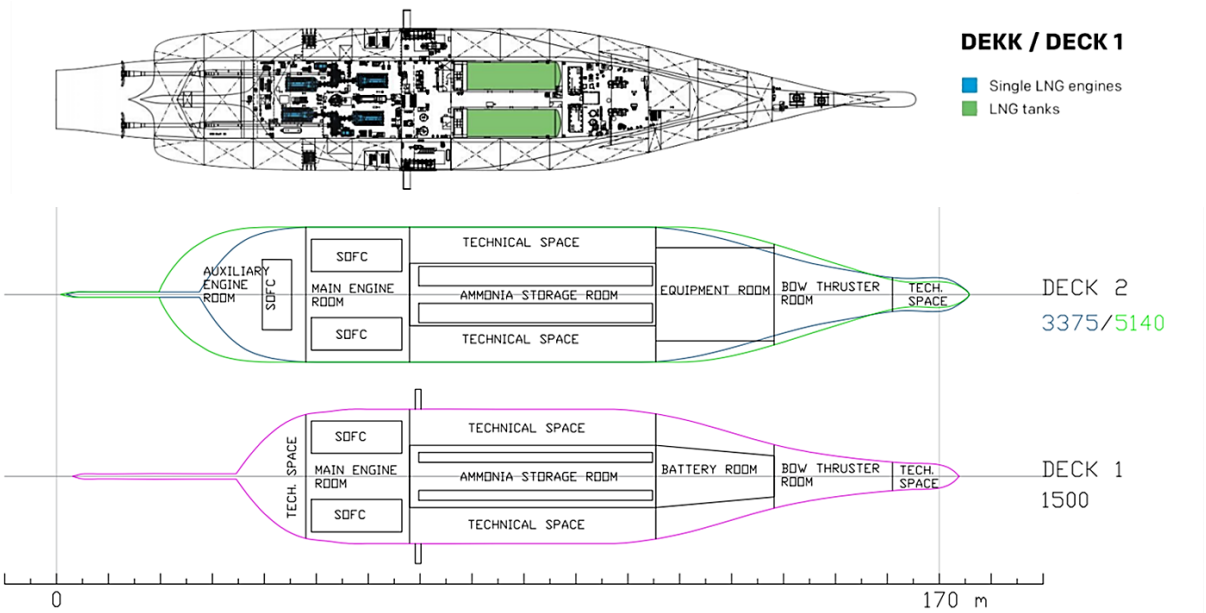

Figure 5-8: Layout of the vessels below the waterline.[6,195]

Table 5-5 presents the weights of the ammonia-fueled SOFC and that of all energy converters of the MS Stavangerfjord. Figure 5-8 and Figure 5-9 indicate that despite the relative small size of the energy converters, the engine room of the MS Stavangerfjord is still of considerable size due to all associated systems. When using SOFCs, considerably less systems are to be expected within the engine room, due to the fact that fuel cell systems already incorporate many of the required systems within the Balance of Plant. Since fuel cells are composed of several systems, a relatively high degree of flexibility, concerning the overall dimensions, can be expected. This favors the placement within the engine room and could therefore also favor the stability of the vessel. Fuel cells provide electric energy, resulting in a more flexible placement of these units and the removal of generators and gearboxes. However, electric motors are required to power the propulsors. These motors are not included in the general arrangement as presented above. This is justified when podded propulsors are used, as will be discussed in paragraph 5.5.4. Figure 5-9 shows a large deck area reserved for these propulsors and affiliated systems.

SOFCs can be directly fueled by pressurized ammonia, thus eliminating the need for a fuel preparation unit as is required when using LNG. This unit is shown in Figure 5-8 and Figure 5-9 as a square unit attached at the aft of the LNG tank.

Another advantage of fuel cells is the low noise level which eliminated the need to have a silencer at the exhaust, saving space at the upper decks where the silencer is commonly situated in modern vessels.

© COPYRIGHT OF C-JOB, WHOSE PROPERTY, THIS DOCUMENT REMAINS. NO PART THEREOF MAY BE DISCLOSED, COPIED, DUPLICATED OR IN ANY OTHER WAY MADE USE OF EXCEPT WITH THE APPROVAL OF C-JOB.

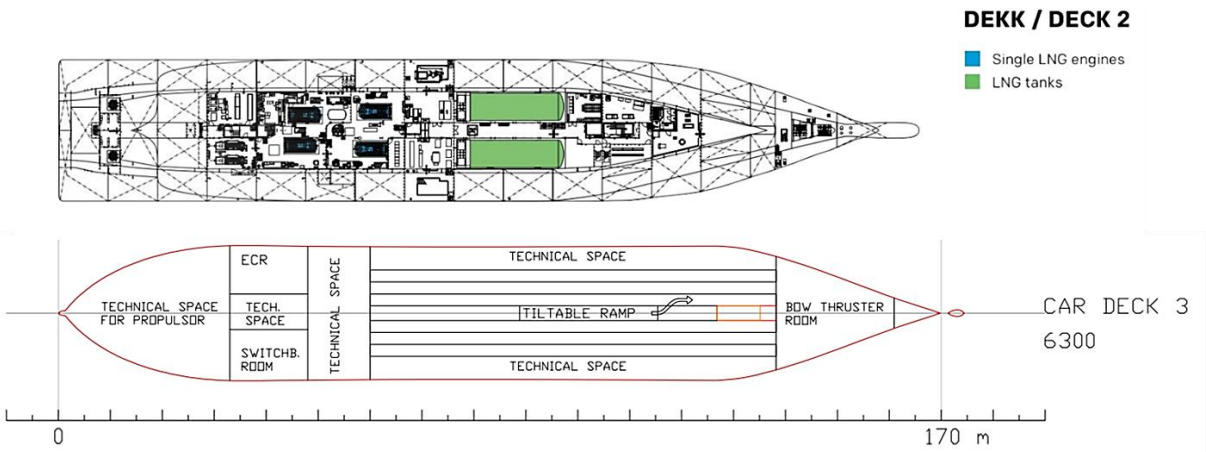

Figure 5-9: First deck above the waterline for both vessels.[6,195]

Another significant difference between these two layouts is the presence of a battery room, shown in Figure 5-8. As discussed in section 5.1.2, an estimated weight of 96 ton of batteries is required to be able to use SOFC as primary energy converter. Due to the relatively high density of these batteries, it is considered to be beneficial to place them as low as possible. This would be beneficial to the stability of the vessel. This is the reason why batteries are placed on the tank top (deck 1).

In conclusion, the ferry of 2050 is characterized by a larger and heavier powerplant, but this is not per definition bad due to the relative spatial flexibility of the power plant components.

The lower energy capacity of ammonia with respect to LNG has resulted in large storage tanks and a higher weight of the required fuel. However, ammonia storage tanks possess, due to the relative mild storage conditions of ammonia, more favorable dimensions with respect to LNG tanks. Moreover, a fuel preparation unit, required when using LNG, is not required when using pressurized ammonia.

The addition of batteries has resulted in an increase in required space, as can be seen in Figure 5-8, but the placement of batteries could have a favorable impact on the ships stability due to the high density.

The total weight of the energy converters is almost identical, but the required volume of SOFCs is considerably larger. However, due to the Balance of Plant of these fuel cells, less additional systems are required supporting the fuel cell. Since a fuel cell has relatively flexible main dimensions, a more favorable placement could be obtained, resulting in a more efficient use of the available space.

© COPYRIGHT OF C-JOB, WHOSE PROPERTY, THIS DOCUMENT REMAINS. NO PART THEREOF MAY BE DISCLOSED, COPIED, DUPLICATED OR IN ANY OTHER WAY MADE USE OF EXCEPT WITH THE APPROVAL OF C-JOB.

5.5 Notable, out of scope, fuel saving measures

Since this thesis concerns the main power plant components and their future, little attention is paid to energy saving measures and their applicability. However, the expected economic challenges implicate a need to operate as efficient as possible. The use of a high temperature fuel cell in combination with ammonia and batteries does allow several systems to be placed on board to improve the overall operational efficiency of the ferry. The following paragraphs will address a selection of fuel saving systems that are likely to improve the overall performance and are considered to be feasible to be used in combinations with the given power plant configuration as specified in sections 4.3 and 5.1.2. Every system will be shortly described and an indication of the total fuel saving potential is provided. First, a waste heat recovery system will be discussed, solar panels, wind assisted propulsion and a podded propulsor will subsequently be elaborated on.

5.5.1 Waste heat recovery system

The possibility of applying a waste heat recovery system has already been touched upon in section 4.3. Several present-day applications of waste heat recovery systems already exist, but not widely used within the maritime industry. During the literature research numerous concept designs of SOFC systems were found which incorporated some form of waste heat recovery.

The most basic form is already discussed in section 3.4.2 and shown in Figure 3-6. This system uses the heat generated by the combustion of unutilized fuel to preheat the fuel and air entering the fuel cell. Since this system is fueled by natural gas, part of this heat is also used to decompose natural gas into hydrogen and carbon dioxide. This decomposition is not necessary when using a SOFC directly fueled by ammonia which implies the presence of excess heat.

Many concept designs of large scale SOFCs, obtained from literature, incorporate gas turbines or steam turbines into the design of the system to generate additional electric energy. These turbines are placed at the outlet of the burner and utilize the pressurized, high temperature exhaust gas to generate electrical energy, as is shown in Figure 5-10. This exhaust gas typically has a temperature in the range of 800 °C and a pressure of approximately 10 bar. Some papers claim a theoretical overall electrical efficiency increase of more than 10 %. Although no data regarding an ammonia fueled SOFC in combination with a turbine is available, the potential of such a configuration is considered to be high. It is therefore advisable to investigate the possibilities of such systems in future studies. [197-200]

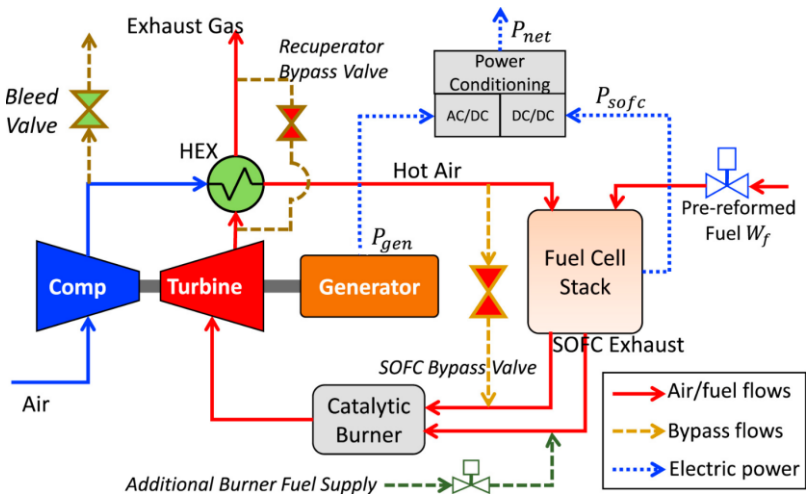

Figure 5-10: Schematic representation of an integrated SOFC/GT system. [200]

© COPYRIGHT OF C-JOB, WHOSE PROPERTY, THIS DOCUMENT REMAINS. NO PART THEREOF MAY BE DISCLOSED, COPIED, DUPLICATED OR IN ANY OTHER WAY MADE USE OF EXCEPT WITH THE APPROVAL OF C-JOB.

5.5.2 Solar panels

The subject of photovoltaic (PV) solar panels has been briefly mentioned in section 2.2.1. Here it was concluded that solar panels are not suitable as main source of energy on board ferries. However, due to the recent price drops of solar panels (current payback period is stated to be 5 – 8 years [201]) and expected future improvements, solar panels are possibly suited to provide additional energy, and by doing so result in fuel savings. The fact that these panels can simply be installed on top of the ferry, without serious difficulty, contributes to the relative attractiveness of the panels.

The amount of solar energy that can be generated using solar panels is largely dependent on the position and location of the panel. According to Figure 5-11, solar irradiances of 4 and 6 kWh/m^2/day are to be expected in the Baltic Sea and Mediterranean Sea, respectively. The performance ratio (amount of available solar irradiance used by the solar panels) of present day systems is reported to be between 80 and 90 %. Current PV systems are considered to have an overall efficiency of approximately 15 %.[26,27]

Taking these efficiencies into account, electric energy generation of PV systems installed on ferries operating in the Baltic Sea is estimated to be $4 * 0.85 * 0.15 = 0.51$ kWh/m^2/day. PV systems operating in the Mediterranean Sea could generate 0.77 kWh/m^2/day.

From the general arrangement of the ferry, as provided in section 5.3, an available roof area of 2600 m^2 is estimated. When this area is exclusively used to place solar panels, an energy generation potential of $2600 * 0.51 \cong 1300$ kWh/day is estimated for the Baltic Sea. 2000 kWh/day could be generated on ferries located in the Mediterranean Sea. Since a total of 1150 GJ/day is estimated to be required for the ferry and $1300\ kWh \cong 4.7\ GJ$, a fuel saving percentage of 0.4 % could be achieved when sailing in the Baltic Sea. 0.6 % of fuel could be saved when operating in the Mediterranean Sea.

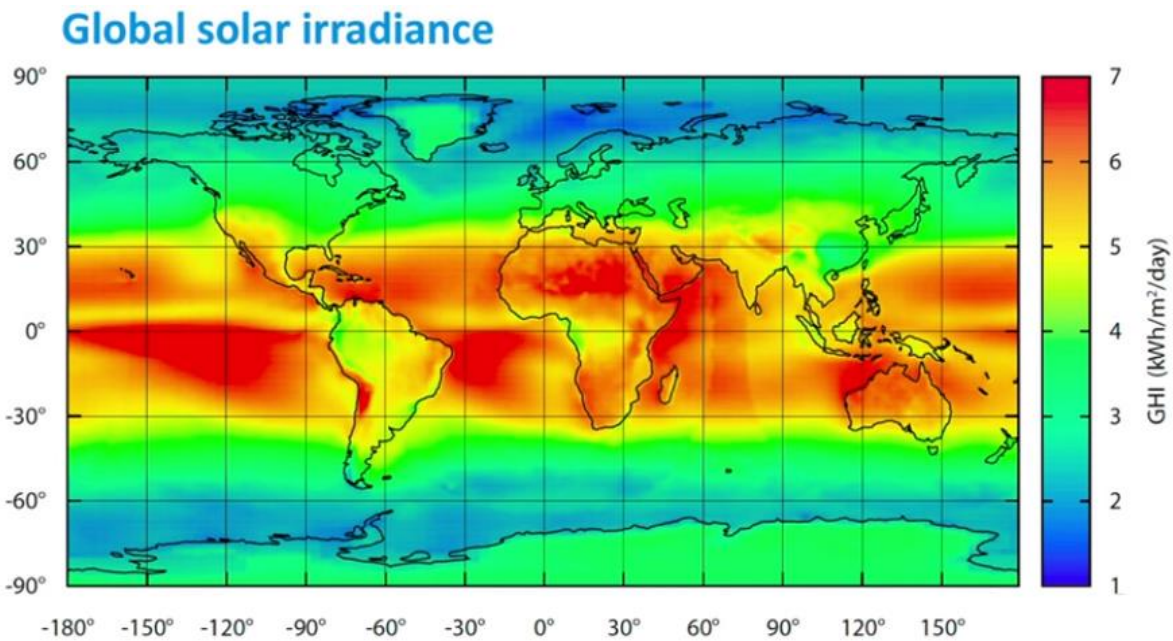

Figure 5-11: Global solar irradiance in kWh/m^2/day. [26]

© COPYRIGHT OF C-JOB, WHOSE PROPERTY, THIS DOCUMENT REMAINS. NO PART THEREOF MAY BE DISCLOSED, COPIED, DUPLICATED OR IN ANY OTHER WAY MADE USE OF EXCEPT WITH THE APPROVAL OF C-JOB.

5.5.3 Wind assisted propulsion

Although wind assisted propulsion was discarded in section 2.2.1 as primary source of energy, it is by an increasing number of companies considered to be a viable measure to reduce fuel consumption. Five basic types of wind propulsion technologies are currently defined: wind turbines, soft sails, fixed sails, kite sails and Flettner rotors[7]. Wind turbines not yet used onboard vessels, while sail-based systems and Flettner rotors are currently in operation.

Flettner rotors in particular are considered to be a viable measure to reduce the fuel consumption due to the relative ease of operation. Only a limited number of ships are currently equipped with these units, despite reported fuel savings of 3 to 25 %. However, the amount of interest in these systems has increased in recent years.[202-205]

Flettner rotors are applicable on ships which have the required installations space available on deck. Norsepower, the main manufacturer of Flettner rotors, states that Ro-Ro ships, tankers, bulk carriers and passenger ships are especially suited for the use of these systems. This corresponds with currently known ships equipped with these rotors, e.g. the Bore's Estraden. In April 2018, the Viking Grace was retrofitted with a rotor sail, making it the first passenger ship equipped with a rotor sail and proving the applicability of such systems on board passenger ships.[204,205]

Figure 5-12: M/S Viking Grace equipped with a Flettner rotor. [205]

5.5.4 Podded propulsor

A podded propulsor is composed of a propeller, an electric motor (located in the underwater housing) and a steering mechanism located inside the hull of the ship, as shown in Figure 5-13. This unit has been identified as a favorable unit to be used as main propulsor, especially for cruise ships and ferries, by MARIN. This unit has several advantages with respect to conventional propulsion units, of which the main advantages are: an increase in propulsive efficiency and maneuverability of the ship. [206-208]

[7] Flettner rotors are smooth vertical cylinders which are rotating and by doing so generate a lift force. This effect is also known as the Magnus-effect.

© COPYRIGHT OF C-JOB, WHOSE PROPERTY, THIS DOCUMENT REMAINS. NO PART THEREOF MAY BE DISCLOSED, COPIED, DUPLICATED OR IN ANY OTHER WAY MADE USE OF EXCEPT WITH THE APPROVAL OF C-JOB.

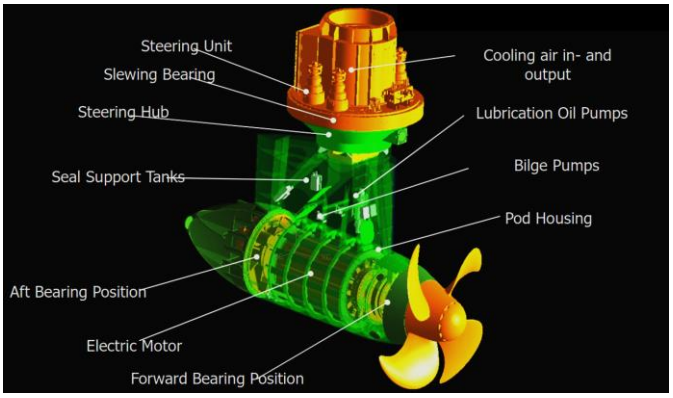

Figure 5-13: General layout of a podded propulsor. [206]

The maneuverability of the vessel increases due to the possibility to generate full thrust in every direction.

The increase of propulsive efficiency is the result of several factors:

- A lower ship resistance due to the absence of appendages such as the shaft line and its supporting struts. A rudder is also not required when using this propulsion unit. Added resistance caused by the podded unit is in general less than the resistance decrease, due to the absence of appendages, resulting in a net resistance decrease.
- An increased hull efficiency due to a more uniform inflow at a podded propulsor compared to a conventional propeller, as illustrated in Figure 5-14. This more uniform inflow is the result of the absence of a shaft line and struts in front of the propeller. This imposes the possibility of better matching the propeller to the wake field of the vessel and therefore the propeller load, resulting in a more efficient propeller. [206]

Total propulsive efficiency increases up to 10 percent are reported, making it a highly attractive unit to be used in combination with the power plant configuration as presented in section 4.3. Manufacturers claim a possible 20 % in energy savings.[209,210]

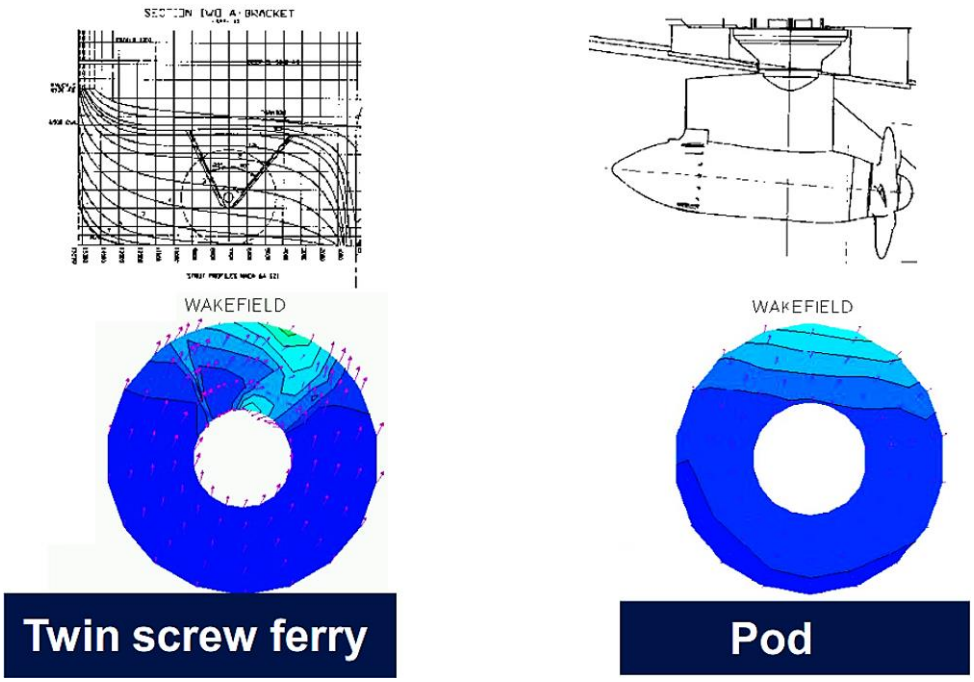

Figure 5-14: Different wake fields of a conventional twin screw ferry and podded propellers. [206]

© COPYRIGHT OF C-JOB, WHOSE PROPERTY, THIS DOCUMENT REMAINS. NO PART THEREOF MAY BE DISCLOSED, COPIED, DUPLICATED OR IN ANY OTHER WAY MADE USE OF EXCEPT WITH THE APPROVAL OF C-JOB.

5.6 Summary

Given the ferry requirements determined in section 2.1 and the power plant design selected in chapter 4, a concept design was developed to prove the feasibility of such a ferry. This has been proven by assessing the differences between an ammonia-fueled SOFC power plant and a present-day LNG based power plant. Differences with respect to safety, dimensions, volume, mass and additional required systems have been discussed. From this analysis, several conclusions can be drawn.

First is the need to ensure the safety of the power plant due to the toxicity of ammonia. Current regulation (IGC and IGF codes) is not considered to be sufficient to ensure a safe operation, but it does provide an indication to what kind of measures are required to ensure a safe operation in the future. The most important safety measures are the placement of toxic gas detectors, a gas containment system and reducing the likelihood that a storage tank will be punctured during an incident. This is in line with the IGC and IGF code. Although such a configuration has not been developed yet, it is deemed to be plausible to design a safe power plant.

When assessing the characteristics of the power plants, as is done in section 5.3, it can be seen that the configuration used for the ferry of 2050 requires a considerable larger amount of space and mass. However, the negative effect of an increasing mass and volume could be limited due to favorable ammonia storage tank dimensions, relative flexible overall fuel cell dimensions and the limited number of supporting systems required when using a fuel cell. It is therefore not possible to conclusively state that an ammonia-based power plant (composed of compressed ammonia storage, batteries and SOFCs) will be less favorable, with respect to weight, volume and general arrangement, than a modern LNG-based power plant.

Previously identified economic challenges of the selected power plant resulted in the consideration of several fuel saving measures. Discussed measures are a waste heat recovery system, solar panels, wind assisted propulsion and a podded propulsor. A waste heat recovery system could utilize the hot exhaust gasses to generate additional electric energy resulting in a possible efficiency increase of more than 10 %. Solar panels only save approximately 0.5 % fuel, but due to the relative ease of installation and the short payback period, it is considered a possible solution. Wind assisted propulsion and podded propulsors can be used to improve the propulsive efficiency of the vessel resulting in less fuel burned to propel the vessel. These systems are reported to save up to ten percent fuel and some theoretical studies imply the possibility of saving over 20 percent of fuel. However, this has not been proven.

© COPYRIGHT OF C-JOB, WHOSE PROPERTY, THIS DOCUMENT REMAINS. NO PART THEREOF MAY BE DISCLOSED, COPIED, DUPLICATED OR IN ANY OTHER WAY MADE USE OF EXCEPT WITH THE APPROVAL OF C-JOB.

6 Conclusion & recommendations

This last chapter of the report will provide a conclusion of the presented research and a discussion of the results. Furthermore, recommended future study topics, following from this thesis, are discussed.

6.1 Conclusion

The goal of this thesis was to come up with a power plant design, emitting minimal amounts of greenhouse gasses, suited to be used on a representative ROPAX ferry built in 2050.

In order to answer this, the following three sub-questions were to be answered:

1. *What requirements does the expected market of 2050 require the representative ROPAX ferry to have?*
2. *What power plant configuration, emitting minimal amounts of minimal greenhouse gasses, is expected to be the most economically and technologically feasible to be used on a ship in 2050?*
3. *How does the selected power plant configuration affect the design of the representative ROPAX ferry compared to current LNG-fueled ferries?*

The first sub-question has been answered in section 2.1 providing a basis for the remainder of the research. This answer is composed of a set of vessel characteristics from which the required energy per day of operation and required output power were used to answer the second sub-question. The remainder of the vessel characteristics were used during the proof of concept used to answer the third sub-question in chapter 5.

Before answering the second sub-question, the considered energy carriers, energy converters and power plant configurations are established. Considered energy carriers are compressed and liquified hydrogen, compressed ammonia and batteries (Li-ion, Li-air and Li-S). Energy converters that are considered are internal combustion engines, fuel cells (PEMFC, SOFC and MCFC) and an ammonia reformer.

Following this, extensive literature research was conducted to provide relevant characteristic values of energy storage and energy converter units. These characteristic values are used to estimate the initial investment cost, cost of energy per day of operation, total weight, total volume and greenhouse gas emissions per power plant configuration. Results of this research are discussed in chapter 4. The following conclusions summarize the findings of this chapter and are used to eliminate power plant configurations from the consideration.

- First and foremost is the need to **reduce the price of hydrogen and ammonia compared to LNG**. Without this price reduction, no single synthetic fuel can be considered economically feasible. Three options to reduce the price of hydrogen and ammonia are identified:
    - a high LNG price including high emission tax;
    - a low commercial electric energy price; or
    - synthetic fuel production using excess renewable energy.

  Especially the last of these three is considered to be a feasible measure due to the expected presence of excess energy from solar and wind farms.
- The second conclusion is that **fuel cells or batteries are the most environmentally friendly** option due to the emission of NO_X when using internal combustion engines.

© COPYRIGHT OF C-JOB, WHOSE PROPERTY, THIS DOCUMENT REMAINS. NO PART THEREOF MAY BE DISCLOSED, COPIED, DUPLICATED OR IN ANY OTHER WAY MADE USE OF EXCEPT WITH THE APPROVAL OF C-JOB.

- Thirdly, **all sustainable configurations require a considerable amount of space** and a 14-day theoretical operational time is not considered feasible for any configuration. However, it has been concluded that ammonia fueled configurations are best suited for longer operational times due to the relative high energy storage density with respect to hydrogen or batteries. Following from this, it is also concluded that compressed hydrogen requires considerable amounts of space, making it only feasible for very short operational times. This also applies to batteries. SOFCs are also expected to require considerable amounts of space, but the effect of this decreases when the energy storage capacity increases. This makes SOFCs better suited for a multiple day theoretical operational time.
- Furthermore, the combination of relative low electrical efficiencies and high hydrogen price has resulted in discarding the hydrogen fueled internal combustion engines and PEMFCs.
- The initial investment price of batteries, in combination with their high weight, has led to the conclusion that batteries are not suited to be used on such a large ship.

Following these conclusions, only three power plant configurations remain. Based on expected safety and logistical concerns and the expected potential for improvements, a single configuration was determined to be the most suitable to be used on a ROPAX ferry in 2050. This power plant configuration is composed of a **SOFC directly fueled by ammonia**.

The last sub-question concerns practical consequences of using the established power plant configuration, an ammonia-fueled solid oxide fuel cell, on board a representative ferry of 2050. Emphasis is hereby put on safety concerns and the general arrangement.

- <u>Regarding the safety concerns</u>: Although current regulation (IGF and IGC Codes) do not account for the use of ammonia as fuel on board a passenger ferry, it is deemed plausible that ammonia can be utilized as fuel in a sufficiently responsible and safe manner.
- <u>Regarding the effect of using an ammonia-fueled SOFC on the general arrangement</u>: When using expected power plant characteristics, such as weight and volume, no radical differences are expected to exist between an LNG- and an ammonia-fueled ROPAX ferry. Despite the fact that the ammonia-based power plant does require more space and weight, the effects are considered to be minimal. This is primary caused by the favorable storage conditions of ammonia with respect to LNG and the possibility of placing heavy units low in the hull favoring the stability of the vessel. The use of fuel cells reduces the number of equipment units required in the engine room resulting in more available space for the fuel cell itself. This is considered to make up for the fact that the fuel cells require more space than conventional engines.

© COPYRIGHT OF C-JOB, WHOSE PROPERTY, THIS DOCUMENT REMAINS. NO PART THEREOF MAY BE DISCLOSED, COPIED, DUPLICATED OR IN ANY OTHER WAY MADE USE OF EXCEPT WITH THE APPROVAL OF C-JOB.

6.2 Recommendations

Following the past report, several recommended topics for future work are given in the following section.

The first is to investigate the total lifetime cost of the power plants including for instance the cost of maintenance and the operational lifetime of different systems. These factors are currently not included but could very well be of great importance in future decision making. The reason for not including these factors is mainly due to the limited amount of information known at the time of conduction the research. However, when considered systems are in further stages of development, it could be possible to include these costs into the consideration. A very rough indication of the lifetime costs, based on estimated initial investment costs and the cost of energy per day of operation, of several power plant configurations is shown in appendix D.5. These indications are far from complete and are therefore only suited as very rough indication of the importance of the cost of energy per day w.r.t. the initial investment costs.

Second is a more detailed safety analysis including a cooperation with class societies such as Lloyd's Register, Bureau Veritas and DNV-GL. This analysis should include a safety analysis of the use of ammonia as fuel and the analysis of using a high temperature fuel cell, in this case a SOFC, as primary energy converter. Although the safe use of ammonia as fuel is expected to be plausible, as discussed in section 5.2, it has not been proven. The use of a high temperature fuel cell as primary energy converter has not been investigated in this thesis, due to a lack of applicable regulation, but it should be investigated in future research. Proving the possibility of safely using such a power plant is required before any final designs can be made. The effect of safety measures on the overall design of the ship has only been briefly investigated, based on current regulation, and is therefore considered to be a possible starting point for future research. Actual safety requirements and their effects on the design of a ship are therefore needed.

Third is a more in-depth research concerning the load profile of the fuel cell. It could be possible to apply some peak shavings due to the presence of batteries, this would reduce the investment cost of the system, the overall volume and weight. This level of power plant optimization is not considered to be possible with currently available information, but the potential of such an optimization is clear.

Four is the more in-depth research concerning operating requirements and output of the fuel cell. This information is now scarcely known, but not considered conclusive enough to incorporate in this research. When and if an ammonia-fueled SOFC is commercially developed, it should be closely examined to establish whether its operating characteristics, such as start-up time, power increasing response time, weight, volume, outlet gas composition, outlet pressure and outlet temperature are within acceptable limits to be operational on a ferry. Some of these characteristics influence the overall volume/mass of the power plant, others influence the need for additional systems such as a waste heat recovery system or an exhaust cleaning unit (to process unburned ammonia if present in the exhaust).

© COPYRIGHT OF C-JOB, WHOSE PROPERTY, THIS DOCUMENT REMAINS. NO PART THEREOF MAY BE DISCLOSED, COPIED, DUPLICATED OR IN ANY OTHER WAY MADE USE OF EXCEPT WITH THE APPROVAL OF C-JOB.

Bibliography

[1] IMO, "UN body adopts climate change strategy for shipping," 13 April 2018. [Online]. Available: http://www.imo.org/en/MediaCentre/PressBriefings/Pages/06GHGinitialstrategy.aspx. [Accessed 5 May 2018].

[2] R. Verbeek, N. Ligterink, J. Meulengrugge, G. Koornneef, P. Kroon, H. De Wilde, B. Kampman, H. Croezen and S. Aarnink, "Natural gas in transport," CE Delft, Delft, 2013.

[3] R. McGill, W. Remley and K. Winther, "Alternative Fuels for Marine Applications," IEA-AMF, 2013.

[4] M. Anderson, K. Salo and E. Fridell, "Particle- and Gaseous Emissions from an LNG Powered Ship," *Environmental Science & Technology,* vol. 49, no. 20, pp. 12568-12575, 2015.

[5] B. Remley, "Alternative Maritime Fuels," Alion Science and Technology, McLean, 2014.

[6] C-job Naval Architects, *Internal source,* Hoofddorp, 2017.

[7] Blue Star Ferries, "Our Ships," Blue Star Ferries, 2018. [Online]. Available: https://www.bluestarferries.com. [Accessed 26 January 2018].

[8] M. Iqbal and A. Trimulyono, "Optimization of catamaran demihull form in early stages of the design process," *Kapal,* vol. 11, no. 3, pp. 126-131, 2014.

[9] V. Dubrovsky and A. Tunik, Ships with outriggers, Backbone Pub., 2004.

[10] International Maritime Organization, "International Convention on Tonnage Measurement of Ships," International Maritime Organization, London, 1969.

[11] G. Myhre, D. Shindell, F.-M. Bréon, W. Collins, J. Fuglestvedt, J. Huang, D. Koch, J.-F. Lamarque, D. Lee, B. Mendoza, T. Nakajima, A. Robock, G. Stephens, T. Takemura and H. Zhang, "Anthropogenic and Natural Radiative Forcing," in *Climate Change 2013: The Physical Science Basis. Contribution of Working Group I to the Fifth Assessment Report of the Intergovernmental Panel on Climate Change*, Cambridge, Cambridge University Press, 2013, pp. 659-740.

[12] N. Olmer, B. Comer, B. Roy, X. Mao and D. Rutherford, "Greenhouse gas emissions from global shipping, 2013–2015," International Council on Clean Transportation, Washington, DC, 2017.

[13] P. Forster, V. Ramaswamy, P. Artaxo, T. Berntsen, R. Betts, D. Fahey, J. Haywood, J. Lean, D. Lowe, G. Myhre, J. Nganga, R. Prinn, G. Raga, M. Schulz and R. V. Dorland, "Changes in Atmospheric Constituents and in Radiative Forcing," in *Climate Change 2007: The Physical Science Basis. Contribution of Working Group I to the Fourth Assessment Report of the Intergovernmental Panel on Climate Change*, Cambridge, Cambridge University Press, 2007, pp. 129-234.

[14] D. Stapersma, Diesel Engines Volume 4 Emissions and Heat transfer, 6th ed., Delft: Royal Netherlands Naval College, 2010.

[15] IPCC, "Climate Change 2014 Mitigation of Climate Change. Contribution of Working Group III to the Fifth Assessment Report of the Intergovernmental Panel on Climate Change," Cambridge University Press, New York, 2014.

[16] U.S. Department of Energy, "Liquified Natural Gas: Understanding the Basic Facts," US Department op Energy, Washington, D.C., 2005.

[17] International Energy Agency, "Transport, energy and CO2 - Moving towards sustainability," OECD Publishing, Paris, 2009.

[18] Ipsos MORI, "Strong global opposition towards nuclear power," 23 June 2011. [Online]. Available: https://www.ipsos.com/ipsos-mori/en-uk/strong-global-opposition-towards-nuclear-power.

[19] J. Spoelstra, "Flettner-rotors besparen 18 % brandstof," *Technisch Weekblad,* no. 34/35, 2015.

© COPYRIGHT OF C-JOB, WHOSE PROPERTY, THIS DOCUMENT REMAINS. NO PART THEREOF MAY BE DISCLOSED, COPIED, DUPLICATED OR IN ANY OTHER WAY MADE USE OF EXCEPT WITH THE APPROVAL OF C-JOB.

[20] C. Willyard, "The answer is blowing in the wind," *Geotimes,* 2008.

[21] R. E. Sheldahl and P. C. Klimas, "Aerodynamic characteristics of seven symmetrical airfoil sections through 180-degree angle of attack for use in aerodynamic analysis of vertical axis wind turbines," Sandia National Labs., Albuquerque, 1981.

[22] E. Benini and A. Toffolo, "Optimal design of horizontal-axis wind turbines using blade-element theory and evolutionary computation," *Journal of Solar Energy Engineering,* vol. 124, no. 4, pp. 357-363, 2002.

[23] R. Schmalensee, "The Future of Solar Energy: An Interdisciplinary MIT Study," Energy Initiative, Massachusetts Institute of Technology, 2015.

[24] K. Granberg, "„Viking Grace- 20 months' experience of Ship to Ship LNG bunkering“," in *Go LNG– Final Conference to the SBSR Project "MARTECH LNG"*, Palanga, 2014.

[25] Fraunhofer ISE and PSG AG, "Photovoltaics report," Fraunhofer Institute for Solar Energy Systems, 12 July 2017. [Online]. Available: www.ise.fraunhofer.de.

[26] K. Jäger, O. Isabella, A. H. Smets, R. A. v. Swaaij and M. Zeman, Solar Energy: Fundamentals, Technology, and Systems, vol. 77, Delft: Delft University of Technology, 2014, p. 78.

[27] V. Frhenakis, "Photovoltaics: Present Status and Future Prospects," Columbia University, New York.

[28] National Academy of Sciences, The Hydrogen Economy: Opportunities, Costs, Barriers, and R&D Needs, Washington, D.C.: The National Academies Press, 2004.

[29] R. Westerwaal and W. Haije, "Evaluation solid-state hydrogen storage systems," *ECN Hydrogen and Clean Fossil Fuels,* 2008.

[30] A. Züttel, A. Remhof, A. Borgschulte and O. Friendrichs, "Hydrogen: the future energy carrier," *Energy materials to combat climate change,* vol. 368, no. 1923, pp. 3329-3342, 2010.

[31] C. Von der Heydt, Interviewee, *Hydrogen storage systems for ships.* [Interview]. 17 November 2017.

[32] T. Mai, "Technology Readiness Level," 7 August 2017. [Online]. Available: www.nasa.gov. [Accessed 12 January 2018].

[33] Fuel Cell Technologies Office, "Hydrogen Storage," U.S. Department of Energy, Washinton, DC, 2017.

[34] U.S. Geological Survey, "Mineral Commodity Summaries: Nitrogen (Fixed)—Ammonia," USGS, 2017.

[35] G. Thomas and G. Parks, "Potential Roles of Ammonia in a Hydrogen Economy: A Study of Issues Related to the Use Ammonia for On-Board Vehicular Hydrogen Storage," US Department of Energy, Washington, DC, 2006.

[36] N. J. Duijm, F. Markert and J. L. Paulsen, "Safety assessment of ammonia as a transport fuel," Risø National Laboratory, Roskilde, 2005.

[37] Hydro Instruments, "Ammonia Handling Manual," Hydro Instruments, Telford, 2013.

[38] L. Van Biert, M. Godjevac, K. Visser and P. V. Aravind, "A review of fuel cell systems for maritime applications," *Journal of Power Sources,* vol. 327, pp. 345-364, 2016.

[39] V. Hans, Interviewee, *Ammonia storage system characteristics.* [Interview]. 5 February 2018.

[40] ISPT, "Power to Ammonia: Feasibility study for the value chains and business cases to produce CO2-free ammonia suitable for various market applications," Institute for Sustainable Process Technology, Amersfoort, 2017.

[41] K. T. Møller, T. R. Jensen, E. Akiba and H.-w. Li, "Hydrogen - A sustainable energy carrier," *Progress in Natural Science: Materials International,* no. 27, pp. 34-40, 2017.

© COPYRIGHT OF C-JOB, WHOSE PROPERTY, THIS DOCUMENT REMAINS. NO PART THEREOF MAY BE DISCLOSED, COPIED, DUPLICATED OR IN ANY OTHER WAY MADE USE OF EXCEPT WITH THE APPROVAL OF C-JOB.

[42] I. Buchmann, "Learn About Batteries," 15 November 2017. [Online]. Available: http://batteryuniversity.com.

[43] M. Lee, J. Hong, J. Lopez, Y. Sun, D. Feng, K. Lim, W. C. Chueh, M. F. Toney, Y. Cui and Z. Bao, "High-performance sodium–organic battery by realizing four-sodium storage in disodium rhodizonate," *Nature Energy 2,* p. 861–868, 2017.

[44] D. L. Chandler, "New lithium-oxygen battery greatly improves energy efficiency, longevity," 25 July 2016. [Online]. Available: http://news.mit.edu/2016/new-lithium-oxygen-battery-greatly-improves-energy-efficiency-longevity-0725.

[45] O. Sapunkov, V. Pande, A. Khetan, C. Choomwattana and V. Viswanathan, "Quantifying the promise of 'beyond' Li–ion batteries," *Translational Materials Research,* vol. 2, no. 4, 2015.

[46] SIS International Research, "Lithium-Ion and Beyond: The Business of a Battery-Powered Future," 2018. [Online]. Available: https://www.sisinternational.com.

[47] N. Imanishi and O. Yamamoto, "Rechargeable lithium–air batteries: characteristics and prospects," *Materials Today,* vol. 17, no. 1, pp. 24-30, 2014.

[48] Battery University Group, "Future Batteries," battery university, 29 August 2017. [Online]. Available: http://batteryuniversity.com. [Accessed 15 January 2018].

[49] X. Zhang, X.-G. Wang, Z. Xie and Z. Zhou, "Recent progress in rechargeable alkali metal–air batteries," *Green Energy & Environment,* vol. 1, no. 1, pp. 4-17, 2016.

[50] T. Zhang, Z. Tao and J. Chen, "Magnesium–air batteries: from principle to application," *Materials Horizons,* vol. 1, no. 2, pp. 196-206, 2014.

[51] B. Evenblij, "Energe storage," [Online]. Available: https://www.tno.nl. [Accessed 18 January 2018].

[52] H. Zhang, X. Li and H. Zhang, Li–S and Li–O2 Batteries with High Specific Energy: Research and Development, S. K. Sharma, Ed., Springer, 2017.

[53] P. Kurzweil, "Lithium Battery Energy Storage: State of the Art Including Lithium-Air and Lithium-Sulfur Systems," in *Electrochemical Energy Storage for Renewable Sources and Grid Balancing*, P. T. Moseley and J. Garche, Eds., Elsevier, 2015, pp. 269-307.

[54] M. Hagen, P. Fanz and J. Tübke, "Cell energy density and electrolyte/sulfur ratio in Li–S cells," *Journal of Power Sources,* vol. 264, pp. 30-34, 2014.

[55] S. S. Zhang, "Liquid electrolyte lithium/sulfur battery: Fundamental chemistry, problems, and solutions," *Journal of Power Sources,* vol. 231, pp. 153-162, 2013.

[56] J. Merkisz, M. Dobrzyński, M. Kozak, P. Lijewsk, P. Fuć, M. Maciej, W. Slawomir, A.-W. Marta, D. Kamil, P. Andrzej, M. Paczuski, M. Marchwiany, R. Pulawski, A. Pankowski, K. Kurpiel, M. Przedlacki and A. Matuszewska, Alternative Fuels, Technical and Environmental Conditions, K. Biernat, Ed., Rijeka, `: InTech, 2016.

[57] J. Larminie and A. Dicks, Fuel Cell Systems Explained, Chichester: John Wiley & Sons Ltd, 2003.

[58] K. Gillingham, "Hydrogen Internal Combustion Engine Vehicles: A Prudent Intermediate Step or a Step in the Wrong Direction?," Stanford University, Stanford, 2007.

[59] U.S. Department of Energy, "A National vision of America's Transition to a hydrogen Economy-To2030 and Beyond," US Department of Energy, Washington, D.C., 2002.

[60] T. Tronstad, H. H. Åstrand, G. P. Haugom and L. Langfeldt, "Study on the use of fuel cells in shipping," DNV GL– Maritime, Hamburg, 2017.

[61] Y. M. A. Welaya, M. M. E. Gohary and N. R. Ammar, "A comparison between fuel cells and other alternatives for marine electric power generation," *International Journal of Naval Architecture and Ocean Engineering,* vol. 3, no. 2, pp. 141-149, 2011.

© COPYRIGHT OF C-JOB, WHOSE PROPERTY, THIS DOCUMENT REMAINS. NO PART THEREOF MAY BE DISCLOSED, COPIED, DUPLICATED OR IN ANY OTHER WAY MADE USE OF EXCEPT WITH THE APPROVAL OF C-JOB.

[62] S. B. Gupta, M. Biruduganti, B. Bihari and R. Sekar, "Natural Gas Fired Reciprocating Engines for Power Generation: Concerns and Recent Advances," in *Natural Gas- Extraction to End Use*, InTech, 2012.

[63] Fuel Cell Technologies Office, "Fuel Cell Technologies Office Multi-Year Research, Development, and Demonstration Plan," U.S. Department of Energy, Washington, DC, 2017.

[64] H. Klein Woud and D. Stapersma, Design of Propulsion an Electric Power Generation Systems, London: IMarEST, 2012.

[65] D. Shekhawat, J. Spivey and D. Berry, Eds., Fuel Cells: Technologies for Fuel Processing, Elsevier, 2011.

[66] R. Lan and S. Tao, "Ammonia as a Suitable Fuel for Fuel Cells," *Frontiers in Energy Research,* vol. 2, p. 35, 2014.

[67] Fuel Cell Today, "Technologies," Johnson Matthey, 2018. [Online]. Available: http://www.fuelcelltoday.com. [Accessed 16 January 2018].

[68] R. Halseid, P. Vie and R. Tunold, "Effect of ammonia on the performance of polymer electrolyte membrane fuel cells," *Journal of Power Sources,* vol. 154, pp. 343-350, 2006.

[69] DNV GL, "Current price development oil and gas," DNV GL, 10 January 2018. [Online]. Available: https://www.dnvgl.com/. [Accessed 26 January 2018].

[70] World Bank, Ecofys and Vivid Economics, "State and Trends of Carbon Pricing 2017," The World Bank, Washington, DC, 2017.

[71] C. Frei, R. Whitney, H.-W. Schiffer, K. Rose, D. A. Rieser, A. Al-Qahtani, P. Thomas, H. Turton, M. Densing, E. Panos and K. Volkart, "World Energy Scenarios: Composing energy futures to 2050," in *World Energy Council*, London, 2013.

[72] Cefic, "European chemistry for growth: Unlocking a competitive, low carbon and energy efficient future," Brussels, 2013.

[73] Y. Demirel, "Energy and Energy Types," in *Energy*, London, Springer, 2012, pp. 27-70.

[74] U.S. Energy Information Administration, "Annual Energy Outlook 2017 with projections to 2050," U.S. Energy Information Administration, Washington, DC, 2017.

[75] European Commission, "EU Reference Scenario 2016 – Energy, transport and GHG emissions - Trends to 2050," European Commission Directorate-General for Energy, Directorate-General for Climate Action and Directorate-General for Mobility and Transport, 2016.

[76] U.S. Department of Energy, "Levelized Cost of Energy (LCOE)," 2015. [Online]. Available: https://www.energy.gov. [Accessed 5 February 2018].

[77] R. Andrews, "UK Electricity 2050 Part 4: Nuclear and renewables cost comparisons," 21 February 2017. [Online]. Available: http://euanmearns.com/.

[78] R. Wiser, K. Jenni, J. Seel, E. Baker, M. Hand, E. Lantz and A. Smith, "Expert elicitation survey on future wind energy costs," *Nature Energy,* vol. 1, no. 10, 2016.

[79] M. Ram, D. Bogdanov, A. Aghahosseini, A. Oyewo, A. Gulagi, M. Child, H.-J. Fell and C. Breyer, "Global Energy System based on 100% Renewable Energy - Power Sector," Lappeenranta, Berlin, 2017.

[80] Agora Energiewende, "Future cost of onshore wind. Recent auction results, long-term outlook and implications for upcoming German auctions.," Berlin, 2017.

[81] International Energy Agency, "Technology Roadmap: Hydrogen and Fuel Cells," International Energy Agency, Paris, 2015.

[82] Y. Bennania, A. Perlb, A. Patila, C. E. Van Somerenb, L. J. Heijneb and M. Van Steenisc, "Power-to-Ammonia: Rethinking the role of ammonia--from a value product to a flexible energy carrier (FlexNH3)," Hanzehogeschool, Groningen, 2016.

© COPYRIGHT OF C-JOB, WHOSE PROPERTY, THIS DOCUMENT REMAINS. NO PART THEREOF MAY BE DISCLOSED, COPIED, DUPLICATED OR IN ANY OTHER WAY MADE USE OF EXCEPT WITH THE APPROVAL OF C-JOB.

[83] J. Hinkley, J. Hayward, R. McNaughton, J. Edwards and K. Lovegrove, "Concentrating solar fuels roadmap – final report," CSIRO, 2016.

[84] V. Subramani, A. Basile and T. Veziro, Eds., Compendium of Hydrogen Energy: Volume 1: Hydrogen Production and Purification, Woodhead Publishing, 2015.

[85] C. Philibert, "Renewable Energy for Industry," International Energy Agency, Paris, 2017.

[86] U. Bossel and B. Eliasson, "Energy and the Hydrogen Economy," Methanol Institute, Arlington, 2003.

[87] International Transport Forum, "Decarbonising Maritime Transport: Pathways to zero-carbon shipping by 2035," Paris, 2018.

[88] K. Lorentsson, Interviewee, *LNG storage and handeling systems.* [Interview]. 22 January 2018.

[89] K. Hirose, Handbook of Hydrogen Storage: New Materials for Future Energy Storage, M. Hirscher, Ed., John Wiley & Sons, 2010.

[90] T. Hua, R. Ahluwalia, J.-K. Peng, M. Kromer, S. Lasher, K. McKenney, K. Law and J. Sinha, "Technical Assessment of Compressed Hydrogen Storage Tank Systems for Automotive Applications," Argonne National Laboratory, Argonne, 2010.

[91] U.S. Department of Energy, "Hydrogen, Fuel Cells & Infrastructure Technologies Program," US Department of Energy, Washington DC, 2007.

[92] K. Law, J. Rosenfeld, V. Han, M. Chan, H. Chiang and J. Leonard, "U.S. Department of Energy Hydrogen Storage Cost Analysis," U.S. Department of Energy, Cupertino, 2013.

[93] B. D. James, "2015 DOE Hydrogen and Fuel Cells Program Review," Strategic Analysis Inc., 9 June 2015. [Online]. Available: https://www.hydrogen.energy.gov.

[94] B. D. James, C. Houchins, J. M. Huya-Kouadio and D. A. DeSantis, "Final Report: Hydrogen Storage System Cost Analysis," Strategic Analysis Inc., Arlington, 2016.

[95] Y. Bicer and I. Dincer, "Comparative assessment of NH3 production and utilization in agriculture, energy and utilities, and transportation systems for Ontario," University of Ontario, Ontario, 2016.

[96] European Fertilizer Manufacturers Association, "Guidance for transporting ammonia by rail," EFMA, Brussels, 2007.

[97] S. Boergert and G. Nyquist, "Super-Safe Large Anhydrous Ammonia Tanks," Mackinaw Associates, 2008. [Online]. Available: https://nh3fuelassociation.org. [Accessed 22 March 2018].

[98] Colorado Department of Agriculture, "Inspection and Consumer Services Division: Storage and Handling of Anhydrous Ammonia," 2015. [Online]. Available: https://www.colorado.gov. [Accessed 22 March 2018].

[99] Lloyd's Register Group Limited & UMAS, "Zero-Emission Vessels 2030. How do we get there?," Lloyd's Register Group Limited, London, 2017.

[100] L. O. Valøen and M. I. Shoesmith, "The effect of PHEV and HEV duty cycles on battery and battery pack performance," in *PHEV 2007 Conference*, 2007.

[101] N. Imanishi, A. Luntz and P. Bruce, Eds., The Lithium Air Battery: Fundamentals, New York: Springer, 2014.

[102] Y. Deng, J. Li, T. Li, X. Gao and C. Yuan, "Life cycle assessment of lithium sulfur battery for electric vehicles," *Journal of Power Sources,* vol. 343, pp. 284-295, 2017.

[103] O. Sharaf and M. Orhan, "An overview of fuel cell technology: Fundamentals and applications," *Renewable and Sustainable Energy Reviews,* vol. 32, pp. 810-853, 2014.

[104] S. Zhang, K. Xu and T. Jow, "Charge and discharge characteristics of a commercial LiCoO2-based 18650 Li-ion battery," *Journal of Power Sources,* vol. 160, no. 2, pp. 1403-1409, 2006.

© COPYRIGHT OF C-JOB, WHOSE PROPERTY, THIS DOCUMENT REMAINS. NO PART THEREOF MAY BE DISCLOSED, COPIED, DUPLICATED OR IN ANY OTHER WAY MADE USE OF EXCEPT WITH THE APPROVAL OF C-JOB.

[105] P. G. Bruce, S. A. Freunberger, L. J. Hardwick and J.-M. Tarascon, "Li–O2 and Li–S batteries with high energy storage," *Nature Materials,* vol. 11, no. 1, pp. 19-29, 2012.

[106] G. Lampič, G. Gotovac, H. Geaney and C. O'Dwyer, "Comparing the suitability of Lithium ion, Lithium Sulfur and Lithium air batteries for current and future vehicular applications," 2016.

[107] Wartsila, "Wartsila 46DF product guide," 4 November 2016. [Online]. Available: https://www.wartsila.com.

[108] H. Thomson, J. Corbett and J. Winebrake, "Natural gas as a marine fuel," *Energy Policy,* vol. 87, pp. 153-167, 2015.

[109] Y. M. Welaya, M. Mosleh and N. R. Ammar, "Thermodynamic analysis of a combined gas turbine power plant with a solid oxide fuel cell for marine applications," *International Journal of Naval Architecture and Ocean Engineering,* vol. 5, no. 4, pp. 529-545, 2013.

[110] Wärtsilä, "Wärtsilä Dual-Fuel LNGC," March 2008. [Online]. Available: http://www.dieselduck.info. [Accessed 4 April 2018].

[111] N. M. Neil Wembridge, "Thermal Power Station Advice - Reciprocating Engines Study," Parksons Brinkerhoff, Auckland, 2009.

[112] CSIRO, "Unlocking Australia's Energy Potential," Newcastle, 2011.

[113] National Energy Technology Laboratory , "Fossil Energy Power Plant Desk Reference," U.S. Department of Energy, Pittsburgh, 2007.

[114] U.S. Energy Information Administration, "Construction cost data for electric generators installed in 2015," 19 May 2017. [Online]. Available: https://www.eia.gov. [Accessed 5 April 2018].

[115] D. Stenersen and O. Thonstad, "GHG and NOx emissions from gas fuelled engines," SINTEF Ocean AS, Trondheim, 2017.

[116] L.-A. Skarbø, "Marine Gas Engines, solutions and possibilities," Rolls-Royce Marine, 2009. [Online]. Available: https://www.sintef.no.

[117] M. Acciaro, "Real option analysis for environmental compliance: LNG and emission control areas," *Transportation Research Part D: Transport and Environment,* vol. 28, pp. 41-50, 2014.

[118] S. Verhelst and T. Wallner, "Hydrogen-fueled internal combustion engines," *Progress in Energy and Combustion Science,* vol. 35, no. 6, pp. 490-527, 2009.

[119] M. E. Soberanis and A. Fernandez, "A review on the technical adaptations for internal combustion engines to operate with gas/hydrogen mixtures," *International Journal of Hydrogen Energy,* vol. 35, no. 21, pp. 12134-12140, 2010.

[120] H. Safaria, S. Jazayeria and R. Ebrahimib, "Potentials of NOX emission reduction methods in SI hydrogen engines: Simulation study," *International Journal of Hydrogen Energy,* vol. 34, no. 2, pp. 1015-1025, 2009.

[121] J. Lee, K. Lee, J. Lee and B. Anh, "High power performance with zero NOx emission in a hydrogen-fueled spark ignition engine by valve timing and lean boosting," *Fuel,* vol. 128, pp. 381-389, 2014.

[122] N. Yamada and M. N. A. Mohamad, "Efficiency of hydrogen internal combustion engine combined with open steam Rankine cycle recovering water and waste heat," *International Journal of Hydrogen Energy,* vol. 35, no. 3, pp. 1430-1442, 2010.

[123] J. Gomes Antunes, R. Mikalsen and A. Roskilly, "An experimental study of a direct injection compression ignition hydrogen engine," *International Journal of Hydrogen Energy,* vol. 34, no. 15, pp. 6516-6522, 2009.

[124] C. Zamfirescu and I. Dincer, "Ammonia as a green fuel and hydrogen source for vehicular applications," *Fuel Processing Technology,* vol. 90, no. 5, pp. 729-737, 2009.

© COPYRIGHT OF C-JOB, WHOSE PROPERTY, THIS DOCUMENT REMAINS. NO PART THEREOF MAY BE DISCLOSED, COPIED, DUPLICATED OR IN ANY OTHER WAY MADE USE OF EXCEPT WITH THE APPROVAL OF C-JOB.

[125] S. Giddey, S. P. S. Badwal, C. Munnings and M. Dolan, "Ammonia as a Renewable Energy Transportation Media," *ACS Sustainable Chemistry & Engineering,* vol. 5, no. 11, pp. 10231-10239, 2017.

[126] C. Mørch, A. Bjerre, M. Gøttrup, S. Sorenson and J. Schramm, "Ammonia/hydrogen mixtures in an SI-engine: Engine performance and analysis of a proposed fuel system," *Fuel,* vol. 90, no. 2, pp. 854-864, 2011.

[127] A. J. Reiter and S.-C. Kong, "Demonstration of Compression-Ignition Engine Combustion Using Ammonia in Reducing Greenhouse Gas Emissions," *Energy & Fuels,* vol. 22, no. 5, pp. 2963-2971, 2008.

[128] M. Comotti and S. Frigo, "Hydrogen generation system for ammonia–hydrogen fuelled internal combustion engines," *International Journal of Hydrogen Energy,* vol. 40, no. 33, pp. 10673-10686, 2015.

[129] C. Duynslaegher, H. Jeanmart and J. Vandooren, "Ammonia Combuston in spark ignition engine conditions," 2012. [Online]. Available: https://nh3fuelassociation.org.

[130] N. Matthias, T. Wallner and R. Scarcelli, "A hydrogen direct injection engine concept that exceeds U.S. DOE light-duty efficiency targets," *SAE International Journal of Engines,* vol. 5, pp. 838-849, 2012.

[131] S. Verhelst, "Recent progress in the use of hydrogen as a fuel for internal combustion engines," *International Journal of Hydrogen Energy,* vol. 39, no. 2, pp. 1071-1085, 2014.

[132] P. V. Blarigan, "Advanced Internal Combustion Engine Research," in *Proceedings of the 2000 U.S. DOE Hydrogen Program Review*, San Ramon, 2000.

[133] L. Van Biert, Interviewee, *Weight and Volume of fuel cells in 2050.* [Interview]. 14 March 2018.

[134] P. Patel and M. Farooque, "DFC Technology Status," FuelCell Energy, Inc., 16 November 2009. [Online]. Available: https://energy.gov/.

[135] P. Breeze, Fuel Cells, Academic Press, 2017.

[136] A. Afif, N. Radenahmad, Q. Cheok, S. Shams, J. H.Kim and A. K. Azad, "Ammonia-fed fuel cells: a comprehensive review," *Renewable and Sustainable Energy Reviews,* vol. 60, pp. 822-835, 2016.

[137] M. Santin, A. Traverso and L. Magistri, "Liquid fuel utilization in SOFC hybrid systems," *Applied Energy,* vol. 86, no. 10, pp. 2204-2212, 2009.

[138] F. Ishak, "Thermodynamic Analysis of Ammonia and Urea fed Solid Oxide Fuel Cells," University of Ontario Institute of Technology, Ontario, 2011.

[139] Q. Ma, R. Peng, L. Tian and G. Meng, "Direct utilization of ammonia in intermediate-temperature solid oxide fuel cells," *Electrochemistry Communications,* vol. 8, no. 11, pp. 1791-1795, 2006.

[140] Y. D. Lee, K. Y. Ahn, T. Morosuk and G. Tsatsaronis, "Environmental impact assessment of a solid-oxide fuel-cell-based combined-heat-and-power-generation system," *Energy,* vol. 79, pp. 455-466, 2015.

[141] V. Contini, "Manufacturing Cost Analyses of Fuel Cell Systems for Non-Transportation Applications," Battelle, 24 Januari 2017. [Online]. Available: https://www.energy.gov. [Accessed 17 March 2018].

[142] C. Thomas, "Fuel cell and battery electric vehicles compared," *International Journal of Hydrogen Energy,* vol. 34, no. 15, pp. 6005-6020, 2009.

[143] B. D. James, J. M. Huya-Kouadio, C. Houchins and D. A. DeSantis, "Mass Production Cost Estimation of Direct H2 PEM Fuel Cell Systems for Transportation Applications: 2016 Update," U.S. Department of Energy, Washington, DC, 2017.

© COPYRIGHT OF C-JOB, WHOSE PROPERTY, THIS DOCUMENT REMAINS. NO PART THEREOF MAY BE DISCLOSED, COPIED, DUPLICATED OR IN ANY OTHER WAY MADE USE OF EXCEPT WITH THE APPROVAL OF C-JOB.

[144] X. Yan, M. Hou, H. Zhang, F. Jing, P. Ming and B. Yi, "Performance of PEMFC stack using expanded graphite bipolar plates," *Journal of Power Sources,* vol. 160, no. 1, pp. 252-257, 2006.

[145] Fuel Cell Store, "H-300 Fuel Cell Stack User Manual," 13 August 2013. [Online]. Available: http://www.fuelcellstore.com. [Accessed 5 March 2018].

[146] A. Mendez, T. J. Leo and M. A. Herreros, "Current State of Technology of Fuel Cell Power Systems for Autonomous Underwater Vehicles," *Energies,* vol. 7, no. 7, pp. 4676-4693, 2014.

[147] Doosan Fuel Cell, "연료전지 시스템," 2018`. [Online]. Available: http://www.doosanfuelcell.com/. [Accessed 5 March 2018].

[148] Battelle Memorial Institute, "Manufacturing Cost Analysis of 100 and 250 kW Fuel Cell Systems for Primary Power and Combined Heat and Power Applications," Battelle Memorial Institute, Columbus, 2016.

[149] U.S. Department of Energy, "DOE Hydrogen and Fuel Cells Program Record," U.S. Department of Energy, Washington, 2017.

[150] OSAKA GAS CO.LTD., "Residential solid oxide fuel cell (SOFC) system," 2012. [Online]. Available: http://www.osakagas.co.jp.

[151] M. Figari and M. Viviani, "Conceptual design of a Fuel Cell Electric Generator for a Ro/Ro Passenger Ferry Vessel," in *HIPER 04: 4th International Conference on High-Performance Marine Vehicles*, Rome, 2004.

[152] P. Jienkulsawad, D. Saebea, Y. Patcharavorachot, S. Kheawhom and A. Arpornwichanop, "Analysis of a solid oxide fuel cell and a molten carbonate fuel cell integrated system with different configurations," *International Journal of Hydrogen Energy,* vol. 43, no. 2, pp. 932-942, 2018.

[153] E. Fontell, T. Kivisaari, N. Christiansen, J.-B. Hansen and J. Pålsson, "Conceptual study of a 250 kW planar SOFC system for CHP application," *Journal of Power Sources,* vol. 131, no. 1-2, pp. 49-56, 2004.

[154] Bloomenergy, "ES5 Data Sheet," 2016. [Online]. Available: http://www.bloomenergy.com. [Accessed 5 March 2018].

[155] T. A. Adams, J. Nease, D. Tucker and P. I. Barton, "Energy Conversion with Solid Oxide Fuel Cell Systems: A Review of Concepts and Outlooks for the Short- and Long-Term," *Industrial & Engineering Chemistry Research,* vol. 52, no. 9, pp. 3089-3111, 2012.

[156] C. Ezgi, M. T. Çoban and Ö. Selvi, "Design and Thermodynamic Analysis of an SOFC System for Naval Surface Ship Application," *Journal of Fuel Cell Science and Technology,* vol. 10, no. 3, p. 031006, 2013.

[157] A. Thaker, M. Mathew, N. Hasib and N. Herringer, "A Review of Ammonia Fuel Cells," *The Royal Society of Chemistry,* 2015.

[158] M. Kishimoto, N. Furukawa, T. Kume, H. Iwai and H. Yoshida, "Formulation of ammonia decomposition rate in Ni-YSZ anode of solid oxide fuel cells," *International Journal of Hydrogen Energy,* vol. 42, no. 4, pp. 2370-2380, 2017.

[159] G. Cinti, G. Discepoli, E. Sisani and U. Desideri, "SOFC operating with ammonia: Stack test and system analysis," *International Journal of Hydrogen Energy,* vol. 41, no. 31, pp. 13583-13590, 2016.

[160] L. Liu, K. Sun, X. Wu, X. Z. M. Li, N. Zhang and X. Zhou, "Improved performance of ammonia-fueled solid oxide fuel cell with SSZ thin film electrolyte and Ni-SSZ anode functional layer," *International Journal of Hydrogen Energy,* vol. 37, no. 14, pp. 10857-10865, 2012.

[161] A. Fuerte, R. Valenzuela, M. Escudero and L. Daza, "Ammonia as efficient fuel for SOFC," *Journal of Power Sources,* vol. 192, no. 1, pp. 170-174, 2009.

© COPYRIGHT OF C-JOB, WHOSE PROPERTY, THIS DOCUMENT REMAINS. NO PART THEREOF MAY BE DISCLOSED, COPIED, DUPLICATED OR IN ANY OTHER WAY MADE USE OF EXCEPT WITH THE APPROVAL OF C-JOB.

[162] G. Fournier, I. Cumming and K. Hellgardt, "High performance direct ammonia solid oxide fuel cell," *Journal of Power Sources,* vol. 162, no. 1, pp. 198-206, 2006.

[163] N. J. J. Dekker and G. Rietveld, "Highly Efficient Conversion of Ammonia in Electricity by Solid Oxide Fuel Cells," *Journal of Fuel Cell Science and Technology,* vol. 3, no. 4, pp. 499-502, 2006.

[164] Q. Ma, R. Peng, Y. Lin, J. Gao and G. Meng, "A high-performance ammonia-fueled solid oxide fuel cell," *Journal of Power Sources,* vol. 161, no. 1, pp. 95-98, 2006.

[165] O. Siddiqui and I. Dincer, "A review and comparative assessment of direct ammonia fuel cells," *Thermal Science and Engineering Progress,* vol. 5, pp. 568-578, 2018.

[166] L. Zhang and W. Yang, "Direct ammonia solid oxide fuel cell based on thin proton-conducting electrolyte," *Journal of Power Sources,* vol. 179, no. 1, pp. 92-95, 2008.

[167] Q. Ma, J. Ma, S. Zhou, R. Yan, J. Gao and G. Meng, "A high-performance ammonia-fueled SOFC based on a YSZ thin-film electrolyte," *Journal of Power Sources,* vol. 164, no. 1, pp. 86-89, 2007.

[168] T. Haneda and A. Akisawa, "Technological assessment of PEFC power generation system using by-product hydrogen produced from a caustic soda plant," *International Journal of Hydrogen Energy,* vol. 42, no. 5, pp. 3240- 3249, 2017.

[169] P. Tomczyk, "MCFC versus other fuel cells—Characteristics, technologies and prospects," *Journal of Power Sources,* vol. 160, no. 2, pp. 858-862, 2006.

[170] M. C. Williams and H. C. Maru, "Distributed generation—Molten carbonate fuel cells," *Journal of Power Sources,* vol. 160, no. 2, pp. 863-867, 2006.

[171] F. Gardner, M. Day, N. Brandon, M. Pashley and M. Cassidy, "SOFC technology development at Rolls-Royce," *Journal of Power Sources,* vol. 86, pp. 122-129, 2000.

[172] M. Rokni, "Addressing fuel recycling in solid oxide fuel cell systems fed by alternative fuels," *Energy,* vol. 137, pp. 1013-1025, 2017.

[173] T. Lipman and N. Shah, "Ammonia as an Alternative Energy Storage Medium for Hydrogen Fuel Cells: Scientific and Technical Review for Near-Term Stationary Power Demonstration Projects, Final Report," UC Berkeley Institute of Transportation Studies, Berkeley, 2007.

[174] J. Ganley, E. Seebauer and R. Masel, "Development of a microreactor for the production of hydrogen from ammonia," *Journal of Power Sources,* vol. 137, no. 1, pp. 53-61, 2004.

[175] R. Z. Sørensen, L. J. Nielsen, S. Jensen, O. Hansen, T. Johannessen, U. Quaade and C. H. Christensen, "Catalytic ammonia decomposition: miniaturized production of COx-free hydrogen for fuel cells," *Catalysis Communications,* vol. 6, no. 3, pp. 229-232, 2005.

[176] M. Wang, J. Li, L. Chen and Y. Lu, "Miniature NH3 cracker based on microfibrous entrapped Ni-CeO2/Al2O3 catalyst monolith for portable fuel cell power supplies," *International Journal of Hydrogen Energy,* vol. 34, no. 4, pp. 1710-1716, 2009.

[177] A. Di Carlo, L. Vecchione and Z. Del Prete, "Ammonia decomposition over commercial Ru/Al2O3 catalyst: An experimental evaluation at different operative pressures and temperatures," *International Journal of Hydrogen Energy,* vol. 39, no. 2, pp. 808-814, 2014.

[178] S. Chiuta, R. C. Everson, H. W. Neomagus, P. d. Gryp and D. G. Bessarabov, "Reactor technology options for distributed hydrogen generation via ammonia decomposition: A review," *International Journal of Hydrogen Energy,* vol. 38, no. 35, pp. 14968-14991, 2013.

[179] W. I. David, J. W. Makepeace, S. K. Callear, H. M. Hunter, J. D. T. J. Taylor and M. O. Jones, "Hydrogen Production from Ammonia Using Sodium Amide," *Journal of the American Chemical Society,* vol. 136, no. 38, pp. 13082-13085, 2014.

[180] J. W. Makepeace, T. J. Wood, H. M. Hunter, M. O. Jones and W. I. David, "Ammonia decomposition catalysis using non-stoichiometric lithium imide," *Chemical Science,* vol. 6, no. 7, pp. 3805-3815, 2015.

© COPYRIGHT OF C-JOB, WHOSE PROPERTY, THIS DOCUMENT REMAINS. NO PART THEREOF MAY BE DISCLOSED, COPIED, DUPLICATED OR IN ANY OTHER WAY MADE USE OF EXCEPT WITH THE APPROVAL OF C-JOB.

[181] R. E. White, C. G. Vayenas and M. E. Gamboa-Aldeco, Eds., Modern Aspects of Electrochemistry 45, New York: Springer, 2009.

[182] B. Leighty, "Costs of Delivered Energy from Large-scale, Diverse, Stranded, Renewable Resources, Transmitted and Firmed as Electricity, Gaseous Hydrogen, and Ammonia," in *Ammonia: Key to US Energy Independence*, Denver, 2006.

[183] V. Alagharu, S. Palanki and K. N. West, "Analysis of ammonia decomposition reactor to generate hydrogen for fuel cell applications," *Journal of Power Sources,* vol. 195, no. 3, pp. 829-833, 2010.

[184] Borel Swiss SA, "Cracked Ammonia Generator 950 °C," 2 February 2015. [Online]. Available: https://www.borel-furnaces.com/.

[185] S. Grannell and D. E. Gillespie, "Ammonia flame cracker system, method and apparatus". United States of America Patent US 20120148925A1 , 2012.

[186] J. Engbaek, "Ammonia cracker for Hydrogen Generation for PEM Application," 2012. [Online]. Available: https://nh3fuelassociation.org.

[187] B. David, "Session: NH3 Fuel Use," in *2016 NH3 Fuel Conference*, Los Angeles, 2016.

[188] M. Afman, S. Hers and T. Scholten, "Energy and electricity price scenarios 2020-2023-2030: Input to Power to Ammonia value chains and business cases," CE Delft, Delft, 2017.

[189] M. Ventura, "RO/RO Ships," Instituto Superior Technico, [Online]. Available: http://www.mar.ist.utl.pt/mventura/Projecto-Navios-I/EN/SD-1.4.4-RO-RO%20Ships.pdf. [Accessed 28 April 2018].

[190] C. Hagemeister and H. O. H. Kristensen, "Environmental performance evaluation of RoPax ferries," *Ship & Offshore,* vol. 3, pp. 10-14, 2011.

[191] National Center for Biotechnology Information, "PubChem Compound Database; CID=222 & CID=297," [Online]. Available: https://pubchem.ncbi.nlm.nih.gov/. [Accessed 15 May 2018].

[192] IMO, "International Code for the Construction and Equipment of Ships Carrying Liquefied Gases in Bulk," IMO Publishing, London, 2016.

[193] IMO, "International Code of Safety for Ships using Gases or other Low-Flashpoint Fuels," IMO Publishing, London, 2016.

[194] D. Watson, Practical Ship Design, 2nd ed., vol. 1, Oxford: Elsevier, 2002.

[195] Fjordline, "MS Stavangerfjord und MS Bergensfjord," 2018. [Online]. Available: https://www.fjordline.com/. [Accessed 25 April 2018].

[196] P. Pospiech, "LNG is a Crystal Clear Alternative," *Maritime Reporter and Engineering News,* pp. 40-45, January 2014.

[197] A. Massardo and F. Lubelli, "Internal reforming solid oxide fuel cell-gas turbine combined cycles (IRSOFC-GT): part A Cell model and cycle thermodynamic analysis," in *International Gas Turbine & Aeroengine Congress & Exhibition*, Stockholm, 1998.

[198] J. Palsson, A. Selimovic and L. Sjunnesson, "Combined solid oxide fuel cell and gas turbine systems for efficient power and heat generation," *Journal of Power Sources,* vol. 86, no. 1-2, pp. 442-448, 1999.

[199] M. A. Azizi and J. Brouwer, "Progress in solid oxide fuel cell-gas turbine hybrid power systems: System design and analysis, transient operation, controls and optimization," *Applied Energy,* vol. 215, pp. 237-289, 2018.

[200] Z. Jia, J. Sun, H. Dobbs and J. King, "Feasibility study of solid oxide fuel cell engines integrated with sprinter gas turbines: Modeling, design and control," *Journal of Power Sources,* vol. 275, pp. 111-125, 2015.

© COPYRIGHT OF C-JOB, WHOSE PROPERTY, THIS DOCUMENT REMAINS. NO PART THEREOF MAY BE DISCLOSED, COPIED, DUPLICATED OR IN ANY OTHER WAY MADE USE OF EXCEPT WITH THE APPROVAL OF C-JOB.

[201] "Is solar power worth the investment?," Empire Renewable Energy, 2018. [Online]. Available: http://solarbyempire.com/. [Accessed 16 May 2018].

[202] E. Grey, "Wind propulsion: an old concept with a modern edge," Ship Technology, 13 March 2016. [Online]. Available: https://www.ship-technology.com/. [Accessed 16 May 2018].

[203] Global Maritime Energy Efficiency Partnerships, "Flettner rotors," [Online]. Available: http://glomeep.imo.org/. [Accessed 16 May 2018].

[204] Lloyd's Register, "Viking Grace installs rotor sail for wind-assisted propulsion.," Lloyd's Register, 30 April 2018. [Online]. Available: https://www.lr.org. [Accessed 16 May 2018].

[205] Norsepower, "Norsepower – your provider of auxiliary wind propulsion," Norsepower Oy Ltd, [Online]. Available: https://www.norsepower.com/. [Accessed 16 May 2018].

[206] J. Grevink, "MT44005 Marine Propulsion Systems College slides: Podded Propulsors," May 2017. [Online]. Available: https://blackboard.tudelft.nl/. [Accessed 17 April 2018].

[207] S. Toxopeus and G. Loeff, "Manoeuvring Aspects of Fast Ships with Pods," in *3rd International EuroConference on High-Performance Marine Vehicles HIPER'02*, Bergen, 2002.

[208] L. Kobylinski, "Problems of handling ships equipped with AZIPOD propulsion systems," *Prace Naukowe Politechniki Warszawskiej. Transport,* vol. 95, pp. 231-245, 2013.

[209] G. Lavini, "Podded Propulsion," in *34th WEGEMT School "Developments in the Design of Propulsors and Propulsion Systems"*, Delft, 2000.

[210] ABB, "ABB Azipod® hydrodynamic efficiency is improved again by more than 2 percent," 22 November 2011. [Online]. Available: http://www.abb.com/. [Accessed 17 May 2018].

[211] M. C. Díaz-de-Baldasano, F. J. Mateos, L. R. Núñez-Rivas and T. J. Leo, "Conceptual design of offshore platform supply vessel based on hybrid diesel generator-fuel cell power plant," *Applied Energy,* vol. 116, pp. 91-100, 2014.

[212] Coinnews Media Group, "US Inflation Calculator," Coinnews Media Group, 2018. [Online]. Available: http://www.usinflationcalculator.com/. [Accessed 30 January 2018].

[213] Statista, "Projection of coal and natural gas prices from 2016 to 2050 (in U.S. dollars per million British thermal units)*," Statista, 2018. [Online]. Available: https://www.statista.com/statistics/189185/projected-natural-gas-vis-a-vis-coal-prices/. [Accessed 25 January 2018].

[214] De Energieconsultant B.V., "De Energyconsultant," De Energieconsultant B.V., 2018. [Online]. Available: http://www.energieconsultant.nl. [Accessed 25 January 2018].

[215] C. Zaiontz, "Creating Box Plots in Excel," 2014. [Online]. Available: http://www.real-statistics.com/. [Accessed 3 May 2018].

[216] Microsoft, "Create a box and whisker chart," Microsoft, 2018. [Online]. Available: https://support.office.com/. [Accessed 3 May 2018].

[217] P. P. Edwards, V. Kuznetsov and W. David, "Hydrogen Energy," *Philosophical Transactions of the Royal Society of London A: Mathematical, Physical and Engineering Sciences,* vol. 365, no. 1853, pp. 1043-1056, 2007.

[218] J. Bartels, "A feasibility study of implementing an Ammonia Economy," Iowa State University, Ames, 2008.

[219] X. Wang, Y. Sone, H. Naito, C. Yamada, G. Segami and K. Kibe, "Cycle-life testing of large-capacity lithium-ion cells in simulated satellite operation," *Journal of Power Sources,* vol. 161, no. 1, pp. 594-600, 2006.

[220] J. Schmalstieg, S. Käbitz, M. Ecker and D. U. Sauer, "A holistic aging model for Li(NiMnCo)O2 based 18650 lithium-ion batteries," *Journal of Power Sources,* vol. 257, pp. 325-334, 2014.

© COPYRIGHT OF C-JOB, WHOSE PROPERTY, THIS DOCUMENT REMAINS. NO PART THEREOF MAY BE DISCLOSED, COPIED, DUPLICATED OR IN ANY OTHER WAY MADE USE OF EXCEPT WITH THE APPROVAL OF C-JOB.

[221] J. Wang, Y. Li and X. Sun, "Challenges and opportunities of nanostructured materials for aprotic rechargeable lithium–air batteries," *Nano Energy,* vol. 2, no. 4, pp. 443-467, 2013.

[222] A. Rahman, X. Wang and C. Wen, "A review of high energy density lithium–air battery technology," *Journal of Applied Electrochemistry,* vol. 44, no. 1, pp. 5-22, 2014.

[223] A. Kraytsberg and Y. Ein-Eli, "A critical review-promises and barriers of conversion electrodes for Li-ion batteries," *Journal of Solid State Electrochemistry,* vol. 21, no. 7, pp. 1907-1923, 2017.

[224] C. Julien, A. Mauger, A. Vijh and K. Zaghib, Lithium Batteries Science and Technology, Springer, 2016.

[225] A. Fotouhi, D. J. Auger, L. O'Neill, T. Cleaver and S. Walus, "Lithium-Sulfur Battery Technology Readiness and Applications—A Review," *Energies,* vol. 10, no. 12, p. 1937, 2017.

[226] F. Cerdas, P. Titscher, N. Bognar, R. Schmuch, M. Winter, A. Kwade and C. Herrmann, "Exploring the Effect of Increased Energy Density on the Environmental Impacts of Traction Batteries: A Comparison of Energy Optimized Lithium-Ion and Lithium-Sulfur Batteries for Mobility Applications," *Energies,* vol. 11, no. 1, p. 150, 2018.

[227] Panasonic Corporation of North America, "Lithium Ion Batteries (Li-Ion): Cylindrical Series," 2018. [Online]. Available: https://na.industrial.panasonic.com/.

[228] P. Moseley and J. Garche, Eds., Electrochemical Energy Storage for Renewable Sources and Grid Balancing, Elsevier, 2015.

[229] M. Zackrisson, K. Fransson, J. Hildenbrand, G. Lampic and C. O'Dwyer, "Life cycle assessment of lithium-air battery cells," *Journal of Cleaner Production,* vol. 135, pp. 299-311, 2016.

[230] M. Winter, "Lithium-Ion Batteries and Beyond," 2017. [Online]. Available: https://www.totalbatteryconsulting.com.

[231] J. Christensen, P. Albertus, R. S. Sanchez-Carrera, T. Lohmann, B. Kozinsky, R. Liedtke, J. Ahmed and A. Kojic, "A Critical Review of Li/Air Batteries," *Journal of the Electrochemical Society,* vol. 159, no. 2, pp. R1-R30, 2012.

[232] J. Kumar and B. Kumar, "Development of membranes and a study of their interfaces for rechargeable lithium–air battery," *Journal of Power Sources,* vol. 194, no. 2, pp. 1113-1119, 2009.

[233] J. P. Zheng, P. Andrei, M. Hendrickson and E. J. Plichta, "The Theoretical Energy Densities of Dual-Electrolytes Rechargeable Li-Air and Li-Air Flow Batteries," *Journal of The Electrochemical Society,* vol. 158, no. 1, pp. A43-A46, 2011.

[234] H. Nagata and Y. Chikusa, "An all-solid-state lithium–sulfur battery using two solid electrolytes having different functions," *Journal of Power Sources,* vol. 329, pp. 268-272, 2016.

[235] W. Xue, L. Miao, L. Qie, C. Wang, S. Li, J. Wang and J. Li, "Gravimetric and volumetric energy densities of lithium-sulfur batteries," *Current Opinion in Electrochemistry,* vol. 6, no. 1, pp. 92-99, 2017.

[236] D. Ainsworth, "Li-S Batteries for Energy Storage Applications," OXIS Energy Ltd, 11 May 2016. [Online]. Available: https://www.slideshare.net.

[237] B. D. McCloskey, "Attainable gravimetric and volumetric energy density of Li-S and li ion battery cells with solid separator-protected Li metal anodes," *The Journal of Physical Chemistry Letters,* vol. 6, no. 22, pp. 4581-4588, 2015.

[238] S. Hardman, A. Chandan and R. Steinberger-Wilckens, "Fuel cell added value for early market applications," *Journal of Power Sources,* vol. 287, pp. 297-306, 2015.

[239] GenCell, "The Big Deal With FUEL CELLS," July 2017. [Online]. Available: http://www.gencellenergy.com/. [Accessed 15 February 2018].

[240] M. Bischoff, "Molten carbonate fuel cells: A high temperature fuel cell on the edge to commercialization," *Journal of Power Sources,* vol. 160, no. 2, pp. 842-845, 2006.

© COPYRIGHT OF C-JOB, WHOSE PROPERTY, THIS DOCUMENT REMAINS. NO PART THEREOF MAY BE DISCLOSED, COPIED, DUPLICATED OR IN ANY OTHER WAY MADE USE OF EXCEPT WITH THE APPROVAL OF C-JOB.

[241] X. Meng, Y. Liu, N. Yang, X. Tan, J. Liu, J. C. D. d. Costa and S. Liu, "Highly compact and robust hollow fiber solid oxide cells for flexible power generation and gas production," *Applied Energy,* vol. 205, pp. 741-748, 2017.

[242] J. Huijsmans, G. Kraaij, R. Makkus, G. Rietveld, E. Sitters and H. Reijers, "An analysis of endurance issues for MCFC," *Journal of Power Sources,* vol. 86, pp. 117-121, 2000.

[243] L. Mastropasqua, S. Campanari and J. Brouwer, "Solid oxide fuel cell short stack performance testing - Part A: Experimental analysis and μ-combined heat and power unit comparison," *Journal of Power Sources,* vol. 371, pp. 225-237, 2017.

[244] T. Ishikawa and H. Yasue, "Start-up, testing and operation of 1000 kW class MCFC power plant," *Journal of Power Sources,* vol. 86, no. 1-2, pp. 145-150, 2000.

[245] J. Zhang, Z. Xie, J. Zhang, Y. Tang, C. Song, T. Navessin, Z. Shi, D. Song, H. Wang, D. P. Wilkinson, Z.-S. Liu and S. Holdcroft, "High temperature PEM fuel cells," *Journal of Power Sources,* vol. 160, no. 2, pp. 872-891, 2006.

[246] S. J. McPhail, L. Leto, M. D. Pietra, V. Cigolotti and A. Moreno, "International Status of Molten Carbonate Fuel Cells Technology," 2015. [Online]. Available: http://www.ieafuelcell.com. [Accessed 6 March 2018].

[247] J. Palsson, A. Selimovic and L. Sjunnesson, "Combined solid oxide fuel cell and gas turbine systems for efficient power and heat generation," *Journal of Power Sources,* vol. 86, pp. 442-448, 2000.

[248] S. D. Vora, "Office of Fossil Energy's Solid Oxide Fuel Cell Program Overview," 22 July 2014. [Online]. Available: https://www.netl.doe.gov.

[249] A. Musa, H. Steeman and M. De Paepe, "Performance of Internal and External Reforming Molten Carbonate Fuel Cell Systems," *Journal of Fuel Cell Science and Technology,* vol. 4, no. 1, pp. 65-71, 2007.

[250] A. Johnson and E. Williams, Fuel cell efficiency, Nova Science Publishers, Inc., 2012.

[251] Stena Line, "Information," 2018. [Online]. Available: https://www.stenaline.co.uk/. [Accessed 25 April 2018].

[252] Tallink, "Booking," 2018. [Online]. Available: https://booking.tallink.com/. [Accessed 25 April 2018].

[253] Viking Line, "Book a voyage," 2018. [Online]. Available: https://www.sales.vikingline.com/. [Accessed 25 April 2018].

[254] P&O Ferries, "Accommodations," 2018. [Online]. Available: http://www.poferries.com/. [Accessed 25 April 2018].

[255] Navier Armas, "Passage," 2018. [Online]. Available: https://www.navieraarmas.com/. [Accessed 25 April 2018].

[256] DFDS Seaways, "Onboard," 2018. [Online]. Available: https://www.dfdsseaways.co.uk/. [Accessed 25 April 2018].

[257] Finnlines, "Booking," 2018. [Online]. Available: https://www.finnlines.com/. [Accessed 25 April 2018].

[258] NorthLink Ferries, "Book a journey with NorthLink Ferries!," 2016. [Online]. Available: https://online.northlinkferries.co.uk/. [Accessed 25 April 2018].

[259] Grimaldi Group SpA, "Vehicles Index," 2018. [Online]. Available: https://www.grimaldi-lines.com/. [Accessed 25 April 2018].

[260] Corsica Ferries Sardinia Ferries,, "Algemene Voorwaarden," 2014. [Online]. Available: https://nl.corsicaferries.com/voorwaarden.html. [Accessed 28 April 2018].

© COPYRIGHT OF C-JOB, WHOSE PROPERTY, THIS DOCUMENT REMAINS. NO PART THEREOF MAY BE DISCLOSED, COPIED, DUPLICATED OR IN ANY OTHER WAY MADE USE OF EXCEPT WITH THE APPROVAL OF C-JOB.

Appendices

A Market research plots

This appendix provides an overview of all statistical plots used during the market research of this thesis as is discussed in section 2.1.

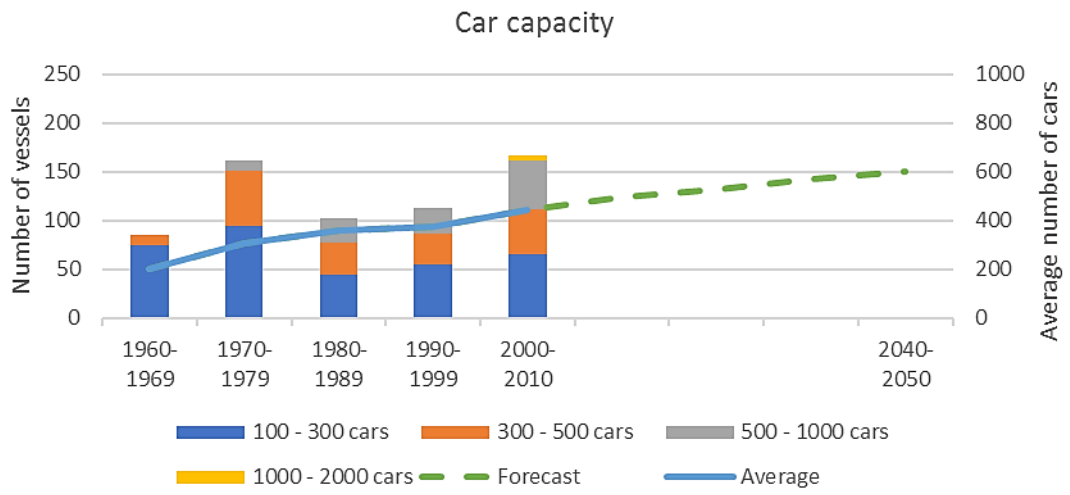

Figure A-1: Car carrying capacity of ROPAX ferries between 1960 and 2010 per decade and a forecasted development for 2050. [6]

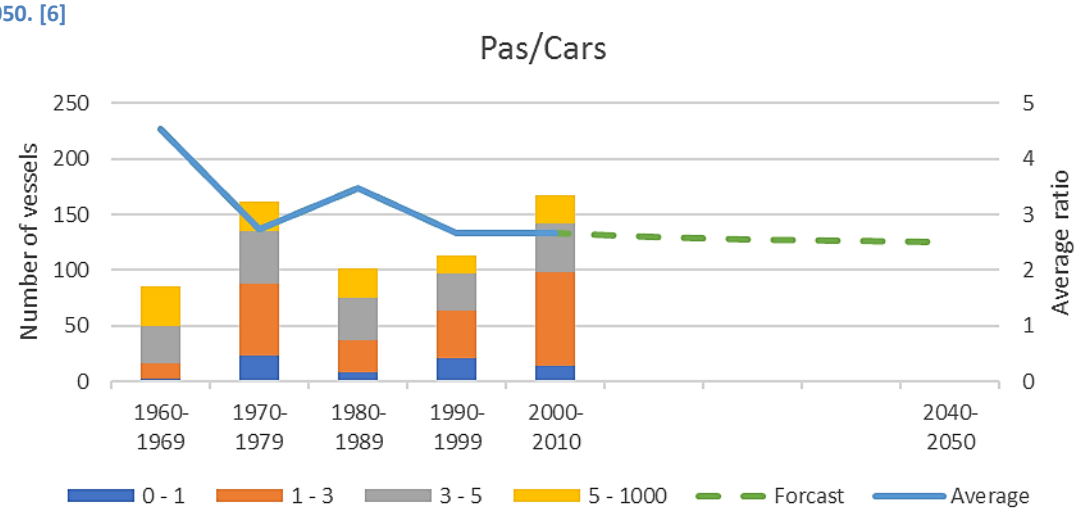

Figure A-2: Passenger/car ratio of ROPAX ferries between 1960 and 2010 per decade and a forecasted development for 2050. [6]

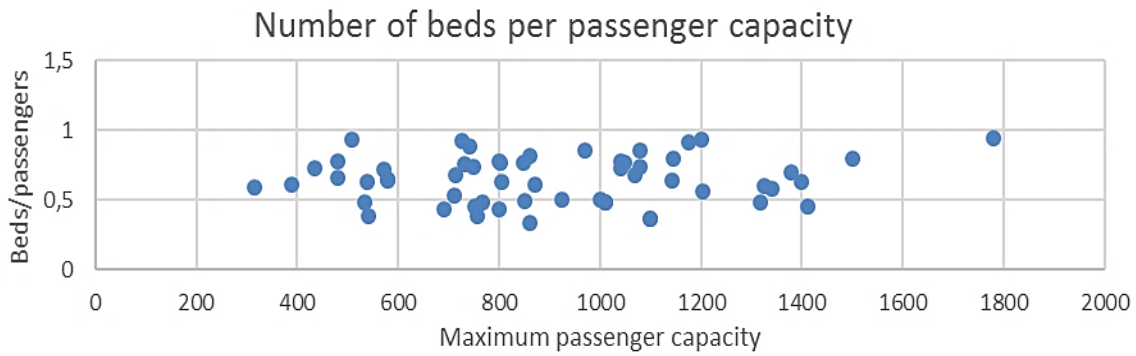

Figure A-3: Number of beds per maximum passenger capacity. [6]

© COPYRIGHT OF C-JOB, WHOSE PROPERTY, THIS DOCUMENT REMAINS. NO PART THEREOF MAY BE DISCLOSED, COPIED, DUPLICATED OR IN ANY OTHER WAY MADE USE OF EXCEPT WITH THE APPROVAL OF C-JOB.

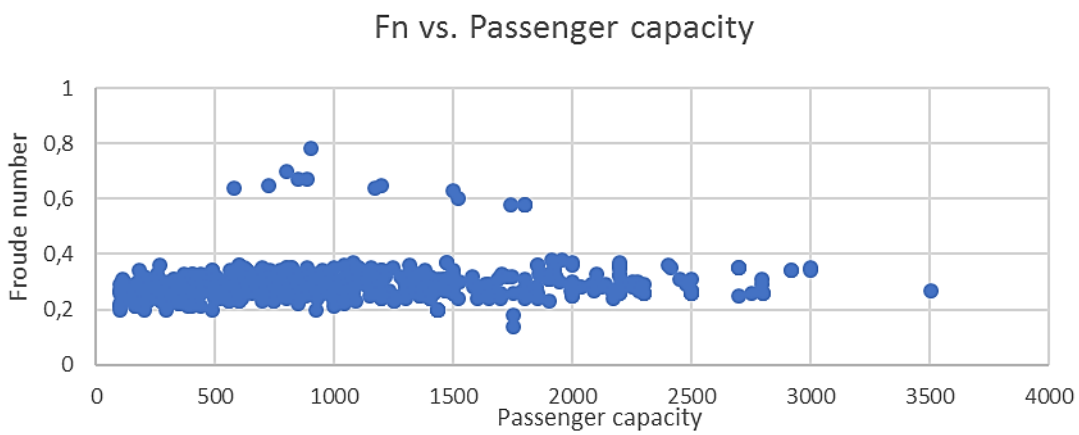

Figure A-4: Froude number versus Passenger capacity. [6]

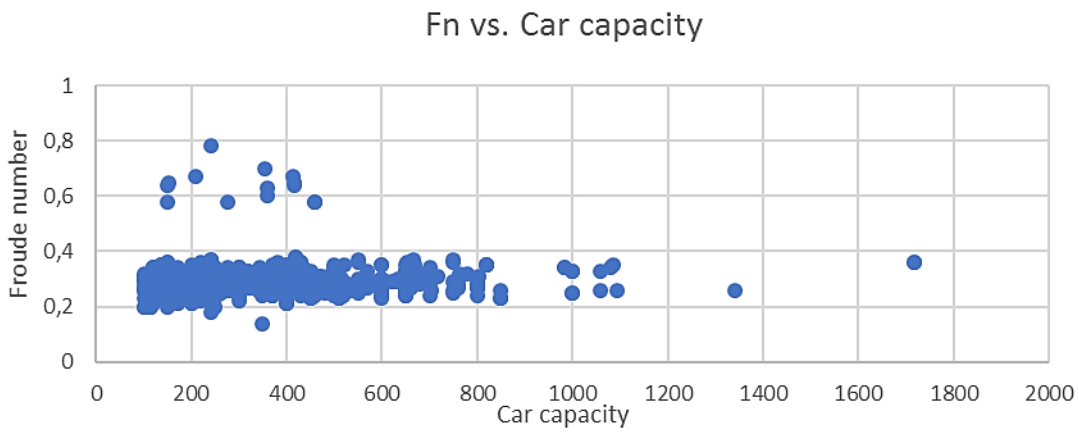

Figure A-5: Froude number versus Car capacity. [6]

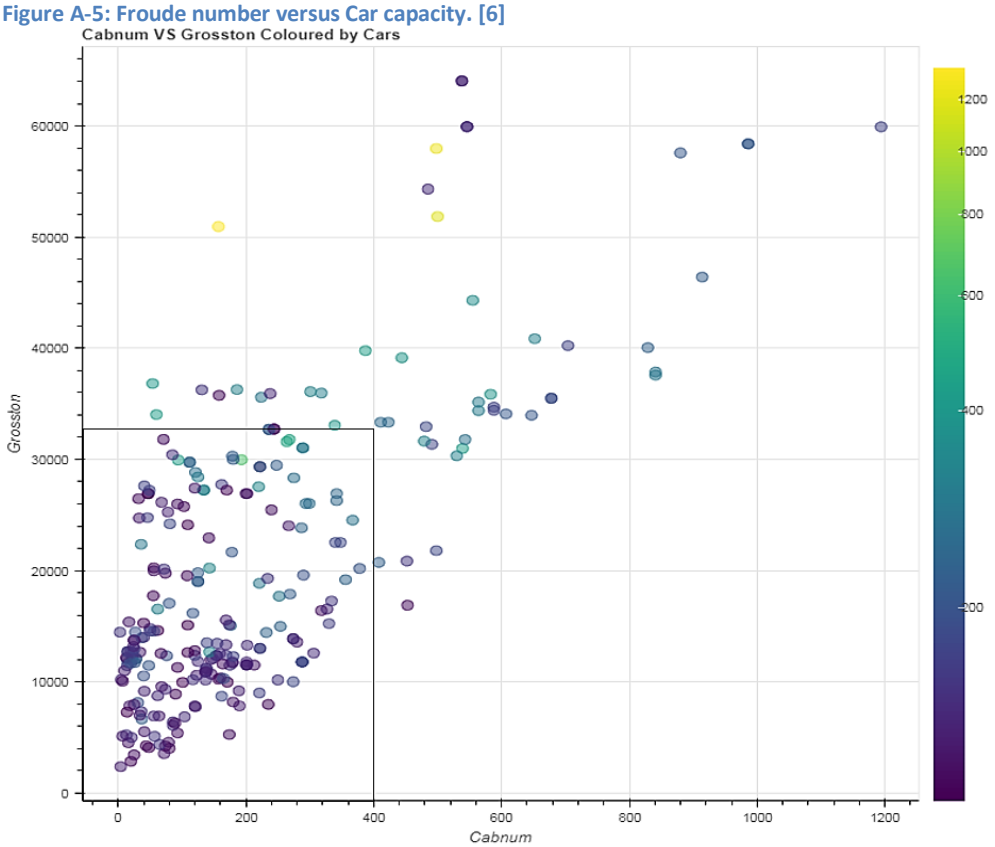

Figure A-6: Gross tonnage of ROPAX ferries as function of the number of cabins and cars. [6]

© COPYRIGHT OF C-JOB, WHOSE PROPERTY, THIS DOCUMENT REMAINS. NO PART THEREOF MAY BE DISCLOSED, COPIED, DUPLICATED OR IN ANY OTHER WAY MADE USE OF EXCEPT WITH THE APPROVAL OF C-JOB.

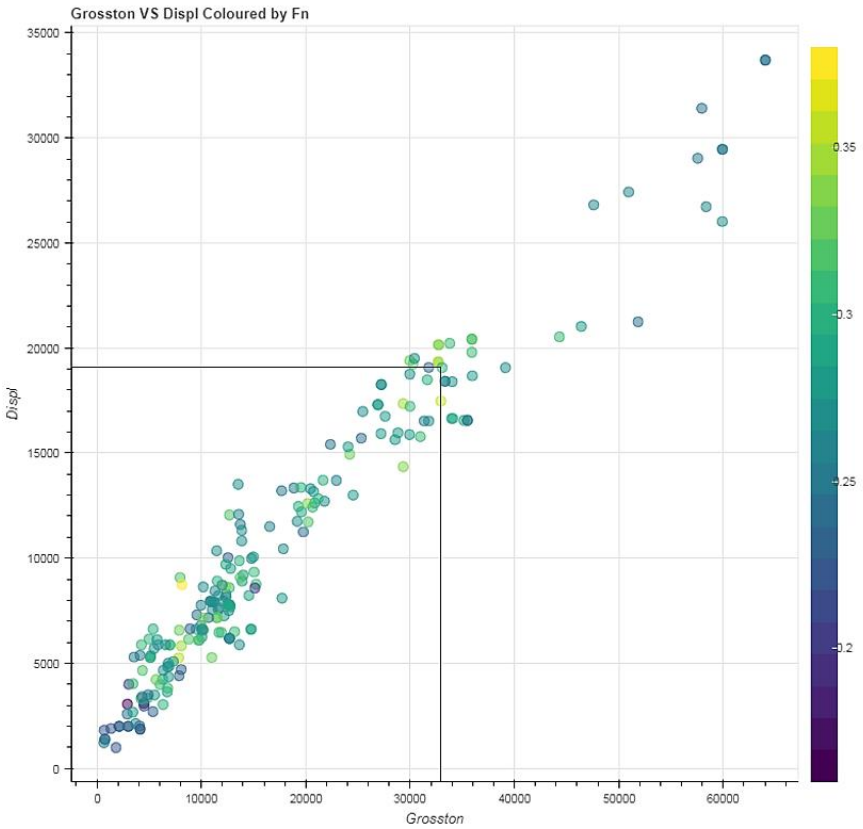

Figure A-7: Displacement of a ROPAX ferry as function of gross tonnage and froude number. [6]

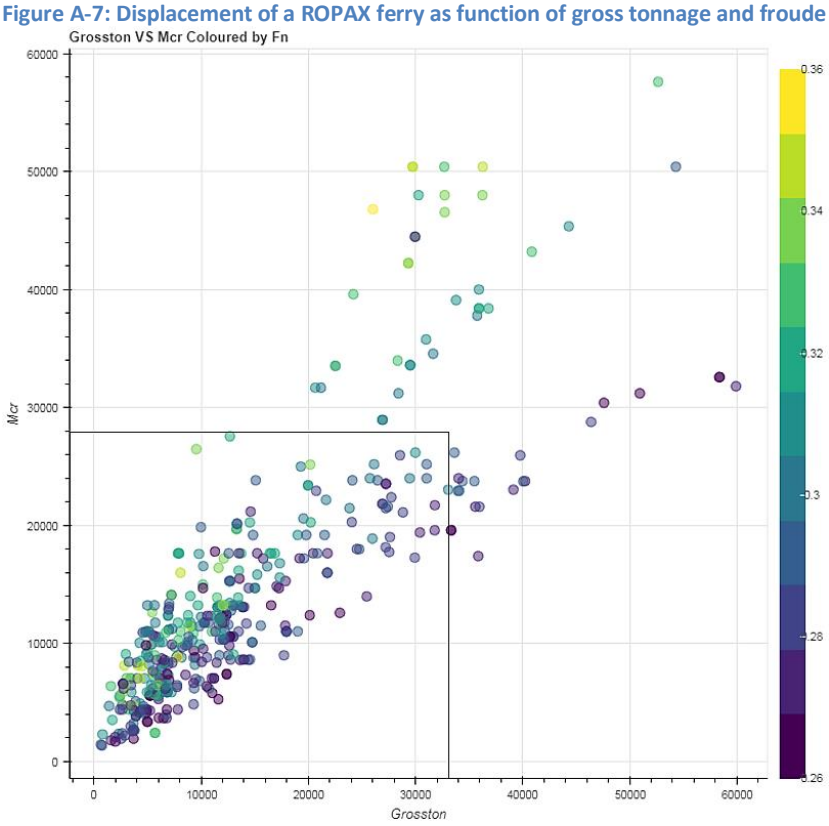

Figure A-8: Total MCR the engines of a ROPAX ferry as function of gross tonnage and Froude number. [6]

© COPYRIGHT OF C-JOB, WHOSE PROPERTY, THIS DOCUMENT REMAINS. NO PART THEREOF MAY BE DISCLOSED, COPIED, DUPLICATED OR IN ANY OTHER WAY MADE USE OF EXCEPT WITH THE APPROVAL OF C-JOB.

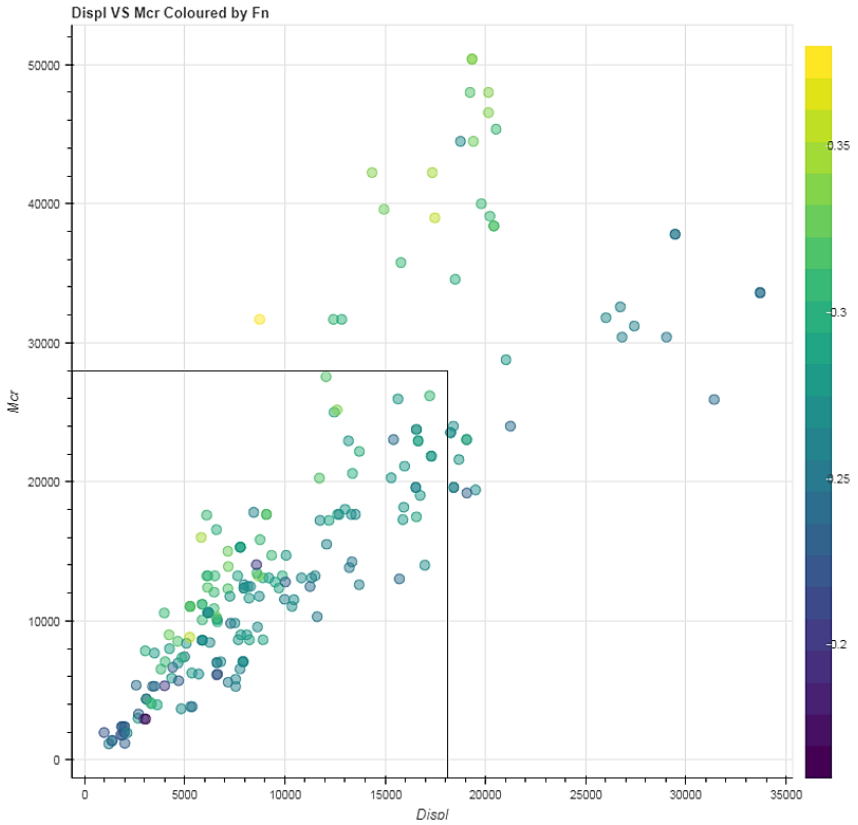

Figure A-9: Total MCR of the engines of a ROPAX ferry as function of displacement and Froude number. [6]

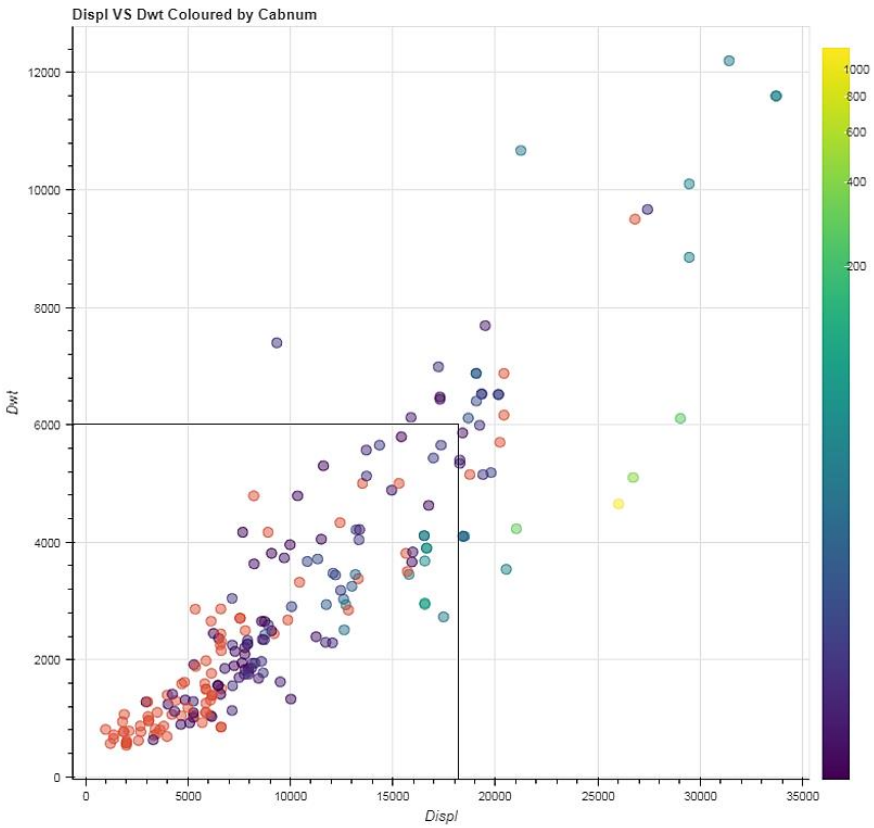

Figure A-10: Deadweight as function of displacement and number of cabins. [6]

© COPYRIGHT OF C-JOB, WHOSE PROPERTY, THIS DOCUMENT REMAINS. NO PART THEREOF MAY BE DISCLOSED, COPIED, DUPLICATED OR IN ANY OTHER WAY MADE USE OF EXCEPT WITH THE APPROVAL OF C-JOB.

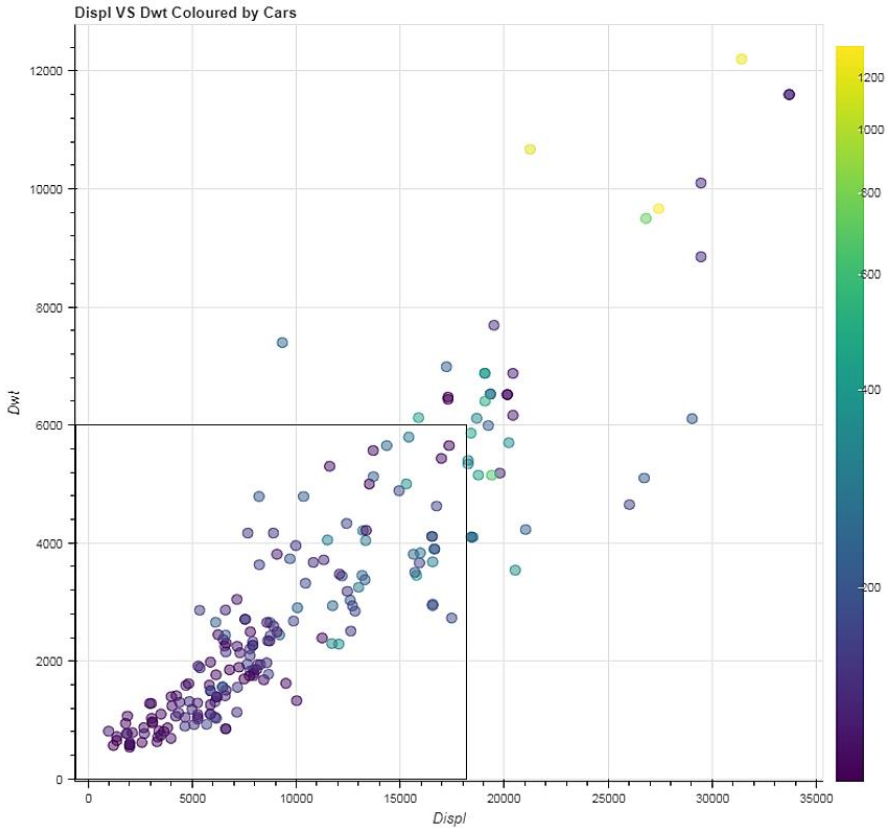

Figure A-11: Deadweight as function of displacement and car carrying capacity. [6]

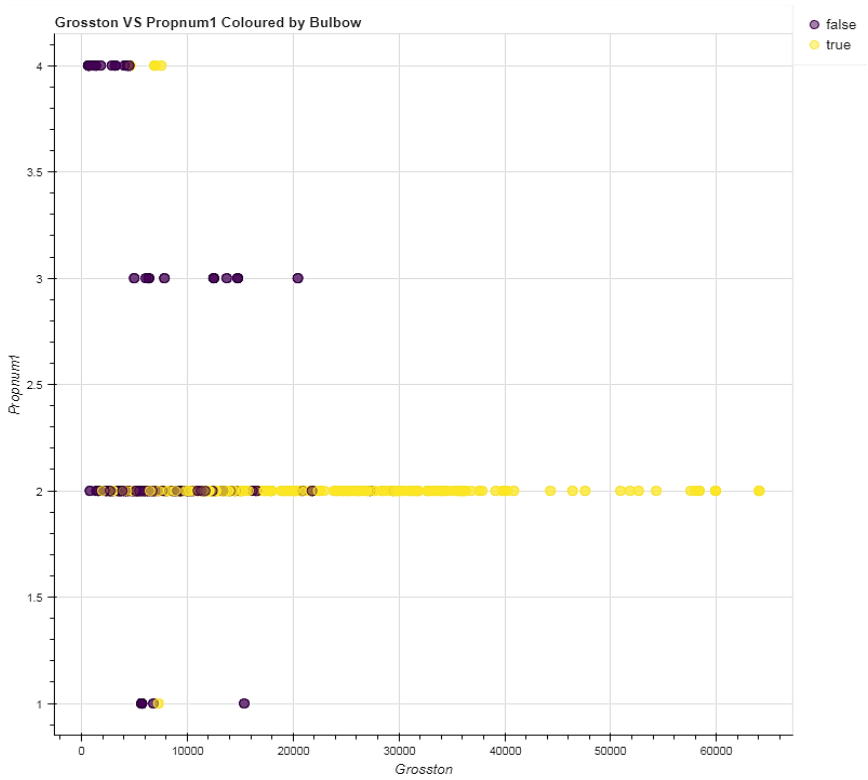

Figure A-12: Number of propellers and whether a ROPAX ferry has a bulbous bow or not displayed as function of the gross tonnage. [6]

© COPYRIGHT OF C-JOB, WHOSE PROPERTY, THIS DOCUMENT REMAINS. NO PART THEREOF MAY BE DISCLOSED, COPIED, DUPLICATED OR IN ANY OTHER WAY MADE USE OF EXCEPT WITH THE APPROVAL OF C-JOB.

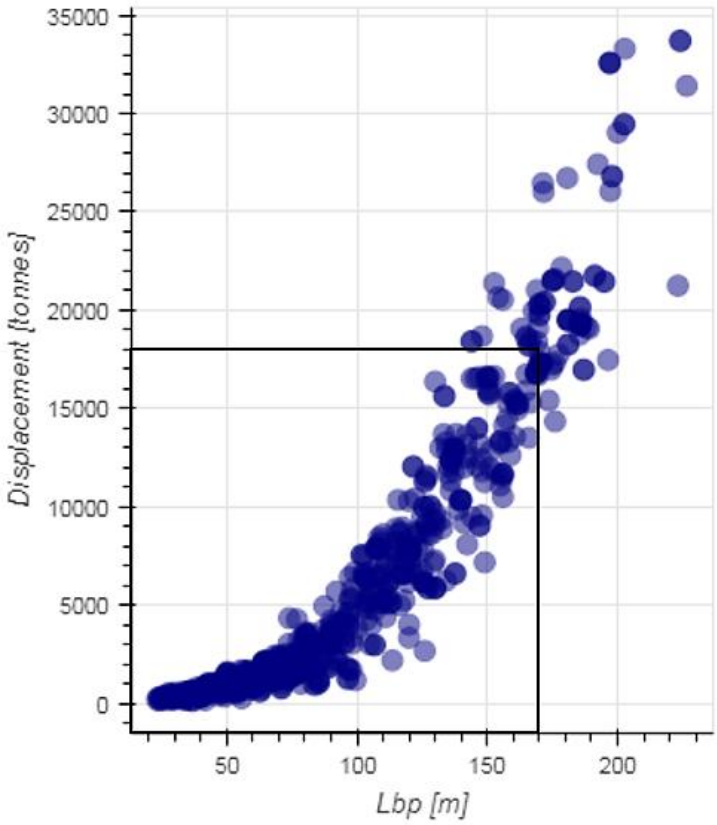

Figure A-13: Displacement as function of the length between perpendiculars (Lbp). [6]

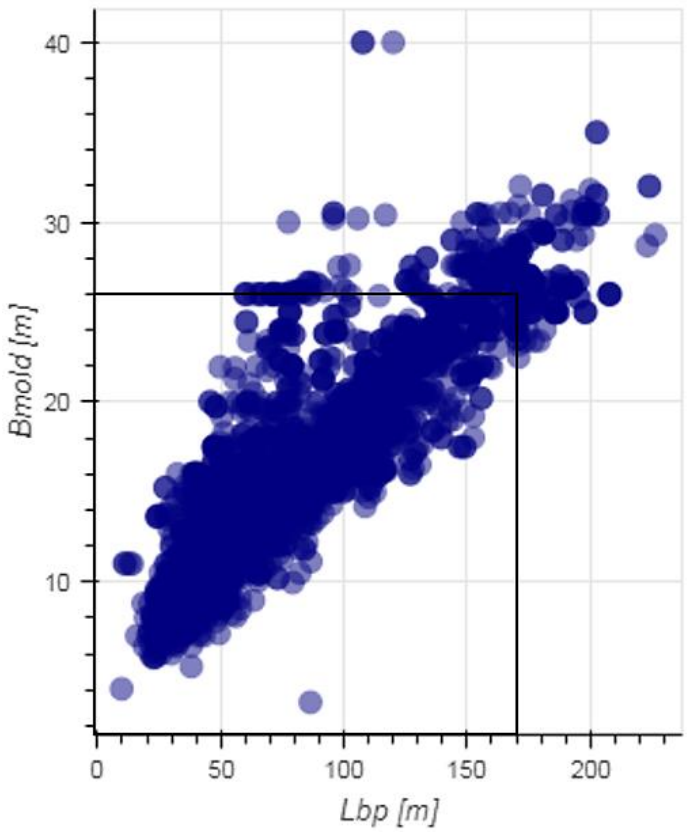

Figure A-14: Molded breadth (Bmold) as function of the length between perpendiculars (Lbp). [6]

© COPYRIGHT OF C-JOB, WHOSE PROPERTY, THIS DOCUMENT REMAINS. NO PART THEREOF MAY BE DISCLOSED, COPIED, DUPLICATED OR IN ANY OTHER WAY MADE USE OF EXCEPT WITH THE APPROVAL OF C-JOB.

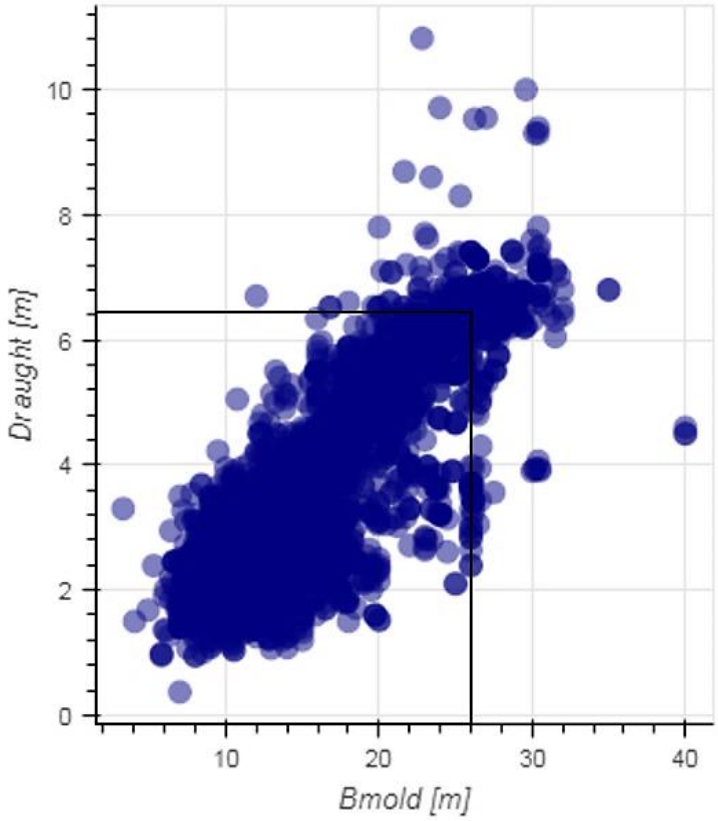

Figure A-15: Draught as function of the molded breadth (Bmold). [6]

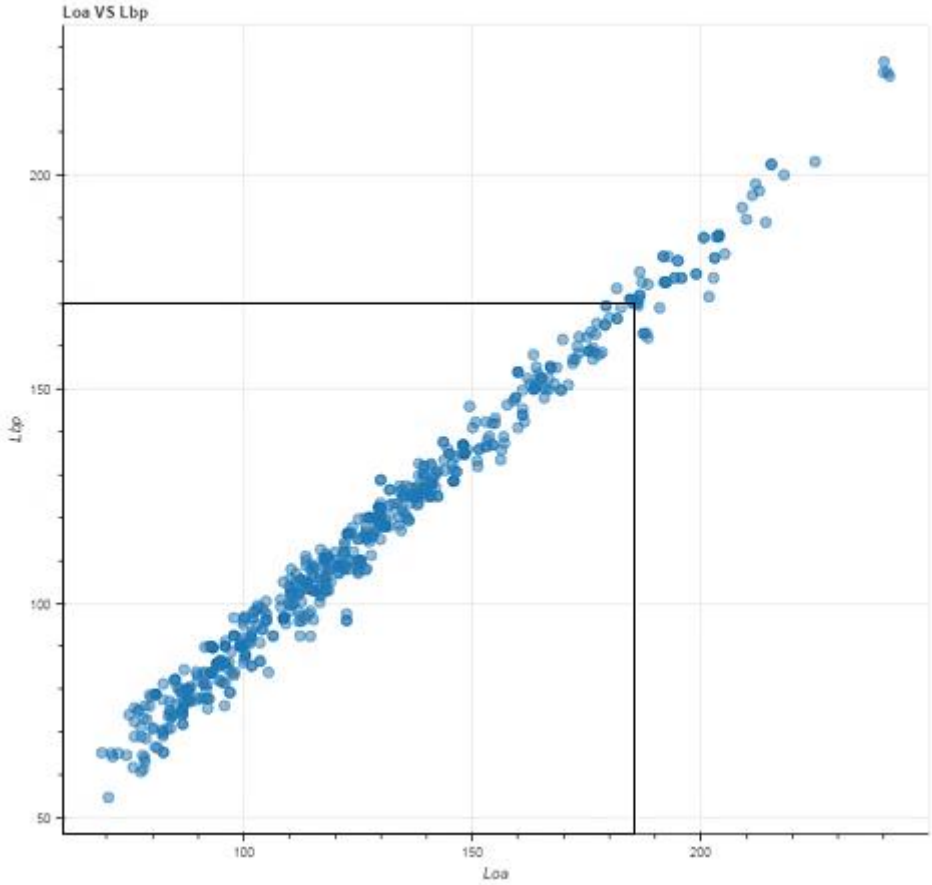

Figure A-16: Length between perpendiculars as function of length over all. [6]

© COPYRIGHT OF C-JOB, WHOSE PROPERTY, THIS DOCUMENT REMAINS. NO PART THEREOF MAY BE DISCLOSED, COPIED, DUPLICATED OR IN ANY OTHER WAY MADE USE OF EXCEPT WITH THE APPROVAL OF C-JOB.

B Background information

This appendix discusses various supporting information. First the technology readiness levels are discussed. Section 2 presents some figures representing schematic representations of fuel cells. The third section provides a calculation example of an ammonia reformer. The forth section provides some conversion tables used during the establishment of the characteristic values of the energy storage and energy converter units. The last section provides an explanation concerning Box & Whiskers plots.

B.1 Technology Readiness Levels (TRL)

Technology Readiness Levels (TRL) are a type of measurement system used to assess the maturity level of a particular technology. Each technology project is evaluated against the parameters for each technology level and is then assigned a TRL rating based on the projects progress. There are nine technology readiness levels. TRL 1 is the lowest and TRL 9 is the highest.

A TRL number is obtained once the description in the diagram has been achieved. For example, successfully achieving TRL 4 (lab environment) does not move the technology to TRL 5. TRL 5 is achieved once there is component/breadboard validation in a relevant environment. The technology remains TRL 4 until the relevant environmental validation is complete. [32]

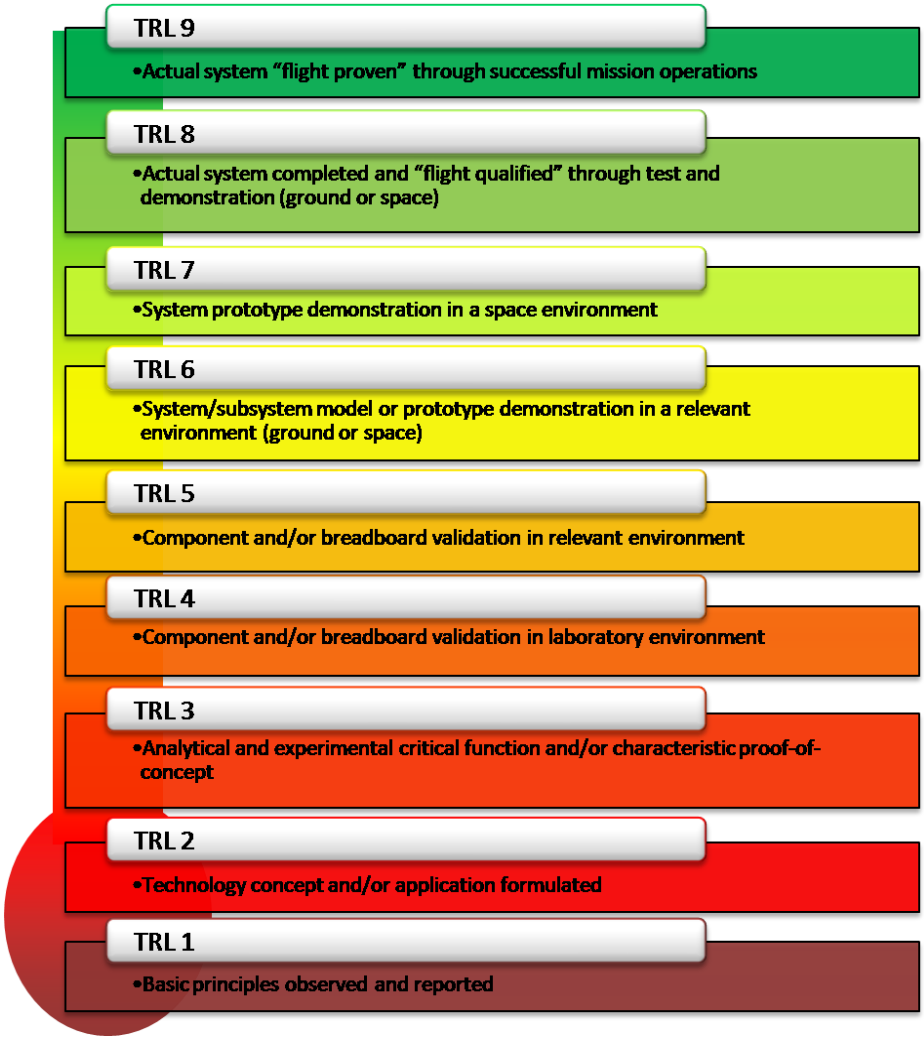

Figure B-1: Technology Readiness Levels according to NASA. [32]

© COPYRIGHT OF C-JOB, WHOSE PROPERTY, THIS DOCUMENT REMAINS. NO PART THEREOF MAY BE DISCLOSED, COPIED, DUPLICATED OR IN ANY OTHER WAY MADE USE OF EXCEPT WITH THE APPROVAL OF C-JOB.

B.2 Fuel cells

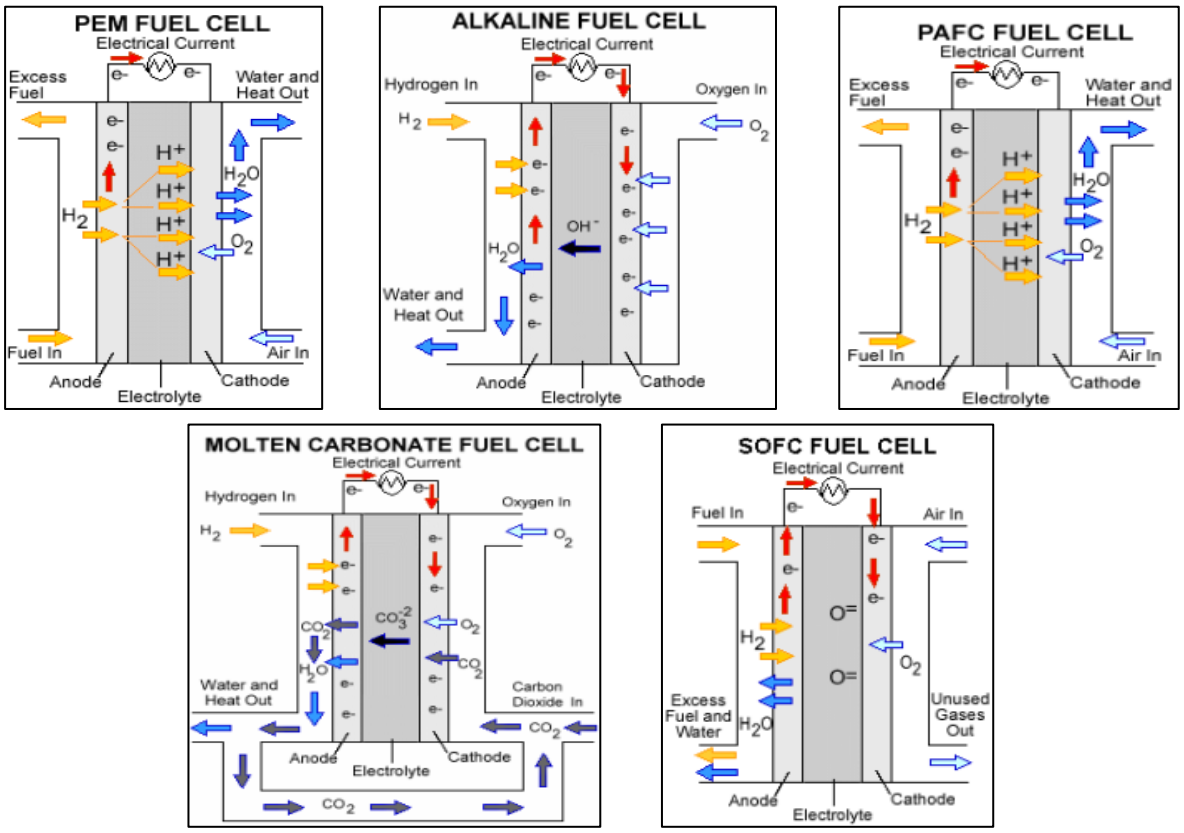

Figure B-2: Schematic representation of a (a) Polymer Electrolyte Membrane fuel cell (PEMFC), (b) Alkaline fuel cell (AFC), (c) Phosphoric Acid fuel cell (PAFC), (d) Molten Carbonate fuel cell (MCFC) and (e) Solid Oxide fuel cell (SOFC). [63]

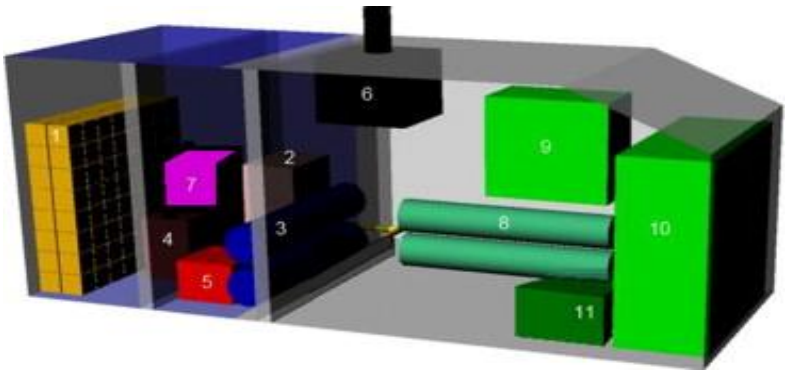

Identifier element	Description	Identifier element	Description
1	SOFC fuel cell stack	7	Anode inlet syn gas pre-heater (HE3)
2	Fuel processor	8	Air fan
3	Fuel conditioner (HE1)	9	Control unit
4	Fuel cell inlet air pre-heater (HE2)	10	Power conversion unit
5	Catalytic burner	11	Back-up power unit
6	Heat recovery unit		

Figure B-3: Main elements of a SOFC system fed by natural gas. [211]

© COPYRIGHT OF C-JOB, WHOSE PROPERTY, THIS DOCUMENT REMAINS. NO PART THEREOF MAY BE DISCLOSED, COPIED, DUPLICATED OR IN ANY OTHER WAY MADE USE OF EXCEPT WITH THE APPROVAL OF C-JOB.

B.3 Ammonia reformer parasitic energy requirement

Section 3.1.2 mentions the possibility that an ammonia reformer requires additional electrical energy to reform sufficient ammonia.

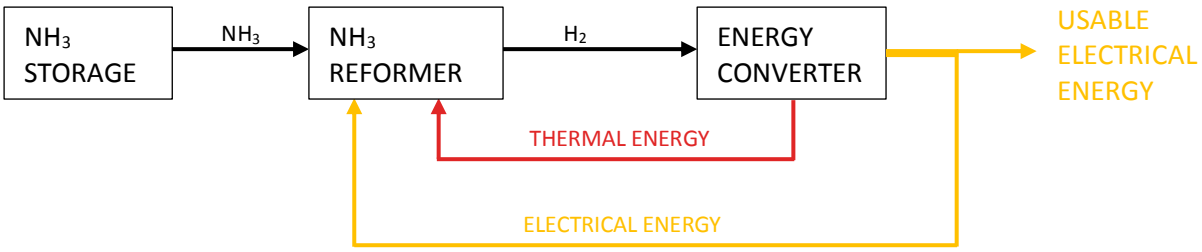

Figure B-4: Schematic layout of a power plant using an ammonia reformer.

As already stated is the usable electrical energy required to be the same for every configuration resulting in an increase in required power and energy when electrical energy is used in for the reforming of ammonia. [181].

The energy efficiency of the ammonia reformer is defined as:

$$\eta_{reformer} = \frac{3 * \Delta H_{H_2}}{2 * \Delta H_{NH_3} + E_{el} + Q}$$

Where ΔH_{H_2} is equal to the LHV of hydrogen (242.7 kJ/mol) and ΔH_{NH_3} is equal to the LHV of ammonia (320.1 kJ/mol). Since two moles ammonia decomposes in three moles hydrogen, the LHV of hydrogen and ammonia are multiplied by three and two, respectively.

When the efficiency of an ammonia reformer is equal to 90 % and there is no thermal energy obtained from the energy converter, a total of 56.3 kJ electrical energy is required to produce one mol H_2. This is equal to 23 % of the LHV of hydrogen, resulting in an equal reduction of electrical efficiency of the energy converter. 23 % of hydrogen energy supplied to the energy converter is needed in the form of electrical energy at the reformer resulting in the following expression for the required hydrogen energy input into the energy converter:

$$E_{H_2,in} = \frac{E_{net,el}}{\eta_{energy\ converter} - E_{MJ\ el\ per\ MJ\ H_2}}$$

Assuming an electrical efficiency of 50 % for the energy converter, the total energy input should be:

$$E_{H_2,in} = \frac{E_{users}}{0.50 - 0.23} = 3.7 * E_{net,el}$$

Note that almost half of the produced electrical energy is required to reform ammonia. This results in an increase in output power of the energy converter by:

$$P_{net,el} = (0.50 - 0.23) * P_{H_2,in} \quad \& \quad P_{converter} = 0.50 * P_{H_2,in} \rightarrow P_{converter} = \frac{0.50}{0.50 - 0.23} * P_{net,el}$$

The output power of the energy converter is therefore 1.85 times as high as the power required by the external users.

Given the LHVs of hydrogen and ammonia per mol, the required input energy in the form of ammonia is known to be:

$$E_{NH_3,in} = E_{H_2,in} * \frac{2 * \Delta H_{NH_3}}{3 * \Delta H_{H_2}} = 0.88 * E_{H_2,in} = 3.3 * E_{net,el}$$

This results in an overall efficiency of 30 %.

© COPYRIGHT OF C-JOB, WHOSE PROPERTY, THIS DOCUMENT REMAINS. NO PART THEREOF MAY BE DISCLOSED, COPIED, DUPLICATED OR IN ANY OTHER WAY MADE USE OF EXCEPT WITH THE APPROVAL OF C-JOB.

B.4 Conversion tables

All prices are calculated in 2017 USD. Prices calculated in other years, are converted to USD 2017 by using the inflation calculator provided by http://www.usinflationcalculator.com/ . This results in the following conversion table:

Table B-1: Currency conversion table based on inflation. [212]. [213]

Year	Year USD	2017 USD	Year Euro
2000	1.00	1.42	1.09
2001	1.00	1.38	1.11
2002	1.00	1.36	1.05
2003	1.00	1.33	0.88
2004	1.00	1.30	0.81
2005	1.00	1.26	0.81
2006	1.00	1.22	0.79
2007	1.00	1.18	0.73
2008	1.00	1.14	0.68
2009	1.00	1.14	0.72
2010	1.00	1.12	0.75
2011	1.00	1.09	0.72
2012	1.00	1.07	0.78
2013	1.00	1.05	0.75
2014	1.00	1.04	0.75
2015	1.00	1.03	0.90
2016	1.00	1.02	0.90
2017	1.00	1.00	0.88

Energy carrier prices are converted to 2017 USD per GJ stored energy based on the LHV. For the following conversion factors are used:

Table B-2: Conversion units used for the calculation of main characteristics of the power plant concepts. [214]

1 mmBTU	1.055 GJ
1 boe	5.8 mmBTU
1 kWh	3.6 MJ
1 kg LNG	49 MJ
1 kg H_2	120 MJ
1 kg NH_3	18.6 MJ
HHV LNG (55 GJ/t)	1.122*LHV LNG (49 GJ/t)
HHV H_2 (142 GJ/t)	1.182*LHV H_2 (120 GJ/t)
HHV NH_3 (22.5 GJ/t)	1.210*LHV NH_3 (18.6 GJ/t)

© COPYRIGHT OF C-JOB, WHOSE PROPERTY, THIS DOCUMENT REMAINS. NO PART THEREOF MAY BE DISCLOSED, COPIED, DUPLICATED OR IN ANY OTHER WAY MADE USE OF EXCEPT WITH THE APPROVAL OF C-JOB.

B.5 Box & Whisker plot

Box and whisker plots are used in chapters 3 and 4 to present the distribution of statistical data obtained from literature. This data is graphically presented using a box, an upper and lower whisker, hence the name. A definition of each aspect of this plot is provided in this section to help the reader to correctly interpret these plots.

Whiskers are vertical lines extending from the box used to provide the minimum and maximum value of the dataset.
25 % of the datapoints have a lower value than the bottom of the box, also known as the 25th percentile or lower quartile of the data.
The median of the dataset is defined as the value where 50 % of the datapoints have a lower value and is given as a horizontal line through the box.
The 75th percentile or upper quartile of the data is given as the top of the box and corresponds with the value higher than 75 % of the data.
Average values are displayed as a x in the box & whisker plot.
Data that is much bigger or smaller than the other data elements are considered outliers. This data is displayed as a dot outside the range of the whiskers. [215], [216]

Table B-3: Explanation of the box & whisker plot elements. [215]

Element	*Meaning*
Top of upper whisker	Maximum value of the sample
Top of box	75th percentile of the sample
Line through the box	Median of the sample
Bottom of the box	25th percentile of the sample
Bottom of the lower whisker	Minimum of the sample
× markers	Mean of the sample
o markers	Outliers of the sample

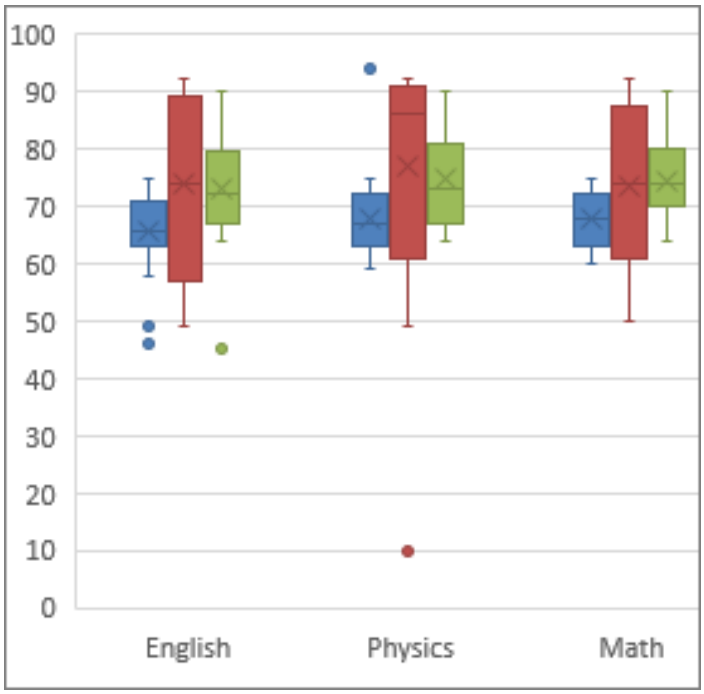

Figure B-5: Example of a box & whisker plot including all previously discussed elements. [216]

© COPYRIGHT OF C-JOB, WHOSE PROPERTY, THIS DOCUMENT REMAINS. NO PART THEREOF MAY BE DISCLOSED, COPIED, DUPLICATED OR IN ANY OTHER WAY MADE USE OF EXCEPT WITH THE APPROVAL OF C-JOB.

C Literature data for energy carriers including storage system

This appendix provides an overview of used energy carrier characteristics including the source from which this data was obtained. Sections C.1 till C.7 provide the gravimetric and volumetric energy storage densities of the considered energy carries including the storage unit (such as an insulated tank). Section C.8 provides an overview of recorded electric efficiencies of fuel cells. A schematic overview of a modern natural gas fueled SOFC is also provided.

Each characteristic is presented in a table which provides the default, minimum and maximum value of the characteristic in the bottom row. These values are used during the assessment of the different power plant configurations as is described in chapter 4.

C.1 Hydrogen at 350 bar

Table C-1: Gravimetric energy density of hydrogen stored at 350 bar according to literature.

DEFAULT [GJ/TON]	MINIMUM [GJ/TON]	MAXIMUM [GJ/TON]	SOURCE
5.8			[3]
9.2 (at 300 bar)			[151]
	3.0	15.0	[30]
6.6			[90]
7.0	**3.0**	**15.0**	

Table C-2: Volumetric energy density of hydrogen stored at 350 bar according to literature.

DEFAULT [GJ/M^3]	MINIMUM [GJ/M^3]	MAXIMUM [GJ/M^3]	SOURCE
1.8			[3]
1.9 (at 300 bar)			[151]
		2.4	[30]
2.1			[90]
2.0	**1.8**	**2.4**	

C.2 Hydrogen at 700 bar

Table C-3: Gravimetric energy density of hydrogen stored at 700 bar according to literature.

DEFAULT [GJ/TON]	MINIMUM [GJ/TON]	MAXIMUM [GJ/TON]	SOURCE
6.5			[3]
7.1			[151]
	2.4	13.2	[30]
	5.4	9.6	[41]
	2.4	6.0	[217]
6.24			[90]
6.5	**2.4**	**13.2**	

Table C-4: Volumetric energy density of hydrogen stored at 700 bar according to literature.

DEFAULT [GJ/M^3]	MINIMUM [GJ/M^3]	MAXIMUM [GJ/M^3]	SOURCE
3.2			[3]
3.3			[151]
	3.6	4.0	[30]
	3.4	3.8	[41]
	2.0	3.0	[217]
3.2			[90]
3.2	**2.0**	**4.0**	

© COPYRIGHT OF C-JOB, WHOSE PROPERTY, THIS DOCUMENT REMAINS. NO PART THEREOF MAY BE DISCLOSED, COPIED, DUPLICATED OR IN ANY OTHER WAY MADE USE OF EXCEPT WITH THE APPROVAL OF C-JOB.

C.3 Hydrogen at -253 °C

Table C-5: Gravimetric energy density of liquid hydrogen storage according to literature.

DEFAULT [GJ/TON]	MINIMUM [GJ/TON]	MAXIMUM [GJ/TON]	SOURCE
7.2			[3]
10.7			[151]
	9.0	15.0	[41]
	6.6	10.8	[217]
9.0			[38]
9.0	**6.6**	**15.0**	

Table C-6: Volumetric energy density of liquid hydrogen storage according to literature.

DEFAULT [GJ/M^3]	MINIMUM [GJ/M^3]	MAXIMUM [GJ/M^3]	SOURCE
4.3			[3]
4.0			[151]
	4.2	5.4	[41]
	4.2	5.2	[217]
4.3			[38]
4.3	**4.0**	**5.4**	

C.4 Ammonia at 10 bar

Table C-7: Gravimetric energy density of compressed ammonia storage according to literature.

DEFAULT [GJ/TON]	MINIMUM [GJ/TON]	MAXIMUM [GJ/TON]	SOURCE
13.7			[218]
13.0			[38]
	13.6	14.6	[39]
13.6	**13.0**	**14.6**	

Table C-8: Volumetric energy density of compressed ammonia storage according to literature.

DEFAULT [GJ/M^3]	MINIMUM [GJ/M^3]	MAXIMUM [GJ/M^3]	SOURCE
10.5			[38]
	10.4	10.7	[39]
10.5	**10.4**	**10.7**	

C.5 Li-ion batteries

Table C-9: Gravimetric energy density of Li-ion batteries according to literature.

DEFAULT [GJ/TON]	MINIMUM [GJ/TON]	MAXIMUM [GJ/TON]	SOURCE
	0.36	0.58	[103]
	0,9	1,08	[219]
0.59			[220]
	0.40	0.58	[221]
0.76			[222]
	0.36	0.61	[223]
0.77			[224]
	0.54	0.90	[54]
1.00			[225]
	0.65	1.08	[105]
0.90			[226]

© COPYRIGHT OF C-JOB, WHOSE PROPERTY, THIS DOCUMENT REMAINS. NO PART THEREOF MAY BE DISCLOSED, COPIED, DUPLICATED OR IN ANY OTHER WAY MADE USE OF EXCEPT WITH THE APPROVAL OF C-JOB.

0.59			[52]
	0.36	0.72	[45]
	0.36	0.58	[53]
	0.18	0.83	[53]
0.54			[89]
	0.50	0.72	[142]
	0,36	0,95	[227]
0.58	**0.18**	**1.08**	

Table C-10: Volumetric energy density of Li-ion batteries according to literature.

DEFAULT [GJ/M^3]	MINIMUM [GJ/M^3]	MAXIMUM [GJ/M^3]	SOURCE
	0,72	1,08	[103], [219]
0.36			[104]
0.97			[89]
2.34			[222]
3.49			[224]
2.44			[226]
1.44	0.72	1.91	[53]
	0.90	2.50	[227]
1.44	**0.36**	**3.49**	

C.6 Li-air batteries

Table C-11: Gravimetric energy density of Li-air batteries according to literature.

DEFAULT [GJ/TON]	MINIMUM [GJ/TON]	MAXIMUM [GJ/TON]	SOURCE
	1.80	2.88	[53], [228]
	1.80	3.24	[105]
6.12			[52]
3.60			[45]
4.86			[229]
	1.19	2.63	[230]
1.26			[228]
	1.80	3.60	[231]
3.60			[232]
	0.97	4.21	[233]
	2.02	3.24	[101]
6.12			[52]
2.52	**0.97**	**6.12**	

Table C-12: Volumetric energy density of Li-air batteries according to literature.

DEFAULT [GJ/M^3]	MINIMUM [GJ/M^3]	MAXIMUM [GJ/M^3]	SOURCE
	0.90	2.52	[230]
1.26			[228]
	2.52	4.68	[231]
3.60			[232]
	2.66	4.68	[101]
2.52	**0.90**	**4.68**	

© COPYRIGHT OF C-JOB, WHOSE PROPERTY, THIS DOCUMENT REMAINS. NO PART THEREOF MAY BE DISCLOSED, COPIED, DUPLICATED OR IN ANY OTHER WAY MADE USE OF EXCEPT WITH THE APPROVAL OF C-JOB.

C.7 Li-S batteries

Table C-13: Gravimetric energy density of Li-S batteries according to literature.

DEFAULT [GJ/TON]	MINIMUM [GJ/TON]	MAXIMUM [GJ/TON]	SOURCE
	0.54	1.36	[53], [228]
1.44			[221]
	0.72	2.16	[54]
1.94			[234]
0.67			[225]
	1.26	2.16	[105], [226]
	0.94	2.88	[52]
	0.79	1.08	[102]
			[53]
	1.44	2.16	[235]
1.98			[42]
1.80			[236]
1.44	1.26	2.16	[237]
	1.26	1.98	[230]
1.40	**0.54**	**2.88**	

Table C-14: Volumetric energy density of Li-S batteries according to literature.

DEFAULT [GJ/M^3]	MINIMUM [GJ/M^3]	MAXIMUM [GJ/M^3]	SOURCE
3.56			[234]
	0.61	1.44	[225]
3.24			[52]
	1.07	1.49	[102]
1.26			[53], [236]
	0.72	2.52	[237]
	1.08	2.34	[230]
	0.72	2.16	[235]
1.26			[101]
1.26	**0.61**	**3.56**	

© COPYRIGHT OF C-JOB, WHOSE PROPERTY, THIS DOCUMENT REMAINS. NO PART THEREOF MAY BE DISCLOSED, COPIED, DUPLICATED OR IN ANY OTHER WAY MADE USE OF EXCEPT WITH THE APPROVAL OF C-JOB.

C.8 Fuel cell electrical efficiencies

Table C-15: Electric efficiencies based on LHV obtained from literature.

PEMFC		MCFC		SOFC		ASOFC	
39 – 52	[61]	50	[60]	55 – 61	[238]	50	[159]
50 – 60	[239]	47	[240]	57 – 65	[241]	50	[163]
40 – 48	[125]	45 – 48	[170]	55 – 68	[171]	60 – 65	[138]
60	[135]	50	[242]	55 – 65	[243]	47 – 70	[172]
40 – 60	[38]	45 – 47	[244]	50 – 55	[125]	60 – 70	[163]
47 – 53	[238]	47 – 53	[151]	52 – 65	[154]		
40 – 50	[245]	49	[246]	45 – 65	[150]		
40 – 65	[168]	45 – 55	[125]	50 – 60	[135]		
35 – 40	[150]	45 – 50	[150]	50 – 55	[247]		
35	[147]	50	[135]	45 – 60	[155]		
45 – 50	[169]	47 – 53	[134]	60	[248]		
		40 – 55	[38]	55 – 65	[103]		
		52	[249]	43 – 60	[250]		
				55	[151]		
				45 – 60	[38]		
				60	[60]		
35 – 65	**47**	**40 – 55**	**50**	**43 – 68**	**55**	**47 – 70**	**60**

© COPYRIGHT OF C-JOB, WHOSE PROPERTY, THIS DOCUMENT REMAINS. NO PART THEREOF MAY BE DISCLOSED, COPIED, DUPLICATED OR IN ANY OTHER WAY MADE USE OF EXCEPT WITH THE APPROVAL OF C-JOB.

D Power plant analysis

Appendix D provides the input and results of the study discussed in chapter 4. The first section concerns the default values of the energy storage media and energy converters characteristics. These are used in section 4.1. input values, calculation results and corresponding figures are documented in this section. Sections 2 and 3 provide tables containing the input values and calculation results of, respectively, the most favorable and least favorable future scenarios per characteristic. Section 4 provides the results of the sensitivity analysis as discussed in section 4.2. This analysis is composed of over 170 different future scenarios which are composed by randomly varying the input variables of the energy storage and energy converter units, within the defined ranges. Statistical representations of the results are shown in section 4. The last section provides plots which indicate the relative importance of the daily energy cost with respect to the initial investment costs.

Electrical efficiencies for ICEs are determined displayed including an electric generator efficiency of 97%.

D.1 All default values

Table D-1: Default input values of the energy storage and energy converter units.

ENERGY STORAGE SYSTEM INPUT									
		LNG	LH2	350 BAR H2	700 BAR H2	NH3	LI-ION	LI-AIR	LI-S
ENERGY PRICE	USD/GJ	10,04	44,97	41,17	41,97	44,29	20	20	20
GRAVIMETRIC DENSITY	GJ/ton	25,4	9	7	6,5	13,6	0,58	2,52	1,48
VOLUMETRIC DENSITY	GJ/m³	15,3	4,32	2	3,2	10,5	1,44	2,52	1,26
STORAGE EFFICIENCY	%	100	100	100	100	100	90	85	85
MAX. FILLING LEVEL	%	95	100	100	100	85	100	100	100
ENERGY STORAGE PRICE	USD/GJ	400	560	560	560	40	20 000	56 000	56 000

ENERGY CONVERTER INPUT									
		LNG ICE	H_2 ICE	NH_3 ICE	PEMFC	MCFC	SOFC	NH_3 SOFC	AM-REF
SPECIFIC MASS	ton/MW	12	15	15	1	40	12	12	4
SPECIFIC VOLUME	m³/MW	15	18,5	18,5	0,7	50	30	30	8
ELECTRICAL EFFICIENCY	%	47	42	44	47	50	53	55	90
INVESTMENT PRICE	USD/kW	350	350	350	300	2 000	750	750	250

Table D-2: Output values of power plant configurations using default values.

OUTPUT										
CONFIG	FUEL COST /DAY	INVESTMENT COST			TOTAL VOLUME			TOTAL WEIGHT		
#	1 000 USD/day	1-day mln$	3.5-day mln$	14-day mln$	1-day m³	3.5-day m³	14-day m³	1-day ton	3.5-day ton	14-day ton
REF	24,8	22,3	24,8	35,1	767	1 337	3 728	558	814	1 889
HC1.1	113,5	22,8	26,7	42,7	2 396	6 784	25 214	936	1 921	6 056
HC1.2	115,7	22,8	26,7	42,7	1 737	4 480	15 999	966	2 027	6 481

© COPYRIGHT OF C-JOB, WHOSE PROPERTY, THIS DOCUMENT REMAINS. NO PART THEREOF MAY BE DISCLOSED, COPIED, DUPLICATED OR IN ANY OTHER WAY MADE USE OF EXCEPT WITH THE APPROVAL OF C-JOB.

HC1.3	124,0	22,8	26,7	42,7	1 457	3 498	12 070	849	1 614	4 831
HC2.1	100,7	9,8	13,2	27,4	1 577	5 472	21 827	378	1 251	4 922
HC2.2	102,7	9,8	13,2	27,4	993	3 427	13 649	404	1 346	5 298
HC2.3	110,0	9,8	13,2	27,4	744	2 555	10 163	300	980	3 834
HC3.1	89,3	22,2	25,2	37,9	2 221	5 675	20 179	646	1 421	4 676
HC3.2	91,1	22,2	25,2	37,9	1 703	3 862	12 927	670	1 504	5 009
HC3.3	97,6	22,2	25,2	37,9	1 482	3 089	9 835	577	1 180	3 711
HC4.1	94,7	57,3	60,5	73,9	2 864	6 525	21 899	1 449	2 270	5 720
HC4.2	96,5	57,3	60,5	73,9	2 315	4 603	14 212	1 474	2 358	6 074
HC4.3	103,4	57,3	60,5	73,9	2 081	3 784	10 934	1 376	2 014	4 698
AC1	115,6	22,6	22,9	24,0	1 118	2 213	6 811	788	1 352	3 722
AC2	188,0	46,1	46,6	48,3	1 692	3 473	10 955	893	1 811	5 667
AC3	84,5	34,3	34,5	35,3	1 372	2 172	5 534	712	1 125	2 858
AC4	89,6	70,1	70,3	71,1	2 187	3 036	6 600	1 519	1 956	3 793
AC5	92,6	21,1	21,3	22,2	1 191	2 068	5 753	517	969	2 868
BC1	25,6	25,9	90,7	362,7	799	2 795	11 181	1 183	4 141	16 564
BC2	27,1	75,2	263,1	1 052,3	456	1 597	6 389	537	1 879	7 516
BC3	27,1	75,2	263,1	1 052,3	913	3 194	12 778	914	3 197	12 789

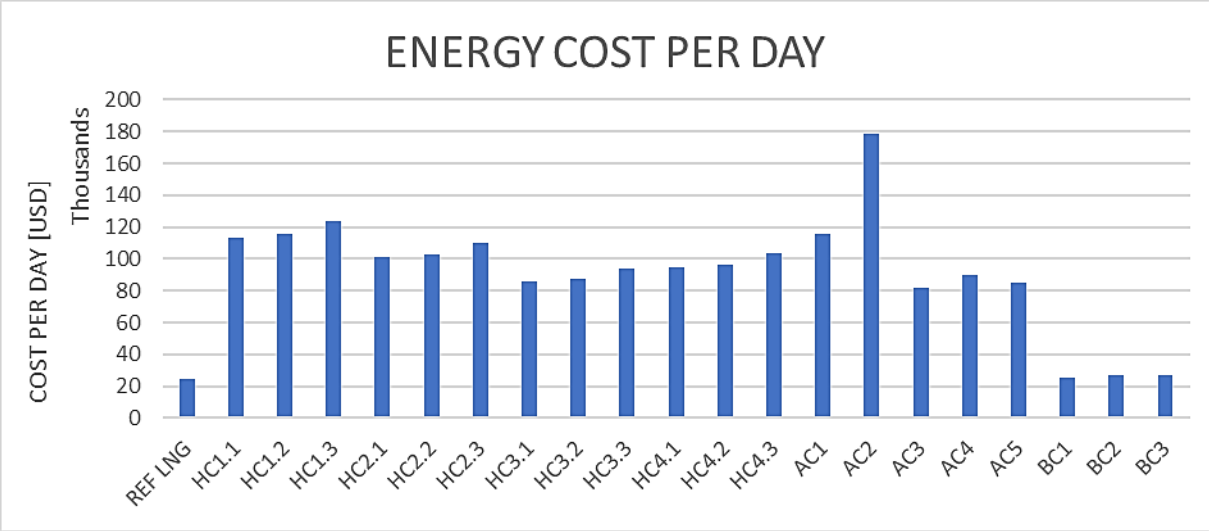

Figure D-1: Energy cost per day 1st set.

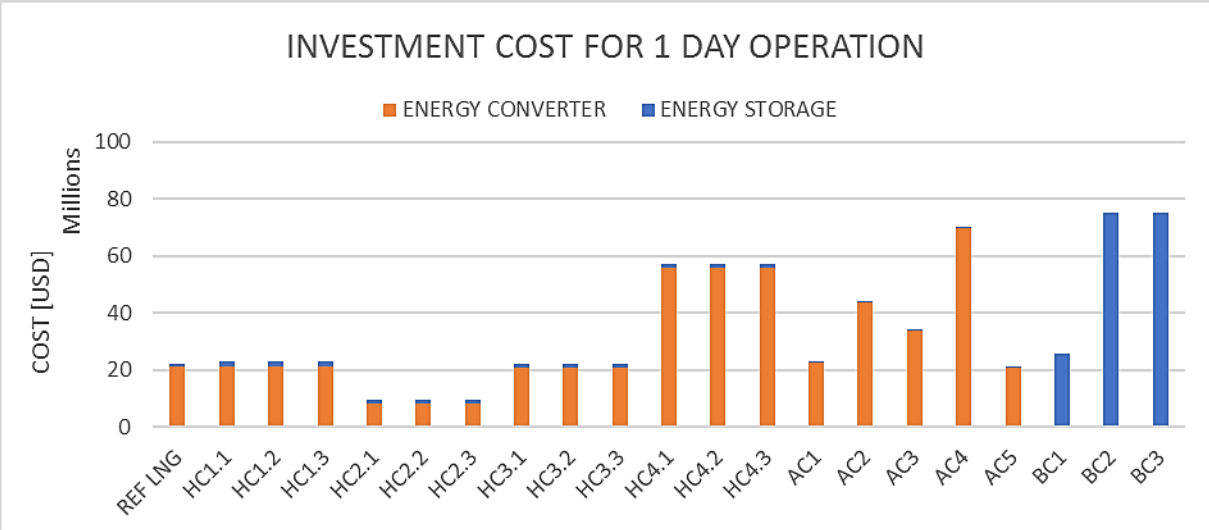

Figure D-2: Investment costs for 1-day operation 1st set.

© COPYRIGHT OF C-JOB, WHOSE PROPERTY, THIS DOCUMENT REMAINS. NO PART THEREOF MAY BE DISCLOSED, COPIED, DUPLICATED OR IN ANY OTHER WAY MADE USE OF EXCEPT WITH THE APPROVAL OF C-JOB.

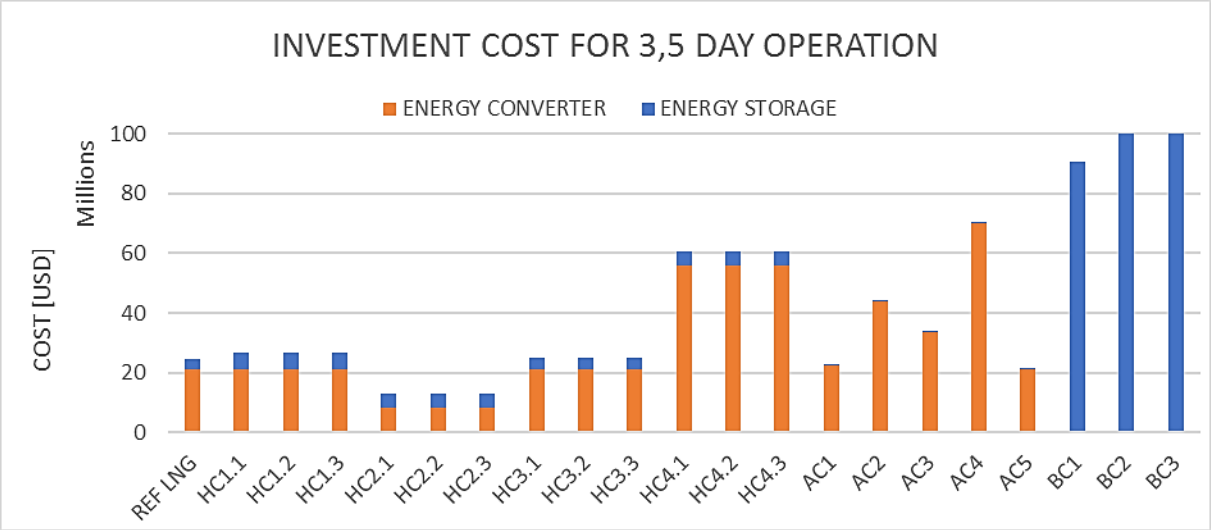

Figure D-3: Investment costs for 3.5-day operation 1st set.

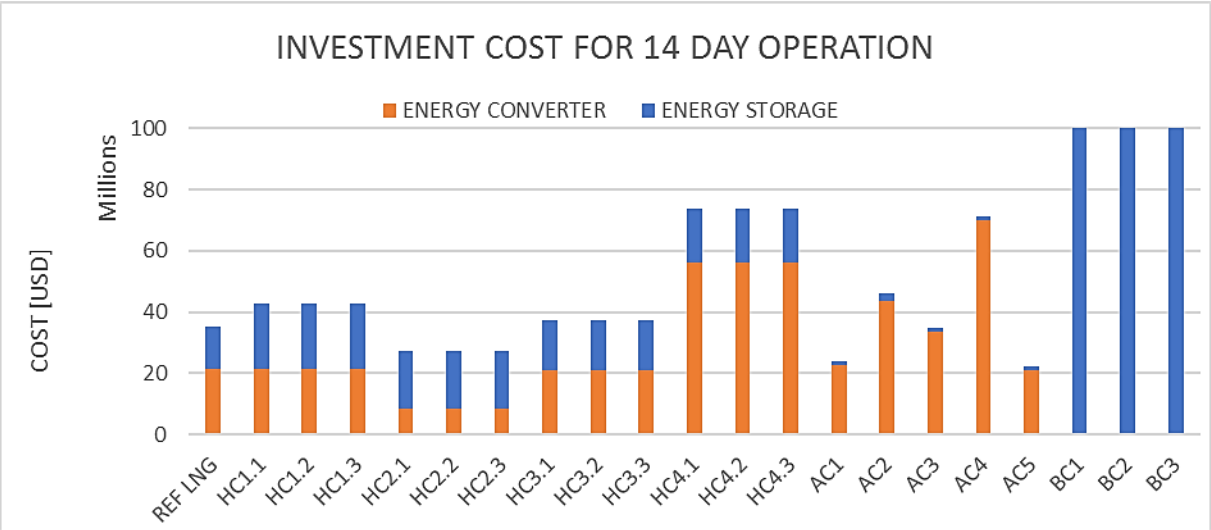

Figure D-4: Investment costs for 14-day operation 1st set.

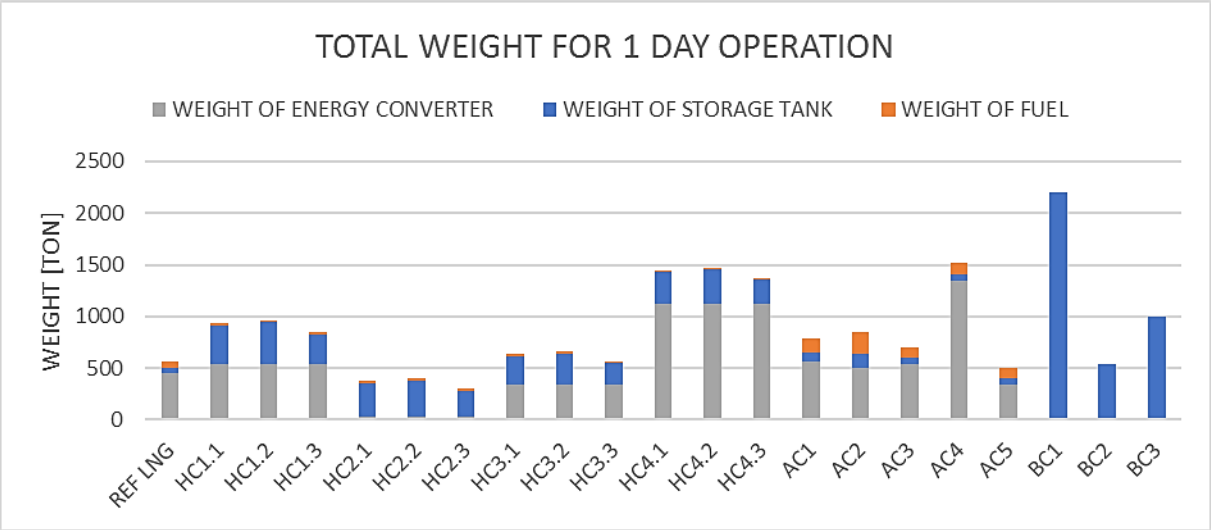

Figure D-5: Weights for 1-day operation 1st set.

© COPYRIGHT OF C-JOB, WHOSE PROPERTY, THIS DOCUMENT REMAINS. NO PART THEREOF MAY BE DISCLOSED, COPIED, DUPLICATED OR IN ANY OTHER WAY MADE USE OF EXCEPT WITH THE APPROVAL OF C-JOB.

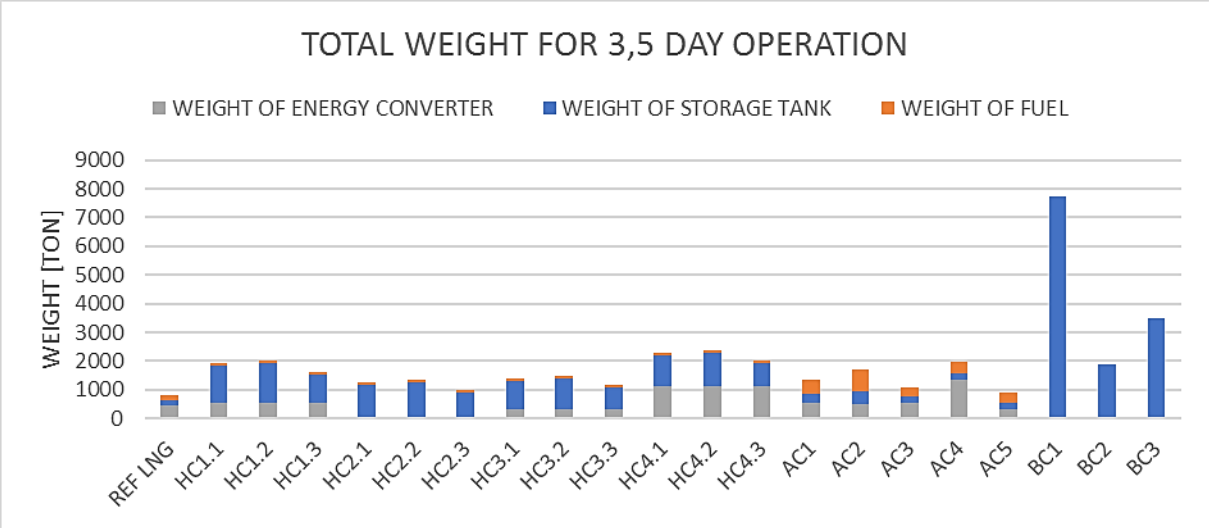

Figure D-6: Weights for 3.5-day operation 1st set.

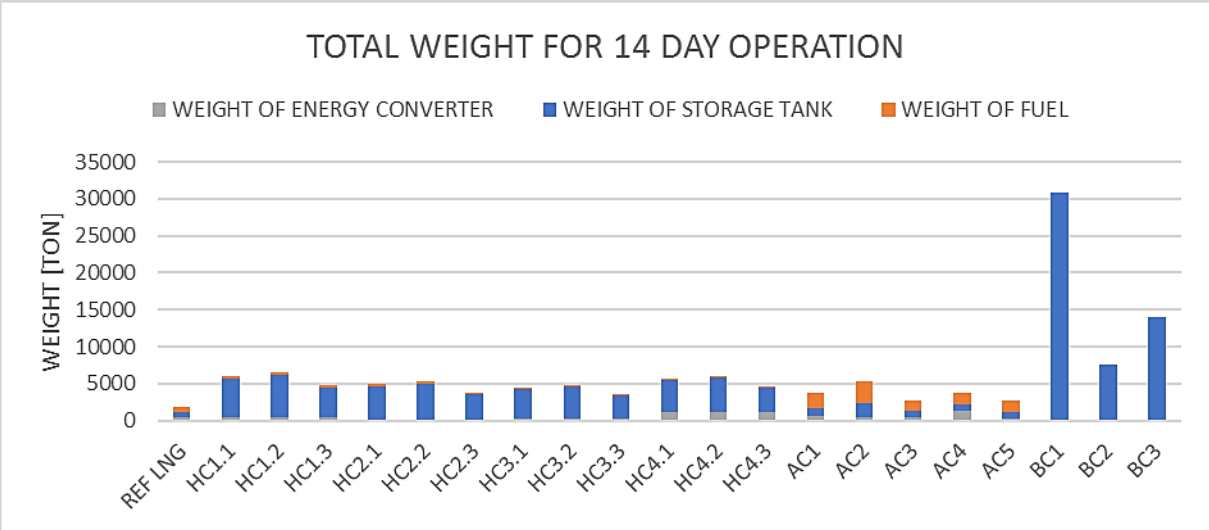

Figure D-7: Weights for 14-day operation 1st set.

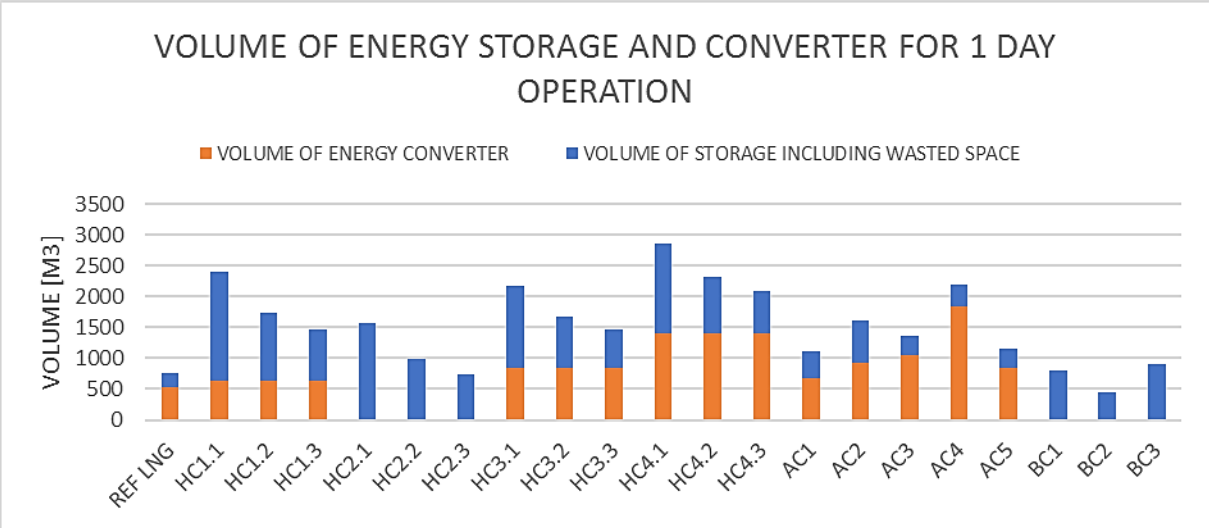

Figure D-8: Volumes for 1-day operation 1st set.

© COPYRIGHT OF C-JOB, WHOSE PROPERTY, THIS DOCUMENT REMAINS. NO PART THEREOF MAY BE DISCLOSED, COPIED, DUPLICATED OR IN ANY OTHER WAY MADE USE OF EXCEPT WITH THE APPROVAL OF C-JOB.

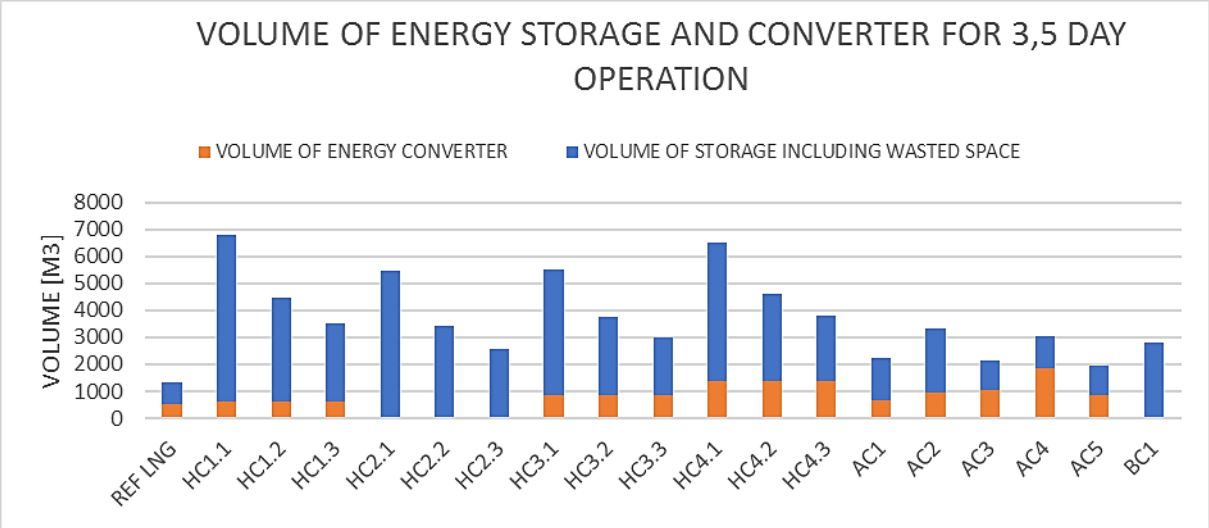

Figure D-9: Volumes for 3.5-day operation 1st set.

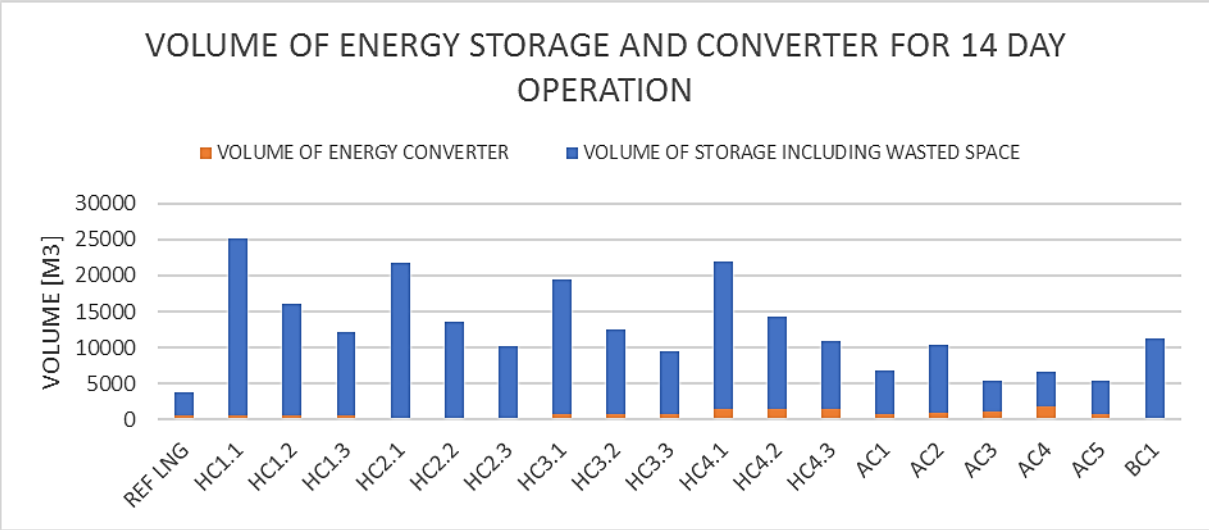

Figure D-10: Volumes for 14-day operation 1st set.

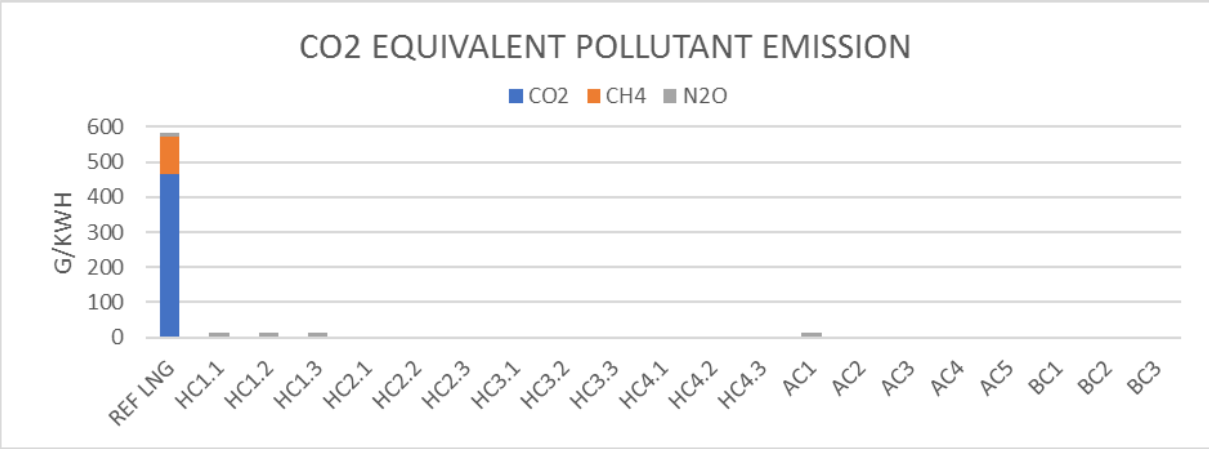

Figure D-11: GHG emissions 1st set.

© COPYRIGHT OF C-JOB, WHOSE PROPERTY, THIS DOCUMENT REMAINS. NO PART THEREOF MAY BE DISCLOSED, COPIED, DUPLICATED OR IN ANY OTHER WAY MADE USE OF EXCEPT WITH THE APPROVAL OF C-JOB.

D.2 As positive as possible

Table D-3: Best-case input values of the energy storage and energy converter units.

ENERGY STORAGE SYSTEM INPUT									
		LNG	LH_2	350 BAR H_2	700 BAR H_2	NH_3	LI-ION	LI-AIR	LI-S
ENERGY PRICE	USD/GJ	6,41	12,5	12,5	12,5	10	6	6	6
GRAVIMETRIC DENSITY	GJ/ton	25,4	15	15	13,2	14,6	1,08	6,12	2,88
VOLUMETRIC DENSITY	GJ/m³	15,3	5,4	2,4	4	10,7	3,49	4,68	3,56
STORAGE EFFICIENCY	%	100	100	100	100	100	95	90	91
MAX. FILLING LEVEL	%	95	100	100	100	85	100	100	100
ENERGY STORAGE PRICE	USD/GJ	400	560	560	560	40	20 000	56 000	56 000

ENERGY CONVERTER INPUT									
		LNG ICE	H_2 ICE	NH_3 ICE	PEMFC	MCFC	SOFC	NH_3 SOFC	AM-REF
SPECIFIC MASS	ton/MW	12	12	12	0,5	20	3	3	2
SPECIFIC VOLUME	m³/MW	15	15	15	0,4	25	7	7	4
ELECTRICAL EFFICIENCY	%	49	53	53	65	55	68	70	97
INVESTMENT PRICE	USD/kW	125	125	125	300	1 000	400	400	250

Table D-4: Output values of power plant configurations using best-case values.

OUTPUT										
CONFIG	FUEL COST /DAY	INVESTMENT COST			TOTAL VOLUME			TOTAL WEIGHT		
#	1 000 USD/day	1-day mln$	3.5-day mln$	14-day mln$	1-day m³	3.5-day m³	14-day m³	1-day ton	3.5-day ton	14-day ton
REF	15,2	15,8	18,1	28,1	758	1 305	3 600	554	800	1 831
HC1.1	26,9	16,0	19,0	31,6	2 064	5 876	21 886	1 174	2 970	10 515
HC1.2	26,9	16,0	19,0	31,6	1 912	5 342	19 751	1 354	3 599	13 030
HC1.3	26,9	16,0	19,0	31,6	1 226	2 941	10 145	782	1 599	5 028
HC2.1	22,1	9,4	11,8	22,2	1 263	4 391	17 532	604	2 078	8 270
HC2.2	22,1	9,4	11,8	22,2	1 138	3 953	15 780	751	2 594	10 335
HC2.3	22,1	9,4	11,8	22,2	574	1 982	7 895	282	952	3 767
HC3.1	21,1	12,1	14,5	24,4	1 392	4 383	16 944	648	2 057	7 976
HC3.2	21,1	12,1	14,5	24,4	1 273	3 964	15 269	789	2 550	9 949
HC3.3	21,1	12,1	14,5	24,4	734	2 080	7 732	340	981	3 671
HC4.1	26,1	29,2	32,1	44,3	2 179	5 877	21 406	1 257	2 999	10 318
HC4.2	26,1	29,2	32,1	44,3	2 031	5 359	19 336	1 431	3 609	12 757
HC4.3	26,1	29,2	32,1	44,3	1 366	3 029	10 018	877	1 669	4 995
AC1	21,3	15,9	16,1	17,0	917	1 822	5 620	657	1 140	3 168
AC2	20,3	25,1	25,3	26,1	583	1 443	5 053	314	773	2 701
AC3	14,9	21,6	21,7	22,3	530	1 160	3 806	301	637	2 050
AC4	18,4	40,8	41,0	41,8	1 215	1 994	5 265	828	1 244	2 991
AC5	16,4	11,3	11,4	12,1	474	1 170	4 093	233	604	2 165
BC1	24,2	24,5	85,9	343,7	3194	11 181	44 722	6 725	23 538	94 152
BC2	25,6	71,0	248,5	993,8	1 278	4 472	17 889	1 323	4 630	18 519
BC3	25,3	70,2	245,7	982,9	1 879	6 577	26 307	2 340	8 191	32 764

© COPYRIGHT OF C-JOB, WHOSE PROPERTY, THIS DOCUMENT REMAINS. NO PART THEREOF MAY BE DISCLOSED, COPIED, DUPLICATED OR IN ANY OTHER WAY MADE USE OF EXCEPT WITH THE APPROVAL OF C-JOB.

D.3 As negative as possible

Table D-5: Worst-case input values of the energy storage and energy converter units.

ENERGY STORAGE SYSTEM INPUT									
		LNG	LH_2	350 BAR H_2	700 BAR H_2	NH_3	LI-ION	LI-AIR	LI-S
ENERGY PRICE	USD/GJ	42.11	89,13	80,96	82,68	92,13	43	43	43
GRAVIMETRIC DENSITY	GJ/ton	25,4	6,6	3	2,4	13	0,18	0,97	0,54
VOLUMETRIC DENSITY	GJ/m³	15,3	4	1,8	2	10,4	0,36	0,9	0,612
STORAGE EFFICIENCY	%	100	100	100	100	100	80	80	78
MAX. FILLING LEVEL	%	95	100	100	100	85	100	100	100
ENERGY STORAGE PRICE	USD/GJ	400	1 390	3 610	4 170	40	42 000	-	-

ENERGY CONVERTER INPUT									
		LNG ICE	H_2 ICE	NH_3 ICE	PEMFC	MCFC	SOFC	NH_3 SOFC	AM-REF
SPECIFIC MASS	ton/MW	12	16	16	5	125	50	50	10
SPECIFIC VOLUME	m³/MW	15	20	20	7	500	125	125	20
ELECTRICAL EFFICIENCY	%	39	39	39	35	40	43	47	60
INVESTMENT PRICE	USD/kW	350	350	350	600	5 000	1 200	1 200	250

Table D-6: Output values of power plant configurations using worst-case values.

OUTPUT										
CONFIG	FUEL COST /DAY	INVESTMENT COST			TOTAL VOLUME			TOTAL WEIGHT		
#	1 000 USD/day	1-day	3.5-day	14-day	1-day	3.5-day	14-day	1-day	3.5-day	14-day
		mln$	mln$	mln$	m³	m³	m³	ton	ton	ton
REF	125,9	22,5	25,5	37,9	813	1 496	4 366	578	886	2 175
HC1.1	240,0	32,0	58,8	171,1	2 780	8 022	30 035	1 559	4 029	14 403
HC1.2	245,1	33,7	64,5	194,2	2 571	7 288	27 100	1 806	4 893	17 861
HC1.3	264,2	25,4	35,7	78,9	1 627	3 986	13 892	1 020	2 143	6 858
HC2.1	266,0	28,7	58,3	182,9	2 520	8 331	32 734	1 235	3 973	15 473
HC2.2	271,7	30,5	64,7	208,5	2 288	7 517	29 481	1 509	4 932	19 307
HC2.3	292,9	21,4	32,8	80,7	1 242	3 857	14 838	638	1 882	7 110
HC3.1	216,5	43,3	67,4	168,8	5 392	10 121	29 985	2 291	4 520	13 881
HC3.2	221,1	44,7	72,6	189,6	5 203	9 459	27 336	2 514	5 300	17 001
HC3.3	238,4	37,3	46,6	85,6	4 351	6 480	15 418	1 805	2 818	7 073
HC4.1	232,8	150,4	176,3	285,3	16 034	21 118	42 471	4 458	6 854	16 917
HC4.2	237,7	152,0	181,9	307,7	15 830	20 406	39 624	4 698	7 693	20 271
HC4.3	256,2	144,0	154,0	195,9	14 915	17 203	26 812	3 936	5 025	9 598
AC1	270,4	22,8	23,1	24,3	1 292	2 536	7 759	892	1 556	4 346
AC2	788,4	109,3	110,2	113,8	6 770	10 395	25 620	3 559	5 495	13 626
AC3	216,6	50,0	50,2	51,2	4 550	5 546	9 730	2 264	2 796	5 031
AC4	232,9	157,6	157,9	158,9	15 828	16 899	21 397	4 429	5 001	7 403
AC5	225,4	33,7	33,9	35,0	3 915	4 951	9 305	1 621	2 175	4 500
BC1	61,8	59,9	209,6	838,5	3 194	11 181	44 722	7 986	27 951	111806
BC2	-	-	-	-	-	-	-	-	-	-
BC3	-	-	-	-	-	-	-	-	-	-

© COPYRIGHT OF C-JOB, WHOSE PROPERTY, THIS DOCUMENT REMAINS. NO PART THEREOF MAY BE DISCLOSED, COPIED, DUPLICATED OR IN ANY OTHER WAY MADE USE OF EXCEPT WITH THE APPROVAL OF C-JOB.

D.4 Sensitivity analysis

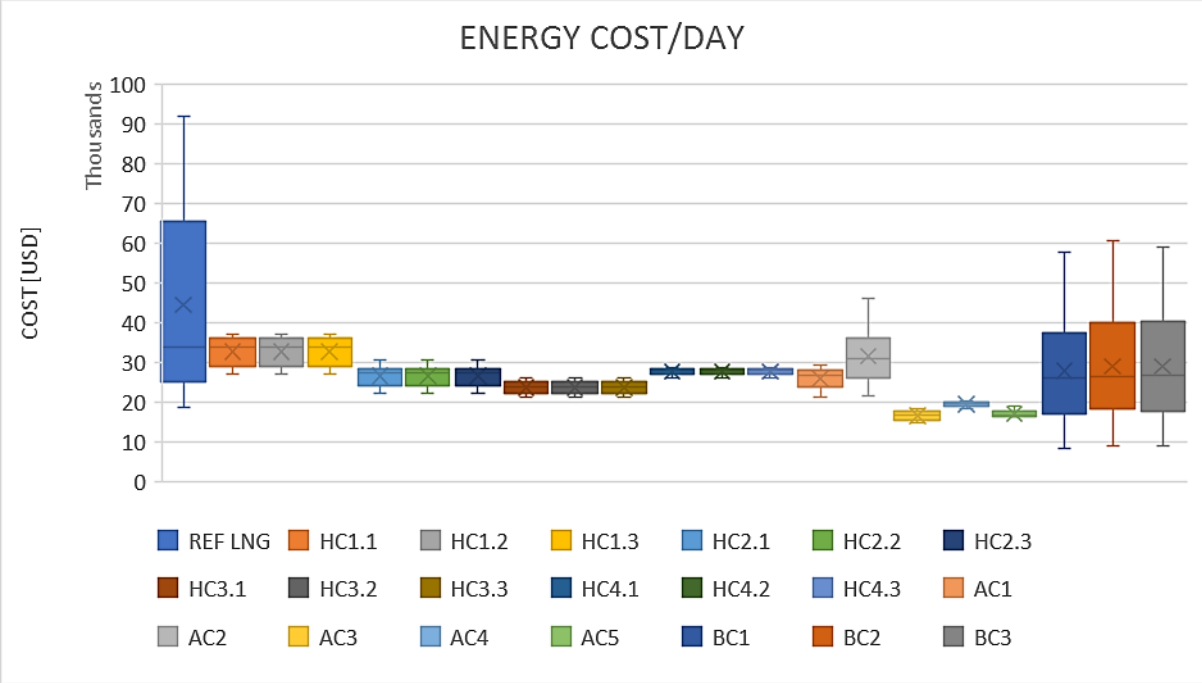

Figure D-12: Daily energy cost per configuration according to the sensitivity analysis.

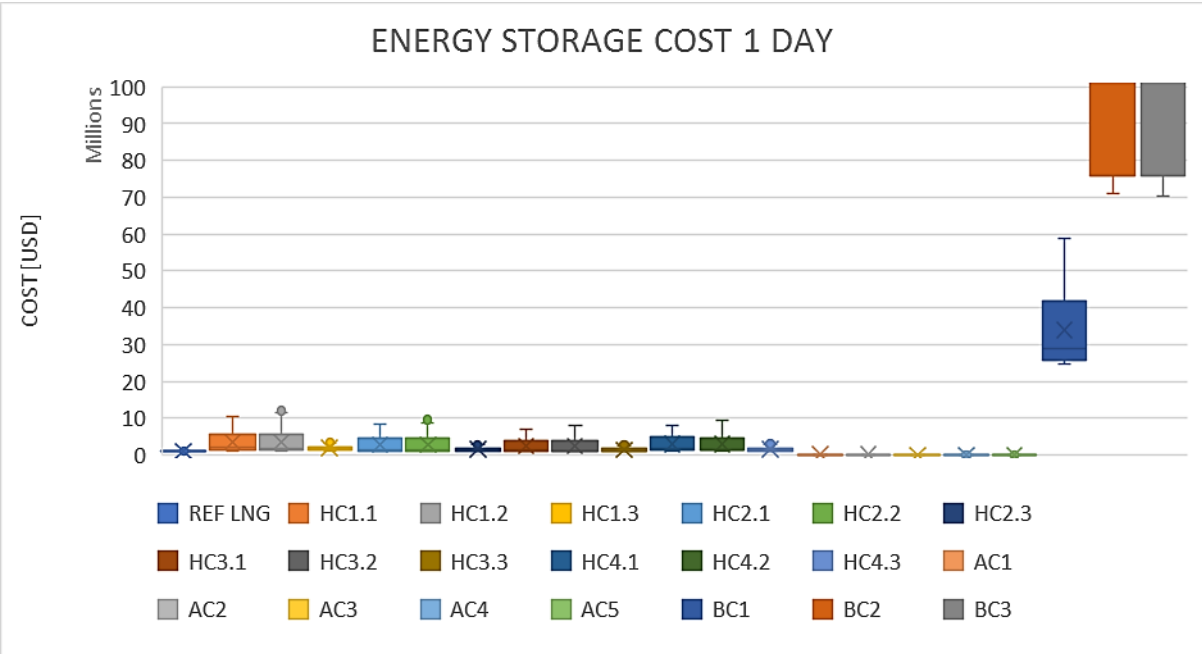

Figure D-13: 1-day energy storage system investment cost per configuration according to the sensitivity analysis.

© COPYRIGHT OF C-JOB, WHOSE PROPERTY, THIS DOCUMENT REMAINS. NO PART THEREOF MAY BE DISCLOSED, COPIED, DUPLICATED OR IN ANY OTHER WAY MADE USE OF EXCEPT WITH THE APPROVAL OF C-JOB.

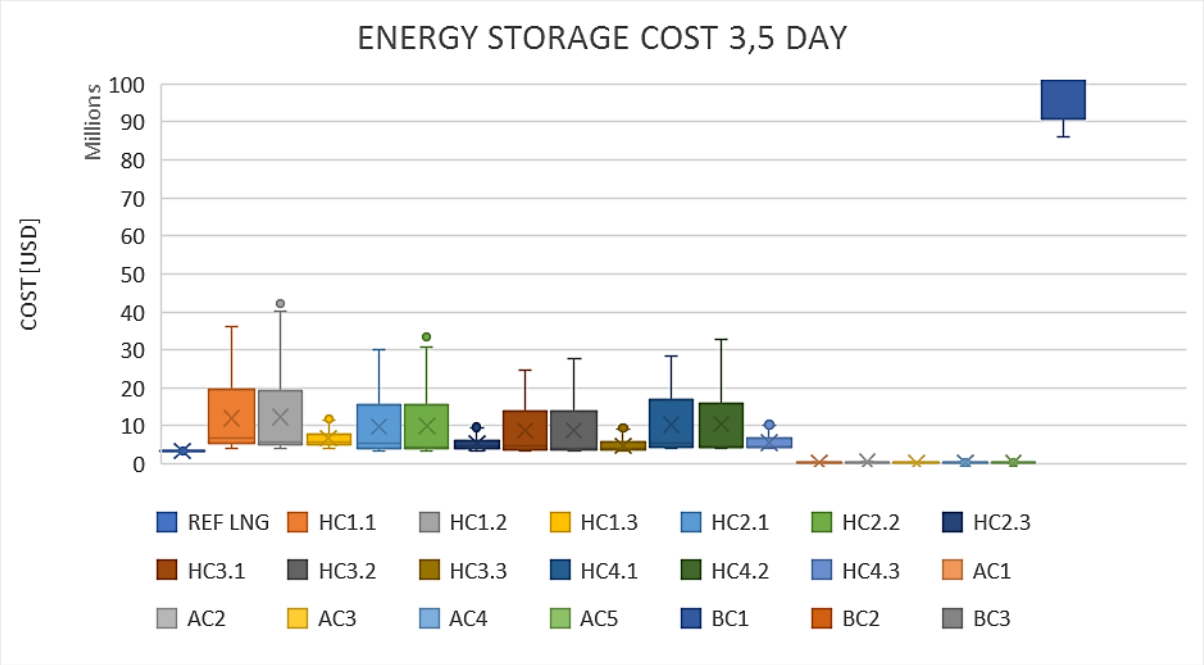

Figure D-14: 3.5-day energy storage system investment cost per configuration according to the sensitivity analysis.

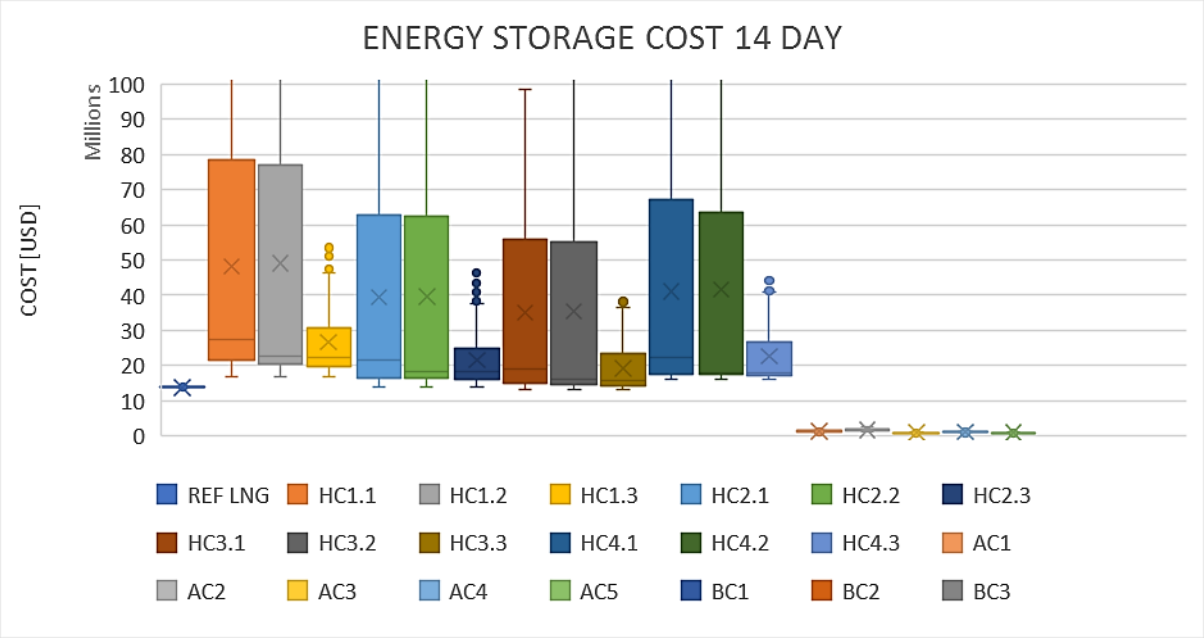

Figure D-15: 14-day energy storage system investment cost per configuration according to the sensitivity analysis.

© COPYRIGHT OF C-JOB, WHOSE PROPERTY, THIS DOCUMENT REMAINS. NO PART THEREOF MAY BE DISCLOSED, COPIED, DUPLICATED OR IN ANY OTHER WAY MADE USE OF EXCEPT WITH THE APPROVAL OF C-JOB.

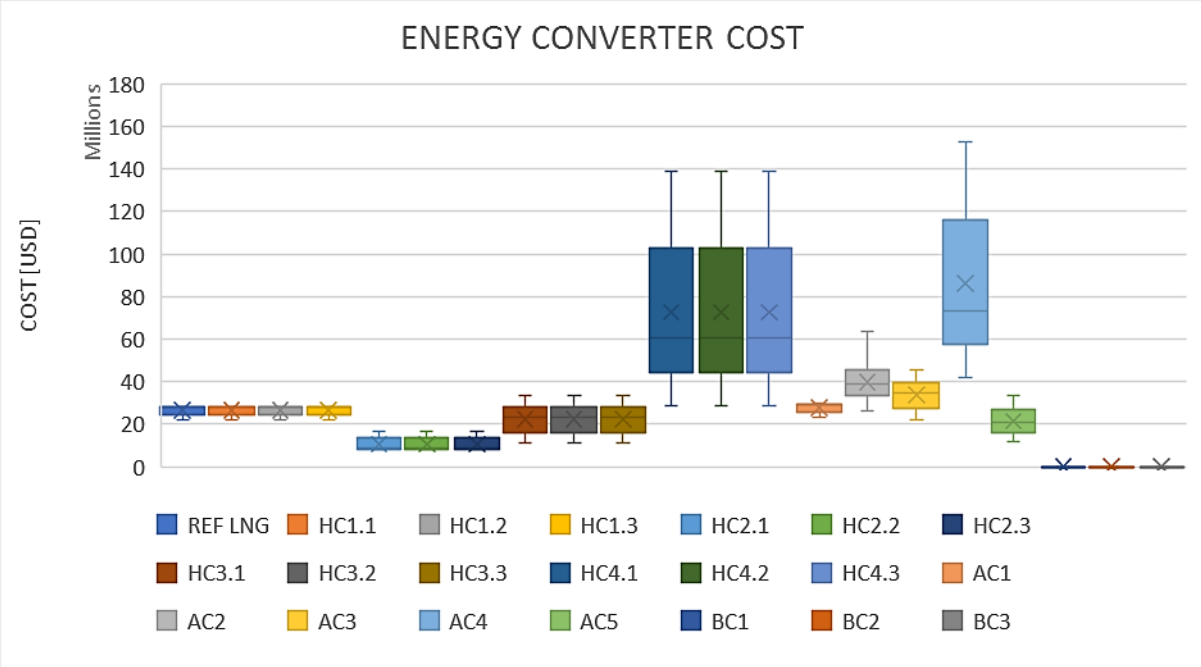

Figure D-16: Energy converter cost per power plant configuration according to the sensitivity analysis.

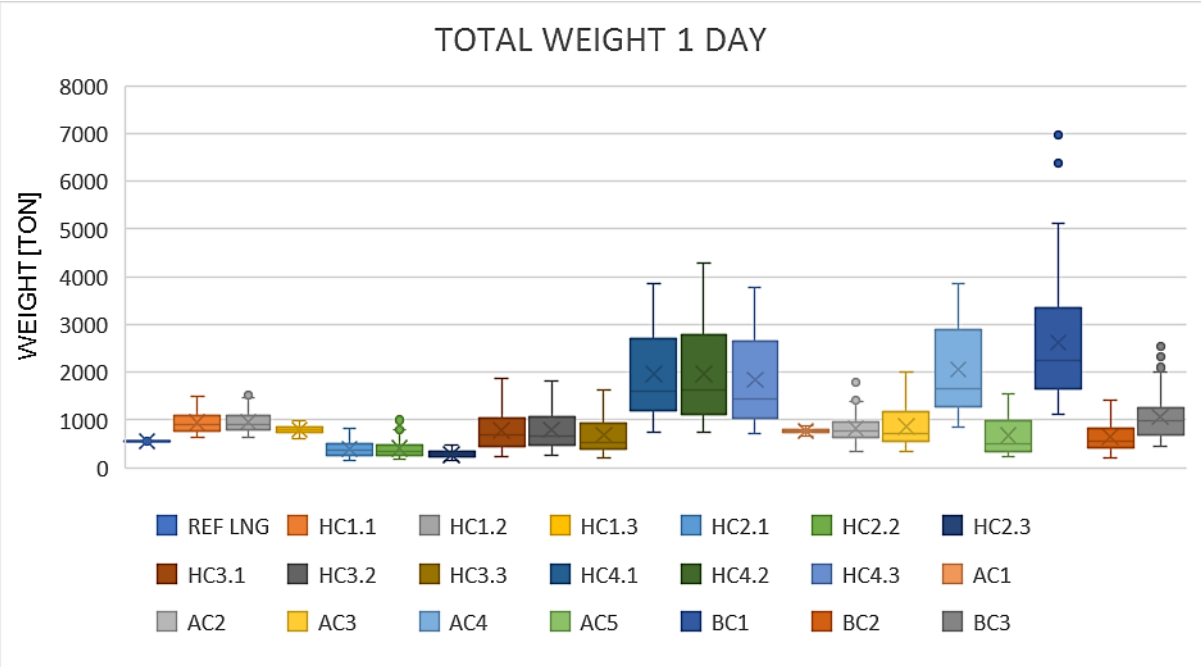

Figure D-17: Total weight of power plants per configuration for 1-day operation according to the sensitivity analysis.

© COPYRIGHT OF C-JOB, WHOSE PROPERTY, THIS DOCUMENT REMAINS. NO PART THEREOF MAY BE DISCLOSED, COPIED, DUPLICATED OR IN ANY OTHER WAY MADE USE OF EXCEPT WITH THE APPROVAL OF C-JOB.

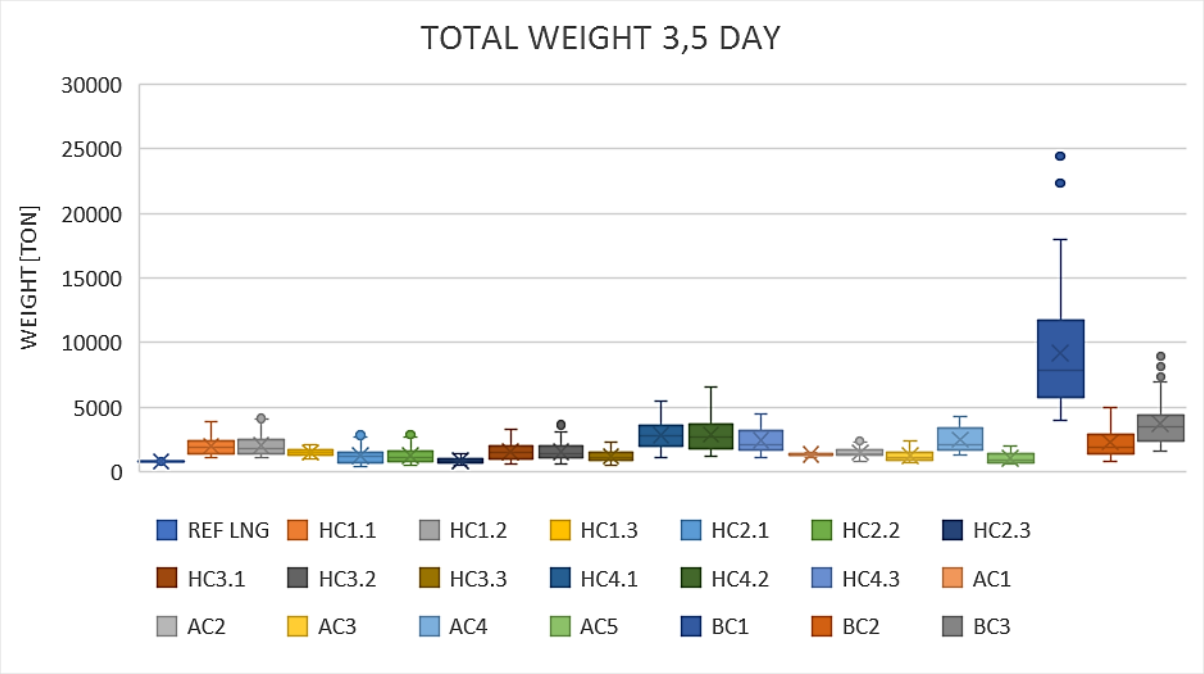

Figure D-18: Total weight of power plants per configuration for 3.5-day operation according to the sensitivity analysis.

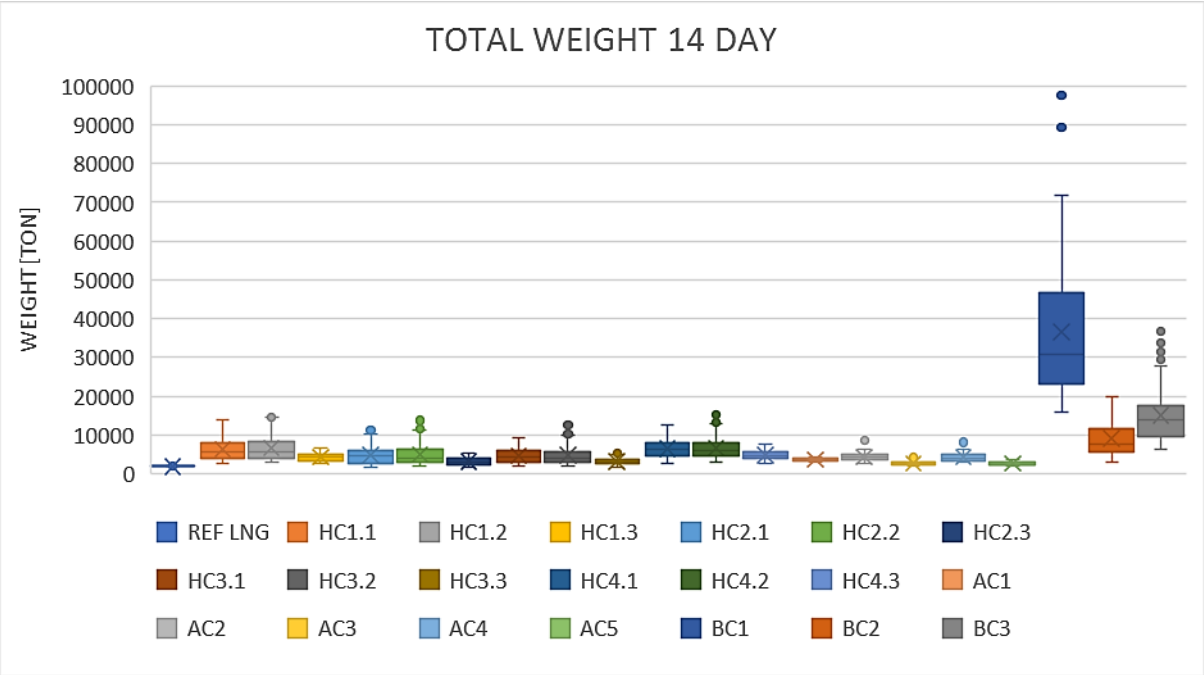

Figure D-19: Total weight of power plants per configuration for 14-day operation according to the sensitivity analysis.

© COPYRIGHT OF C-JOB, WHOSE PROPERTY, THIS DOCUMENT REMAINS. NO PART THEREOF MAY BE DISCLOSED, COPIED, DUPLICATED OR IN ANY OTHER WAY MADE USE OF EXCEPT WITH THE APPROVAL OF C-JOB.

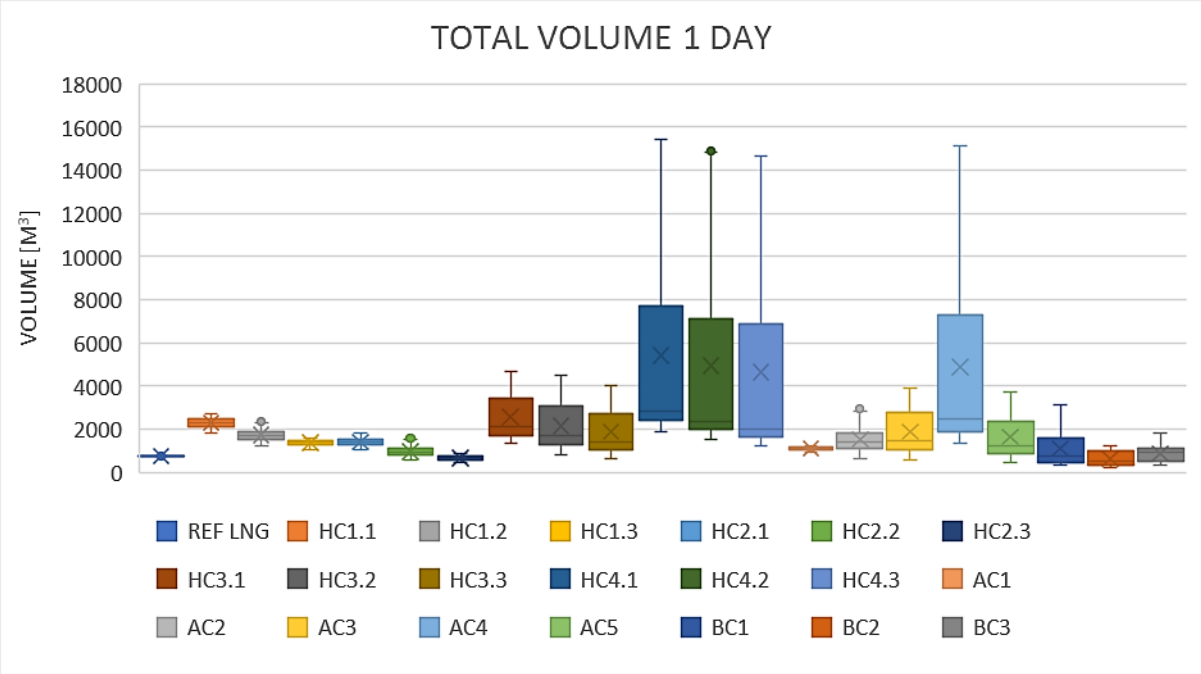

Figure D-20: Total volume of power plants per configuration for 1-day operation according to the sensitivity analysis.

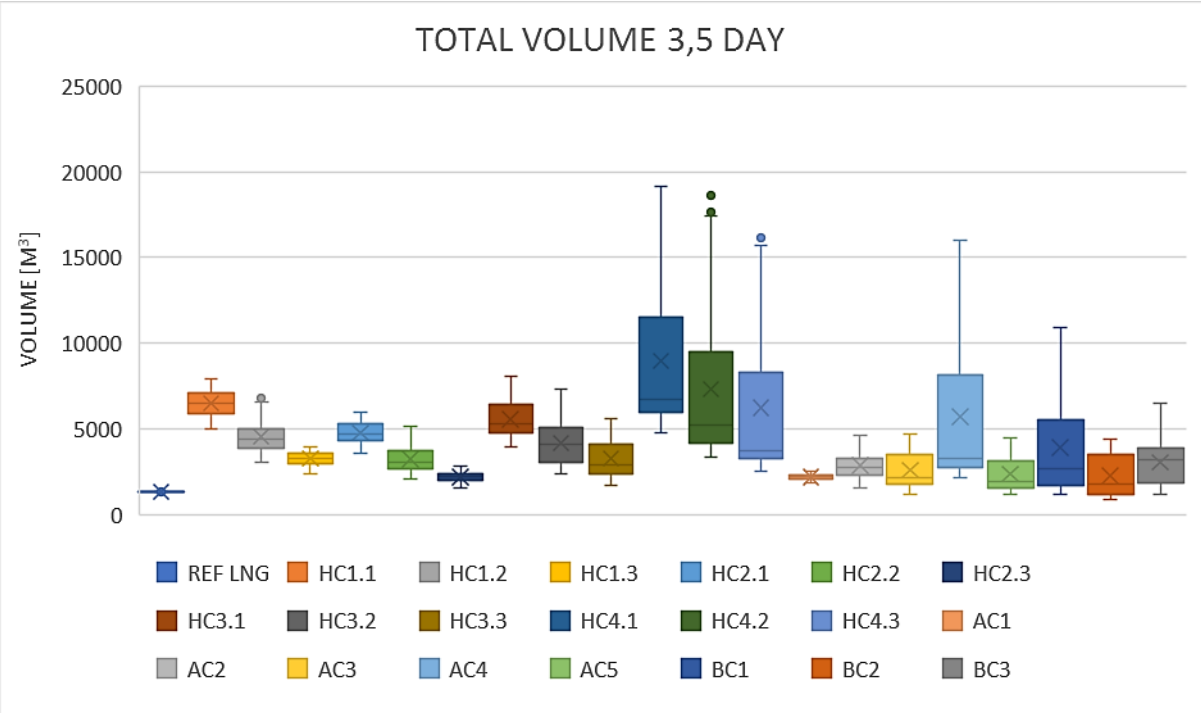

Figure D-21: Total volume of power plants per configuration for 3.5-day operation according to the sensitivity analysis.

© COPYRIGHT OF C-JOB, WHOSE PROPERTY, THIS DOCUMENT REMAINS. NO PART THEREOF MAY BE DISCLOSED, COPIED, DUPLICATED OR IN ANY OTHER WAY MADE USE OF EXCEPT WITH THE APPROVAL OF C-JOB.

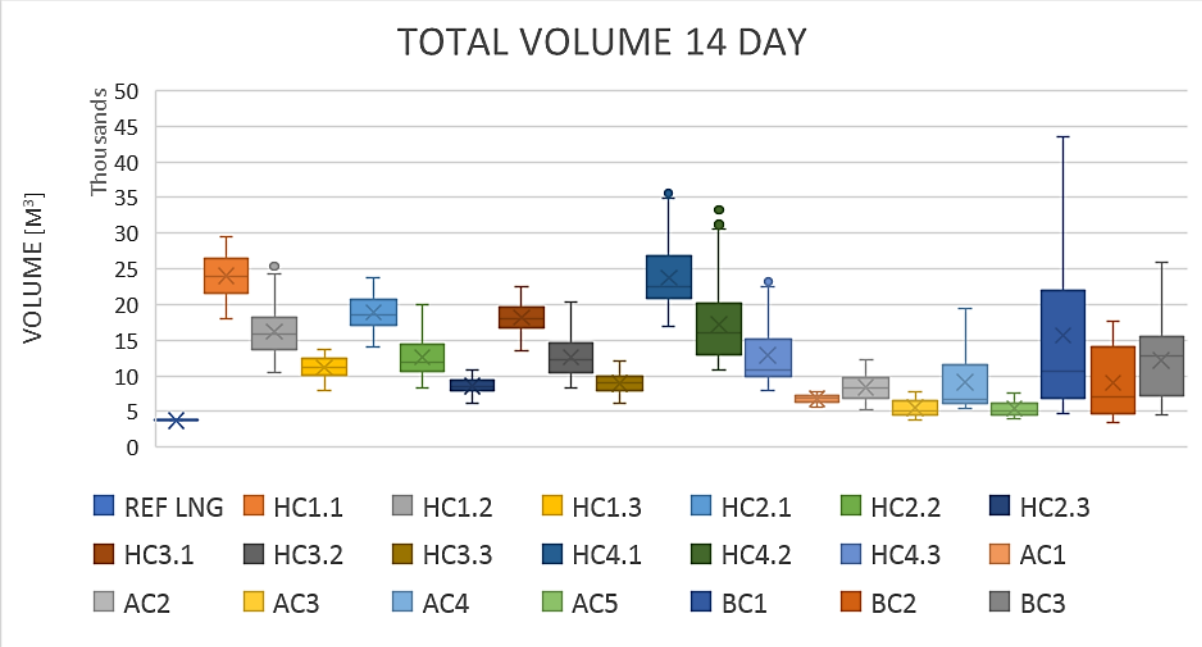

Figure D-22: Total volume of power plants per configuration for 14-day operation according to the sensitivity analysis.

© COPYRIGHT OF C-JOB, WHOSE PROPERTY, THIS DOCUMENT REMAINS. NO PART THEREOF MAY BE DISCLOSED, COPIED, DUPLICATED OR IN ANY OTHER WAY MADE USE OF EXCEPT WITH THE APPROVAL OF C-JOB.

D.5 Financial considerations

As discussed in section 4.1 are synthetic fuels characterized with high daily energy costs caused by the high price of synthetic fuels when using commercial energy. The relative importance of the price of energy is indicated in Figure D-23, Figure D-24 and Figure D-25. These figures present the cumulative lifetime costs of five power plant configurations based on a one-time purchase and a constant daily cost based on the cost of energy required per day of operation. These figures do not account for energy price fluctuations, maintenance and (partial) replacement of units resulting in a very rough representation of the expected lifetime costs of power plants.

The five power plants that are included in these figures are:

- The default power plant being an LNG fueled internal combustion engine, theoretically capable of operating for 3.5 days without refueling.
- The power plant fueled by liquid hydrogen and a using a SOFC (HC3.3), theoretically capable of operating for 3.5 days without refueling.
- The power plant using an ammonia converter and SOFC, fueled by ammonia (AC3), theoretically capable of operating for 3.5 days without refueling.
- The power plant configuration using an ammonia fueled SOFC (AC5), theoretically capable of operating for 3.5 days without refueling.
- The Li-ion battery-based configuration (BC1), theoretically capable of operating for one day without recharging.

Three lines are shown for every power plant configuration, representing the default, minimum and maximum costs associated with the corresponding power plant. The default, minimum and maximum cost per power plant are obtained from Table D-2, Table D-4 and Table D-6, respectively. The cumulative costs of power plant configurations, as displayed in the figures below, are calculated using the following formula:

$$cum.cost = investment\ cost + nr.of\ years * 365 * daily\ energy\ cost$$

These figures show that the daily costs are very important when assessing the cumulative expenses of power plants during the total lifetime. For example, it is clearly visible that the power plants using ammonia or hydrogen are by default very expensive due to the daily energy costs, as already stated in section 4.1. When these power plant configurations are compared to the default expenses of LNG or Li-ion based power plants, it is shown that the total costs in 30 years are over three times as high when using synthetic fuels manufactured using commercial energy. This implies the need to reduce the price of these fuels by using excess energy from renewable resources. This assumption is also used in section 4.2.

Minimal price scenarios as displayed in Figure D-23, Figure D-24 and Figure D-25 correspond with utilizing excess energy from renewable energy resources for the production of synthetic fuels. These scenarios result in a relatively low cumulative cost over the lifetime of the vessel which is only surpassed by a very low energy cost scenario for the battery configuration. Despite the fact that the battery configuration could cost the least amount of money on the long term, it is not chosen as most favorable configuration due to the relative weight of the configuration. This has been established in sections 4.2 and 4.3.

© COPYRIGHT OF C-JOB, WHOSE PROPERTY, THIS DOCUMENT REMAINS. NO PART THEREOF MAY BE DISCLOSED, COPIED, DUPLICATED OR IN ANY OTHER WAY MADE USE OF EXCEPT WITH THE APPROVAL OF C-JOB.

However, when synthetic fuels are not fabricated using excess renewable energy, are configurations using these fuels not likely to be the most economically favorable. In this case, the battery configuration will most likely be the most economically feasible option to power the ship, despite the high weight of the configuration and the need to recharge after every trip. Again, this does not take regular costs such as maintenance and unit replacements into account.

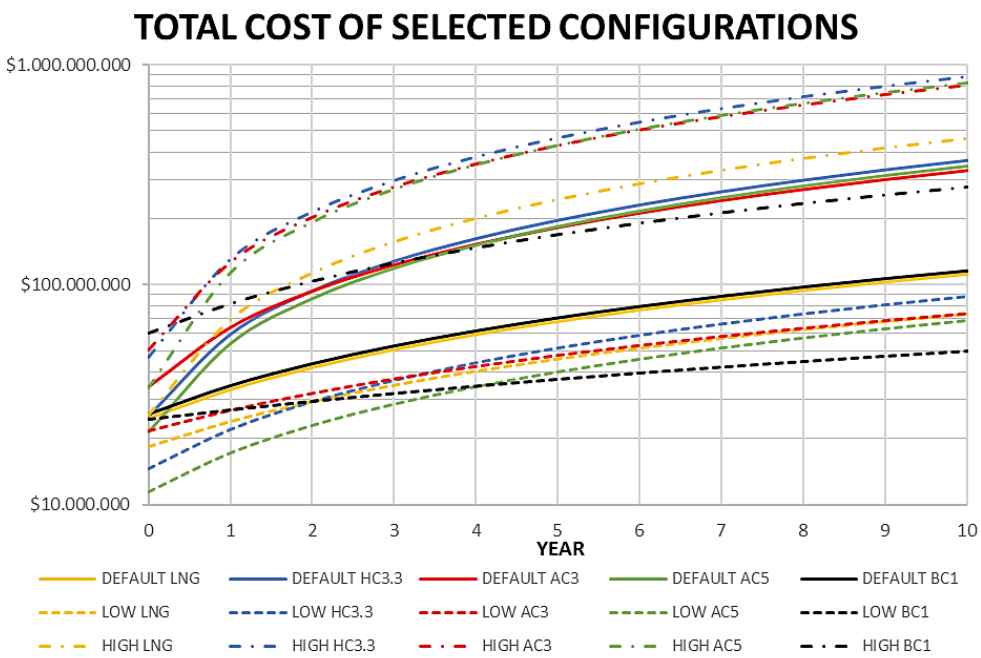

Figure D-23: Cumulative expenses over 10 years of operation of selected power plant configuration based on their default, best-case and worst-case scenarios.

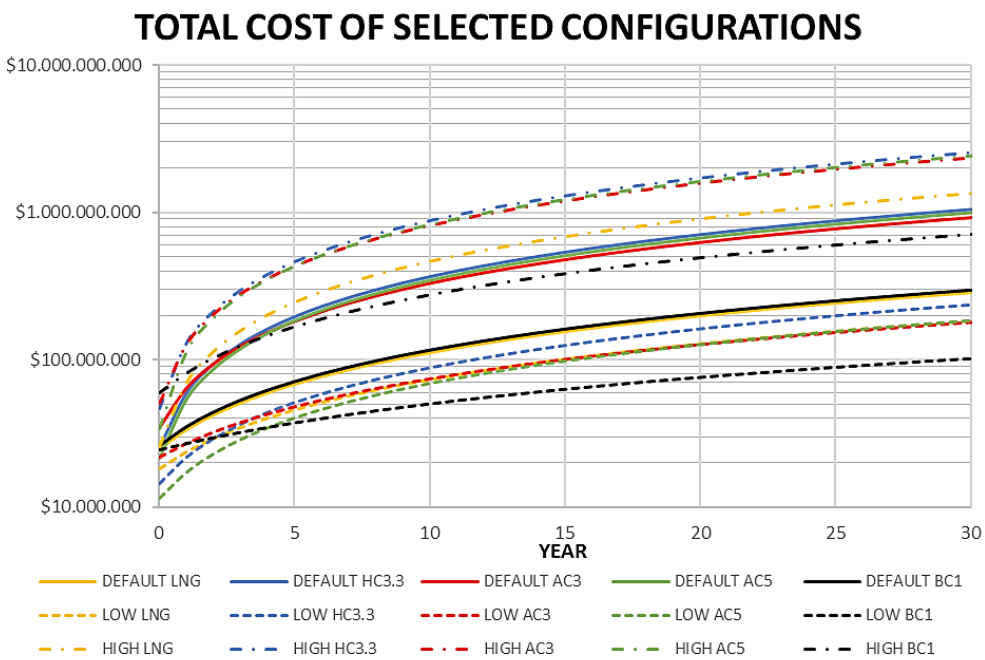

Figure D-24: Cumulative expenses over 30 years of operation of selected power plant configuration based on their default, best-case and worst-case scenarios.

© COPYRIGHT OF C-JOB, WHOSE PROPERTY, THIS DOCUMENT REMAINS. NO PART THEREOF MAY BE DISCLOSED, COPIED, DUPLICATED OR IN ANY OTHER WAY MADE USE OF EXCEPT WITH THE APPROVAL OF C-JOB.

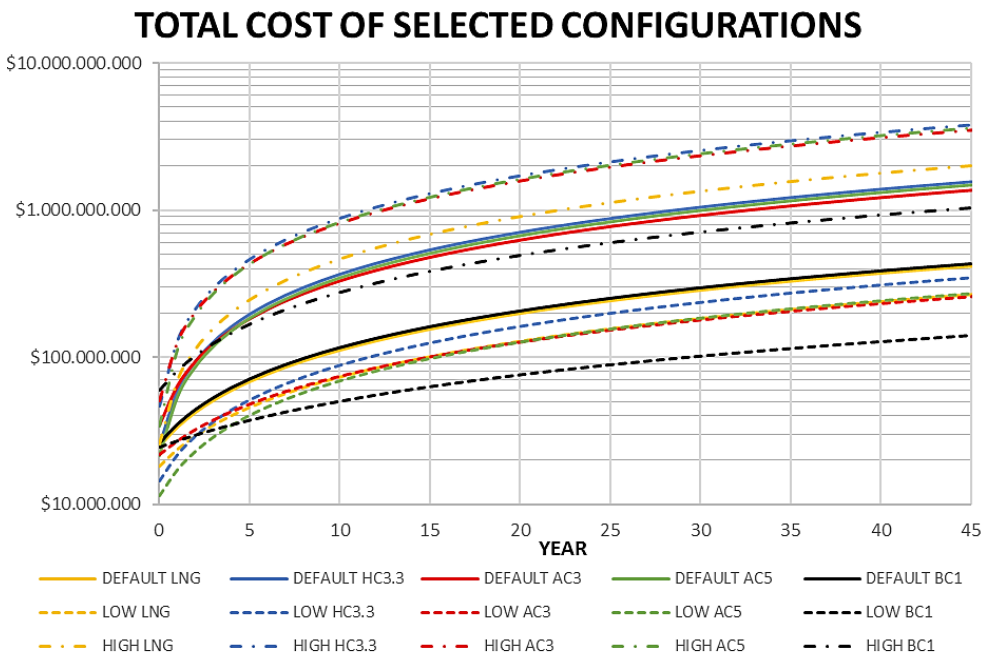

Figure D-25: Cumulative expenses over 45 years of operation of selected power plant configuration based on their default, best-case and worst-case scenarios.

© COPYRIGHT OF C-JOB, WHOSE PROPERTY, THIS DOCUMENT REMAINS. NO PART THEREOF MAY BE DISCLOSED, COPIED, DUPLICATED OR IN ANY OTHER WAY MADE USE OF EXCEPT WITH THE APPROVAL OF C-JOB.

E Concept design

This appendix is used during the composition of the general arrangement of a representative ROPAX ferry to be constructed in 2050. This design incorporates the power plant configuration established chapter 4 into the design to indicate the feasibility of such a power plant to be used onboard a ferry.

The first section provides an overview of current space requirements of berthed passengers and cars. These measurements are used during the composition of the general arrangement of the ferry.

The total general arrangement of the MS Stavangerfjord is provided in the second section. This vessel is used as reference vessel in section 5.3 and 5.4.

E.1 Passenger and car requirements

Table E-1: Cabin and car requirements according to ferry operators.

FERRY OPERATOR	CABIN REQUIREMENTS	STANDARD CAR DIMENSIONS		SOURCE
STENA LINE	2 – 6 m^2/berth 4 m^2/ berth average	L < 6 m B < 2.1 m	H < 2 m	[251]
TALLINK	2 – 4 m^2/berth	L < 5 m	H < 1.9 m	[252]
VIKING LINE	2.5 – 4 m^2/berth	L < 5 m	H < 1.9 m	[253]
P&O FERRIES	2 – 4 m^2/berth	L < 6 m	H < 1.8 m	[254]
NAVIER ARMAS		Small L < 4.85 m Medium L = 4.85 – 5 m Large L = 5 – 6 m	 H < 1.85 m H = 1.86 – 2 m H > 2 m	[255]
FJORDLINE	2 – 6 m^2/berth 3 – 4 m^2/berth average			[195]
DFDS SEAWAYS		L < 5 m	H < 1.85 m	[256]
FINNLINE	2.5 – 5 m^2/berth	L < 6 m	H < 2.1 m	[257]
NORDLINK			H < 2.2 m	[258]
GRIMALDI		L < 5 m		[259]
CORSICA FERRIES		L < 5 m B < 2 m	H < 1.9 m	[260]
	2 – 4 M^2/BERTH	**L < 5 M**	**H < 2.1 M**	

© COPYRIGHT OF C-JOB, WHOSE PROPERTY, THIS DOCUMENT REMAINS. NO PART THEREOF MAY BE DISCLOSED, COPIED, DUPLICATED OR IN ANY OTHER WAY MADE USE OF EXCEPT WITH THE APPROVAL OF C-JOB.

E.2 General Arrangement of MS Stavangerfjord

This part of the appendix E is used to provide the total general arrangement of the LNG-fueled vessel used to compare with the representative ROPAX ferry design.

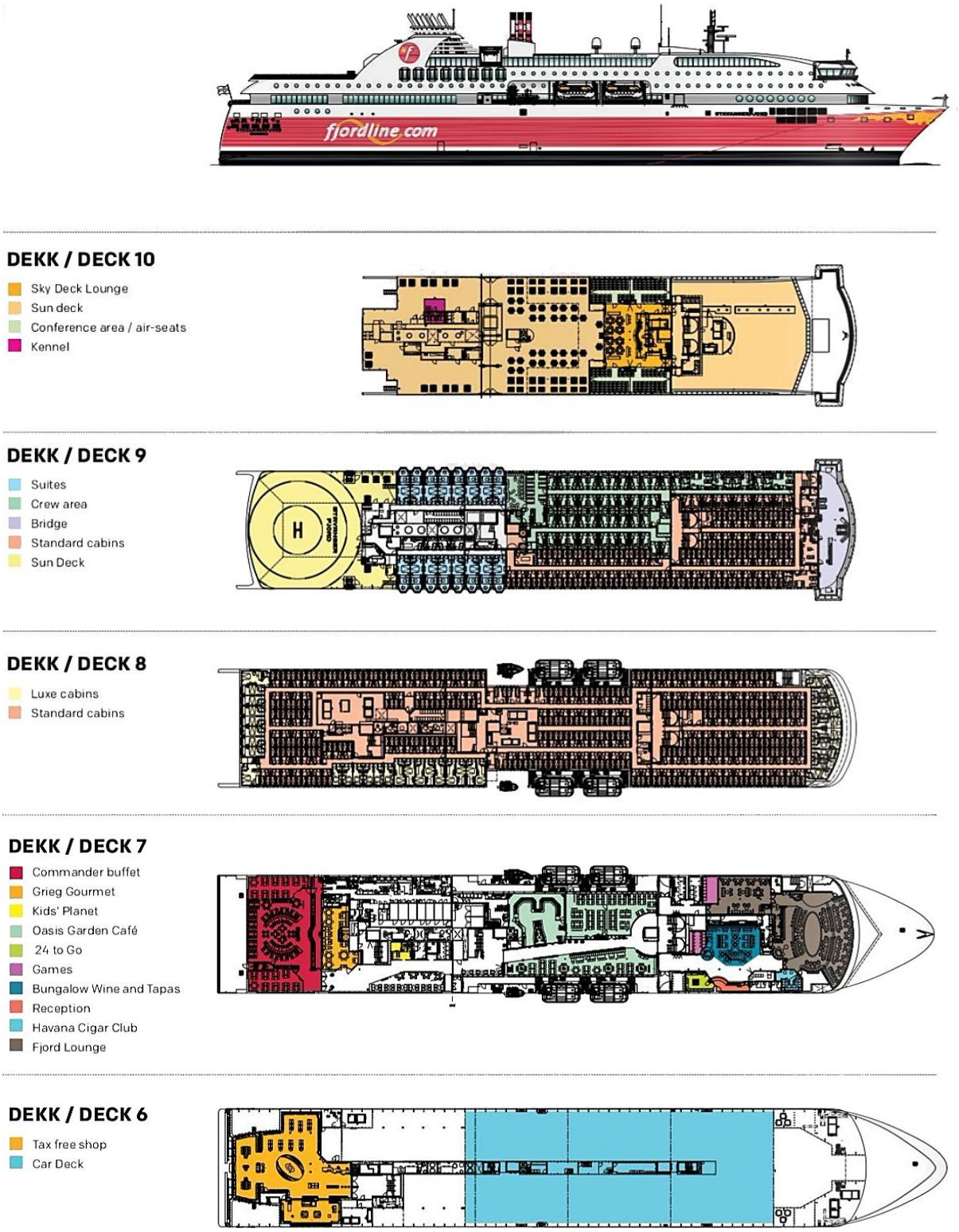

Figure E-1: General arrangement of the MS Stavangerfjord part 1. [195]

© COPYRIGHT OF C-JOB, WHOSE PROPERTY, THIS DOCUMENT REMAINS. NO PART THEREOF MAY BE DISCLOSED, COPIED, DUPLICATED OR IN ANY OTHER WAY MADE USE OF EXCEPT WITH THE APPROVAL OF C-JOB.

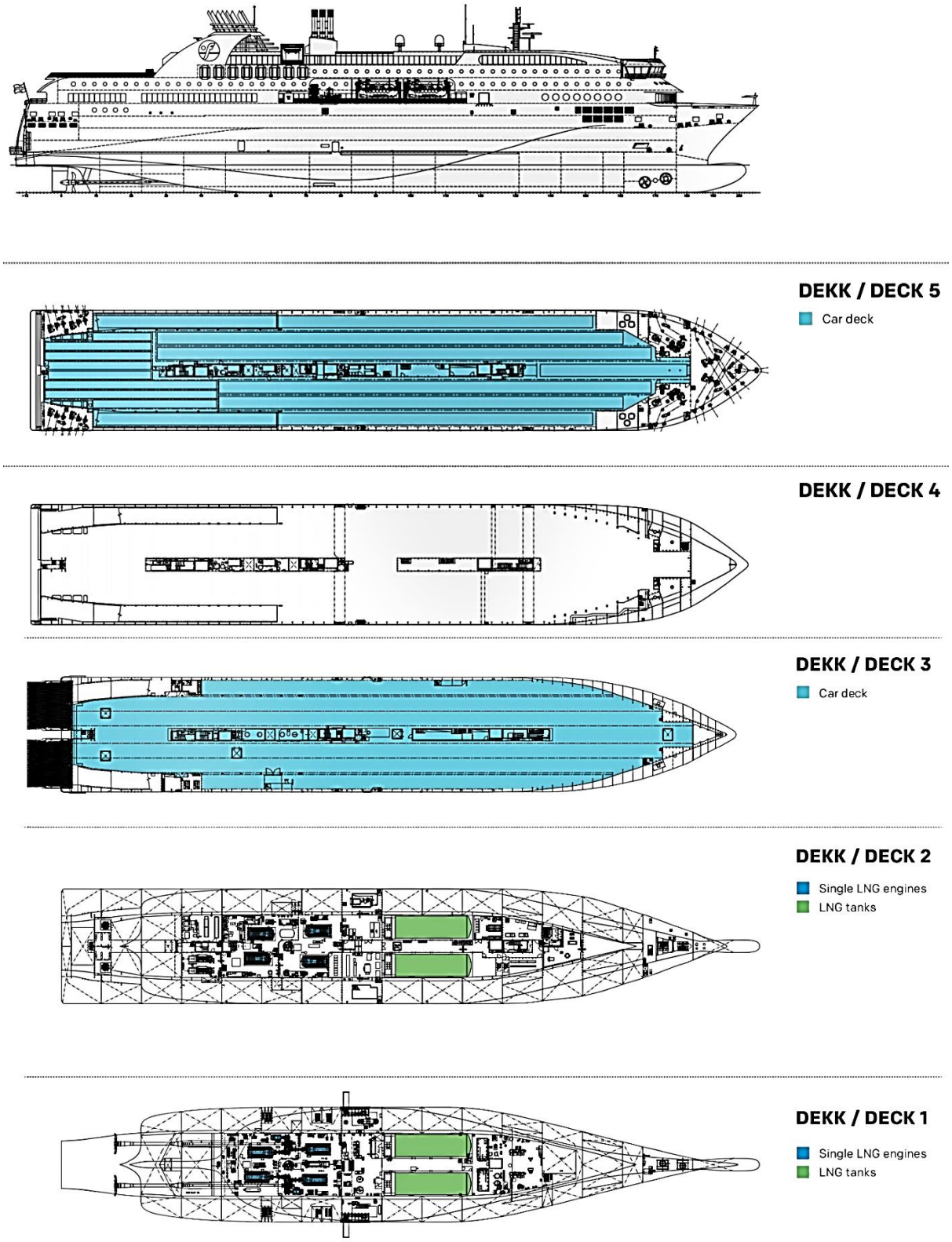

Figure E-2: General arrangement of the MS Stavangerfjord part 2. [195]

© COPYRIGHT OF C-JOB, WHOSE PROPERTY, THIS DOCUMENT REMAINS. NO PART THEREOF MAY BE DISCLOSED, COPIED, DUPLICATED OR IN ANY OTHER WAY MADE USE OF EXCEPT WITH THE APPROVAL OF C-JOB.